BEHAVIOUR OF BEAM-TO-COLUMN END PLATE CONNECTIONS IN STRUCTURAL STEELWORK

by

Mohammad Bahrami B.Sc. (Hon)

A Thesis presented for the award of the
Degree of Doctor of Philosophy
of the
Council for National Academic Awards

Department of Civil Engineering,
Surveying & Building
Dundee Institute of Technology
December 1991.

Acknowledgements

The author wishes to express his sincere gratitude to his two supervisors Dr. B. Bose (Director of Studies) and Prof. S. Sarkar for their invaluable support, encouragement and guidance given to the author throughout the course of this research, without which this research would not be possible. The author is greatly indebted to his external supervisor Prof. W. M. Jenkins for the valuable advice received on various aspects of the investigation during frequent meetings with the author.

Mr. S. Gardener, Mr. S. Ballas and other staff of the computer centre of the Dundee Institute of Technology had assisted the author on many occasions when he required special computer facilities or encountered difficulties with computing. The author thanks them for their ungrudging help.

Acknowledgement is also due to the staff at Finite Element Analysis Ltd. for their cooperation at early stages of the finite element analysis.

Thanks are also due to the technical staff of the Department of Civil Engineering, Surveying and Building, in particular Messers Galloway, Thompson, Smart and Webster, for their valuable assistance in preparing and testing the specimens.

Author is also grateful to the Research Committee, Dundee Institute of Technology for financial assistance towards the research project.

Last but not the least, the author wishes to express his deep gratitude to his parents, sister and brother for their understanding, love and support during the long and sometimes frustrating years of his research work.

Dedicated to my Parents for their love and support.

Behaviour of beam-to-column end plate connections
in Structural Steelwork

M. BAHRAMI

ABSTRACT

End plate connections are extensively used as moment-resistant connections between members in steel frames. The popularity of these connections can be attributed to the simplicity and economy associated with their fabrication and erection. Both the 'flush' and 'extended' end plate types are widely used in steel construction industry.

The overall objectives of the research project were to carry-out an in-depth study into the behaviour of unstiffened beam-to-column extended end plate connections by applying finite element technique and to formulate a limit state design method for this type of connection.

A finite element model of the connection is presented in the thesis. In addition to the solid and bar elements used to discretize the plates and bolts respectively, non-linear joint elements were employed to model the interactive forces induced between the end plate and column flange. The properties of the joint elements were chosen to ensure displacement compatibility at nodes where end plate and column flange were in contact but allow separation at the other nodes except at bolt locations. A three-dimensional elastic-plastic analysis of the connection was carried out with the aim of predicting the ultimate moment capacity and moment-rotation characteristics of the connection over the entire range of the loading until collapse occurred.

Twelve full scale tests involving three column-beam sets, and four end plate thicknesses for each of the three column-beam sets were conducted and the results were analysed. Comparison was made between the results obtained by the finite element analysis and the experimental investigation. A parametric study was also carried out for the purpose of the separating the contribution of the end plate, column and bolt towards the stiffness of the connection. A limit state design method for the end plate connection is described.

List of Tables

List of Figures

CHAPTER 1

CHAPTER 2

CHAPTER 3

CHAPTER 4

CHAPTER 5

CHAPTER 6

CHAPTER 7

CHAPTER 8

CHAPTER 9

CHAPTER 1

Introduction

1.1 Definition of Semi-Rigid Connection

Economy is the theme of today's industrial climate and in structural steelwork the key to it often lies in the type of connection selected for a particular structure. The main function of the connection is to transfer the load applied to the beam and floor system to columns, and its rotational characteristics will influence the strength and stability of the steel structure. Desired economy and performance of the structure can be achieved by adopting appropriate connections. Currently the design approaches for steel connections are based on the assumption that joints behave either as:

(1) fully rigid, where the joints provide full rotational continuity between the connected members or

(2) pinned, where the connections act as shear pins only.

However, the research work on connections which started as early as 1900 had demonstrated that neither of these connections can truly be reproduced in practical situation. Rigid connections will generally be somewhat less rigid than assumed and a certain degree of flexibility will exist. Also, pinned joints demonstrate a degree of rigidity ignored in the design process. Therefore, all connections fall under the semi-

rigid category with ideally pinned and fully rigid joints representing only the extreme conditions which are rarely encountered in real structures.

Behaviour of semi-rigid connections has been of great interest for a long time. It produces a closer balance between the end moment and mid-span moment in the beam resulting in economy for both beam and column design by increase in the load capacity of the beam, reduction in overall deflection of the beam and reduction in the effective length of column. A semi-rigid connection in a steel structure should meet the following requirements:

(i) sufficient strength;

(ii) adequate rotation capacity;

(iii) sufficient stiffness; and

(iv) economic fabrication.

In order to fulfill the above requirements and to formulate simple design rules for this type of connection, it is necessary fully to understand the response of the connection under loading. The early research on semi-rigid connections was conducted on welded or riveted specimens [1, 2, 3] and the design charts given in document PD3343[4] were based on the information obtained by studying the behaviour of column-beam connections typical of the period before 1930-45 (mainly riveted joints). The design curves were based on allowable stresses and load factors in use at that time. By the early 1950's riveting was largely replaced by bolts, in particular H.S.F.G. bolts, which provided a greater and more consistent clamping force. It was also more economical than riveting [5]. Such developments brought a new wave of research into bolted

connections which is still continuing. The result of such studies and a survey of steel industry indicated that the use of H.S.F.G. bolts can increase the connection rigidity; however their use is limited to cases where there is a danger of nut working loose with dynamic loading or connection rigidity is critical or slip is an important factor. In these cases it is important to ensure that the bolts are fully tightened under proper supervision which will lead to higher labour cost. Although there are other means of fastening, like welding and grade 8.8 bolts, each has its own shortcomings. The grade 8.8 bolts are susceptible to premature stripping of the threads in the nuts. Recent comparative studies of grade 8.8 and H.S.F.G. bolts [6] have shown that the grade 8.8 bolt is not significantly weaker in tension than H.S.F.G. bolts provided grade 10 nut is used with grade 8.8 bolt to avoid premature stripping of the threads in the nut. However, the idea of mixing the two different grade is not covered by any existing code of practice. Therefore, grade 8.8 bolts can be replaced by general grade H.S.F.G. bolts which have larger heads and nuts (equivalent to grade 10 nut) and used without any load indicating washers. They are treated in a manner similar to that for normal high strength bolts and are not fully torqued. In the absence of bolt tightening under proper supervision the use of H.S.F.G. bolts will not increase the cost significantly.

Welding is also used as a means of fastening, but direct site welding is expensive and difficult and should be avoided wherever possible. Generally welded joints require tighter tolerance than the bolted ones; it also requires skilled labour for fabrication and inspection. Devices such as the use of an additional seating cleat attached to column to act as a temporary seat during erection will often be required. Moreover,

during fabrication jigs may be required to hold parts in position for tack welding before the full joints are made which involve more operation than that for bolted connections. The advantages of bolted connections over welded joints, which have been indicated by several writers [7, 8] in the past, can be summarised as below:

(i) labour costs for structural steel erection involving site welding have risen to a level where it is not practical in many situations to use fully welded beam-to-column moment connections. Net savings have been achieved by using bolted connections instead of site welded ones;

(ii) bolted joints are quicker to fabricate than the welded joints;

(iii) error in alignment can be corrected with bolted joints, while the alignment of the welded frames is difficult and distortion in the members are likely to cause inconvenience or difficulty in fit up.

1.2 Extended End Plate Connection, Advantages and Design Practices

Although bolted connections have long been employed for shear joints, the extension of their use as moment resisting connections is a recent trend in steel construction. In a report on end plate connections in 1962 Disque [9] described the advantages and disadvantages of the end plate connections from a practical and fabricating point of view. Some of the advantages over other types of bolted connections (ie. T-stub and angle cleat connections) are:

(i) saving in material weight and fabricating costs;

(ii) reduced number of detail pieces to handle which results in saving;

(iii) alignment with connecting member is not affected by beam depth variation;

(iv) workmanship is simpler when all drilling is confined to plates which are then welded to beams.

Both flush and extended end plate connections are widely used as moment resisting joints in steel frame construction. Extended end plate is more rigid and has a higher moment capacity than that of a flush end plate and is frequently used in order to achieve a rigid connection. A typical extended end plate connection comprises a rectangular steel plate welded to the end of the beam section which in turn is connected to the flange of a column by two pairs of high strength steel bolts positioned symmetrically on either side of the beam tension flange and a pair of bolts placed adjacent to the beam compression flange. Also, in order to ensure that the joint has the ability to transfer the anticipated load from beam to the column and to develop the desired restraint additional column stiffeners may be provided at the level of beam flanges. However, column stiffening involves costly fabrication and may interfere with the connection of cross beam to the web of the column; therefore it may be preferable to use a heavier column section to avoid column stiffening.

In extended end plate connections the beam end moment is transferred through the end plate to the column flange via the bolts. This results in tension force acting on the column flange at bolt location in the tension region and compression force acting over some bearing zone in the compression region. The column flange,end plate

interaction is a complex problem in that the interface condition between the bodies varies depending on the level of interaction and loading. This can be further complicated by the existence of prying forces and bolt tightening. The prying forces had been frequently disregarded even though they can have significant influence and in many cases they can lead to joint strength being controlled by premature bolt failure.

While it could be said that in an ideal design all parts of connection should fail simultaneously for maximum efficiency, this cannot be regarded as a good practice. Bolts and welds behave in a brittle manner and their failure in a connection would cause a sudden loss of strength. This type of failure occurs if a thick end plate is used such that there is negligible bending deformation of the end plate, provided the column is strong enough to resist the external moment. Therefore it is necessary to establish a right balance between the performances of the individual components in order to obtain the desired stiffness and strength. Semi-rigid connections are allowed in BS5950 [10] where it recommends that semi-rigid connections shall be designed as idealised pinned joints and allowance of 10% of free moment shall be made for the end restraint moment. This design method is neither efficient nor economical and is not widely used. Another approach is based on the yield line method where various yield line configurations are assumed in order to consider the plastic behaviour of the various components forming the connection. It assumes the connection to be rigid with no elastic deformation in the end plate and column flange. This approach tends to oversimplify the behaviour of the connection and is limited to beam plastic

moment of resistance of 420 kNm. Also, the occurrence of prying forces is acknowledged but no attempt is made to present a method for evaluating these forces. It is suggested that an increase of upto 33% in the tension bolt forces will be adequate to compensate for the prying action. This method results in conservative formulas for the design of end plate, column flange and bolts.

Recent developments in computer technology ie, advent of large core, high speed digital computers and many powerful finite element packages provide an ideal tool to carry out an in-depth study of the connection behaviour. Early attempts to analyse the end plate connections using finite element technique were based on two dimensional analysis, treating the connection as a plane stress problem in the plane of the beam web. Also the column flange was treated either as a rigid base with no contribution towards the rotational characteristics of the connection or the column flange was stiffened with similar geometrical properties as the end plate and had limited deformability. Although some attempts were made to model the interaction between the end plate and column flange and determine the position of the prying forces, they were mainly unsuccessful. Hence they either ignored the prying effects or suggested a percentage increase in the tension bolt forces to account for the prying action.

It should be recognised that an extended end plate moment connection is essentially a complex three dimensional problem. Although a three dimensional finite element analysis of the connection is much more complicated than a two dimensional one and is lot more demanding in respect of computer time and facilities, it is nevertheless

preferable as it enables a realistic and meaningful solution to the extremely complex problem. In order to bridge the existing gap in the theoretical analysis of the extended end plate connection and highlight the relevance, applicability and accuracy of the three dimensional finite element technique a thorough investigation was carried out by the author. Some of its findings were reported in a paper [11] which was presented at the International Conference on 'Computational Structures Technology' held at Heriot-Watt university, Edinburgh in August, 1991. A copy of the paper published in the Structural Engineering Review is enclosed at the end of the thesis.

1.3 Aim and Scope of Present Study

End plate connections are increasingly used as moment-resistant connections in framed structures. Popularity of this type of connection is due to the economy and simplicity of construction associated with their fabrication and erection. The behaviour of this type of connection is extremely complex and is dependent on a large number of parameters. It is therefore necessary to carry out an in depth investigation of this type of connection at both ultimate and service loads.

The aim of this project is to carry out an investigation into the behaviour of unstiffened beam-to-column extended end plate connection in steel structure. This report discusses the overall problem concerning semi-rigid joints. It also describes theoretical finite element modelling and analysis of the extended end plate connection, and testing programme which was carried out to enable the validity of the theoretical analysis to be checked. A non-linear three dimensional finite element

analysis was carried out utilising the computer software package 'LUSAS'. It simulated the connection characteristics which included the effects of end plate flexure, column flange deformation and extension of the bolts on the rotational behaviour of the joint.

Twelve full scale tests were conducted and the data obtained from the tests were analysed. These were compared with the results obtained from the finite element analysis in order to assess the validity of the assumptions made and the accuracy of the finite element model. Finally a limit state design method for this type of connection was discussed.

CHAPTER 2

Review of Previous Research Work

2.1 Introduction

Since the beginning of 20th century researchers have been investigating the behavioural characteristics of the semi-rigid connections with the aim of providing a easier and more precise method of incorporating these joints into the structural steel design. These investigators were concerned with the performance of the connections themselves as well as the way in which connection behaviour influences the performance of the whole structure. A prerequisite of such studies is an understanding of the strength, stiffness and rotational capacity of the connection. However, the complexity of the behaviour of most structural steelwork connections has resulted in considerable simplification in the traditional approaches to design. The classification of connection types has been based on the concepts of 'rigid' and 'pinned' joints. In reality most of the connections normally regarded as pinned possess some rotational stiffness, while connections which are regarded as rigid often display some flexibility. It would therefore seem more correct to classify all steel connections under the semi-rigid category, while recognising 'pinned' and 'rigid' as extreme cases. The most

obvious advantage of a design utilising semi-rigid connections is that the beam moments are reduced leading to lighter beams. Such economy in design can only be achieved if the rotational characteristic of the connection is known. It is therefore not surprising to find that the main thrust of research has been towards providing an accurate method of predicting the moment-rotation behaviour of the connections. These studies have resulted in a variety of methods for the analysis of semi-rigid connections ranging from purely empirical curve fitting of test data, through behavioural analogy to finite element method. The available literature on the subject can be divided into three categories:

(1) experimental research involving testing to failure;

(2) theoretical research based on the yield-line theory; and

(3) analytical research using finite element technique.

This chapter contains a brief survey of available literature on extended end plate connections.

2.2 Experimental Research

Early work on connections was directed towards the determination of rigidity of riveted connections under tensile forces. This was spearheaded by Wilson and Moore[12] in 1917. They conducted twelve tests in order to assess the rigidity of various types of connections and highlighted the importance of end restraint provided by semi-rigid connections. In the 1930's Batho [1], and Young et al [2] in Britain and Canada established the relationship between the moment transmitted and the relative angle

changes between the beam and the column in an attempt to provide data for semi-rigid connection design. Batho proposed a graphical method for predicting the end restraint provided by a connection for which experimentally derived moment-rotation relationship was known. Such proposals were based on extensive experimental programmes. During the 1940's Hetchman and Johnson [13] conducted a large experimental programme on 47 riveted specimens which led to the prediction of 15%-20% economy in design that could be achieved using riveted connections as compared with pinned connections.

Upto this point in time joint behaviour could only be found by conducting large testing programmes and this was mainly confined to riveted connections which were being used extensively. However, the appearance of H.S.F.G. bolts in the 1950's brought a new wave of research in various countries. The popularity of H.S.F.G bolts was due to the following reasons [5].

(1) A more consistent clamping force was provided.

(2) Installation did not require expensive heating equipment.

(3) Bolting crew required less training to operate simpler equipment.

(4) Fire risk was reduced.

(5) Field erection cost was lower.

Therefore, it was necessary to establish theories for bolted moment connections and numerous design procedures were proposed based on theoretical and experimental studies.

In 1959, Schutz [14] investigated the behaviour of T-stub and end plate connections and proposed a design method based on 'prying force' concept. When a tensile load was applied to a T-stub, the bolts were subjected to tension and prying force was induced due to flexure of the flange. The design methods developed to determine the flange thickness and bolt size were based on experimental data. Also prying forces were assumed to act at the extreme edge of the flange of the T-stub.

Sherbourne [15] investigated the characteristics of end plate connections in 1961 with particular reference to the detailing of the end plate and column stiffening. His experimental programme focussed on the ability of columns, with or without stiffeners, to develop the full plastic moment of the connection member. The effect of column axial load was not considered and no attempt was made to determine the stress or strain distribution in the end plate, column and stiffeners. For a connection employing only four bolts he assumed that the tension flange force would be divided equally between them. From the test results it was concluded that a nominal amount of stiffening was required for the column with thin flanges. The size and the point at which stiffeners were needed were not established. Generally the main emphasis was laid on the overall behaviour of the connection, and it was recommended that the component parts of end plate connections be proportioned so that they reach the required strength and all yield simultaneously.

In 1965 Douty and McGuire [16] published a refined version of Schultz's suggestions and developed semi-empirical equations for prying force based on experimental and analytical studies on double T-stub connections. They concluded that the prying force increased with increasing bolt stiffness and local compressive stiffness of the T-stub flange and decreased with increasing bolt to flange edge distance. Similar work was done by Nair, Birkemore and Munse [17] in 1974 on the behaviour of high strength bolts in T-stub connections in the elastic and inelastic ranges. They developed an alternative formula to Douty and McGuire's which was simpler and it was determined that prying action can significantly reduce the ultimate load and fatigue strength of the bolted connection.

This trend of research was continued by Grundy etal [18] (1980) which resulted in a semi-empirical design procedure for end plate, bolt and column reinforcement based on the experimental investigation. They assumed that the connection stiffness depends on the strength of individual components. Therefore, it is only necessary to design each component without considering their interacting effects. It was assumed that the flange forces in tension and compression regions were independent of each other and should be designed separately. This assumption ignores the rotational nature of the deformed end plate and the fact that the welded end plate transmits both tension and compression. It was also assumed that the prying action would increase the tension bolt forces by a factor of 1.2.

2.3 Theoretical Analysis Based on Yield-Line Method

Early studies of semi-rigid joint action relied on representation of test data as the most appropriate means of including the contribution of the joint. Whilst this led to an improved understanding of the role of connection stiffness, it was expensive and time consuming. Therefore a new wave of research started in various countries in order to find an analytical method for predicting the performance of moment connections. One of these methods was presented by Surtees and Mann [19]. In developing the proposed formula for end plate thickness, these authors included the restraint offered to the end plate by beam web, assuming that the pattern of yield lines extended down to approximately half the depth of the beam. In the tests on beam-to-column connections reported by them the end plate and column flange were of similar thickness and the behaviour of the extended end plate rather than T-stub model was examined. Although their experimental results did not verify the assumed yield line pattern exactly, the results nevertheless confirmed their estimation of end plate thickness.

Zoetemeijer's [20] work was based on the ultimate load approach employing yield line theory. The 'equivalent length' of yield line was expressed in terms of geometrical and physical properties of connected parts for two possible yield line patterns. The pattern that gave the lower moment capacity was the failure pattern. The theory was based on the plastic behaviour of the T-stub flanges and bolts. Formulae were given to compute the design load of the connection based on two possible means of failure, bolt fracture and flange failure. The effect of prying force was not considered in the

method. It was also shown that the given formulae could be applied to end plate and T-stub beam-to-column connections. The method did not provide deformation or stress distribution when the material was in the elastic and plastic range.

Packer and Morris [21] also used yield line theory to predict the end plate moment capacity but most of the effort was directed at the failure of the column flange. Although prying force was not considered in their method it was suggested that the bolt load should be increased by 33% to account for prying. They studied the behaviour of column flanges which were decidedly less stiff than the end plate. It was found that in such circumstances though the behaviour of the extended end plate is not quite analogous to the T-stub, the latter proved to be a reasonable model. This pattern assumes that double curvature has developed, with yield lines forming at the bolt lines and at the plate-flange junction.

It can be seen that this method only predicts the ultimate strength of the connection, and does not provide any information relating to the actual deformation occurring in the connection. Therefore it cannot predict the bending moment based on stiffness. A satisfactory approach to comprehensive analysis of a connection must include the performance at both service and ultimate loads. It should also be capable of determining the actual bolt forces occurring, since they should not be greater than the maximum design load of the bolt.

2.4 Analytical Research using Finite Element Techniques

The ability to predict the structural response of a building frame to loading depends on accurate prediction of rotational behaviour of the connections. Such characteristics are the sum of the contributions from the individual components as well as the interaction between the member components. The basic mechanism of this interaction needs to be fully understood and is prerequisite for any simpler approach to joint behaviour. Whilst the previous methods of analysing semi-rigid connections provide valuable insight into the problem, they fail to measure important parameters and local effects. Also the huge expense involved in full scale testing has made it a less viable approach for research. The finite element technique offers an ideal tool to handle the complex problem. The finite element method of analysis has developed concurrently with the increasing use of high speed computers to the extent where it is now possible to obtain the solution of complex problems in engineering structures. The displacements (hence the rotations) and the stresses of a structure at any stage of loading can be obtained by using the finite element method.

Krishnamurthy [22, 23, 24, 25] used finite element technique to carry out 2 and 3 dimensional analyses of the end plate connections. He adopted an iterative procedure to determine the location of contact points between the end plate and the column flange support. However, he neither proposed a method of direct calculation of prying forces nor acknowledged their effects by increasing the bolt capacity. Also the contribution of the column section was not considered. The comparison of the

theoretical and experimental results illustrated the important role played by the bolt head and weld, both of which should be included in the numerical analysis.

Tarpy's [26] work was focussed on the unstiffened beam-to-column flange end plate connections. He produced equations which predicted the behaviour of the unstiffened beam-to-column connection by using linear elastic finite element method. By introducing joint elements in the model the interaction between end plate and column flange was taken into account. The investigation was limited to elastic analysis and no attempt was made to extend it to the inelastic range. Furthermore, it did not suggest a method to determine bolt forces.

An elastic-plastic layered finite element model was used to study the behaviour of extended end plate and cleated connections by Maxwell, Jenkins and Howlett [27, 28]. Some limited experimental testing and theoretical studies on the end plate connection were reported. The importance of moment rotation characteristic for beam-to-column joints was stressed. Previous work using the finite element method was based on the so called 'classic Kirchhoff thin plate' theory in which shear deformations were neglected. In fact in most steel connections the relative dimensions of the joint makes it a 'thick' plate problem. They pointed out that shear deformation effects might be important in end plate connections.

A very simple equivalent bar system was adopted by Patel and Chen (1985) [29, 30] in order to account for the bolt action, when simulating the response of a fully bolted moment connection. They used plane stress isoparametric elements for modelling the beam, column and connection plates, while three bar elements were used to simulate the pretension and shear carrying behaviour of the bolts. A linear stress-strain characteristic was assumed for the bars, whose parameters were derived from experimental results. The proposed system did not, however, take into account the possibility of slip. This factor was suggested as the main reason for the discrepancies found between the numerical results and test data in the inelastic range.

In 1986, Jenkins, Tong and Prescott [31, 32] also used 2-dimensional finite element method to produce design charts for stiffened beam-to-column connections. The theoretical moment-rotation curves produced were obtained by combining the separate analysis of end plate and column flange. The first analysis was based on the assumption that the rotation is principally due to deformation of end plate with no contribution from the flange, and the second analysis considered the column flange only with no deformation in the end plate. The theoretical modelling of the column flange deformation was considerably simplified by using column flange stiffeners in the tension and compression region. Although the bolts were not theoretically modelled, in order to account for the contribution of bolt stretching to connection rotation, the actual force-extension relationship of the bolts was used. For extended end plate connections the effect of prying was considered by applying a point load on

the column flange at the outer corners of the extension plate. They proposed standard details for both flush and extended end plate connections for a limited range of U.B. sections and a sample of only two U.C. sections, but their attention was mainly concentrated on flush end plate with at least four tension bolts. Extended end plate connections were considered only in passing and information concerning their structural behaviour was not reported.

Gendron and Beaulieu [33] proposed a 2-dimensional finite element model which takes account of plasticity for the behaviour of bolted steel connections. They used a similar technique to the one used by Patel and Chen to simulate the bolt behaviour. However a contact element was added to model the shear behaviour of the bolt and account for the existing gap between the shank of the bolt and the edge of the hole. Four of these bolt arrangements were placed in each beam flange at actual bolt locations. Nevertheless, since the entire connection assembly was modelled in two dimensions, the shear plate bolted to the beam web was allowed to overlap in the same plane while having different elements and different nodes, except at the bolt positions where they had common nodes. From the theoretical analysis they produced a load-deflection curve and a series of stress distribution graphs which did not reflect the true behaviour of finite element model. This model does not consider the effect of prying on the bolt behaviour. Therefore a more thorough check by comparison and calibration studies against an extensive range of tests on the bolted plates and full connection is necessary.

2.5 Survey of the Structural Steel Industry

In today's construction industry an important element in cost reduction is the more economic use of manpower brought about by automated and semi-automated procedures. This presupposes a measure of standardization not currently present in the British Constructional Steelwork Industry. The introduction of standardization not only reduces the numerous number of parameters involved in any connection design but also allows the designers to choose between a range of connections once the beam and column section have been decided on. This method provides a more efficient and economical design than the present methods where all connections are designed individually. This can only be achieved if adequate knowledge of connection responses is available. It is therefore essential to carry out a detail study in order to understand the moment-rotation characteristics of most connections.

Traditional design approach which classifies the connections based on the concept of 'rigid' and 'pinned' ignores the end restraint provided by the practical connections. The consideration of this end restraint will provide efficiency in design and a saving of up to 15% in steel [28]. The saving is the result of more realistic design without alteration to the existing design procedure; hence fabrication and erection costs remain unchanged. However, the recent increase in labour cost has overwhelmed the saving which can be made in material. It is therefore essential that the connection details be rationalized and the design procedure standardized. This is an ideal method

for incorporating the computerised design and fabrication which allows mass production and stock piling of the joint components. The combination of the reduction in material and manpower cost will have a significant effect on overall cost of construction. The Australian Steel Industry with only a single large fabricator has achieved a measure of standardization of connections and has adopted a 20mm diameter bolt (commercial grade) as standard. The diversity of fabricators and designers in Britain complicates the issue and contributes to the large number of different types of connections, bolts, weld size, plate thickness, etc. As a result it will need considerable effort and a lot of convincing before standard connections will be adopted in the U.K.

A survey of the Structural Steelwork Industry [34, 35] was carried out by Hatfield Polytechnic to review current practices and the validity of existing design methods in Britain. Two part questionnaires were sent to steelwork fabricators and consulting engineers. The first part was concerned with industrial practice in the use of various beam-to-column connection types, use of stiffeners, bolt types and size, preloading of bolts and unused holes. It was also seeking the frequency of universal beam and column usage, weld size and plate thicknesses. Other questions were related to design practice and 'in service' performance. The second part of the questionnaire was intended to obtain industry's response to certain proposals for standardization of end plate types of beam to column connection.

A collection of ten popular connections from pinned to rigid as identified in the BCSA 'Manual on Connections' [36] were sent to industry (Fig. 2.1). These connections were classified into three groups dependent upon their stiffness. Of the three basic types into which the connections can be divided ie, flexible, semi-rigid and rigid, one overwhelmingly predominated in each category. The survey indicated that connection types 1, 6, 7 and 10 were being used frequently by 48%, 83%, 31% and 71% of the suppliers respectively as shown in Fig. 2.2. The popularity of the connection type 10 is due to its extensive use in portal frame construction. End plate connection 6, 7 and 10 can be prefabricated in-shop which allows a higher standard of quality control. Also the frequency of replies clearly indicates the connection types for which standardization of detail is a worthwhile task. Conversely the connections with the need for on-site welding were the most unpopular with less than 10% of respondent claiming a frequent use. This clearly highlights the preference of steel industry for in-shop opposed to on site-welding.

Similar convergence occurs with bolts. Despite the popularity of M16 and M24 grade 8.8 bolts, the one overwhelmingly preferred is M20 grade 8.8 (Figs. 2.3- 2.6). The use of H.S.F.G. bolts, except where there is degree of nut working loose with dynamic loading or rigidity is critical or slip is an important factor, is quite low. This is due to the need for on-site supervision and access for pretensioning which lead to higher labour cost. This has contributed to general limitation in the use of preloaded bolts. Another pattern of practice shows that the grade 4.6 bolts are mostly used in flexible

connections with grade 8.8 being used in semi-rigid and rigid connections where bolt tension is a more important factor than shear. A recent comparative study of grade 8.8 and H.S.F.G [7] bolts has shown that grade 8.8 bolts are not significantly weaker in tension than H.S.F.G. bolts provided that grade 10 nuts are used to avoid premature stripping of the thread in the nuts. However, the discussion on that paper indicated that such mixing of grades is not practical and controllable on the site. Therefore grade 8.8 can be replaced by general grade H.S.F.G. bolts, which have larger head and nut (equivalent to grade 10 nut), used without preload to prevent stripping and provide economy.

While grade 43 steel is almost universally in use, there is still a wide range of universal sections being used and the trend is for shallower beam and column sections to be used. 69% of universal beams used are within the range 203x133 UB - 475x191 UB and 81% of column sections used are between 152x152 UC - 305x305 UC. Although it has been considered more economical to select heavier column and beam sections rather than introducing stiffeners, there was little support from the replies for the suggestion. This indicates a lack of understanding of the behaviour of the unstiffened column flange. When stiffeners are introduced, tension/compression stiffeners are popular and limited to flush, extended end plate and fully rigid connections. Table 2.1 summarizes the results of the survey.

The thickness of end plate seems to be related to moment-rotation capacity requirements of the connection and therefore, not specifically predictable, but there is a relationship between the thickness of the end plate and the size of the weld as expressed by the rule of thumb formula;

$$t_w = 2\sqrt{t_p}$$

where t_w = weld size

t_p = thickness of end plate

In general the industry seems willing and indeed eager to accept the standardization of connections as long as such standardization entailed no more expenditure of time or effort than the present methods. There were, however, two areas where reluctance was shown. First, replies indicated an unwillingness to make use of heavier columns instead of using horizontal stiffeners in the column flange, despite the saving in manpower. Second, the suggestion that fabricated end plates should be provided with more holes than needed for a specific connection was rejected on ground of susceptibility to corrosion and adverse public reaction.

It seems that in view of the results of the questionnaire a standardized design should be sought. While complete mass production of end plate is not popular and there is marked opposition to unfilled holes and punched holes, consideration should be given to the use of standard universal flat rolled to width at the mill for end plates.

Standardization of bolts can be split into two groups, according to bolt diameter with M16 and M20 for beams in one group while M20 and M24 bolts can be used for beams in the other giving a choice between three bolt diameters with a variation in bolt pitch and horizontal spacing. It can therefore be concluded that standardization is unlikely to result in saving in the amount of steel used, but even if there is a slight increase this should be more compensated for by saving in labour cost. Additional results collected by the Hatfield Survey are summarized in tables 2.2 to 2.6.

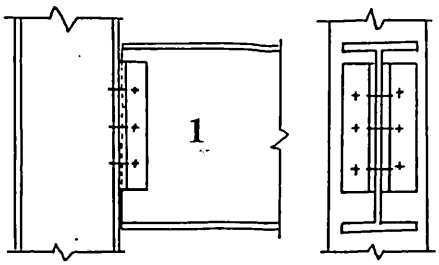

Web cleat

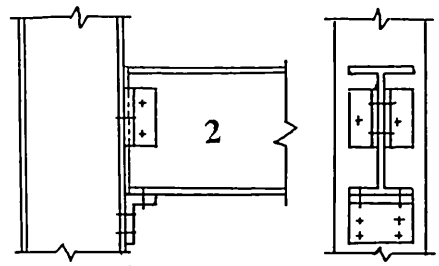

Bottom flange cleat with web cleat

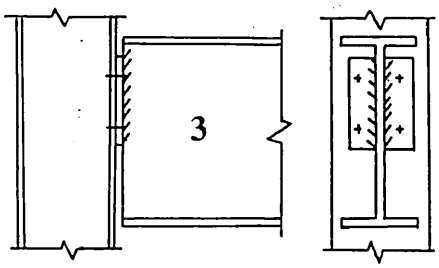

Flexible end plate

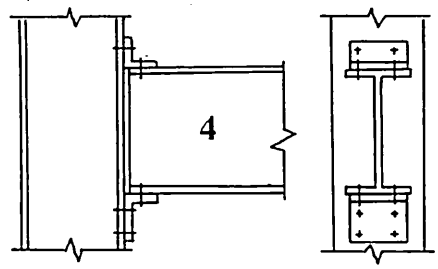

Flange cleat

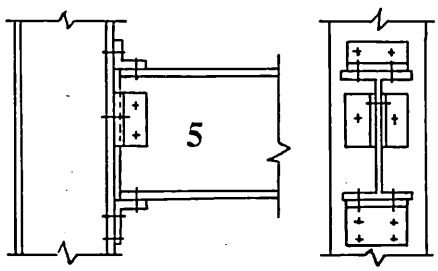

Web and flange cleat

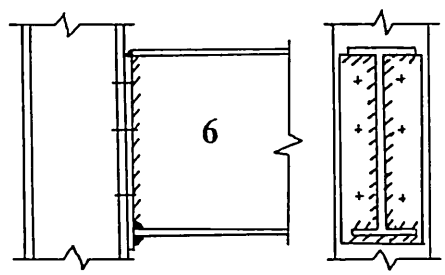

Flush end plate

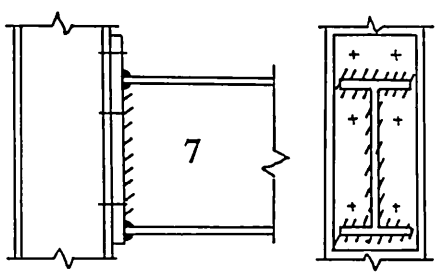

Extended end plate

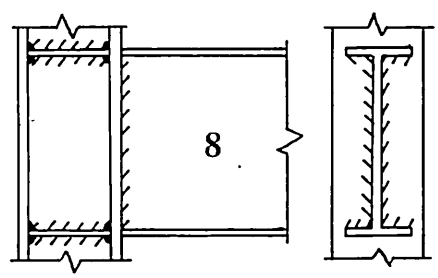

Directly welded with horizontal stiffeners

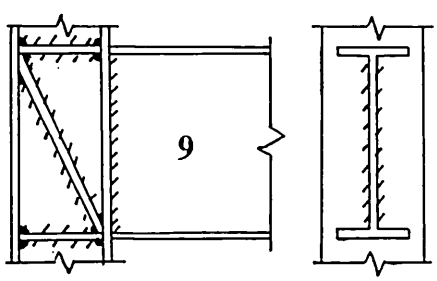

Directly welded with diagonal stiffeners

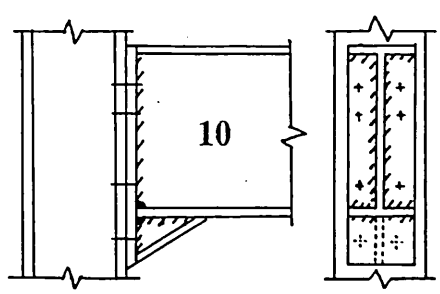

Extended end plate with haunch

Fig. 2.1 Connection types (Reproduced from Ref. 34)

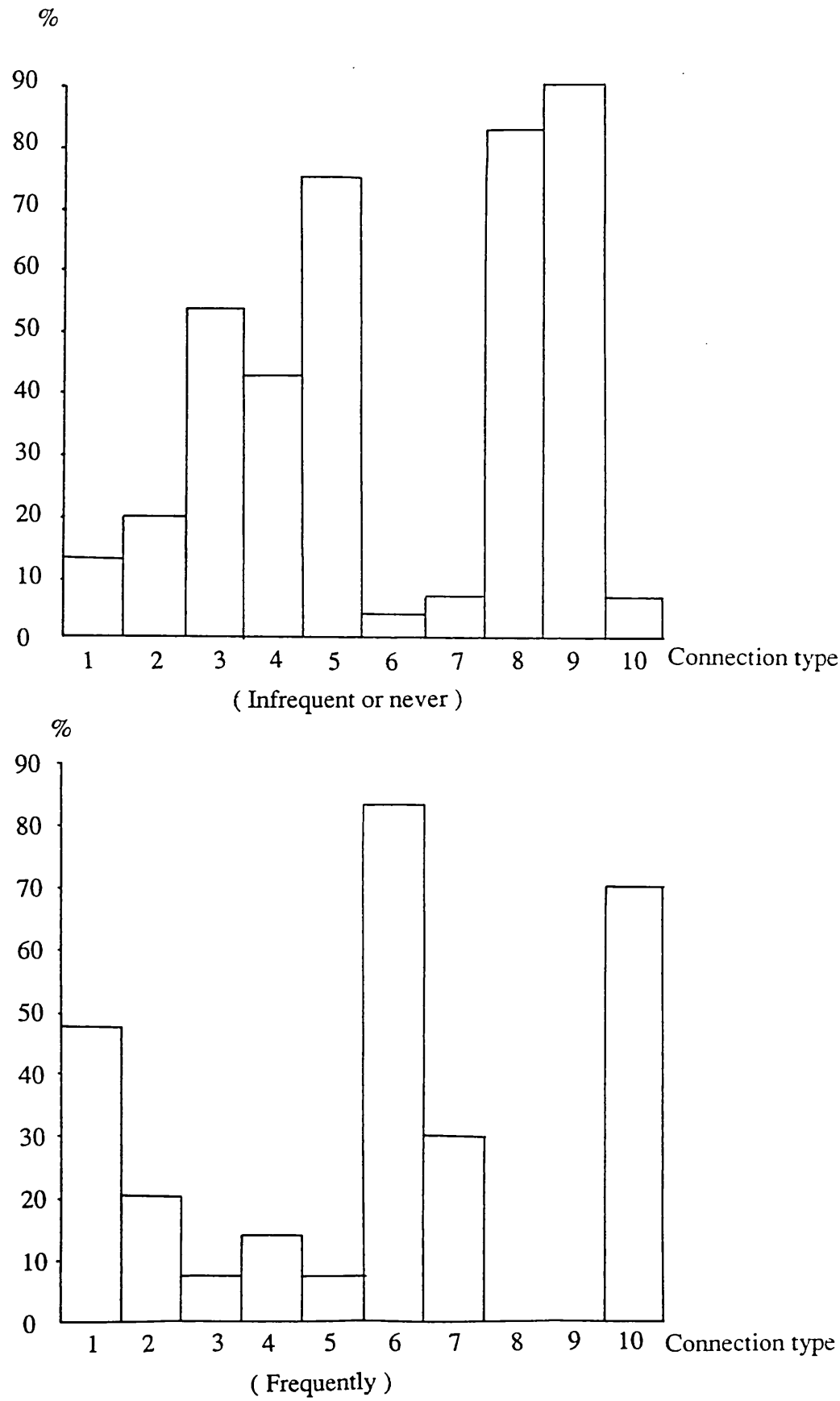

Fig. 2.2 Usage of connection types (Reproduced from Ref. 34)

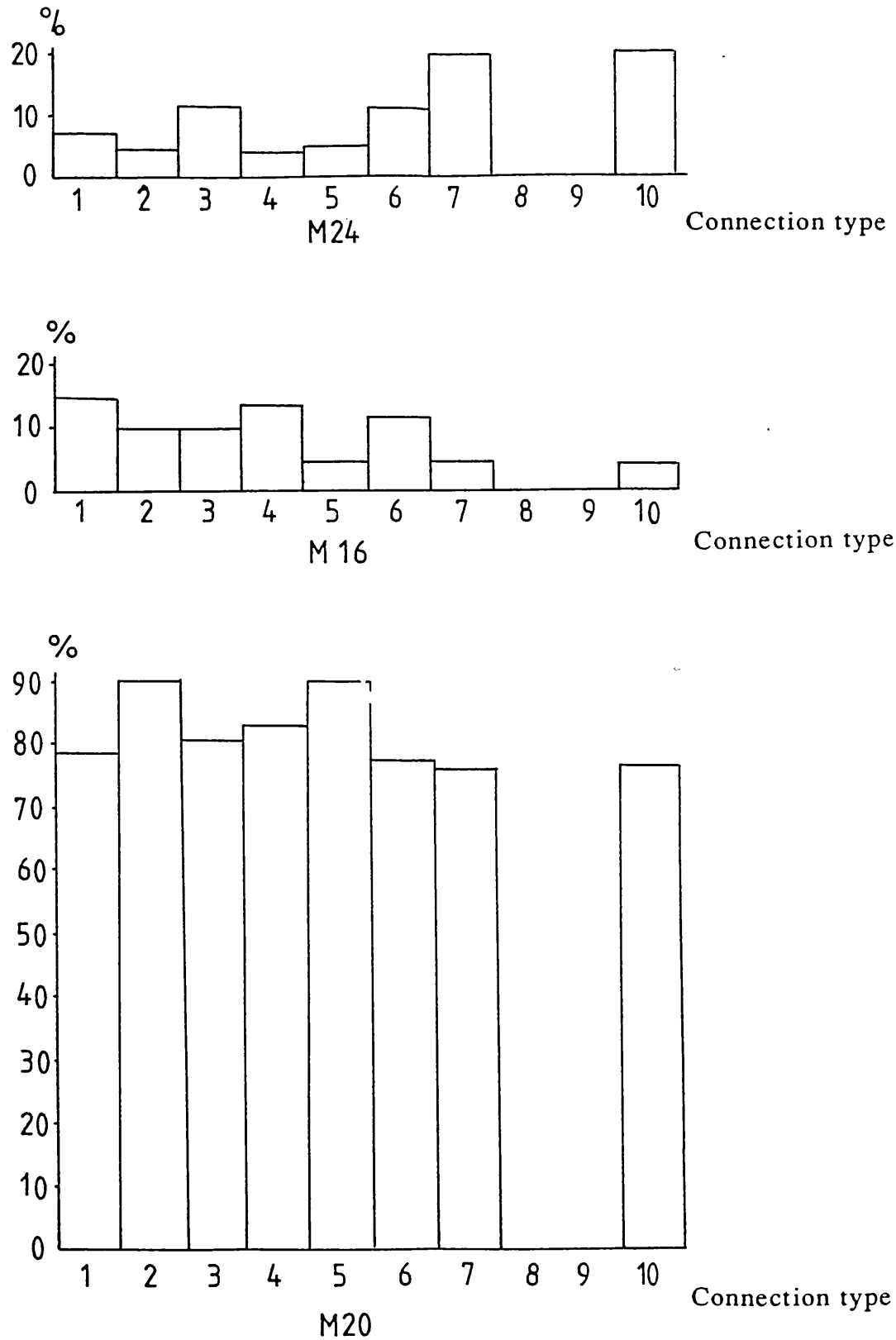

Fig. 2.3 Most frequently used bolt diameter (Reproduced from Ref. 34)

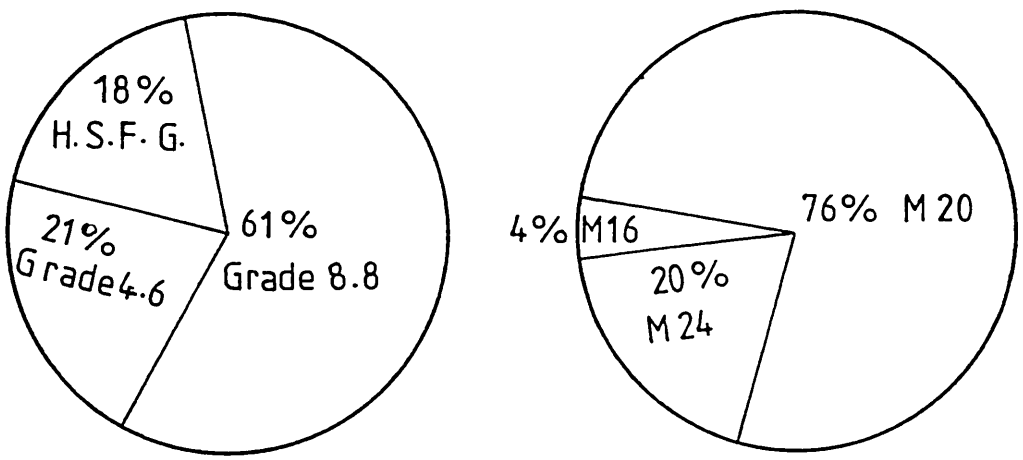

Bolt type

Bolt diameter

Fig. 2.4 Frequently used bolt type and diameter for extended end plate connections (Reproduced from Ref. 34)

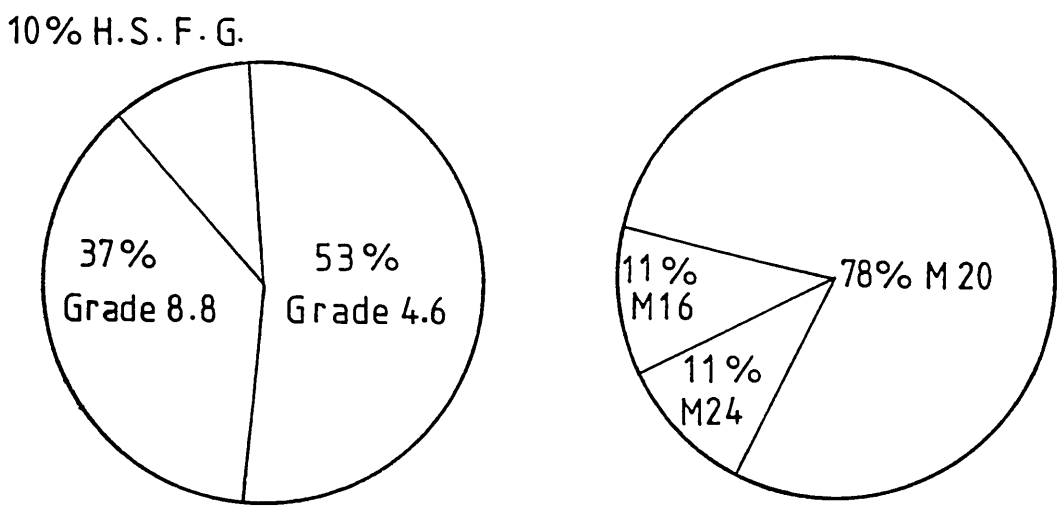

Bolt type

Bolt diameter

Fig. 2.5 Frequently used bolt type and diameter for flush end plate connections (Reproduced from Ref. 34)

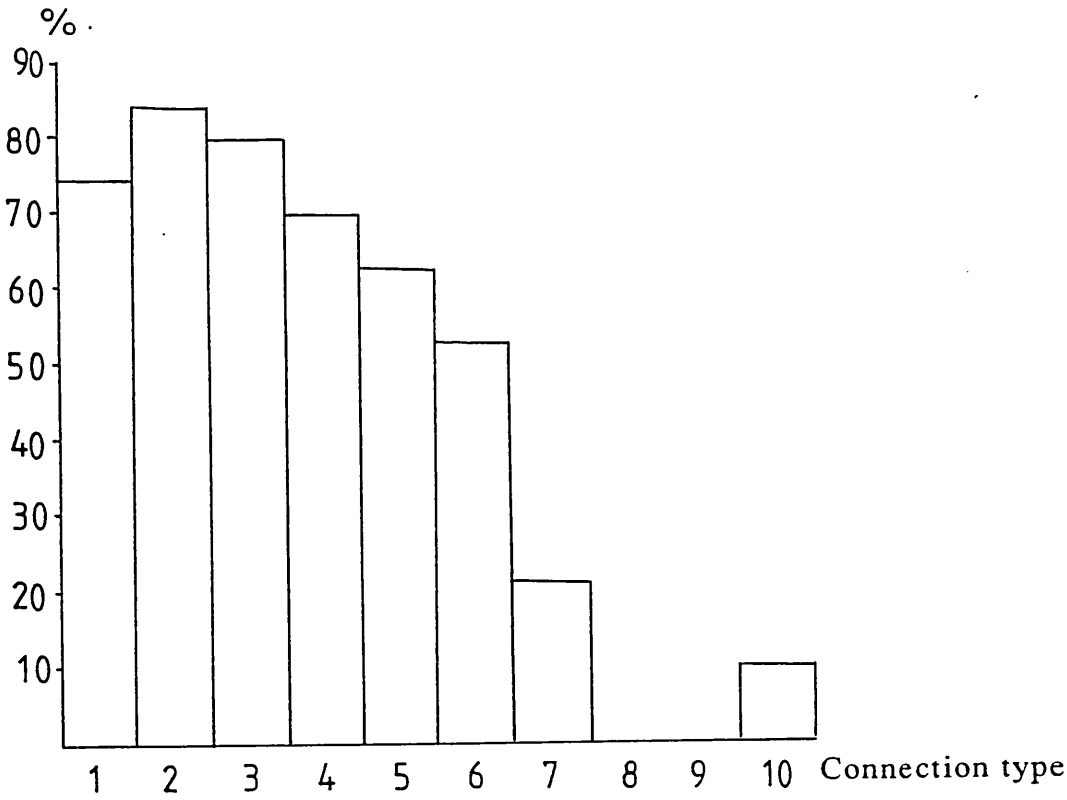

(Grade 4.6 bolt)

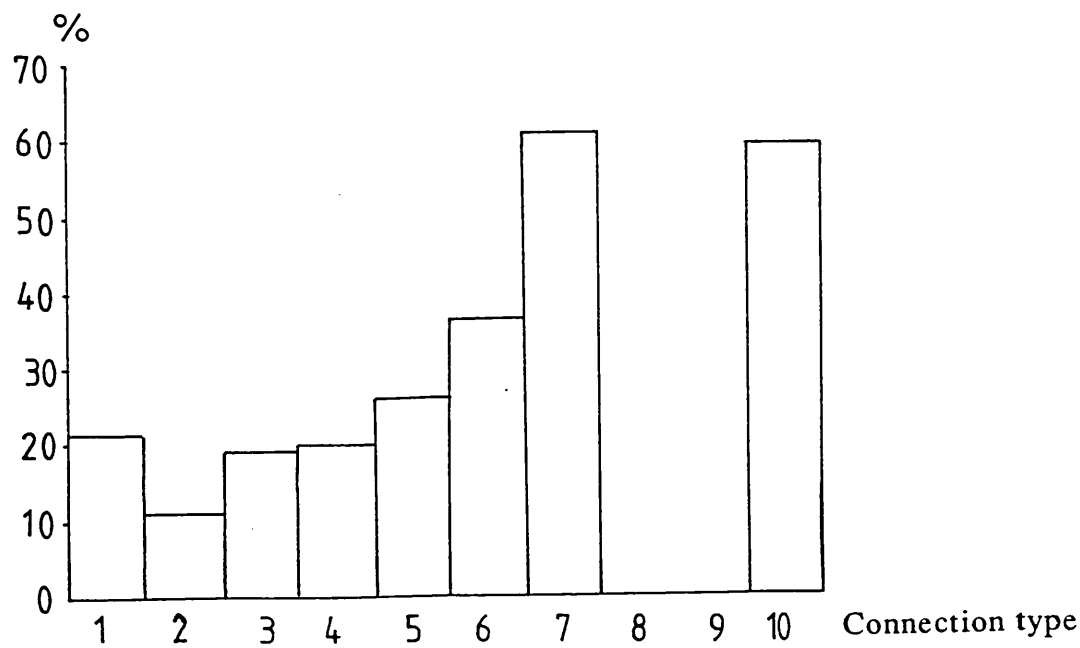

(Grade 8.8 bolt)

Fig. 2.6 Most frequently used bolt in connections (Reproduced from Ref. 34)

	Connection type				
	6	7	8	9	10
Stiffeners in tension/ compression	31	54	40	23	66
Diagonal Stiffeners	3	6	6	10	10
Column web reinforcing plate	6	11	11	3	11
Flange backing plate	6	14	0	0	14

(Figures indicate % of respondents using stiffeners frequently)

Table 2.1 Use of column stiffeners (Reproduced from Ref. 34)

	% range of holes punched						
	0-10	10-20	20-30	30-40	40-50	50-60	60
(%) Respondents	48	8	19	8	7	7	3

Table 2.2 Use of punched holes (Reproduced from Ref. 34)

	% of bolt preloaded					Measuring method		
	0	4-5	6-10	11-15	>15	Torque Wrench	Part Turn	Load Indicating Washers
Respondents %	24	31	28	7	10	20	12	68

Table 2.3 Preloading of bolts (Reproduced from Ref. 34)

UB / UC	914X 419 to 762X267	686 X 254 to 533X 210	457X191 to 356X127	305X165 to 203X133	Total (UC)
356X406 to 356X368	5	7	3	4	19
305X 305 to 254X 254	4	11	20	8	43
203X203 to 152X152	0	4	13	21	38
Total (UB)	9	22	36	33	100

(Figures are percentages)

Table 2.4 Usage of UB and UC (Reproduced from Ref. 34)

t_p (mm) \ UB	914 X 419 to 762 X 267	686X 254 to 533X 210	457X191 to 357X127	305X165 to 203X133
40	59	47	37	37
40-30	68	74	52	52
30-20	79	85	76	70
20-10	70	95	100	95
<10	45	57	80	90

Table 2.5 Percentage of respondents using end plate (Reproduced from Ref. 34)

t_p (mm) \ UB	914X419 to 762X267	686X254 to 533X210	457X191 to 357X127	305X165 to 203X133
40	12	12	10	10
40-30	10	10	10	8
30-20	8	10	8	8
20-10	8	8	6	6
<10	6	6	6	6

Table 2.6 Average weld size (mm) quoted by respondents

(Reproduced from Ref. 34)

CHAPTER 3

Theory of finite elements

3.1 Introduction

The limitations of the human mind are such that it cannot grasp the behaviour of its complex surroundings and creations in one operation. Thus the process of subdividing all systems into their individual components or 'elements', whose behaviour is readily understood, and then rebuilding the original system from such components to study its behaviour is a natural way in which the engineer, the scientist or even the economist proceeds.

In the determination of a system of stresses and displacements for a given design problem an adequate model is obtained using a finite number of well-defined components, in each of which the behaviour is described by a separate set of assumed functions representing the stresses or displacements in that region.

There are many excellent texts on Finite Element Method and the theory described in this chapter are extracted from references 37, 38 and 39.

The simplest three dimensional continuum element is a tetrahedron [37], with four nodal corners and this chapter will deal with the basic formulation of such an element. Although the detailed algebra is concerned with shape functions which arose from triangular and tetrahedral shapes, other element forms could equally be treated.

Indeed, once the element and the corresponding shape functions are determined, subsequent operations follow a standard, well defined path. A progressive increasing number of nodes improves accuracy and presumably decreases the number of such elements required to obtain an adequate solution. The additional complexity will require more computer time to be spent in their formulation.

3.2 Tetrahedral Element Characteristics

3.2.1 Displacement Function

Fig.3.1 illustrates a tetrahedral element i, j, m, p in space defined by the x, y, and z co-ordinates.The state of displacement of a point is defined by three displacement components u, v, and w in the direction of three co-ordinates x, y, and z. Thus :

$$\{u\}=\begin{Bmatrix} u \\ v \\ w \end{Bmatrix} \tag{3.1}$$

where {u} is the displacement vector and u, v, w are the three displacement components.

Just as in a plane triangle, where a linear variation of quantity is defined by its three nodal values, here a linear variation will be defined by the four nodal values. Thus we may write:

$$u = \alpha_1 + \alpha_2 x + \alpha_3 y + \alpha_4 z \tag{3.2}$$

where α_1 , α_2 , α_3 , α_4 are constants.

Substituting the values of displacement at the nodes we have four equations :

$$\begin{aligned} u_i &= \alpha_1 + \alpha_2 x_i + \alpha_3 y_i + \alpha_4 z_i \\ u_j &= \alpha_1 + \alpha_2 x_j + \alpha_3 y_j + \alpha_4 z_j \\ u_m &= \alpha_1 + \alpha_2 x_m + \alpha_3 y_m + \alpha_4 z_m \\ u_p &= \alpha_1 + \alpha_2 x_p + \alpha_3 y_p + \alpha_4 z_p \end{aligned} \qquad (3.3a)$$

In matrix form they can be expressed as:

$$\begin{Bmatrix} u_i \\ u_j \\ u_m \\ u_p \end{Bmatrix} = \begin{bmatrix} 1 & x_i & y_i & z_i \\ 1 & x_j & y_j & z_j \\ 1 & x_m & y_m & z_m \\ 1 & x_p & y_p & z_p \end{bmatrix} \begin{Bmatrix} \alpha_1 \\ \alpha_2 \\ \alpha_3 \\ \alpha_4 \end{Bmatrix} \qquad (3.3b)$$

From Eq. (3.3b) the constants α_1 ,α_2 ,α_3 and α_4 can easily be solved in terms of nodal displacements u_i ,u_j ,u_m and u_p as :

$$\{\alpha\} = \begin{Bmatrix} \alpha_1 \\ \alpha_2 \\ \alpha_3 \\ \alpha_4 \end{Bmatrix} = \begin{bmatrix} 1 & x_i & y_i & z_i \\ 1 & x_j & y_j & z_j \\ 1 & x_m & y_m & z_m \\ 1 & x_p & y_p & z_p \end{bmatrix}^{-1} \begin{Bmatrix} u_i \\ u_j \\ u_m \\ u_p \end{Bmatrix}$$

$$= \frac{1}{6V} \begin{bmatrix} a_i & a_j & a_m & a_p \\ b_i & b_j & b_m & b_p \\ c_i & c_j & c_m & c_p \\ d_i & d_j & d_m & d_p \end{bmatrix} \begin{Bmatrix} u_i \\ u_j \\ u_m \\ u_p \end{Bmatrix} \qquad (3.4)$$

in which

$$6V = \det \begin{vmatrix} 1 & x_i & y_i & z_i \\ 1 & x_j & y_j & z_j \\ 1 & x_m & y_m & z_m \\ 1 & x_p & y_p & z_p \end{vmatrix}$$

where V represents the volume of the tetrahedron and

$$a_i = \det \begin{vmatrix} x_j & y_j & z_j \\ x_m & y_m & z_m \\ x_p & y_p & z_p \end{vmatrix}, \quad b_i = -\det \begin{vmatrix} 1 & y_j & z_j \\ 1 & y_m & z_m \\ 1 & y_p & z_p \end{vmatrix}$$

$$c_i = -\det \begin{vmatrix} x_j & 1 & z_j \\ x_m & 1 & z_m \\ x_p & 1 & z_p \end{vmatrix}, \quad d_i = -\det \begin{vmatrix} x_j & y_j & 1 \\ x_m & y_m & 1 \\ x_p & y_p & 1 \end{vmatrix}$$

with the other constants defined by cyclic interchange of the subscripts in the order p, i, j, m.

Substituting the values of the constants from Eq.(3.4) into Eq.(3.2) we get the displacement component u as :

$$\begin{aligned} u = \frac{1}{6V} \{ & (a_i + b_i x + c_i y + d_i z)\, u_i \\ & +(a_j + b_j x + c_j y + d_j z)\, u_j \\ & +(a_m + b_m x + c_m y + d_m z)\, u_m \\ & +(a_p + b_p x + c_p y + d_p z)\, u_p \} \end{aligned} \qquad (3.5)$$

The ordering of the nodal numbers p, i, j, m must follow a 'right-hand' rule obvious from Fig.3.1. In this the first three nodes are numbered in an anti-clockwise manner when viewed from the last one.

The element displacement is defined by the twelve displacement component of the nodes as :

$$\{a^e\} = \begin{Bmatrix} a_i \\ a_j \\ a_m \\ a_p \end{Bmatrix} \tag{3.6}$$

with

$$\{a_i\} = \begin{Bmatrix} u_i \\ v_i \\ w_i \end{Bmatrix} \text{ etc.}$$

where $\{a_i\}$, $\{a_j\}$, $\{a_m\}$, $\{a_p\}$ are the nodal displacements and $\{a^e\}$ is the element displacement.

can write the displacements of an arbitrary point as:

$$\{u\} = [IN_i,\ IN_j,\ IN_m,\ IN_p\ ]\ \{a^e\} \tag{3.7}$$

where [I] is three by three identity matrix,

N is the displacement shape function defined as :

$$N_i = (a_i + b_i x + c_i y + d_i z)/6V \text{ etc.} \tag{3.8}$$

Once again the displacement functions used will obviously satisfy continuity requirements on interfaces between various elements. This is a direct corollary of the linear nature of the variation of displacements.

3.2.2 Strain Matrix

Six strain components are relevant in a full three dimensional analysis. The strain matrix can be defined as :

$$\{\xi\} = \begin{Bmatrix} \xi_x \\ \xi_y \\ \xi_z \\ \gamma_{xy} \\ \gamma_{yz} \\ \gamma_{zx} \end{Bmatrix} = \begin{Bmatrix} \dfrac{\partial u}{\partial x} \\ \dfrac{\partial v}{\partial y} \\ \dfrac{\partial w}{\partial z} \\ \dfrac{\partial u}{\partial y} + \dfrac{\partial v}{\partial x} \\ \dfrac{\partial v}{\partial z} + \dfrac{\partial w}{\partial y} \\ \dfrac{\partial w}{\partial x} + \dfrac{\partial u}{\partial z} \end{Bmatrix} = [\ L\ ]\ \{u\} \qquad (3.9)$$

where $\{\xi\}$ is the strain vector; ξ_x, ξ_y, ξ_z, γ_{xy}, γ_{yz}, γ_{zx} are components of direct and shear strains; and

$$[\ L\ ] = \begin{bmatrix} \dfrac{\partial}{\partial x} & 0 & 0 \\ 0 & \dfrac{\partial}{\partial y} & 0 \\ 0 & 0 & \dfrac{\partial}{\partial z} \\ \dfrac{\partial}{\partial y} & \dfrac{\partial}{\partial x} & 0 \\ 0 & \dfrac{\partial}{\partial z} & \dfrac{\partial}{\partial y} \\ \dfrac{\partial}{\partial z} & 0 & \dfrac{\partial}{\partial x} \end{bmatrix}$$

Therefore we can write :

$$\{\xi\} = [B]\ \{a\}^e = \left[\ [B_i]\ [B_j]\ [B_m]\ [B_p]\ \right]\ \{a\}^e \qquad (3.10)$$

in which

$$[\ B_i] = \begin{bmatrix} \dfrac{\partial N_i}{\partial x} & 0 & 0 \\ 0 & \dfrac{\partial N_i}{\partial y} & 0 \\ 0 & 0 & \dfrac{\partial N_i}{\partial z} \\ \dfrac{\partial N_i}{\partial y} & \dfrac{\partial N_i}{\partial x} & 0 \\ 0 & \dfrac{\partial N_i}{\partial z} & \dfrac{\partial N_i}{\partial y} \\ \dfrac{\partial N_i}{\partial z} & 0 & \dfrac{\partial N_i}{\partial x} \end{bmatrix} = \frac{1}{6V} \begin{bmatrix} b_i & 0 & 0 \\ 0 & c_i & 0 \\ 0 & 0 & d_i \\ c_i & b_i & 0 \\ 0 & d_i & c_i \\ d_i & 0 & b_i \end{bmatrix} \qquad (3.11)$$

with other submatrices obtained in a similar manner simply by interchange of subscripts.

3.2.3 Elasticity Matrix

With complete anisotropy the [D] matrix relating the six stress components to the same number of strain components can contain 21

independent constants. In general:

$$\{\sigma\} = \begin{Bmatrix} \sigma_x \\ \sigma_y \\ \sigma_z \\ \tau_{xy} \\ \tau_{yz} \\ \tau_{zx} \end{Bmatrix} = [D]\ (\xi - \xi_0) + \{\sigma_0\} \qquad (3.12)$$

where ξ_0 and σ_0 are the initial strain and stress respectively.

No difficulty is encountered in computation when dealing with such materials, since the multiplication will never be carried out explicitly. For an isotropic material the elasticity matrix [D] in terms of usual elastic constants E (modulus) and ν (poisson's ratio), can be written :

$$[D] = \frac{E(1 - \nu)}{(1 + \nu)(1 - 2\nu)}$$

$$\times \begin{bmatrix} 1 & \frac{\nu}{1-\nu} & \frac{\nu}{1-\nu} & 0 & 0 & 0 \\ & 1 & \frac{\nu}{1-\nu} & 0 & 0 & 0 \\ & & 1 & 0 & 0 & 0 \\ & & & \frac{(1-2\nu)}{2(1-\nu)} & 0 & 0 \\ & \text{symmetric} & & & \frac{(1-2\nu)}{2(1-\nu)} & 0 \\ & & & & & \frac{(1-2\nu)}{2(1-\nu)} \end{bmatrix} \qquad (3.13)$$

3.2.4 Stiffness and Load Matrices

The stiffness matrix defined by general relationship Eq.(3.14) can be explicitly integrated since the strain and stress components are constant within the element.

$$[K^e] = \int_{V^e} [B]^T [D] [B] \, dV \tag{3.14}$$

The general ij submatrix of the stiffness matrix will be a three by three matrix defined as :

$$[K^e{}_{ij}] = [B_i]^T [D][B_j]V^e \tag{3.15a}$$

where V^e represents the volume of the elementary tetrahedron.

Similarly the nodal force due to initial strain becomes:

$$[F^e{}_{ij}] = -[B_i]^T [D] \{\xi_0\}V^e \tag{3.15b}$$

3.3 Rectangular Prisms

In section 3.2 it was shown how linear elasticity problems could be formulated and solved using simple finite element form. Although the detailed algebra was concerned with shape functions associated with tetrahedral shapes only, it should be obvious that other element forms could equally well be used. Indeed, once the element and the corresponding shape functions are determined, subsequent operations follow a standard, well defined path. In fact it is possible to program a computer to deal with wide classes of problems by specifying the shape functions only.

For further investigation it will be convenient to use normalized co-ordinates shown in Fig.3.2. They are chosen so that on the faces of

the rectangle their values are ±1.

$$\xi = (x - x_c)/a \quad , \quad \frac{d\xi}{dx} = \frac{1}{a}$$

$$\eta = (y - y_c)/b \quad , \quad \frac{d\eta}{dy} = \frac{1}{b} \tag{3.16}$$

Once the shape functions are known in the normalized co-ordinates, translation into actual co-ordinates or transformation of the various expressions occurring, for instance, in stiffness derivation is quite simple.

It is usually most convenient to make the shape functions dependent on nodal values placed on the element boundary. Consider for instance the three elements of Fig.3.3. In each a progressively increasing and equal number of nodes is placed on the element boundary. Using now three normalized co-ordinates and introducing new variables

$$\xi_0 = \xi\xi_i \qquad \eta_0 = \eta\eta_i \qquad \zeta_0 = \zeta\zeta_i$$

we have the following shape functions:

Linear element (8 nodes)

$$N_i = \frac{1}{8}(1 + \xi_0)(1 + \eta_0)(1 + \zeta_0) \tag{3.17}$$

Quadratic element (20 nodes)

Corner nodes

$$N_i = \frac{1}{8}(1 + \xi_0)(1 + \eta_0)(1 + \zeta_0)(\xi_0 + \eta_0 + \zeta_0 - 2) \qquad (3.18)$$

Typical mid-side node

$$\xi_i = 0 \qquad \eta_i = \pm 1 \qquad \zeta_i = \pm 1$$

$$N_i = \frac{1}{4}(1 - \xi^2)(1 + \eta_0)(1 + \zeta_0) \qquad (3.19)$$

Cubic elements (32 nodes)

Corner node

$$N_i = \frac{1}{64}(1 + \xi_0)(1 + \eta_0)(1 + \zeta_0)[9(\xi^2 + \eta^2 + \zeta^2) - 19] \qquad (3.20)$$

Typical mid-side node

$$\xi_i = \pm\frac{1}{3} \qquad \eta_i = \pm 1 \qquad \zeta_i = \pm 1$$

$$N_i = \frac{9}{64}(1 - \xi^2)(1 + 9\xi_0)(1 + \eta_0)(1 + \zeta_0) \qquad (3.21)$$

3.4 Non-linear Theory

The performance of any structure is governed by the behaviour of its parent material and a successful finite element analysis should be able to simulate the true material responses [38, 39]. In this case the steel behaviour comprises two consecutive stages, elastic and plastic.In the elastic range a linear analysis would be adequate to predict the correct deformed configuration of structure. However, in

the plastic range there is significant non-linearity in the stress and strain relationship which is due to a decrease in the material stiffness subsequent to yielding. Therefore to model the correct material behaviour a non-linear analysis is necessary.

In general elasto-plastic theory is based on five concepts [38, 39] :

(i) A stress-strain law is assumed prior to plastic straining.

(ii) A yield surface exists beyond which plastic straining occurs.

(iii) A flow rule is assumed which defines the direction of plastic straining .

(iv) A hardening rule exists which defines the change in the yield surface during the course of plastic straining.

(v) The total strain may be decomposed into an elastic and plastic parts.

3.4.1 Elastic Stress-Strain Law

All the materials refered to in LUSAS are based on the assumption that prior to yielding the stress-strain relationship is linear and is defined by:

$$d\{\sigma\}_e = [D]\, d\{\xi\}_e \qquad (3.22)$$

where:

[D] is the elastic modulus matrix

$\{\sigma\}_e$ is the elastic stress vector

$\{\xi\}_e$ is the elastic strain vector

3.4.2 Yield Function

The yield function is dependent upon the state of stress $\{\sigma\}$ and strain hardening parameter (κ) and can be written as:

$$F(\{\sigma\}, \kappa)=0 \qquad (3.23)$$

where:

$\{\sigma\}$ is the effective stress hardening according to yield criterion adopted.

κ is the strain hardening parameter.

This function can be interpreted by Fig.(3.4) which shows for:

$F(\{\sigma\}, \kappa)<0$ stress state is elastic

$F(\{\sigma\}, \kappa)=0$ plastic flow occurring

$F(\{\sigma\}, \kappa)>0$ has no physical meaning since a stress state can not exist outside the yield surface.

In order to formulate the continuum plasticity four yield criteria are available:

(i) Tresca (ii) Von-Mises	suitable for ductile materials that exhibit little volumetric plastic strain eg. metals
(iii)Mohr-Coulomb (iv) Drucker-prager	suitable for materials that exhibit substantial volumetric plastic strain eg. concrete

For the purpose of this research Von-Mises yield criterion is chosen, since it is most universally accepted yield criteria for metals as shown in Fig.3.5. This criterion is based on the consideration of

distortional strain energy and its function can be written as:

$$F=(\{\sigma\},\ \kappa) = \bar{\sigma} - \sigma_y(\kappa) \tag{3.24}$$

where

$$\bar{\sigma} = \sqrt{3(J_2')^{1/2}} = \sqrt{3\kappa} \tag{3.25}$$

and $\bar{\sigma}$ is known as the effective or equivalent stress

σ_y is the current uniaxial yield stress

J_2' is the second deviatoric stress variant

3.4.3 Flow Rule

For multi-axial stress state it is necessary to define the direction and magnitude of plastic hardening. This is achieved by using the flow rule, which is defined as:

$$d\{\xi\}_p = d\lambda \frac{\partial Q}{\partial \{\sigma\}} \tag{3.26}$$

where :

$\{\xi\}_p$ is the plastic strain vector

$d\lambda$ is a constant of proportionality known as plastic multiplier

Q is the plastic potential.

If the plastic potential (Q) is equal to yield function (F) then the direction of plastic flow is normal to the yield surface. This flow rule is termed an associated flow rule. In this package associated flow rules are used with all of the four yield criteria. Therefore :

$$d\{\xi\}_p = d\lambda \frac{\partial F}{\partial \{\sigma\}} \tag{3.27}$$

This is termed normality condition, since $\frac{\partial F}{\partial \{\sigma\}}$ is a vector directed normal to the yield surface.

3.4.4 Hardening Law

After initial yielding, the yield stress may depend on the current degree of plastic straining. This phenomenon is denoted as strain hardening or softening. The two most common hardening hypotheses are isotropic and kinematic hardening. Isotropic hardening assumes that a uniform expansion of the yield surface occurs without any translation, whilst kinematic hardening assumes that the yield remains fixed in size but undergoes a translation, Fig.3.6. Isotropic hardening is adopted for the elastic-plastic models in LUSAS and work hardening hypothesis is used to relate the total plastic work (W_p) to the amount of expansion of the yield surface. Thus the hardening parameter κ can be written as :

$$F(\{\sigma\},\kappa) = F(\{\sigma\}) - K(\kappa) = 0 \tag{3.28}$$

and the equation (3.28) can be rewritten as :

$$F(\{\sigma\}) - \sigma_y(\kappa) = 0 \tag{3.29}$$

Also by partially differentiating equation (3.28) :

$$dF = \frac{\partial F}{\partial \{\sigma\}} d\{\sigma\} + \frac{\partial F}{\partial \kappa} d\kappa \tag{3.30}$$

or

$$dF = \{a\}^T d\{\sigma\} - A d\lambda \tag{3.31}$$

where

$$\{a\}^T = \frac{\partial F}{\partial \{\sigma\}} = \left[\frac{\partial F}{\partial \sigma_x}, \frac{\partial F}{\partial \sigma_y}, \frac{\partial F}{\partial \sigma_z}, \frac{\partial F}{\partial \tau_{yz}}, \frac{\partial F}{\partial \tau_{zx}}, \frac{\partial F}{\partial \tau_{xy}} \right] \tag{3.32}$$

and

$$A = - \frac{1}{d\lambda} \frac{\partial F}{\partial \kappa} d\kappa \tag{3.33}$$

where {a} is the flow vector.

Also the variation of strain hardening parameter produces :

$$d\kappa = \{\sigma\}^T d\{\xi\}_p = d\lambda \{a\}^T \{\sigma\} \tag{3.34}$$

substituting equation (3.34) in (3.33) will result in :

$$A = - \frac{\partial F}{\partial \kappa} \{a\}^T \{\sigma\} \tag{3.35}$$

However, for the uniaxial case $\{\sigma\} = \bar{\sigma} = \sigma_y$ and $d\{\xi\}_p = d\bar{\xi}_p$ where $\bar{\sigma}$ and $\bar{\xi}_p$ are the effective stress and strain respectively. Thus equation (3.34) becomes :

$$d\kappa = \bar{\sigma} \, d\bar{\xi}_p \tag{3.36}$$

giving

$$\frac{\partial F}{\partial \kappa} = \frac{1}{\bar{\sigma}} \frac{\partial F}{\partial \bar{\xi}_p} \tag{3.37}$$

Noting that for Tresca and Von-Mises yield criteria only, the yield stress is the function of plastic strain and using the equations (3.35) and (3.37) we obtain :

$$A = H_1 \frac{1}{\bar{\sigma}} \{a\}^T \{\sigma\} \tag{3.38}$$

where H_1 is the slope of the uniaxial yield stress versus the effective plastic strain curve as shown in Fig.3.7.

3.4.5 Decomposition of Elastic and Plastic Strain

For small strain the total strain increment $d\{\xi\}$ may be divided into elastic ($d\{\xi\}_e$) and plastic ($d\{\xi\}_p$) parts. Therefore

$$d\{\xi\} = d\{\xi\}_e + d\{\xi\}_p \tag{3.39}$$

For elastic material the constitutive relationship may be written as:

$$d\{\sigma\} = [D]\ d\{\xi\} \tag{3.40}$$

D is the elastic modulus matrix.

For yielded material the relationship is:

$$d\{\sigma\} = [D]_{ep}\ d\{\xi\} \tag{3.41}$$

where $[D]_{ep}$ is the elasto-plastic modulus matrix. $[D]_{ep}$ may be derived using the assumptions outlined previously ie. the elastic strain definition and the flow rule. Then the total strain is defined by :

$$d\{\xi\} = [D]^{-1}\ d\{\sigma\} + d\lambda\ \frac{\partial Q}{\partial \{\sigma\}} \tag{3.42}$$

$$W_p = \kappa = \int \{\sigma\}\ d\{\xi\}_p \tag{3.43}$$

where W_p is the total plastic work done.

Noting the equations (3.30), (3.33) and premultiplying equation

(3.42) by $\left\{\frac{\partial F}{\partial \{\sigma\}}\right\}$ [D] the plastic multiplier ($d\lambda$) is given by

$$d\lambda = \frac{\left[\frac{\partial F}{\partial \{\sigma\}}\right]^T [D]\, d\{\xi\}}{\left\{\left[\frac{\partial F}{\partial \{\sigma\}}\right]^T [D] \left[\frac{\partial Q}{\partial \{\sigma\}}\right]\right\} + A} = \frac{\{a\}^T [D] \{a\}\, d\{\xi\}}{A + ([\{a\}^T [D] \{a\}])} \qquad (3.44)$$

Then combining equations (3.43) and (3.44) together and eliminating $d\lambda$ identifies the elasto-plastic modulus matrix as:

$$[D]_{ep} = [D] - \frac{[D] \left[\frac{\partial Q}{\partial \{\sigma\}}\right] \left[\frac{\partial F}{\partial \{\sigma\}}\right]^T [D]}{\left\{\left[\frac{\partial F}{\partial \{\sigma\}}\right]^T [D] \left[\frac{\partial Q}{\partial \{\sigma\}}\right]\right\} + A} \qquad (3.45)$$

3.5 Non-linear Analysis

In the analysis discussed so far a linear form of stress-strain relationship had been assumed. Many problems of practical significance exist in which such linearity is not preserved and it is of interest to extend the numerical processes described to cover these. In this context we have a whole range of solid mechanics situations in which such phenomena as plasticity, creep etc. supersede the simple linear elasticity assumption.

These classes of problems can often be dealt with simply, without reformulation of the complete problem. If a solution to the non-linear problem can be arrived at by some 'trial and error' process in

which, at the final stage, the material constants are so adjusted that the appropriate new constitutive law is satisfied, then a solution is achieved.

Because a direct solution of the non-linear equation is extremely difficult, an iterative solution is adopted. There are two main forms of this trial and error method, both having their advantages and disadvantages. They are

(a) The Newton Raphson method, and
(b) The modified Newton Raphson method

3.5.1 Newton Raphson Method

In this method the computer makes an initial guess at the displacements by using the linear stiffness equation, with the stiffness value being that for the previous load conditions. A value of strain is then calculated for this guess for which there is a specified stress value given by the computer model of the strain/stress curve, as contained in the input data. The stress level actually existing due to the applied loads is then compared with the stress from the curve, and any difference is called the RESIDUAL.

If this residual value is within strict limits of acceptance then the process is finished, and the strains that have been calculated are adopted as the true strains that the mass had been subjected to. If however, the residual value falls outside the limits, then it updates the stiffness of the mass and another guess is made about the

displacements that occur, and the residual values again checked for the tolerance. The stiffness is updated for the calculation of each guesses and is taken as a tangent to the stress and strain graph at the point it previously considered.

As can be seen from Fig.3.8 this method converges quickly to an answer but due to the numerical methods involved and some of the stress/strain curves that have to be modelled, problems can occur that produce incorrect results or prevent the computer from actually reaching an answer.

3.5.2 Modified Newton Raphson Method

This process is almost exactly the same as Newton Raphson method, except that it uses the same stiffness value for all guesses. Information about each approximation is considered, thus allowing an improved result for the displacements each time, to enable the computer to converge towards an answer (Fig.3.9).

3.6 Convergence

A measure of convergence of the solution is required using the incremental/iterative solution algorithms eg. Newton-Raphson technique. The selection of appropriate convergence criteria is of utmost importance since an excessively tight tolerance may result in unnecessary iteration and consequent waste of computer resources, and a slack tolerance may result in incorrect answers. Therefore, effective convergence criteria used with a realistic tolerances are preconditions for accurate and economic solution.

The values used are very much a matter of experience. In general, with predominantly material non-linearity problems, large local residuals may be tolerated. The method of monitoring convergence within LUSAS considers five criteria :

(i) Euclidian Residual Norm

The Euclidian residual norm γ_Ψ is defined as the norm of the residuals as a percentage of the norm of the external forces and is written as :

$$\gamma_\Psi = \frac{||\{\Psi\}||_2}{||\{R\}||_2} \times 100$$

where $\{R\}$ is a force vector containing external loads and reactions and $\{\Psi\}$ signifies the residual of forces.Owing to the inconsistency of the units of displacement and rotation, only translational degrees of freedom are considered. For problems involving predominantly geometric non-linearity, a tolerance of $\gamma_\Psi<0.1$ is suggested. Where plasticity predominates, a more flexible tolerance of $1.0 < \gamma_\Psi < 5.0$ is suggested.

(ii) Euclidian Displacement Norm.

The Euclidian displacement norm γ_d is defined as the norm of the iterative displacements as a percentage of the norm of the total displacements and is written as :

$$\gamma_d = \frac{||\{\delta a\}||_2}{||\{a\}||_2} \times 100$$

As in the residual norm only translation degrees of freedom are considered. The criterion is a physical measure of how much the structure has moved during the current iteration. Typical values are:

$$0.1 < \gamma_d < 1.0 \qquad \text{(reasonable)}$$

$$0.001 < \gamma_d < 0.1 \qquad \text{(tight)}$$

(iii) Work Norm

The work measure is defined as the work done by the residuals on the current iteration as a percentage of the work done by the external forces on the first iteration.

$$\gamma_w = \frac{\{\Psi\}^T \{\delta a\}_i}{\{q\}^T \{\delta a\}_1} \times 100$$

$$1.0E\text{-}3 < \gamma_w < 1.0E\text{-}1 \qquad \text{(slack)}$$

$$1.0E\text{-}6 < \gamma_w < 1.0E\text{-}3 \qquad \text{(reasonable)}$$

$$1.0E\text{-}9 < \gamma_w < 1.0E\text{-}6 \qquad \text{(tight)}$$

(iv) Root Mean Square of Residuals

This criterion evaluates the root mean square value of all the residuals in the problem ie.

$$\gamma_\Psi = ||\{\Psi\}||_2$$

The criterion is dependent upon the units of the problem.

(v) Maximum Absolute Residual

This criterion limits the maximum absolute residual in a problem ie.:

$$\gamma_\Psi = \max[\ |\{\Psi\}|\ ]$$

The criterion is dependent upon the units of the problem. It is an extremely stiff criterion, which may be useful near bifurcation points of sensitive geometrically non-linear problems where large residuals may pollute the solution.

3.5 Frictional Gap Model

3.5.1 Theory

The frictional gap material model for joint elements provides frictional and gapping connection between nodes [40]. The frictional and gapping capabilities of the model only act on the translational degrees of freedom. Rotational degrees of freedom are always considered to behave linearly. The maximum forces in the local y and z direction are given by the compressive force in the local x direction times the coefficient of friction. If the gap is open all forces are set to zero.

The "strains" in the element are given by :

$$\{\xi\} = \begin{Bmatrix} \xi_x \\ \gamma_{xy} \\ \gamma_{xz} \end{Bmatrix} = \begin{Bmatrix} u_2 \\ v_2 \\ w_2 \end{Bmatrix} - \begin{Bmatrix} u_1 \\ v_1 \\ w_1 \end{Bmatrix} \qquad (3.46)$$

where u, v, w are the local displacements in the x, y, z directions respectively and $\{\xi\}$ is the strain vector. The corresponding stresses

are :

$$\{\sigma\} = \begin{Bmatrix} \sigma_x \\ \tau_{xy} \\ \tau_{xz} \end{Bmatrix} \tag{3.47}$$

The constitutive relationship is presented in figure (3.10). For elastic behaviour the constitutive relationship is given by:

$$\begin{Bmatrix} \sigma_x \\ \tau_{xy} \\ \tau_{xz} \end{Bmatrix} = \begin{bmatrix} K_x & 0 & 0 \\ 0 & K_y & 0 \\ 0 & 0 & K_z \end{bmatrix} \begin{Bmatrix} \xi_x \\ \gamma_{xy} \\ \gamma_{xz} \end{Bmatrix} \tag{3.48}$$

The shear limit τ_0 is generalized to a circle as :

$$(\tau_0)^2 = (\tau_{xy})^2 + (\tau_{xz})^2 \tag{3.49}$$

Thus the yield function is defined as

$$F(\tau, \sigma_x) = \sqrt{(\tau_{xy})^2 + (\tau_{xz})^2} - (\tau_0) \leq 0 \tag{3.50}$$

Decomposition of elastic and plastic strain gives

$$d\{\gamma\} = d\{\gamma\}_e + d\{\gamma\}_p \tag{3.51}$$

where :

$$\{\gamma\} = \begin{Bmatrix} \gamma_{xy} \\ \\ \gamma_{xz} \end{Bmatrix} \tag{3.52}$$

It is assumed that frictional slip is directed normal to the yield surface, thus :

$$d\{\gamma\}_p = d\lambda \left[\frac{\partial}{\partial\{\tau\}} \right]^T (\sqrt{(\tau_{xy})^2 + (\tau_{xz})^2} - \tau_0) = 2d\lambda\{\tau\} \tag{3.53}$$

where

$$\{\tau\} = \begin{Bmatrix} \tau_{xy} \\ \\ \tau_{xz} \end{Bmatrix} \frac{1}{\sqrt{(\tau_{xy})^2 + (\tau_{xz})^2}} \tag{3.54}$$

The variation in shear stress is related to the variation of the elastic component of strain as

$$d\{\tau\} = [D](d\{\gamma\} - d\{\gamma\}_p) \tag{3.55}$$

where

$$[D] = \begin{bmatrix} K_y & 0 \\ 0 & K_z \end{bmatrix} \tag{3.56}$$

Substituting from equation (3.53) gives

$$d\{\tau\} = [D](d\{\lambda\} - 2d\lambda\{\tau\}) \tag{3.57}$$

Differentiating the yield function (3.50) gives

$$dF = \frac{\partial F}{\partial \{\tau\}} d\{\tau\} + \frac{\partial F}{\partial \sigma_x} d\sigma_x = 0 \tag{3.58}$$

which can be written explicitly as

$$\{\tau\}^T d\{\tau\} - \tau_0 \frac{\partial \tau_0}{\partial \sigma_x} d\sigma_x = 0 \tag{3.59}$$

Substituting from equation (3.55) gives

$$\{\tau\}^T [D] d\{\gamma\} - 2d\lambda\{\tau\}^T [D]\{\tau\} - \tau_0 \frac{\partial \tau_0}{\partial \sigma_x} d\sigma_x = 0 \tag{3.60}$$

Rearranging gives the constant $d\lambda$ as

$$d\lambda = \frac{\{\tau\}^T [D] d\{\gamma\} - \tau_0 \frac{\partial \tau_0}{\partial \sigma_x} d\sigma_x}{2\{\tau\}^T [D] \{\tau\}} \tag{3.61}$$

Substituting into equation (3.57) gives

$$d\{\tau\} = [D]d\{\gamma\} - \frac{[D]\{\tau\}\{\tau\}^T [D]}{\{\tau\}^T [D]\{\tau\}} d\{\gamma\} - \frac{\mu \tau_0 [D]\{\tau\}}{\{\tau\}^T [D]\{\tau\}} d\sigma_x \tag{3.62}$$

It should be noted that the last term in equation (3.62) leads to an unsymmetric constitutive matrix, which is to be expected since friction is nonconservative. Neglecting the non-symmetric term in equation (3.62) gives the "elasto-plastic" constitutive relationship as :

$$d\begin{Bmatrix}\sigma_x\\ \tau_{xy}\\ \tau_{xz}\end{Bmatrix} = \left\{\begin{bmatrix}K_x & 0 & 0\\ 0 & K_y & 0\\ 0 & 0 & K_z\end{bmatrix} - \left[\begin{array}{c|cc} 0 & 0 & 0\\ \hline 0 & \multicolumn{2}{c}{\dfrac{[D]\{\tau\}\{\tau\}^T[D]}{\{\tau\}^T[D]\{\tau\}}}\\ 0 & & \end{array}\right]\right\} d\begin{Bmatrix}\xi_x\\ \gamma_{xy}\\ \gamma_{xz}\end{Bmatrix} \qquad (3.63)$$

If the shear stresses are zero then equation (3.63) becomes indeterminate. Under these circumstances the elastic constitutive relationship, equation (3.48), is used. If the gap is open the constitutive matrix is taken as zero.

3.5.2 Stress Evaluation

To allow for the initial gap the strains are modified according to

$$\begin{Bmatrix}\xi_x\\ \gamma_{xy}\\ \gamma_{xz}\end{Bmatrix} = \begin{Bmatrix}u_2\\ v_2\\ w_2\end{Bmatrix} - \begin{Bmatrix}u_1\\ v_1\\ w_1\end{Bmatrix} + \begin{Bmatrix}GAP\\ 0\\ 0\end{Bmatrix} \qquad (3.64)$$

If the direct strain ξ_x obtained from equation (3.64) is greater than zero then all stresses for the element is zero since the gap is open. The elastic stresses are evaluated from equation (3.48)

The shear yield stress is then evaluated from

$$\tau_0 = -\mu\ \sigma_x \qquad (3.65)$$

The effective stress level is evaluated from

$$\tau_{eff} = \sqrt{(\tau_{xy})^2 + (\tau_{xz})^2} \qquad (3.66)$$

If the "effective stress level" is greater than the shear yield stress then frictional slip occurs and the shear stresses are scaled according to

$$\begin{Bmatrix} \tau_{xy} \\ \tau_{xz} \end{Bmatrix} = \frac{\tau 0}{\tau_{eff}} \begin{Bmatrix} \tau_{xy} \\ \tau_{xz} \end{Bmatrix} \tag{3.67}$$

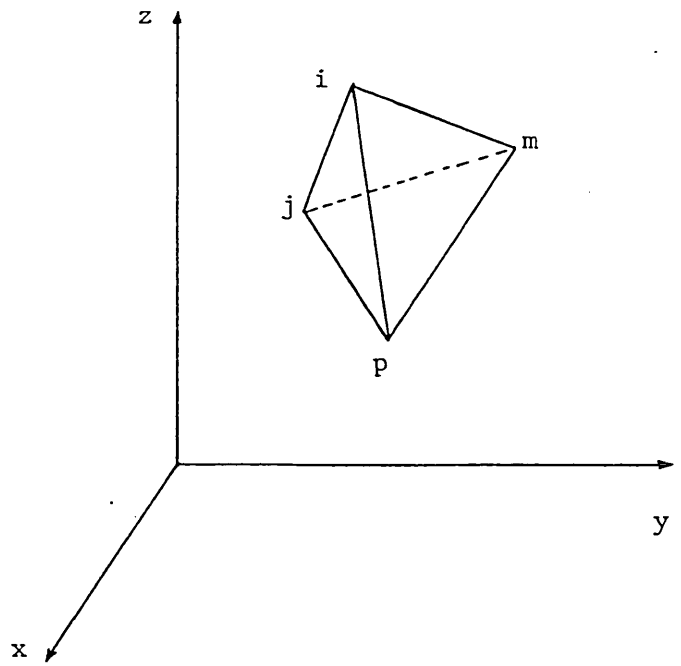

Fig. 3.1 Tetrahedral element i, j, m p in space defined by x, y and z direction (Reproduced from Ref. 37)

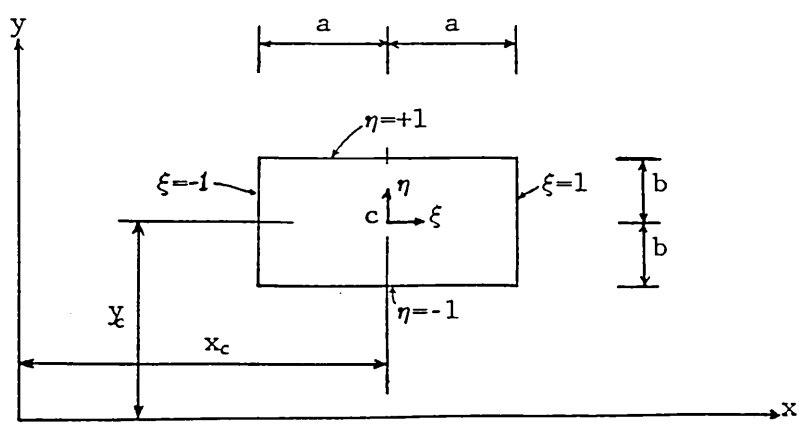

Fig. 3.2 Normalised coordinates for a rectangle (Reproduced from Ref. 37)

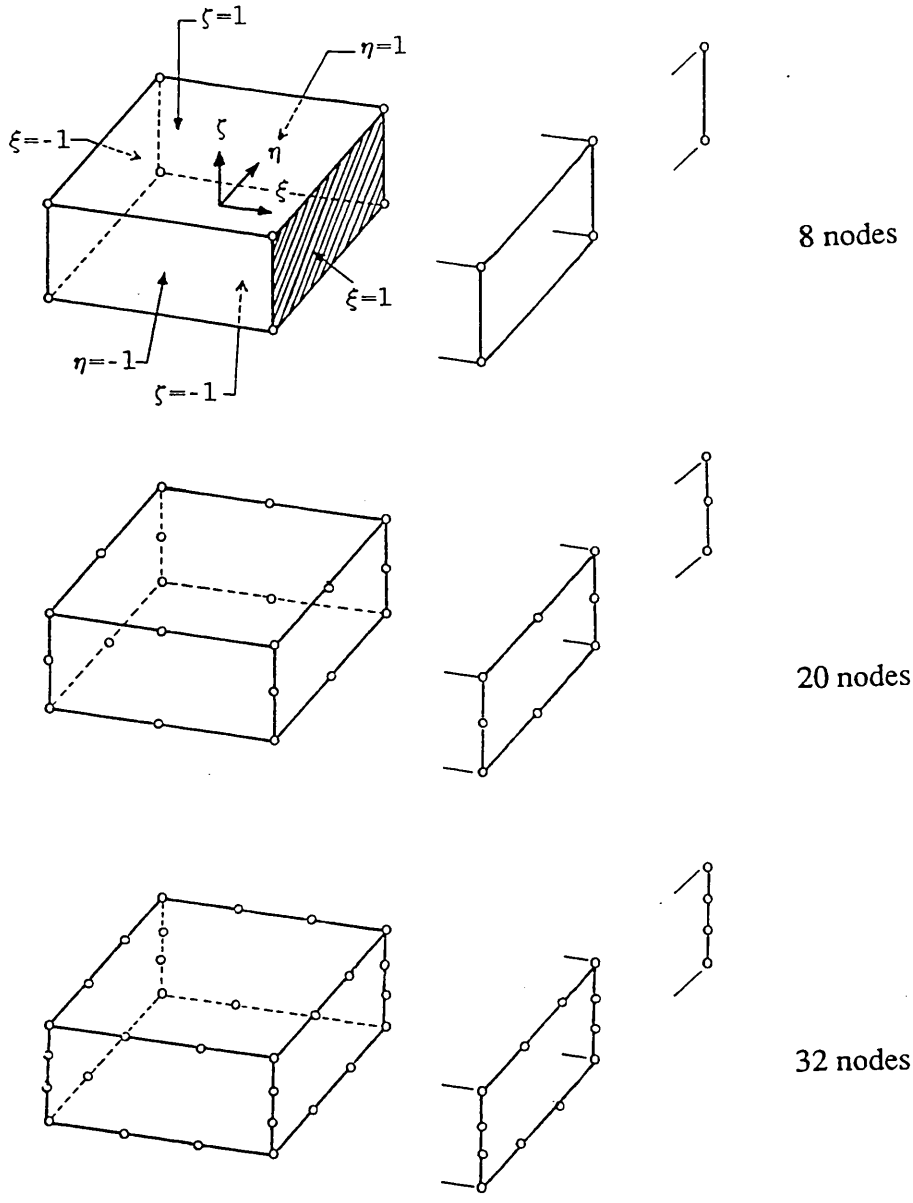

Fig. 3.3 Right prisms of boundary nodes (serendipity) family with corresponding sheet and line element (Reproduced from Ref. 37)

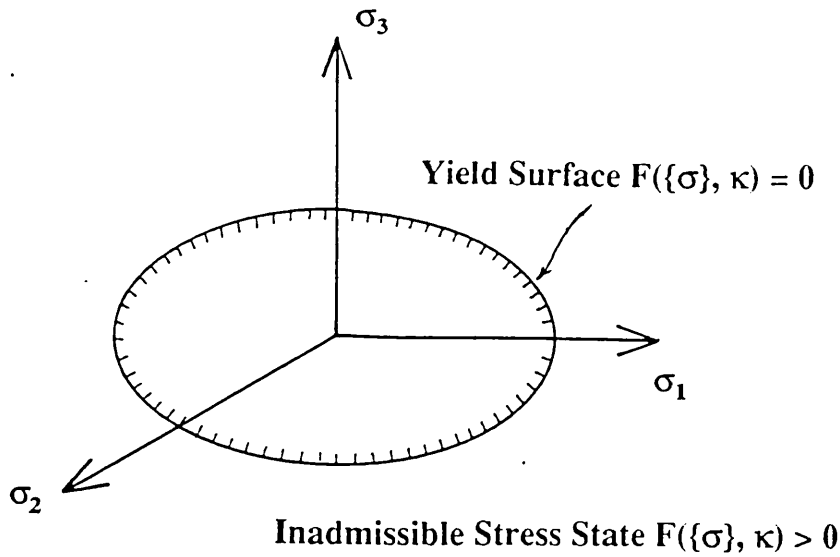

Fig. 3.4 Yield surface in the principal stress span (Reproduced from Ref. 39)

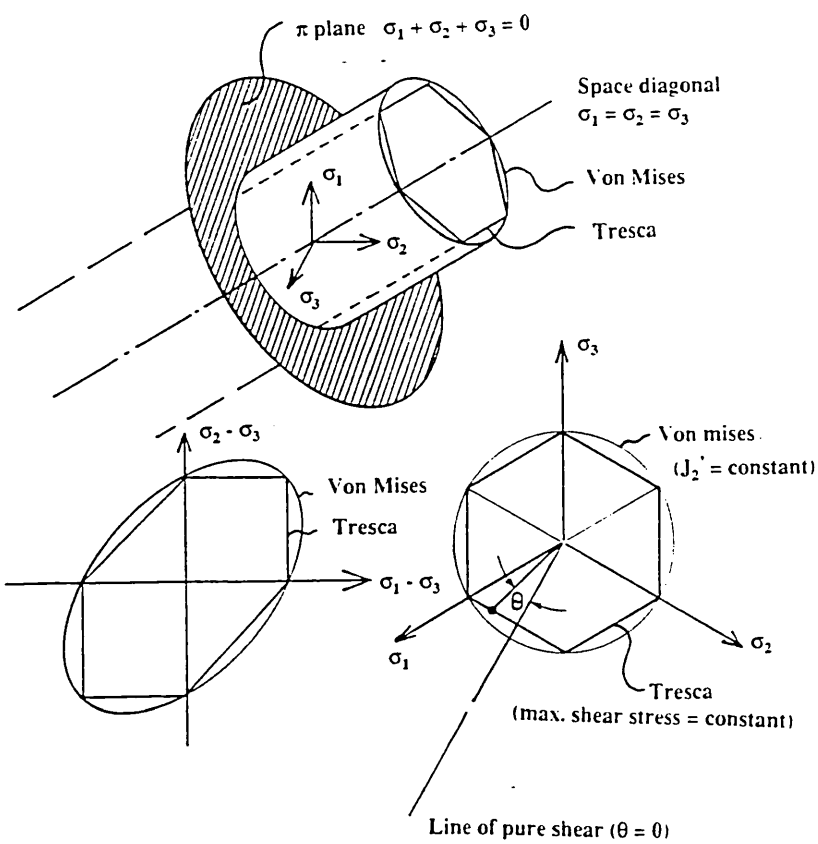

Fig. 3.5 Tresca and Von Mises yield criteria (Reproduced from Ref. 39)

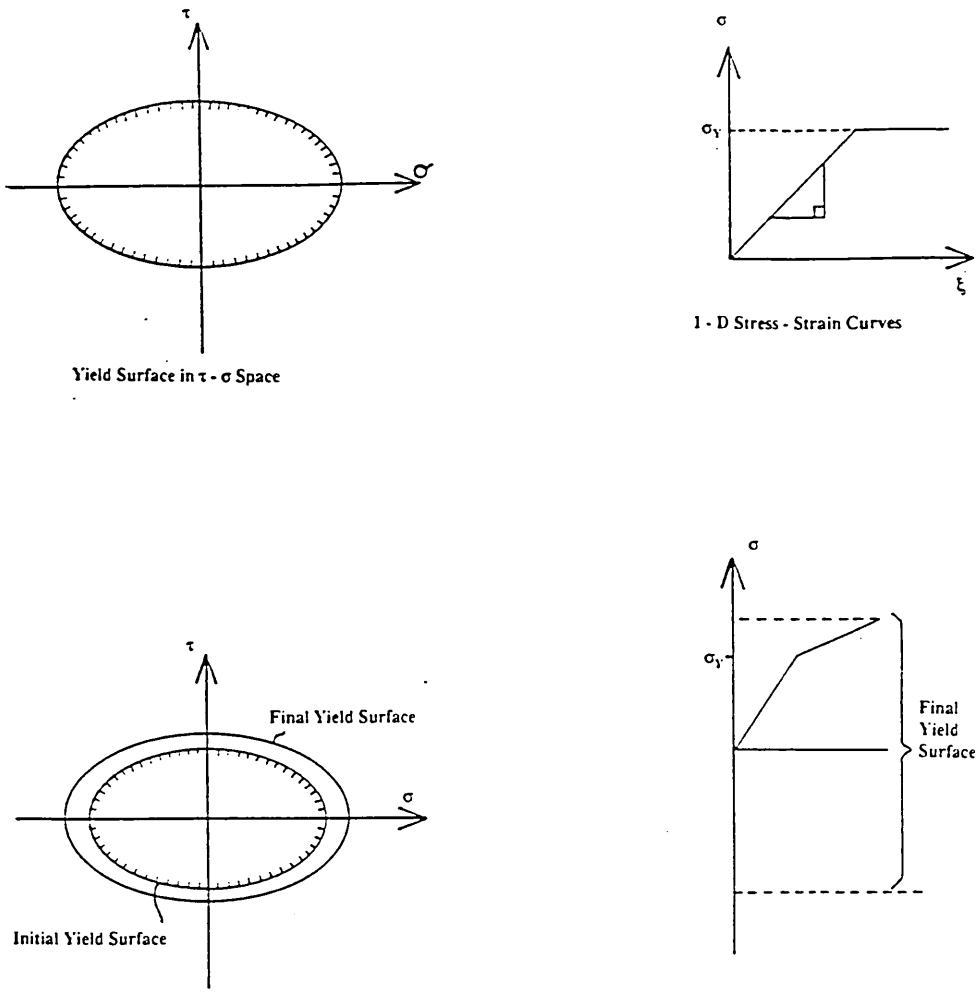

(a) Isotropic Hardening behaviour

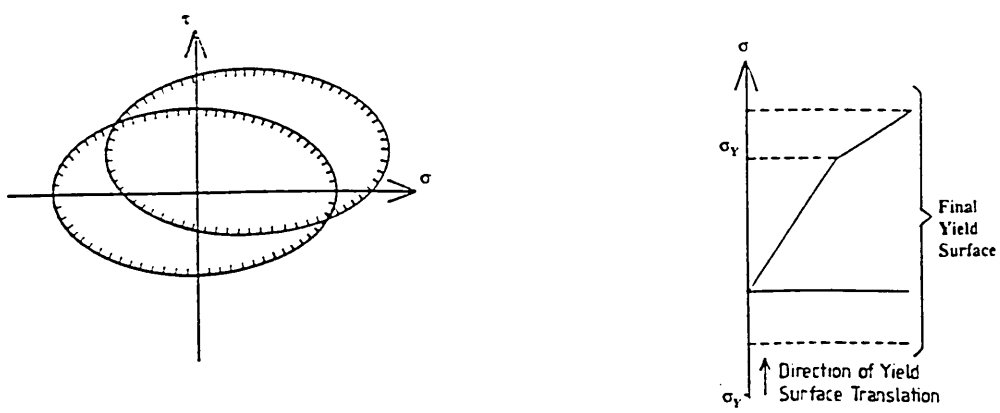

(b) Kinematic Strain Hardening behaviour

Fig. 3.6 Strain Hardening behaviour (Reproduced from Ref. 39)

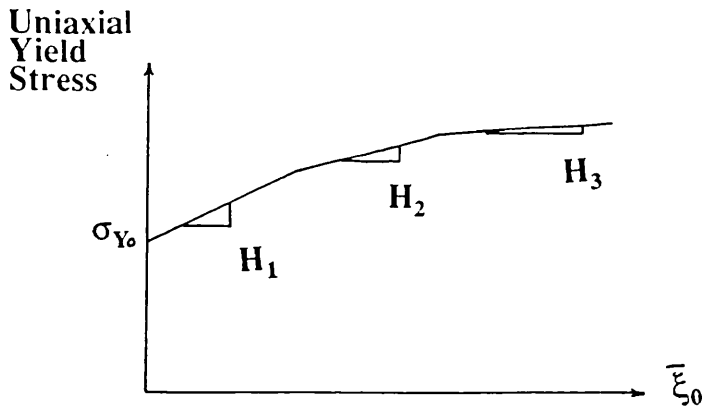

Fig. 3.7 hardening curve for Von Mises/Tresca criteria

(Reproduced from Ref. 39)

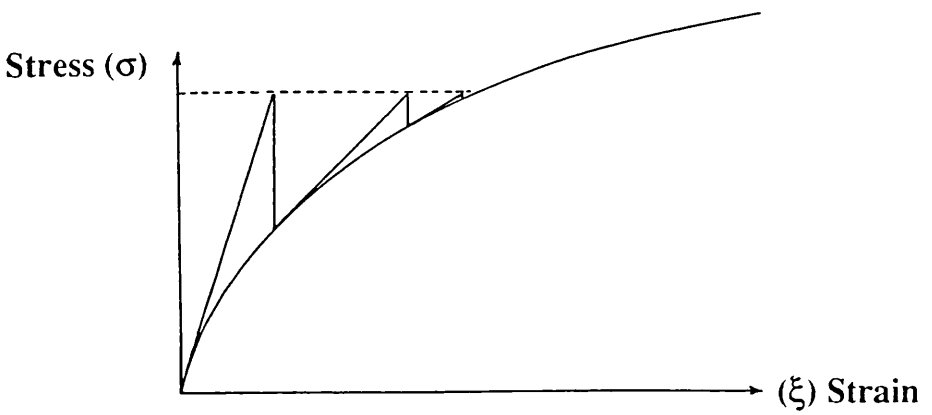

Fig. 3.8 Newton Raphson process (Reproduced from Ref. 39)

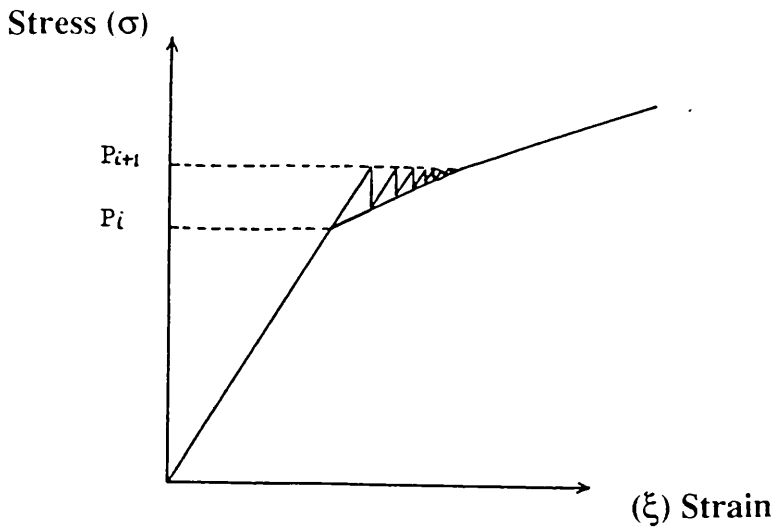

Fig. 3.9 Modified Newton Raphson process (Reproduced from Ref. 39)

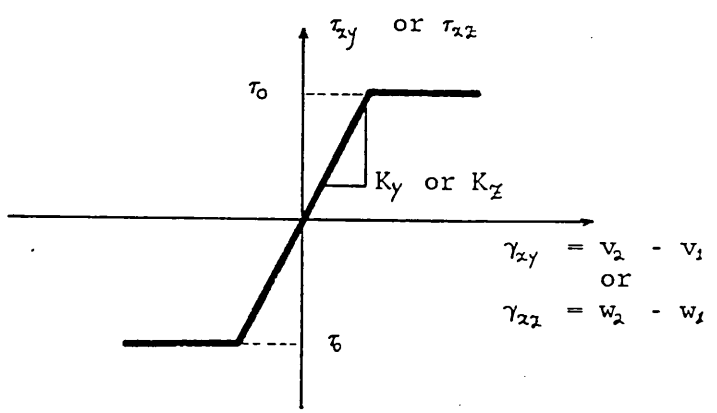

Fig. 3.10 Relationship between local y and x direction forces and strain (Reproduced from Ref. 39)

CHAPTER 4

Finite Element Modelling Of The Extended End Plate Connection

4.1 Introduction

The main objectives of the research project were to investigate the behaviour of extended end plate connections, and to formulate design criteria for this type of joint. The design process should account for certain requirements, such as strength, rotation capacity and stiffness for a satisfactory connection performance. In order to quantify the above parameters, the moment-rotation curves for this type of connection must be available. Thus the ability to produce with adequate accuracy the moment-rotation curves of the connection which takes account of the non-linear nature of joint behaviour is of paramount importance. This necessitates an understanding of the very complex interaction between the member components, connection components and the fasteners ie; column, beam, bolts and welds in the elastic as well as plastic states.

Since 1900, researchers have adopted various methods including full scale testing and curve fitting of experimental data, behavioural analogy and semi-emperical techniques and finite element analysis for the determination of the moment-rotation behaviour of semi-rigid connections. Although full scale testing and curve fitting of

data can provide an insight into joint characteristics and as a method of predicting moment-rotation curves can be extremely accurate , its use is limited to the range of available data. Whilst the final product of this method fails to recognise the contribution of all individual components towards the overall joint response, it might be neither physically nor economically feasible to expand the data to cover all influencing parameters.

Popular design methods based on behavioural analogy were derived using the yield-line method[19, 20]. While these methods had served to calculate the ultimate load capacity of the joints, they failed to calculate deformation as a continuous function of load. They are therefore unsuitable for predicting the moment-rotation characteristics of semi-rigid connections. A realistic approach for a comprehensive analysis of connection response must include elastic and plastic behaviour. The theoretical analysis must also be capable of predicting the bolt forces, since they are crucial in the connection design. It must also identify the force-deformation relationship of each component ie; column(flange and web), end plate and bolts since joint flexibility is dependent on the behaviour of individual parts. The development of interacting forces further complicates the analysis. In view of the above complexities the finite element technique represents the most suitable tool presently available for conducting such exhaustive investigation.

Recently, the finite element method has been extensively used to investigate the behaviour of end plate connections, which is the product of interaction between

various components. It has been established that most of the connection rotation originates from three separate sources ie; deformation of end plate, deformation of column(flange and web) and extension of bolts. Researchers[31, 32] have used the finite element method to analyse these components independently and determine the overall connection response from superimposition of individual member deformation. However, this method of analysis ignores the interaction of different parts and the resulting prying forces. Although it is widely recognised that moment transmitting extended end plate connection behaviour is highly non-linear and three dimensional in nature with bi-axial bending of plate, the bulk of the investigations have been carried out by two-dimensional finite element analysis. Whilst a three dimensional analysis is much more complicated and is a lot more demanding in respect of computer time and size, it enables a realistic and meaningful solution to this extremely complicated problem.

4.2 Modelling Criteria

The important aspects of this analysis include an examination of the overall response of the unstiffened extended end plate connection over the entire elastic-plastic range until failure occurs, the prediction of moment-rotation characteristic of the joint, magnitude and position of interacting forces and magnitude of bolt forces. It is also intended to single out the contribution of different components, since the capability of assessing the contribution made by each joint member is important for the development of suitable design method for the connection.

In order to study the behaviour of unstiffened extended end plate connections the LUSAS (London University Structural Analysis System) finite element software package was used. LUSAS [41] is a general purpose engineering analysis system which incorporates facilities for linear and non-linear, static or dynamic stress analysis. This system is based on the finite element displacement method of analysis and contains a comprehensive range of elements and solution procedures. The model representing the unstiffened extended end plate connection incorporates the following LUSAS element types:

(i) **HX16** This is a three dimensional isoparametric thick shell element capable of modelling curved boundaries, Fig.(4.1a) This element comprises 16 nodes with three degrees of freedom u, v, w at each node. Its formulations are based on the standard isoparametric approach which uses the same interpolation functions to define the element shape or geometry as well as the field variables within the element.

(ii) **BRS2** This is a straight isoparametric bar element in three dimensions which can accommodate varying cross-sectional area, Fig.(4.1b). It includes two nodes with three degrees of freedom u, v, w at each node. The axial force along the length is constant for this element.

(iii) **JNT4** This is a three dimensional joint element which connects two nodes (not necessarily coincidental) by three springs in the local x, y, z directions, Fig.(4.1c). This element has four nodes with

three degrees of freedom at each of the two active nodes while the third and forth nodes are passive nodes used only to define the element's local x-axis and the xy-plane.

Symmetry of the connection configuration and the load resisted by the joint about both the major and minor axes permits the analysis of only a quarter of the entire connection Fig.(4.2). The finite element model incorporates HX16 solid elements for plates, BRS2 bar elements for bolts and JNT4 joint elements for the interactive forces generated between the end plate and column flange. A length of column equal to three times the depth of the beam is considered in the model. It is assumed that most of the column deformation is limited to this length. The column web, column flange and end plate are modelled such that there exist corresponding nodes on the column flange for every node on the end plate as shown in fig.(4.3), and column web and flange share common nodes at their junction. The two corresponding nodes for the column flange and the end plate are connected to each other by two bar elements, BRS2, at the centre of tension bolt holes and joint elements, JNT4, at other locations. The joint elements employed have non-linear properties with infinite (very large) stiffness in compression and zero stiffness in tension. This ensures displacement compatibility at nodes where end plate and column flange are in contact but allows separation at all other nodes except at the tension bolt locations. Friction between column flange and end plate is ignored and the only degrees of freedom that are made compatible between the bodies are lateral displacements. The contribution of the beam towards the rotational stiffness of the connection is small and is not considered. However, its

contribution towards the bending behaviour of the end plate is recognised and included in the model. A short length of the beam is incorporated in the model with artificially high modulus of elasticity to ensure that the boundary of the end plate, where it is connected to the beam flanges and web, remains in a plane at all times.

In view of the complexity of the problem and in order to achieve economy in computer time and space several simplifying assumptions are made in modelling the extended end plate connection. The bolts in the compression region are not included in the model, since they do not contribute towards the moment resistance of the connection and are meant to transmit shear only. The weld and the changes in yield stress of steel in the heat-affected zone caused due to welding are ignored. Also no consideration is given in the model to account for the fillets in the column. On the same economic consideration bolt holes are not considered in the model. It can be argued that exclusion of bolt holes will affect the rigidity of the model and create a void in the understanding of their effect on the end plate and column flange in the immediate vicinity of the hole. However, since the welds and stress changes in the heat affected zone of the end plate are ignored in this study, this will compensate for the increased stiffness of the connection due to lack of bolt holes.

In simulating the response of extended end plate connection, it is generally agreed that the moment acting at the beam end can be replaced by a couple whose forces act at the level of the beam flanges. Hence the loads were applied to this structure at nodal points of beam flanges as shown in Fig.(4.4). The accuracy of higher order

finite element analysis is attributed to proper allocation and consistent distribution of nodal forces. Consequently, to attain greater precision, the unnatural but consistent nodal force distribution ratios proposed by Zienkiewicz [37] were adopted as shown in Fig.(4.5).

4.3 Finite Element Mesh Generation

For the purpose of comparing the results of the finite element analysis with the experimental results, the prototypes for the basic models were chosen to be the actual unstiffened extended end plate connections, fabricated as part of the experimental investigation carried out by the author. The experimental details of the connections are given in Chapter 6. Three connection set-ups (254x254x132 UC, and 305x165x54 UB with 15mm end plate; 254x254x89 UC and 406x178x74 UB with 15mm end plate; 203x203x60 UC and 305x127x48 UB with 12mm end plate) were modelled and represented by three-dimensional isoparametric elements. Taking advantage of symmetry the models of only a quarter of the whole connection are shown in Figs.(4.6), which illustrate the subdivision of column, end plate, beam and their boundary conditions.

4.4 Bolt Representation

It is commonly assumed that the moment acting at the beam end can be replaced by a couple whose forces act at the level of beam flanges and are given by:

$$F_t = F_c = \frac{M}{D}$$

These forces are transferred through the plate and act on the column flange. The tension component F_t of the beam moment is carried primarily by the tension group of bolts while the compression component F_c is carried by bearing acting over an area near the bottom of the connection. Therefore compression bolts only act as shear pins, carrying a negligible amount of axial load. For practical end plate thickness the latter will also bear on the column flange near the top of connection. As a result prying force will develop which increases the force carried by the tension bolts.

A reliable prediction of connection behaviour depends on a number of factors including a knowledge of the load elongation characteristic of bolts. It is therefore necessary to include the bolts in the finite element model of an extended end plate connection.

The tension group bolts were represented by two-noded bar elements which are connected to the nodes on the inside surface of the column flange and the outside surface of the end plate along the longitudinal axis of the bolt, as shown in Fig.(4.7). While high strength friction grip or grade 8.8 bolts were used with a small amount of pretensioning in the test programme, in the mathematical model the bolts were assumed to be without any pretensioning.

4.5 Boundary Conditions

As stated previously the finite element model represents a quarter of the whole connection. Therefore, appropriate assumptions with regard to boundary conditions are essential. In the model only half of the actual thickness of the column web is considered. Since the web is subjected only to in-plane action, all the nodes situated in the column web and lying in the yz plane, through the web centreline are allowed vertical and horizontal in-plane displacements (y and z direction). Thus out-of-plane displacements and rotations in the outer plane of the web are restrained. Also at the column mid-depth all the nodes in the xy plane of symmetry are restrained in all directions. For the nodes in the column flange, end plate, beam flanges and web which lie in the yz plane of symmetry through the column web centreline, the horizontal displacement in the x direction is restrained.

4.6 Material Properties

The response of the end plate connection is controlled by the behaviour of its components and their interaction. Although finite element technique provides the most suitable means for a comprehensive investigation of their behaviour, the accuracy of such an investigation can only be relied upon if correct and relevant information has been utilized. One of the most influential parameters which affects the joint's response is the mechanical characteristics of each member. It is therefore

essential to distinguish and include the various material properties of each component within the theoretical analysis.

As stated previously, each connection model comprises beam section, column section, end plate and bolts (grade 8.8 or H.S.F.G). Although grade 43A steel was used for all members, welding the end plates to beam sections alters their material properties in the immediate vicinity of the welded area (Heat Affected Zone) and creates residual stresses in that region. These changes result from high temperature variation during the welding process which affects the microstructure of the steel. Although, there is no established law governing the mechanical properties of the heat affected zone, there is an increase in the yield point and ultimate strength of the material in that region. The extent of such increases are dependant upon the material composition, heat input, cooling rate, etc. Tong [33] found that the yield stress in the HAZ is about 18% greater than the parent metal. The weld and its effects have not been considered in these analyses in order to satisfy the need for economy in computer resources. Also the absence of bolt holes in the finite element models will result in higher rigidity of the connection which is expected to compensate for the loss of rigidity as a result of neglecting the weld and HAZ. Similarly, the residual stresses are omitted since the results of the studies by Wilson and Ho [42] show that:

(1) Residual stress significantly affects only those phenomena that occur under a low applied stress, such as brittle fracture and stress corrosion cracking.

(2) As the level of the applied stress increases, the effect of residual stress decreases.

(3) The effect of residual stress on the performance of a welded structure is negligible when applied stress has been increased beyond the yield point.

(4) The residual stress tends to decrease as the structure is subjected to a repeated loading.

Therefore, homogeneous material properties were assumed for end plate and column section. For the beam elements artificially high values of yield stress and modulus of elasticity were chosen to prevent any bending deformation of the beam.

In order to produce the necessary data for a non-linear analysis in LUSAS (ie. modulus of elasticity, yield stress and gradient of the local tangents in the plastic region) a series of tensile tests were carried out for grade 43A steel plate cut from test specimens, grade 8.8 and H.S.F.G. bolts. For grade 43A steel four suitably shaped test pieces were gripped in tensile testing machine and subjected to an increasing force at constant rate, until fracture occurred. Continuous readings were taken of the force required to produce the measured extension of the test pieces. The four resulting load-elongation graphs were averaged to limit or possibly eliminate the effects of the various types of defects present in the industrial steel including cracks, pores, etc. Hence an average stress-strain graph was produced for the steel. In the elastic range grade 43A steel was found to have a modulus of elasticity of 197 kN/mm^2 and yield stress of 285.5 N/mm^2. Thereafter, the material response was approximated with the continually varying local tangents to the curve. These tangent moduli are characterised in LUSAS by their gradient and the limit of the effective plastic strain up to which the tangent is valid as shown in Fig.(4.8). The same procedure was

followed for grade 8.8 and H.S.F.G. bolts which resulted in the calculation of modulus of elasticity of 178.7, 186.6 kN/mm^2 and yield stress of 541.1 and 620.7 N/mm^2 respectively.

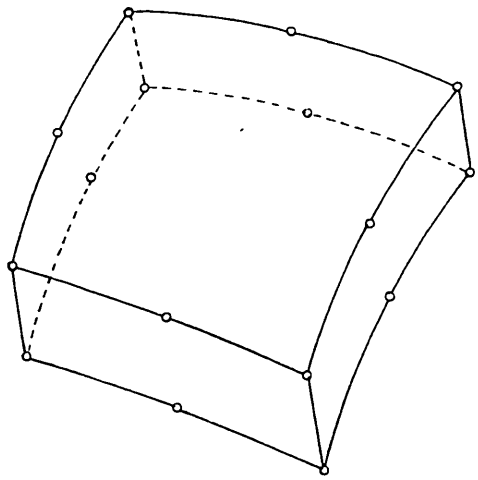

(a) HX16 Element

(b) BRS2 Element

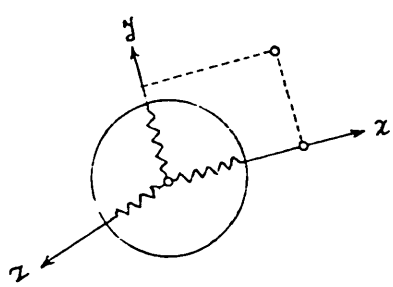

(c) JNT4 Joint element

Fig. 4.1 Element types used in the model (Reproduced from Ref. 39)

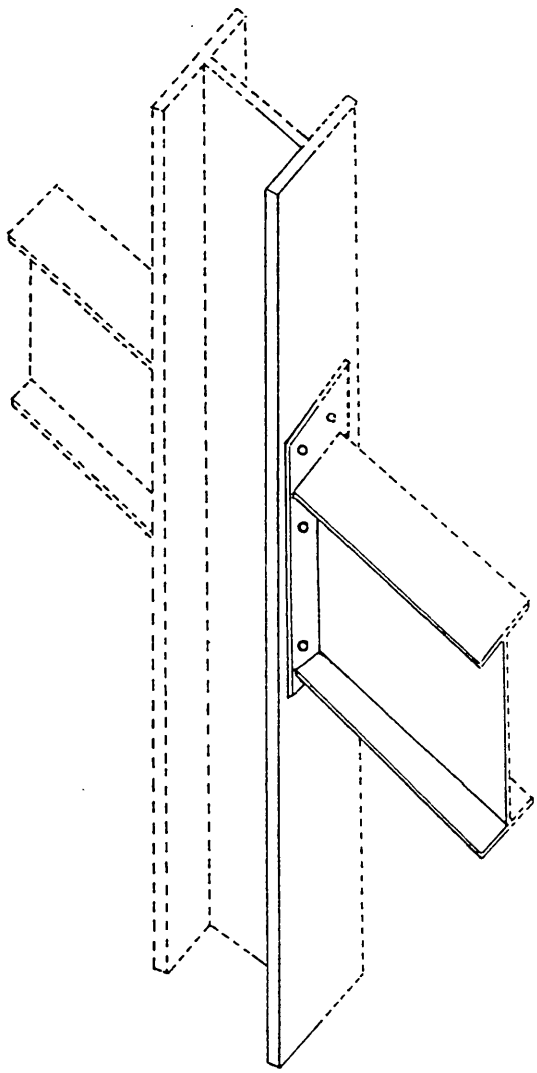

Fig. 4.2 Area of the connection considered in the finite element modelling

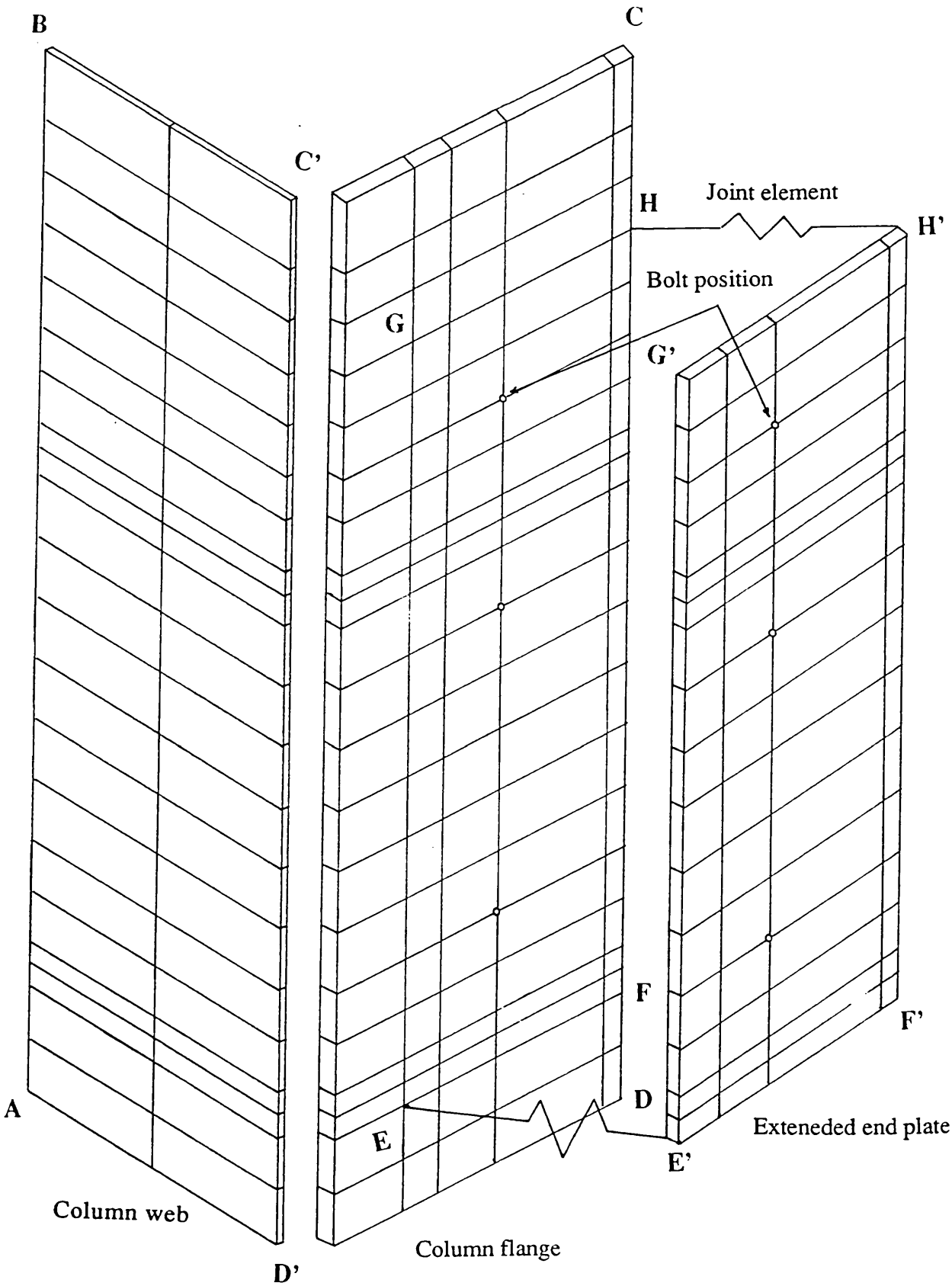

Fig. 4.3 Position of joint elements to model the interaction of end plate and column flange

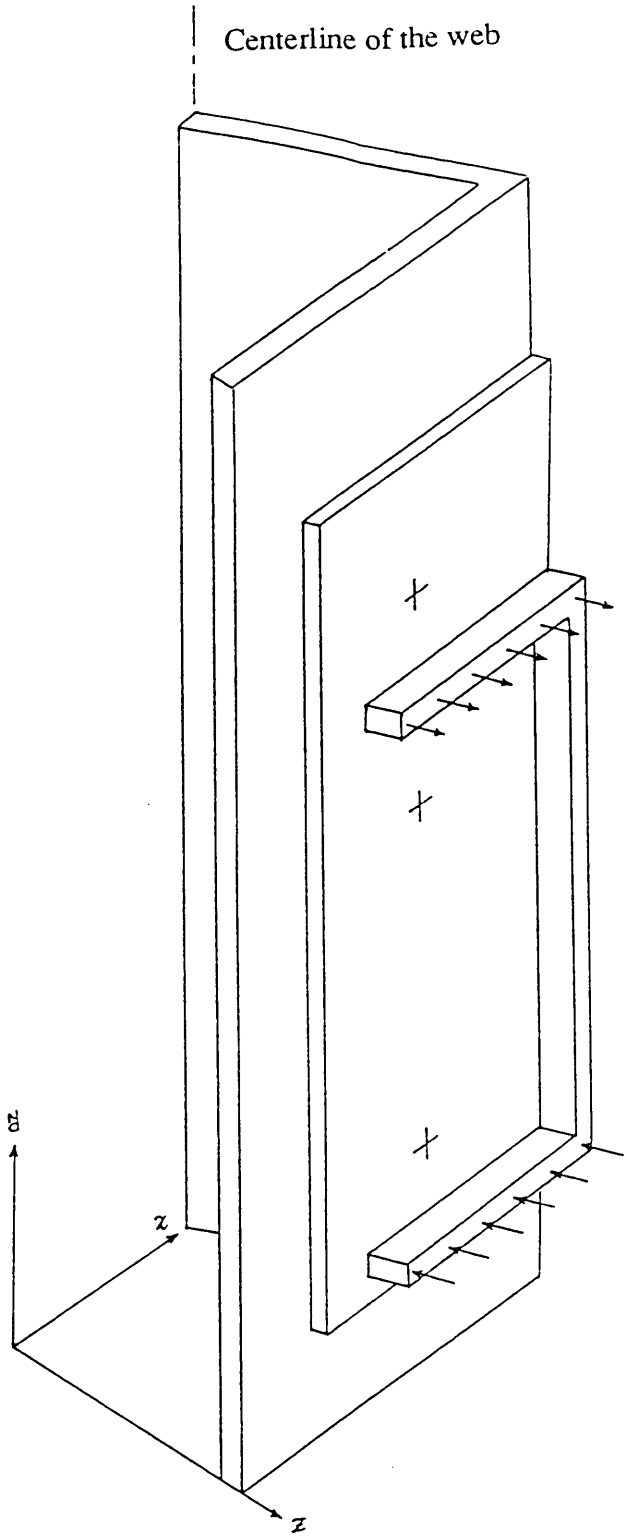

Fig. 4.4 Force applied to the extended end plate connection

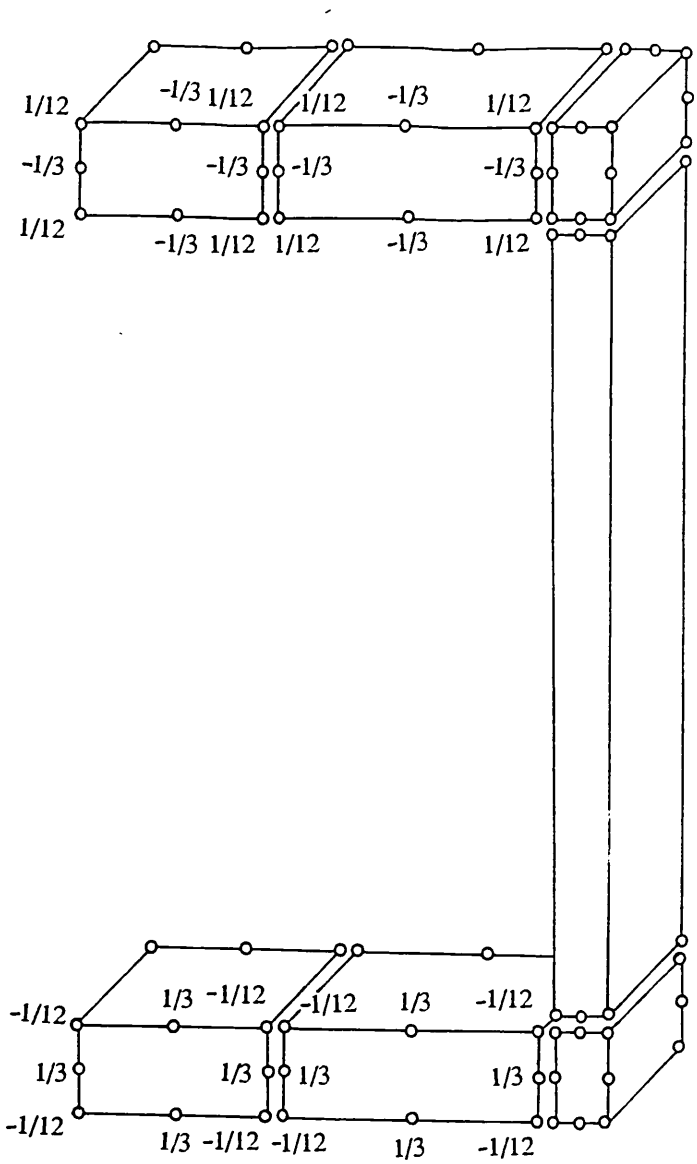

Fig. 4.5 Force distribution factors proposed by Zienkiewicz for nodal forces

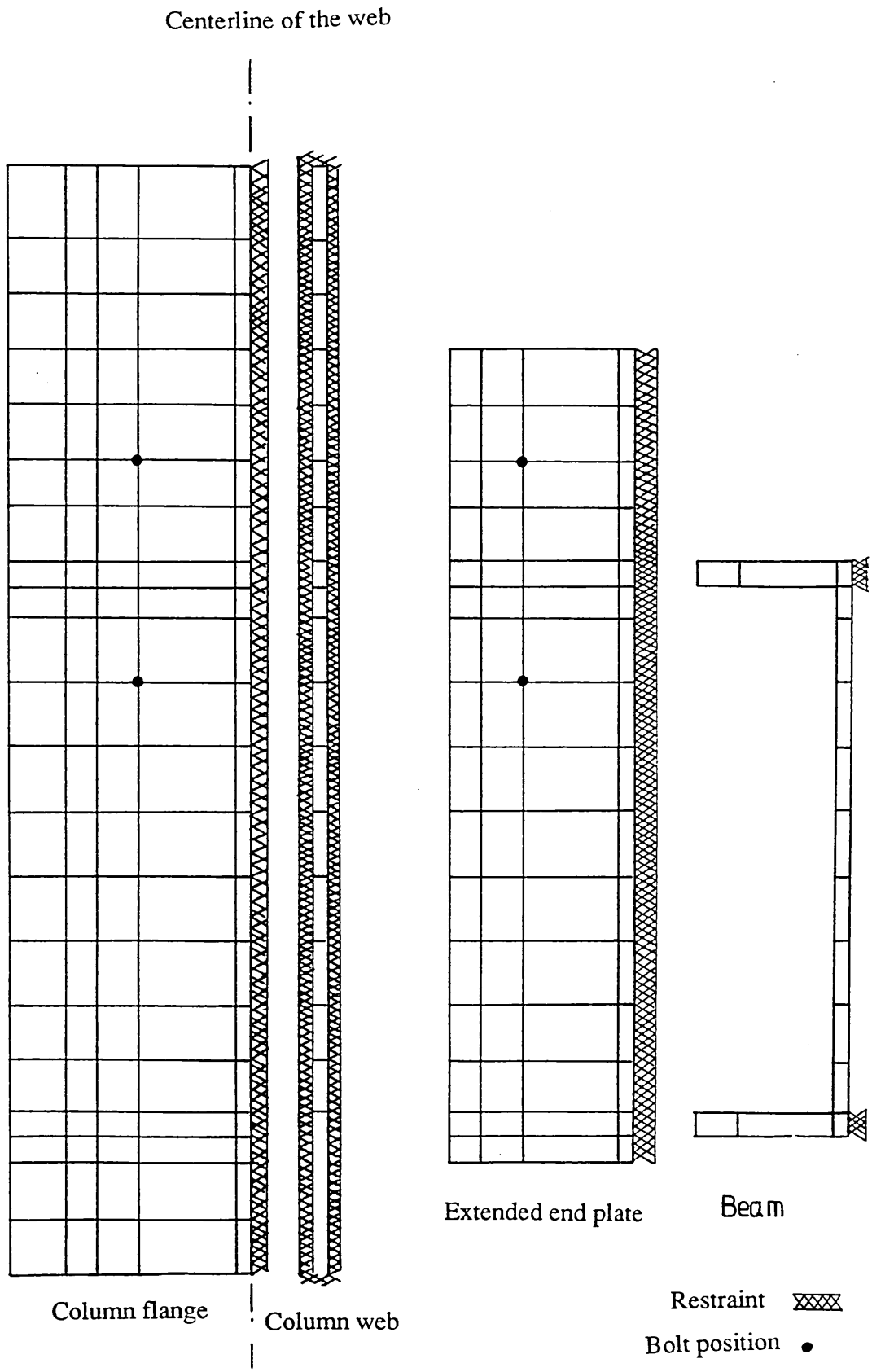

Fig. 4.6 Finite element mesh for extended end plate connection

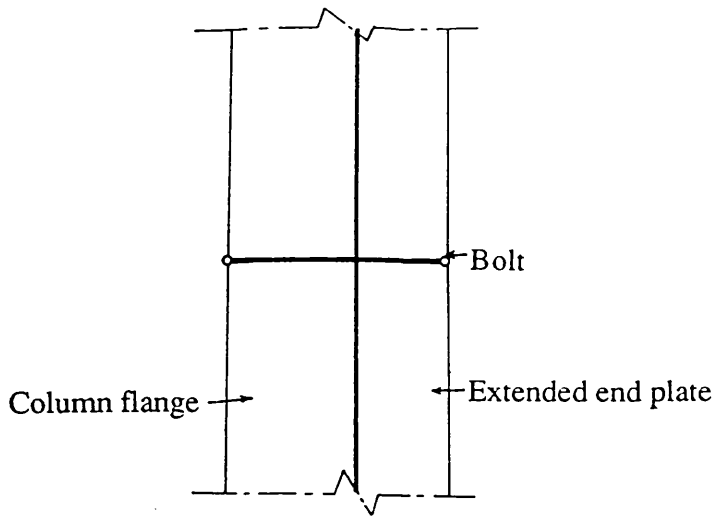

Fig. 4.7 Bolt representation in the theoretical model

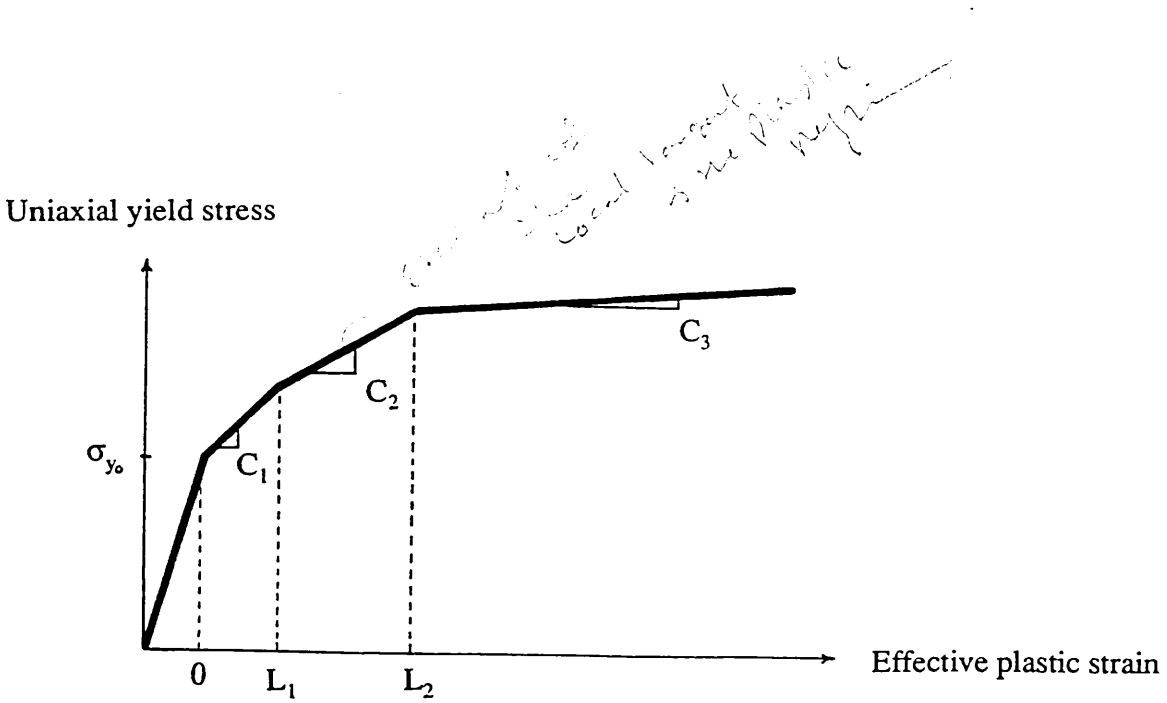

Fig. 4.8 Stress - Strain relationship for non-linear material model

CHAPTER 5

Moment-Rotation Characteristics

5.1 Introduction

Connection is a medium through which forces and moments are transmitted from one member to another and its stiffness and strength can influence the response and stability of the steel structure. Therefore, the joint behavioural characteristics are of great significance which should be correctly ascertained and incorporated in the analysis and design of the structure. Traditional approach to joint design disregards the actual connection behaviour and assumes the ideal models of perfectly rigid or pinned connections. Although the use of these idealized joint behaviour greatly simplifies the analysis and design procedure, the predicted response of the frame may not be realistic as most connections used in actual practice transmit some moment and experience some rotational deformation upon loading. The ideally pinned and fully rigid joint assumptions represent only extreme conditions which are rarely encountered in real structures. There is a need for a more realistic design approach based on the actual performance of the connection.

If semi-rigid nature of the practical connection types is to be correctly allowed for, the moment-rotation characteristics of such connections must be available. Such

characteristics express the rotational deformation of the connection as a function of the moment acting at the connection. When a moment M, is applied to a connection it rotates by an amount θ which represents the change in angle between the beam and column from its original configuration. The moment-rotation curves, spread over a large spectrum for very flexible to fully rigid joints, can be used as a means of distinguishing between different classes of behaviour as well as featuring in the actual design calculations. Thus a knowledge of the moment-rotation curves and the ability to predict them are of outmost importance. Early studies of the joint behaviour relied upon test data as the most appropriate means of determining the moment-rotation curves. However, recent attempts to assemble these data into a usable collection indicated that only a patchy coverage will ever be available[43]. Although careful study of these test data and selective additional testing can ensure that their value is maximised in terms of interpolation between cases, identification of similarities etc, comprehensive coverage requires the availability of the analytical techniques that can be used to predict the moment-rotation behaviour and generate parametric studies. Numerous attempts have been made to provide a suitable analytical approach for producing the response of the connections but they only considered some of the characteristic parameters defining the moment-rotation curves. This could also be true with finite element techniques since previous researchwork mostly considered the two dimensional aspects of the beam-to-column connection and was mainly limited to the analysis of isolated plates. Nevertheless this technique is suitable for predicting the overall connection behaviour as well as the contribution of individual components. It

allows both in plane and out of plane response to be simulated with a high degree of accuracy including the representation of large strain and/or displacements and accounts for spread of plasticity over the surface and through the thickness as well as for strain hardening and instability effects.

5.2 Moment Rotation Curves for Extended End Plate Connections

Extended end plate connections are usually designed to resist both bending moments and shear forces. It has however been shown by earlier research [3] that the effect of shear on the moment-rotation characteristics is negligible. Hence the present investigation is confined to the performance of the joint when subjected to bending only. The scope of this study is limited to the analysis of extended end plate connection using only four tension bolts forming two rows adjacent to the tension flange of the beam. It is known[34] that additional bolts within the web area will not contribute significantly to the bending strength of the connection. The centre of compression of the moment couple on the connection is located at or near the compression flange. The tension component of the couple resisting moment is carried by connection bolts, loaded predominantly in direct tension. High strength bolts are capable of transmitting high shear forces, and act more efficiently in tension and as such are ideal for use in end plate connections. One disadvantage associated with the use of high strength bolts in tension is that high yield stress has been achieved in the bolt material at the cost of some loss in ductility. This is of great importance in ultimate limit state design where local ductility is relied upon to bring about

redistribution of moments in framed structures. As mentioned earlier the rotation of the connection is mainly due to the extension of the bolts, flexure of the end plate and the deformation of the column flange.

The deflection of the end plate at the beam tension flange position obtained by finite element method is the transverse displacement ab related to the undeformed beam shown in Fig. 5.1. This deformation resulted from the contribution of the bolts, end plate and column flange. If the point of the rotation is assumed to be at the mid-depth of the compression flange the rotation can the be obtained by the following relationship:

$$\theta = \frac{ab}{D - T}$$

where:

D is the depth of the beam; and

T is the thickness of the beam flange.

The end plate may be subdivided into two parts, one the end-plate between the beam flanges and other the extension plate. When the extension plate becomes plastic the end-plate between the beam flanges still remains elastic. At this stage the moment-rotation relationship is solely controlled by this part of end plate. Structural failure occurs when this portion becomes fully plastic.

Experimental results suggest that the forces in the tension bolts are not equally or linearly distributed between bolts. The distribution of this force among the bolts is dependent on the ratio of end plate and column flange thicknesses. If the end plate and column flange were infinitely stiff a linear load distribution would be imposed on the bolts, the outer bolt row carrying a large proportion of the load. Prying forces would of course be absent. However, as the end-plates have finite thickness, their inevitable flexibility produces a redistribution of load. The plate below the beam tension flange is stiffer than that above and consequently the bolts supported by it have more of the direct load transferred to them. At the same time the flexibility of the extension plate generates prying forces due to which additional forces are induced in the tension bolts. The force distribution within the bolt group is a complex problem which is further complicated by the presence of prying forces produced by end-plate flexure.

It is therefore evident that in addition to direct tension the bolts are subjected to additional forces due to prying action brought about by flexure of the end-plate. This secondary factor must be accounted for in the moment-rotation characteristics studies and in any design method. This prying action increases the forces in the bolts and helps in developing the maximum strength of the plate by forcing it into double curvature.

In previous research [25, 26, 31, 32] it can be seen that there has been a lot of simplifying assumptions about the location and magnitude of the prying forces. The prying forces

which develop and change position during loading are very difficult to determine accurately. In recent years new developments in finite element (i.e. nonlinear joint element) have made it possible to calculate the exact position and amount of prying force at each loading stage which will be discussed in chapter 7.

5.3 Unstiffened Column Flange Deformation

Earlier analytical methods were based on the assumption that the moment-rotation characteristics exhibited by the connected parts were caused predominantly by the flexure of the end plate. Even though the column flange deformation was taken into account in some of the methods, the forces on the column flange were derived form the principal assumption stated above.

As mentioned before, tension forces act on the column flange at the bolt locations in the tension region and compression forces act over some bearing zone in the compression region. The critical design considerations for the compression region of the column occur in the column web and the area over which the load is transferred from the end plate to the column flange. In the tension region it occurs primarily in the column flange. The mode of failure can be either by buckling of the column web or by material yielding of the column web in the compression region, and by yielding of the column flange in bending about the column web in tension region. These can occur when there are compressive line load acting over flange effective width in the

compression region, and concentrated bolt forces acting some gauge distance apart in the tension region.

Most of the investigation carried out in this country have been based on the assumption that column flanges and web are very stiff, and do not deform. In 1961 Sherbourne [15] conducted an experimental investigation of beam-to-column end plate connections that focussed on the ability of columns, with or without stiffeners, to develop the full plastic moment capacity of the connecting beam. It was concluded that a nominal amount of stiffeners was required in column with thin flanges. It was further concluded that too thick an end-plate might seriously restrict the rotation capacity of the connection and may also reduce the connection strength by imposing an elastic stress distribution in the bolts of extended end plate connections. Bolt tension failure of the outermost bolts could occur, since high strength bolts could not deform plastically and equalize forces within bolt groups. This can be prevented only by permitting plastic deformation to occur in the end plate.

Tarpy and Cardinal [26] conducted a series of tests with various configuration, in order to determine the effect of the end plate forces on the column flange and web. The end plate thickness ranged from 1.5 to 4 times the column flange thickness. Some of the tests were identical but with column stiffeners included at the tension and compression regions. They produced formulas for maximum transverse displacement

of column flange and average stress at the toe of the fillet in the tension region of column flange by two dimensional elastic finite element analysis.

In most steel connections the relative dimensions of the joint components make each one of them a thick plate problem rather than the classical Kirchhoff thin plate problem. Shear deformation becomes important. When the end plate thickness is large, a full three dimensional analysis is needed [37]. Also when the end plate thickness is almost equal to the column flange thickness, better analytical results can be obtained by including the column flange deformation.

5.4 Bolt Behaviour

In bolted end plate connections applied loads are normally transferred to the bolts through the end plates, and the combined deflection due to end plate flexure, column flange deformation and extension of the bolts produces an effective rotation of the joint. In order to understand the overall behaviour of the connections the understanding of the bolt performance is of great significance. Bolt forces are induced from the nut through the threads, and the stress varies along the bolt from the threaded area to the shank area. The threaded portion is the weakest section of a bolt in tension and the tensile strength depends on the threaded area which is about 78 percent of the area of the shank [44]. Previous research [45] indicated that BS449 [46] assumed a relatively large factor of safety against failure for black bolts. Godly and Needham [6] carried out comparative tests on grade 8.8 and H.S.F.G. bolts in tension and shear. They

concluded that grade 8.8 bolt is not significantly weaker than the H.S.F.G. bolt in direct tension, provided grade 10 nut was used with grade 8.8 bolts. Their recommendation of employing different grades of bolt and nut is impractical and uncontrollable on site. Therefore grade 8.8 bolts can be replaced by general grade H.S.F.G. bolts which have larger heads and nuts and used as ordinary bolts without pretension. This will prevent failure due to bolt stripping and in the absence of site supervision will not significantly increase the cost.

Presence of bolt preload can increase the joint stiffness but at ultimate loading stage the connected faces separate and therefore the behaviour of the joint will be similar to the behaviour of the identical joint without preload. As far as connection strength is concerned there is clearly no advantage to be gained by pretensioning the bolts, unless the rigidity of connection is an important factor. Godly and Needham did not produce load-elongation characteristic of the bolts, even though 146 tests were conducted by them. Due to lack of such information most of the research work has ignored the bolt extension and assumed that the major source of rotation is attributable to flexure of the end plate and deformation of the column flange. But work by Shakir-Khalil and Ho [45] on the moment rotation relationship for end plate connection clearly indicated that the contribution due to bolt extension might be important.

The reliable prediction of connection behaviour depends on a number of factors including a knowledge of the load-elongation characteristics of bolts. Some tests were

conducted by Anderson [47] to obtain the load-elongation characteristics of M20 grade 8.8 bolts in direct tension. He also recorded and compared the yield strength and ultimate tensile strength of the M20 grade 8.8 with the results obtained by Godly[6] and BS3692 [48]. He concluded that all bolts failed in the threaded length and all stresses were within the limit specified in BS3692. He also agreed with Godley's findings. Similar tests were also carried out by him for mild steel bolts which indicated that the elastic behaviour for mild steel bolts and high tensile steel bolts was almost identical. Beyond the yield, the load-elongation curve for the grade 8.8 bolts displayed a sharp bend, unlike the load-elongation curve for a mild steel bolt. For grade 8.8 bolt the load-elongation curve can be represented by a bilinear relationship with very small elastic elongation and significantly large plastic deformation.

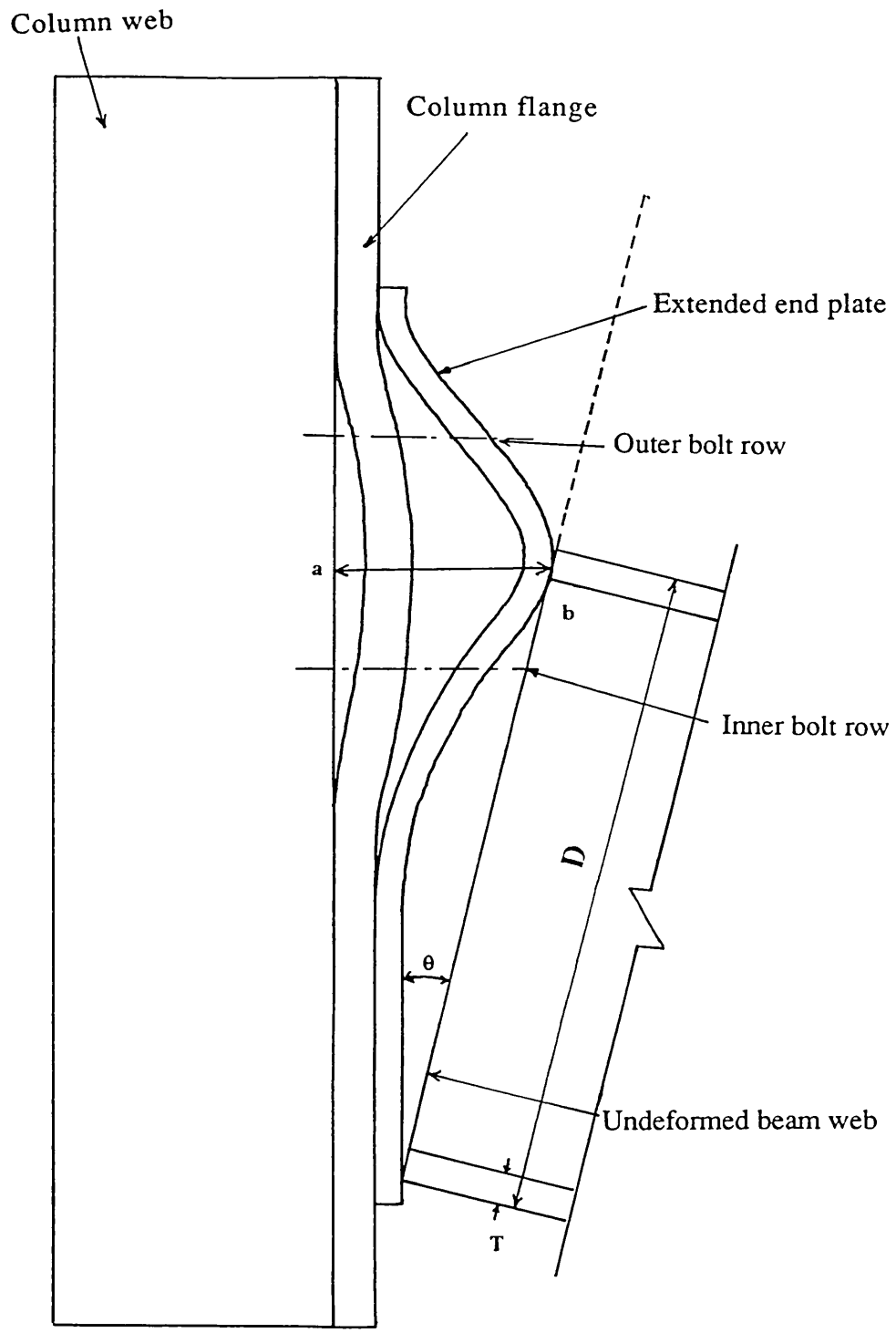

Fig. 5.1 Rotation of extended end plate connection

CHAPTER 6

Experimental Investigation

6.1 Introduction

In order to develop a semi-rigid design method for structures with unstiffened extended end plate connections, a knowledge of the strength, stiffness and deformation capacity of the joint from elastic, through plastic, up to the failure is essential. The determination of such characteristics requires a full understanding of the behaviour of each component of the connection as well as the way in which they interact. Although the finite element technique represents an economical and efficient tool for conducting a comprehensive investigation into the overall joint response and interaction of individual components, nevertheless the accuracy and adequacy of the analytical models should be determined through comparison with experimental data. If good agreement between the analytical model and experimental results are achieved, then generalized design equations or charts could be produced and applied to a large spectrum of semi-rigid connection design. In order to establish the validity of the finite element model and to permit observation of the overall behaviour of the unstiffened extended end plate connections when subjected to pure moment, an experimental investigation was conducted in conjunction with the analytical investigation. All the tests were continued until failure, which occurred due to a

variety of reasons. The details of of the comprehensive test programme are included in this chapter.

The experimental investigation was concerned with determining the effect of the column flange and web thickness, the end plate thickness, and depth of the beam and column on moment-rotation characteristics of connection. Similarly stress distribution and deformation propagation along the column flange and web and their effect on joint response were investigated. Also the moment-rotation relationship of the connection for the entire loading range and bolt force distribution were examined.

6.2 Test Rig

The test set up for the extended end plate connection is shown in Figure 6.1. The load was applied by a 1000kN capacity jack and monitored by a similar capacity console. Although connections were subjected to pure moment in the finite element model, all the specimens were tested under combined moment and shear. Previous attempts to avoid shear at the joint by the use of spreader beam encountered great difficulty in achieving stability of the spreader beam. The complex set up was discarded in favour of a simple one in which the load was applied directly on the column causing combined moment and shear at the joint. As stated previously the effect of the shear on the joint rotation is small and can be ignored.

During the first test the flange of the cross beam of the loading frame was deformed and the jack was mis-aligned. Modification was made to the loading frame to provide

the necessary stiffness for the flanges of the cross beam. Also two channel sections were welded to both sides of the frame to provide lateral support for column stub if necessary. Steel rollers were placed at the points of support to ensure free movement of the beam under load and in all cases care was taken to reduce friction between the steel rollers and the supports.

The testing components consisting of two beams with end plates welded on the ends and a column stub were lined up on the floor. The end plates were secured to the column flanges by inserting and tightening twelve dummy bolts. The whole structure was then placed into the loading frame, centred and plumbed using a theodolite which was also used to check any out of plumb movement during the loading programme. Having set up the bracing channels, the dummy bolts were replaced by the strain gauged bolts all of which had their initial strain readings recorded. The bolts were tightened to an initial degree of tightness. It was noticed that during the tightening of the bolts, there was some reduction in the preload of those bolts which had been previously tightened to the required preload. In order to achieve a constant preload in all the bolts several rounds of the tightening were necessary. Even then it was not possible to apply a constant preload in all bolts. Preloading of all the bolts within an acceptable range was however achieved in all the tests.

During the erection of each joint some degree of lack-of-fit in the structure due to rolling and welding distortion and mis-alignment of the bolt holes was noticed. It was found that by virtue of the use of bolts in clearance holes no adjustment or

enlargement of the bolt holes was necessary and the rolling distortions were within the specified BS4 tolerances. Earlier tests [49, 50, 51, 52] have shown that lack-of-fit arising from end plate distortion during welding does not have a significant effect on the moment-rotation response of end plate connections. However, several rounds of bolt tightening were necessary to bring the end plates and column flanges into some degree of contact, although a full surface contact between them was not possible.

6.3 Test Specimen

A series of twelve tests was carried out in the Heavy Structure Laboratory of the Dundee Institute of Technology to determine the overall behaviour of the extended end plate connection and to ascertain the accuracy of the finite element model by comparison of experimental with theoretical results. Table 6.1 shows a summary of test results. The twelve experiments were divided into three sets each consisting of four tests. Each set comprised a pair of identical beams connected to the flanges of a column stub by four different end plate thicknesses. The sizes of column and beam sections were chosen on the basis of survey of structural steel industry carried out by the Hatfield Polytechnic, which indicated the most popular types of joints, steel sections, types and sizes of bolts in todays construction industry. Three sections, namely 254x254x132 UC, 254x254x89 UC and 203x203x60 UC, were selected for the column stubs. These sections had a length of 1100mm, approximately three times the depth of the beams which they were connected to. To ensure the stability of the column stub and uniformity of the applied load, two 20mm thick plates were welded to the top and bottom of each column section. It might be argued that these plates

would limit the deformation along the length of the column stub, but previous research [34] has shown that the column deformation will dissipate within that length. For beam members 305x165x54 UB, 406x178x74 UB and 305x127x48 UB sections were used. These relatively heavy sections were chosen to limit their rotational contribution and to examine the effect of beam depth on joint characteristics. They were reinforced at the support position by welding stiffeners to prevent any web buckling.

The effect of end plates on joint behaviour and bolt force distribution was studied by fabricating four different end plate thicknesses in every set (10, 15, 22 and 25mm for the first; 10, 15, 20, 25mm for the second and 10, 12, 15 and 20mm for the third set). The end plate dimensions were based on beam size to which it was welded (Table 6.2). As suggested by Jenkins et al_{31} the universal beams are divided into two groups, A and B as shown in Table 6.2. For group A, the standard details are based on the use of M24 bolts but either M24 or M20 may be used in design. For group B the standard details are based on the use of M20 bolts but either M20 or M16 may be used in design. In the above range M20 is the most frequently used bolt diameter and bolts out with this range are rarely used. In view of its extensive use in steel construction hand tightened M20 HSFG or grade 8.8 bolts were chosen for these tests. The pretensioning of these bolts was kept to minimum, since it has been established [34, 35] that the effect of pretensioning bolts is to increase the stiffness of the connection at bending moments below the ultimate but has little effect on the strength and long term reliability of the semi-rigid connections.

The beam and column sections and end plates used for fabricating test specimens were all grade 43 steel. End plates were arc welded to the end of the beam section by 10mm all round fillet welds.

6.4 Instrumentation and Measurements

The most important characteristic of a semi-rigid joint is the relationship between the moment M transmitted by the joint and the angular rotation θ between the members connected at the joint. The bolt forces in an extended end plate connection are modified by prying action between the end plate and the column flange. In order to determine the accuracy of the finite element model of the connection the following connection properties were obtained from the test programme and compared with the results of finite element analysis:

(i) moment-rotation relationship of the connection;

(ii) bolt forces; and

(iii) strains at various points on column (flange and web), end plate and beam.

The rotation, θ is the difference in angular movements between the central axes of the column and beam at their intersection point. Although the importance of the correct measurement of these angular changes has been stressed by different researchers there is still not a standard method of measurement. During the past fifty years of research

on semi-rigid connections various techniques have been devised to measure the moment-rotation characteristics. In the author's investigation, a system of two arms cut from aluminum angle sections were connected to the specimen, one to the column web at the intersection of the beam and column centre-lines (point A), and the other to the beam web (point B) as shown in Figure 6.2. Point B was positioned as close as physically possible to the end section of the beam such that the flexural effect of the beam on the rotation of the arm at B was insignificant. Two dial gauges were mounted on the strong floor of the laboratory with their pointers resting on the arm connected to the point B at a known distance apart. From this set up the rotation of the connection can be found by subtracting one reading from the other and dividing it by the distance between the gauges. To check the above rotation another two dial gauges were connected at a known distance apart to the arm at point B with their pointers resting on the arm at point A. The difference between these two gauge readings divided by the distance between them determined the relative rotation of the beam and column. The two sets of rotation results were found to be in a very good agreement, and the average value was taken as the rotation for the connection. Similar arrangement was set up on each of the two beams connected to column flanges and it was found that by and large cases both beams behaved similarly.

As stated previously an understanding of the bolt behaviour and the load distribution is vital in the design of semi-rigid connections. In the tests the bolt forces were determined by means of strain gauges attached at 120 degree interval to the shank of the bolts between the threaded region and the head [34]. Three PL5 strain gauges were

mounted longitudinally in 1mm deep recesses milled in the shank and were connected to the data-logger through 3mm holes drilled into the head of the bolts. To protect the strain gauge connecting wires from any damages, they were covered by plastic tubing and reinforced using epoxy resin adhesive. A typical M20 bolt with recesses is shown in Figure 6.3.

In order to relate the measured strain to the applied force, it was necessary to calibrate the bolts. This was achieved by using an apparatus similar to the one developed by Godly and Needham [6]. This device comprises two interlinked boxes with a central hole through the two inner plates. A strain gauged bolt was inserted in the central hole and it was hand tightened connecting the two inner plates together as shown in Figure 6.4. By applying a compression force to the box, the inner plates separate and in turn exerts a tensile force to the bolt. The resultant strain from each gauge was measured using a Solartron data-logger. The gauge readings were averaged to eliminate any variability in the measured strains due to possible bolt bending. This method was used to calibrate M20 H.S.F.G. and M20 grade 8.8 bolts up to bolt failure. For all the bolts tested the failure was either due to fracture which occurred in the threaded region or slippage of the nut. This indicated that milling 1mm of the shank to place the gauges and drilling into the bolt head had no adverse effect on the ultimate strength of the bolts.

In order to determine the stress distribution strain gauges were mounted at the following critical points of the connection components:

(i) column flange and web in the tension and compression regions;

(ii) end plate; and

(iii) beam flanges and web near the end plate in tension and compression regions.

In order to achieve economy advantage was taken of the symmetry of the test specimens. At the first stage of testing only a quarter of the whole column was gauged. The strain gauges were mounted along the length of the column on the inner and outer surfaces of the flange and on the neutral axis of the web at 100mm intervals, to measure the horizontal and vertical strains at these positions as shown in Figure 6.5. The results obtained indicated that the deformation along the column flange in tension or compression region diminishes quickly and strain in the tension region of the web can be ignored. Hence at the second stage of experiment, some of the gauges were omitted from column flange and web and extra strain gauges were attached to the end plate at points where it was thought to be subjected to high bending stress as shown in Figure 6.6. Finally, for the third and final stage both the beam web and inner and outer surfaces of beam flanges were gauged to asses the stress distribution in the flanges and its reversal from tension to compression (Figure 6.7).

6.5 Test Procedure

As stated previously, each test specimen was lined up on the laboratory floor and assembled together using dummy bolts. It was then placed in the testing frame and aligned as accurately as possible using plumb-line and theodolite. The safety panels

were set up and the dummy bolts were replaced by strain gauged bolts for which the initial readings had been noted. Due to twisting of the beam sections some difficulties were encountered regarding stability of the connection, but this was remedied by using packing materials on the support. Other lack-of-fit problems e.g., beam and column not being parallel, mis-alignment of the bolt holes and weld distortion were ignored, since they were within the British Standard tolerances and would be typical of practice in the construction industry.

In order to measure the rotational characteristic of the connection, the aluminum arms were connected to the column and beam webs and levelled using a precise engineering level. The dial gauges were mounted at the predetermined positions and the strain gauges were connected to the data logger. Once the instrumentation was completed and checked, zero load readings were taken for all dial and strain gauges.

The load was applied to the top of the column stub through a hydraulic jack. Each specimen was loaded and unloaded in the elastic range once before being finally loaded to destruction. At every load increment the appropriate readings were taken and the axial load was kept constant during the measurement period. In the plastic region there was creep in the metal causing dial gauges to run. Load increments were reduced in the region and adequate time was allowed for dial gauge movement to either stop or become imperceptible. It was found that after the initial loading and unloading, there was a certain degree of slackness in the bolts. This was due to welding distortion of end plate which prevented complete contact between the end

plate and column flange. This phenomenon was more noticeable with thin end plates. The loss of bolt pretension was very small and did not effect the overall performance of the connection.

The connection was inspected after each load increment for plumbness, physical state of all instrumentation and any visible signs of deformation.

6.6 Summary of Results

A series of twelve tests were conducted and in all cases the connections were subjected to combined moment and shear. In the tests both the friction grip and grade 8.8 bolts were only hand tightened and slip of the end plate caused the bolts to be in shear and bearing. It is however, reasonable to assume that in the bolts tension caused due to moment predominates. Furthermore in small to medium span beams the two bolts in the compression region are adequate to resist the end shear from the beam. Therefore the four bolts in the tension region may be assumed to transfer bending moment from the beam to the column flange and web via the end plates.

It was observed that although the twelve test specimens differed in column, beam sizes and end plate thicknesses the pattern of the moment-rotation curves depended primarily on the relative thicknesses of the end plate and column flange. The factors influencing the connection rotation are the end plate deformation, stretching of bolts and column flange and web deformation. In general if the end plate is relatively thin, the first sign of deformation is the separation of the extended part of the end plate and

column flange in the tension region. At subsequent loading, as the lack-of-fit is overcome, the end plate is forced into double curvature and separation between the end plate and column flange at the position of beam tension flange and between the tension and compression region bolts started to appear. In this case the rotation is mainly due to the end plate bending with some possible contribution from bolt stretching. However, if the end plate is thick enough to resist any significant deformation, the connection rotation is attributed to column (flange and web) deformation and bolt extension. The column flange behaviour is similar to the behaviour of the end plate fixed on one side with some degree of rotational restraint on the other two sides when subjected to concentrated loads from the end plate through the connection bolts. In addition, the end plate serves to restrain the bending of the flanges by providing a degree of fixity at the bolt location and other point of contacts. This results in the column flange bending away from the column web.

From the observation made in the experimental investigation it is obvious that the mode of failure of the connection is dependent upon the relative thicknesses of the end plate, column flange and column web. For those connections with thin end plates, failure was by excessive plate bending, which in one case resulted in punching through the end plate around the inner tension bolts as shown in Figure 6.8 and in another caused the cracking of the weld at the outer edge of the beam tension flange, Figure 6.9 . However, from close inspection of the weld it was apparent that insufficient weld penetration caused by poor workmanship had significantly reduced the connection strength. This was remedied in all subsequent tests by adequate

supervision. For connection with thick end plate and heavy column section, it was the bolt fracture or slipping which gave rise to the final failure Figure 6.10 and 6.11. Also the combination of thick end plate and lighter column section resulted in excessive deformation of column flange and at final stage buckling of the column web as shown in Figure 6.12.

In the first series of tests the column stub (flange thickness of 25.3mm and web thickness of 19.3mm) made very little contribution towards the connection rotation. Test(1) with 10mm thick end plate indicated that at failure the end plate had been excessively deformed while the applied moment was about 192.5 kNm. The type of failure for test(2) with 15mm end plate was the same as test(1) and occurred at 225.5 kNm. These two tests show visible sign of deformation, but as the end plate thickness increased (ie. 22 and 25mm) column flange and end plate deformed mainly in the elastic range. Failures for tests(3) and (4) were due to fracture of inner tension bolts.

Although for the second set of tests a lighter column stub (254x254x89 UC) was used, the end plates were kept approximately the same as in the first set. In test(5) the 10mm end plate was excessively deformed and an applied moment of 246.4 kNm caused a physical failure ie. bolts punched through the end plate. For tests(6) and (7), with 15 and 20mm end plate respectively there were considerable deformation of the column flange and end plate but the physical failures were caused by bolt stripping and column web buckling respectively at moments 281.5 kNm and 316.4 kNm respectively. In test(8) with 25mm end plate there was little end plate deformation,

but the column flanges deformed considerably. Finally at 370.2 kNm moment the column web buckled.

In the third set light column section (203x203x60 UC) made significant contribution towards joint rotation. In tests(9) and (10) with 10 and 12mm end plates, it was the excessive deformation of both the end plate and column flange which caused failure, while the applied moments of 160.3 and 157.2 kNm respectively were achieved. A premature failure was recorded in test(11) with 15mm end plate. The failure occurred at an applied moment of 145.4 kNm due to weld fracture. It became apparent that lack of weld penetration was the reason for such a mode of failure. In test(12) with 20mm end plate excessive column flange deformation occurred and failure was caused by web buckling at 153.2 kNm.

6.7 Moment-Rotation Curves

The moment-rotation relationship for a connection is expressed by a curve which plots the moment, M transmitted by the connection against the rotation, θ of the connection.For an ideally rigid joint the rotation is zero and the M-θ relationship is represented by the y axis of the graph. In the case of an ideally pinned connection the moment transmitted is zero and the relationship is expressed by the x axis. From tests it is observed that connections which are termed as rigid exhibit some joint rotations where as connections which are classified as pinned offer appreciable moments of

resistance. Hence all practical joints can be termed as semi-rigid connections. Moment-rotation curves are the product of a complex interaction between the member components with significant effects from a number of geometrical and mechanical parameters. The many components which may contribute to the connection rotation are:

(i) the end plate;

(ii) the beam;

(iii) the column (flange and web);

(iv) the weld material;

(v) the bolts and nuts; and

(vi) washers.

Each of these components possesses unique material properties and its response depends upon its position within a connection. However, the rotational characteristic of the extended end plate joint can be attributed to its principal contributors ie. end plate, column and bolts.

The moment-rotation curves of all connections tested were non-linear through their entire loading history irrespective of their material and geometrical properties. This non-linearity at the lower load range arises from the combination of lack-of-fit, imperfection of the connected parts and bolt pretensioning. The end plate distortion caused by welding prevents a full contact between the end plate and column flange. Also, all bolts were only hand tightened. Therefore each connection possessed a

certain degree of in-built slackness, which depending on the load level in the elastic range, could cause slip and relative local deformation between the end plate and column flange. These deformations were to some degree irrecoverable. In all tests the connections were initially loaded and unloaded, and the subsequent paths were different due to joint bedding in and permanent take up of some of the lack-of-fit. This non-linearity is more evident for thin end plates but could be more significant for thick end plates. For thick end plates showing lower rotational ability, this non-linearity could count for a high proportion of its elastic rotation. For thinner end plates, where comparatively larger rotations are experienced, the proportion of rotation coming from these effects is significantly less. Hence, to limit or if possible to eliminate rotation caused by lack-of-fit or slip, the connections were loaded and unloaded in the elastic range before testing them to failure.

In the plastic region the rotational non-linearity is caused by elastic-plastic material properties of the connection components.

The scope of this study was limited to extended end plate connections using only four tension bolts, forming two rows adjacent to the tension flange of the beam. These connections are divided into three sets based on beam section, column section and bolt grade variation. Each set incorporates connections with similar beam and column combination with variable end plate thicknesses. For the three sets, the end plate thicknesses are approximately the same, and it is the beam and column sections which are varied. In all the tests, 20mm diameter bolts were used as fastener, but for the first

set H.S.F.G. bolts and for the second and third sets grade 8.8 bolts were chosen. Therefore the end plate thickness is the only variable in every set. The moment-rotation curves obtained for the three sets (Figures 6.13-6.15), clearly indicate that the end plate thickness is highly critical which influences the rotational response of that particular beam column combination. Increase in end plate thickness would result in substantial increase in connection stiffness, provided that bolt fracture or weld failure did not occur. The curves also show that initial response of each group of connection is almost identical and their curve separation is at the on set of non-linearity based on the relative thickness of the end plates. This is more true with the first set, since the column section was relatively heavy and showed very little visible signs of deformation. It is therefore reasonable to assume that the connection rotation is derived from the contribution of the end plate and the bolts only. In the lower range of end plate thicknesses (10,15mm), the connection responses are attributed mainly to the end plates, with very little or no input from the bolts. The bolts and in particular H.S.F.G. bolts possess higher yield value than the mild steel; they also exhibit low extension properties. As the end plate thickness increases (22, 25mm) higher force is transferred to the tension bolts which in turn demands a higher contribution from the bolts towards the joint rotation. As their extensibility is limited, the increasing moment forces the end plate into double curvature by contact forces. The effect of these contact forces is to limit the rotation and increase the actual bolt forces which finally cause their fracture. Figure 6.10 shows the fractured tensile bolts with some degree of necking before failure. The fracture of H.S.F.G. bolts were sudden and violent which can have catastrophic consequences in structural steel. Therefore

establishing a right balance between the end plate and column (flange and web) thicknesses is very important in order to achieve the desired rigidity and to avoid certain failure modes of the connection.

Throughout the experimental programme the H.S.F.G. and grade 8.8 bolts were only hand tightened. From previous investigation[34, 35] it is known that pretensioning has insignificant influence on the moment-rotation response of the joint. The only difference in rotation between the hand- tightening and pretensioning arises from the absence of any contribution from the extension of the bolts in the preloaded connection, until the initial pretensioning has been overcome. Therefore a pretensioned joint shows a stiffer rotational response to the applied moment in the lower range. As far as connection strength is concerned, there is clearly no advantage to be gained by pretensioning the bolts. This effect is however less apparent with thin end plate and column flange.

In order to assess the effect of column size on the rotational characteristics of a joint, lighter column sections were used for second and third set of tests. In general the column is subjected to tensile forces acting on the flange at bolt locations in the tension region and compressive forces acting over some bearing zone in the compression region. The effect of column on the rotational behaviour of the connections depends on the performance of the two distinct tension and compression regions. In the tension part most of the deformation occurs in the flange, especially in the vicinity of the bolt holes, with some extension in the web. In the compression

region the column flange and end plate simply act as bearing plates to transfer the load to the web. Although the centre of rotation of the beam changes during the experiment which in turn changes the compression zone, it is reasonable to assume that the compressive load is applied at beam flange position. This can result in failure of the web by buckling. The rotation curves (Figures 6.16 - 6.18) indicate that the extent of column contribution to the overall joint behaviour is dependent upon the rigidity of the end plate and the fasteners as well as the column itself. Also the major contribution of the column towards the rotation of connection is due to the flange deformation in the tension zone. A thick column flange can have a restricting effect on the rotational ability of the joint which can lead to premature failure of the connection, while a thin column flange can exhibit excessive flexibility.

6.8 Bolt Force Results

Throughout the experimental programme the end plate is connected to column flange via six bolts, four of which are situated in the tension and the other two in the compression region. This pattern of bolting is adopted with the knowledge that additional bolts within the beam web area will not contribute significantly to the bending strength of the connection. Tension bolts are positioned in two rows near the beam tension flange, inside and outside the depth of the beam. The remaining two bolts are placed near the compression flange of the beam as shown in Figure 6.19. They are termed inner, outer and compression bolts respectively for ease of reference. These were hand tightened with tension of up to 30 kN. Application of constant tension to all the bolts proved to be difficult which arose from lack-of-fit (ie. welding

distortion) in the connection. These variations in the tightening tension have no significant influence on their performance. Preloading only affects the elastic stiffness of the connection and after the initial tightening is overcome the pattern of bolt responses are similar. The tightening force in the bolts and their subsequent increase due to applied moment were determined from direct conversion of the average strain in the bolts using 'Load-Strain' graphs obtained from the calibration tests. In order to produce 'Load-Strain' graphs a number of strain gauged bolts were tested according to the method mentioned previously, and for each bolt the average strain was plotted against the load. Since a direct tensile load was applied to the bolts in these calibration tests, very little bending should develop, and averaging the strain for each bolt would eliminate any bending effects which might be present. Also to limit the discrepancies due to any material or manufacturing deficiencies, the mean of all Load-Strain values were used to create one Load-Strain graph. This method was applied to M20 HSFG as well as M20 grade 8.8 bolts to develop two calibration curves. This method of obtaining bolt force is an accurate approach and takes account of any plastic flow which might occur in the bolt provided the bolts are not subjected to severe bending. However, in combination with thin end plates or column flange the accuracy of this might decrease due to bending of the bolts at high moment. This can be remedied by increasing the number of strain gauges attached to the shank. However, such action lowers the strength of the bolts.

The experimental results demonstrate clearly that the tensile force is not equally distributed between the tension bolts. The distribution of this force is dependent on

the depth of the beam and the relative rigidity of end plate and column flange. The whole bolting system can be divided into two sub-systems, one for the end plate between the beam flanges and another for the extension plate. If the end plate and column flange were infinitely stiff a linear load distribution would be imposed on the bolts, with outer bolt row carrying higher load. This is indicated in Figure 6.20 (25mm end plate, second set) where the outer bolt row absorbs higher loads than the inner row. However, as the end plate thickness decreases, the resulting flexibility produces a redistribution of load and the inner tension bolts carry a higher percentage of the applied load as shown in Figure 6.21 to 6.27. The plate below the tension flange is stiffer than the plate above due to the support provided by the welded beam. As a consequence the bolts in that zone have more of the direct load transferred to them. But in the case of the 22mm and 15mm end plates in the first and second set respectively, the inner and outer bolt rows were carrying equal loads over the entire loading process (Figures 6.28 and 6.29). This might be considered to be an intermediate case falling between the two categories described earlier. For these particular connections the ratio of the end plate to column flange thickness is 0.87. Lack of adequate data prevents the establishment of the range of thickness ratio for each of the two categories of bolt force distribution.

Moment-Bolt force graphs also show that there is no significant change in bolt force until the moment is sufficient to overcome the preload. It then commences to increase linearly. At a higher moment level, the increase deviates from its linear path and a sudden rise in the bolt force occurs. This rapid upsurge of force is due to the

excessive bending of the end plate and column flange, inducing bending of the bolts. This behaviour is thickness dependent and bolts used in conjunction with thin end plate and column flange are more susceptible. The compression bolts are seen to lose some of their initial preload at lower moment as a result of end plate elastic bending about the inner bolt row. This causes a certain amount of flexural movement providing a bedding-in effect between the end plate and column flange. At higher moment, when the bedding-in effect is overcome and yielding occurs in either the tension bolts, the column flange or the end plate the compression bolts will gradually pick up load. The pattern of compression bolt responses is similar to the tension bolts with nominal loss of preload at low moment followed by a linear increase in bolt force and finally settling to a steady state with a constant force. For these bolts a maximum tensile force of 40kN was recorded.

The interplay of forces within a bolt group is made complicated by the presence of the prying forces. These are contact forces developed between the end plate and column flange and caused by the bending deformation of the end plate, Figure 6.30). The force resulting from the applied moment is transferred through the beam flanges to the end plate and is resisted by tension bolts. Since the bolts have limited extensibility and there is significant bending of the end plate, the end plate is forced into double curvature by the contact forces. The effect of such behaviour is to increase the force in the bolts as well as the ultimate strength of the end plate. The prying forces will not develop until the gaps between the end plate and column flange caused by the welding distortion close up under a certain amount of external force. Therefore, the

contact forces will act only at higher moment and the area over which they act vary with the load. In general they act on the outer edge of extension plate and some part of the vertical edge near the inner tension bolts. This is more noticeable in thin extended end plate connections which are more flexible.

The accurate determination of prying forces is difficult. In order to prove their existence as well as determine their magnitude a comparison is made between the applied moment and the moment from the bolt forces. For this purpose it is therefore necessary to assume a point of rotation. Initially it is located at the bottom edge of the end plate. However, with increasing load and resulting deformation of end plate this point will move to the middle of the beam compression flange. For the purpose of calculation the lower edge of the compression flange was chosen as the rotational point of the connection. The moment induced by the bolts is determined by the summation of bolt forces multiplied by its respective lever arm, ie.

$$M = T_1 d_1 + T_2 d_2$$

where M = calculated moment due to bolt forces;

T_1 = force in the outer bolt row;

T_2 = force in the inner bolt row; and

d_1 and d_2 = respective lever arms for outer and inner bolt rows

This moment resulting from bolt forces was plotted against the moment applied to the connection. In the absence of prying the curve should be a straight line inclined at 45

degree angle, once the effect of the initial preload has been overcome. This was found to be the case for thick end plates as shown in Figs. 6.31 - 6.33. The points are lying on the 45 degree angle line indicating that the moment calculated from the bolt forces is equal to the applied moment. However, for 20mm end plate in second set of tests (Fig. 6.32), the curve departs from the straight line at 250kNm which marks the start of prying. The prying occurs at the upper edge as can be seen in Figure 6.34. For thinner end plate the prying is found to develop at lower moment. For the 10mm and 12mm end plate in the first and third sets prying is present almost from the beginning and the curves representing moment due to the bolt forces are above the 45 degree angle line at all times (Figs. 6.35 - 6.37).

The development of prying does not depend on the end plate thickness only, but is also affected by the column flange rigidity. Therefore the percentage increase in bolt forces for similar end plates with various sets of connections were different. It was found that for these connections the percentage increase in tensile bolt forces due to prying varied between 8.5% for 20mm end plate connection in the second set and 30% for 10mm end plate connection in the first set.

6.9 Column Flange Deformation

In order to understand the true connection behaviour it is necessary to investigate the column response and the extent of its contribution towards the overall rotational behaviour of the connection. Such information has not been available, since most of previous research has only considered the action of reinforced column section.

However, the expense incurred in the fabrication and the inconvenience of the column reinforcement have meant that the role of unreinforced column stub in the semi-rigid connections be investigated. Throughout the experimental programme a range of heavy, medium and light size column sections were used in conjunction with various end plate thicknesses to examine the column deformation and its interaction with other components incorporated within a connection.

In the extended end plate connections, column sections are subjected to tensile force acting at the bolt locations in the tension region and compression force acting over some bearing zone in the compression region. These forces are resisted by an effective length of column in both regions.

The results of the first series of tests where relatively heavy column stubs (254x254x132UC) were associated with varying end plate thicknesses suggest that the rotation of these joints was mainly composed of end plate deformation and the extension of the bolts. The lack of contribution from column increased the rigidity of the connection specially when associated with thick end plate and would cause failure due to bolt fracture. Heavy column stub with thin end plates resulted in excessive plate deformation which consequently produced higher prying force and higher bolt force. These effects are highlighted by the modes of failure of the joints as shown in Table 6.1. The decrease in the weight of the column stub results in significant increase in the joint rotation which can be attributed to higher column deformation. The column sections in these tests followed similar deformation pattern. In the

tension region the deformation occurs mainly in the flange with some extension of the web. The flange deforms bi-axially about the web and an axis perpendicular to it, which travel some distance along the length of the column. In the compression region the applied load is transferred from the end plate to the web which spreads out as it penetrates into the column. Therefore, the intensity of the resulting stress decreases with deeper penetration. If the spread of stress is insufficient to reduce their intensity at some point below the base of the column compression flange, the web will not be able to provide sufficient resistance to the applied compressive force. The resulting effect is the buckling of the web which occurs in the region opposite the beam compression flange. These observations point out the need to establish the right balance between the behaviour of individual components of the connection to achieve the necessary strength and rotation. This can only be accomplished with an accurate knowledge of each member's behaviour, and the experimental method is expensive in reaching this goal

6.10 End plate Deformation

The deformation of the end plate is governed by the forces it is resisting and the support conditions. Each end plate is subjected to the forces from the connecting beam, bolts and the forces resulting from its interaction with the column flange. The tension and compression forces resulting from the applied moment are transferred to the end plate through the respective beam flanges. The bolts positioned on either sides of the beam tension flange will chiefly resist these loads. The induced pressure will force the plate to bend about the flange and web of the beam. The bending of the

extended part of the plate about the tension flange will result in its prying into the column at positions of contact. This system of forces will create areas of high stress and strain at the junction of end plate and at bolt locations. The end plate will undergo bi-axial bending and depending upon the nature and magnitude of stresses, local buckling or punching through at bolt position might occur. The severity of end plate deformation depends on the intensity of the stresses. The strain gauges attached to the end plates to measure the true strain and its distribution pattern proved to be insufficient. The factors which limited the number of gauges attached were primarily the lack of adequate space in the critical regions and to a much lesser extent the expense it entailed. The limited strain results were used for comparison with the results obtained from the finite element model to check their accuracy.

FIRST SET (With M20-H.S.F.G. Bolts, hand tightened)

Test No.	Universal Column Section	Universal Beam Section	End Plate Size (mm)	Col. Fla. Thickness (mm)	Maximum Recorded Rotation (θ) (Rad. x 10^{-3})	Load at Maximum Recorded Rotation (kN)	Moment at Maximum Recorded Rotation (kNm)	Failure Load (kN)	Failure Moment (kNm)	Mode of Failure
1	254x254x132	305x165x54	440x200x10	25.3	21.21	230	126.5	350	192.5	End plate Failure
2	"	"	" x15	"	18.22	390	214.5	410	225.5	End plate Failure
3	"	"	" x22	"	12.51	430	231.0	440	242.0	Bolt Fracture
4	"	"	" x25	"	11.15	380	209.0	390	214.5	Bolt Fracture

SECOND SET (With M20-Grade 8.8 bolts, hand tightened)

5	254x254x89	406x178x74	555x240x10	17.3	25.54	310	173.6	440	246.4	End plate Failure
6	"	"	" x15	"	22.37	500	278.8	505	281.5	Bolt Stripping
7	"	"	" x20	"	22.92	560	310.8	570	316.4	Col. web Buckling
8	"	"	" x25	"	28.99	660	364.7	670	370.2	Col. web Buckling

THIRD SET (With M20-Grade 8.8 bolts, hand tightened)

9	203x203x60	305x127x48	450x205x10	14.2	44.34	210	120.2	280	160.3	End plate & Column flange Failure
10	"	"	" x12	"	49.27	240	137.2	275	157.2	End plate & Column flange Failure
11	"	"	" x15	"	57.12	250	142.5	255	145.4	Weld Fracture
12	"	"	" x20	"	51.12	230	130.5	270	153.2	Col. web Buckling

Table 6.1 Experimental results

UB	Dp	Wp	H	S1	S2	S3	G1	G2
914x419	1050	440	115	60	205	945	120	70
914x305	1060	330	"	"	200	950	"	"
838x292	980	315	"	"	195	880	"	"
762x267	900	290	"	"	190	800	"	"
686x254	825	275	"	"	190	725	"	"
610x305	765	335	"	"	195	655	"	"
610x229	750	250	"	"	190	650	"	"
533x210	675	235	"	"	190	580	"	"
457x191	600	215	"	"	185	505	"	"
457x152	595	200	"	"	185	505	"	"
406x178	545	200	"	"	185	455	"	"
356x171	495	200	"	"	185	405	"	"
305x165	440	200	"	"	180	355	"	"

Group A

M20/M24 bolts

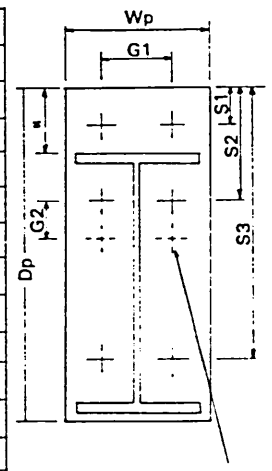

UB	Dp	Wp	H	S1	S2	S3	G1	G2
457x152	580	175	100	50	165	490	100	60
406x178	525	200	"	"	165	440	"	"
406x140	515	170	"	"	165	435	"	"
356x171	480	200	"	"	165	390	"	"
356x127	465	170	"	"	165	390	"	"
305x165	425	200	"	"	165	340	"	"
305x127	425	170	"	"	165	340	"	"
305x102	425	170	"	"	160	345	"	"
254x146	375	170	"	"	165	290	"	"
254x102	375	170	"	"	160	295	"	"
203x133	320	170	"	"	160	245	"	"

Group B

M16/M20 bolts

Table 6.2 Proposed end plate dimensions(Reproduced from Ref. 31)

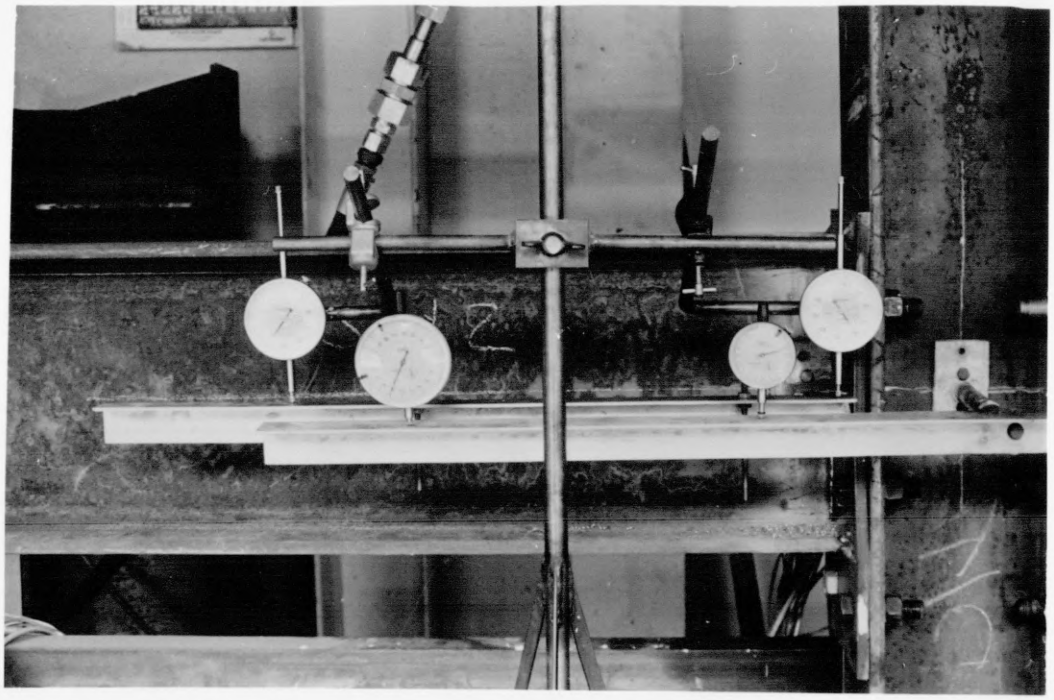

(a)

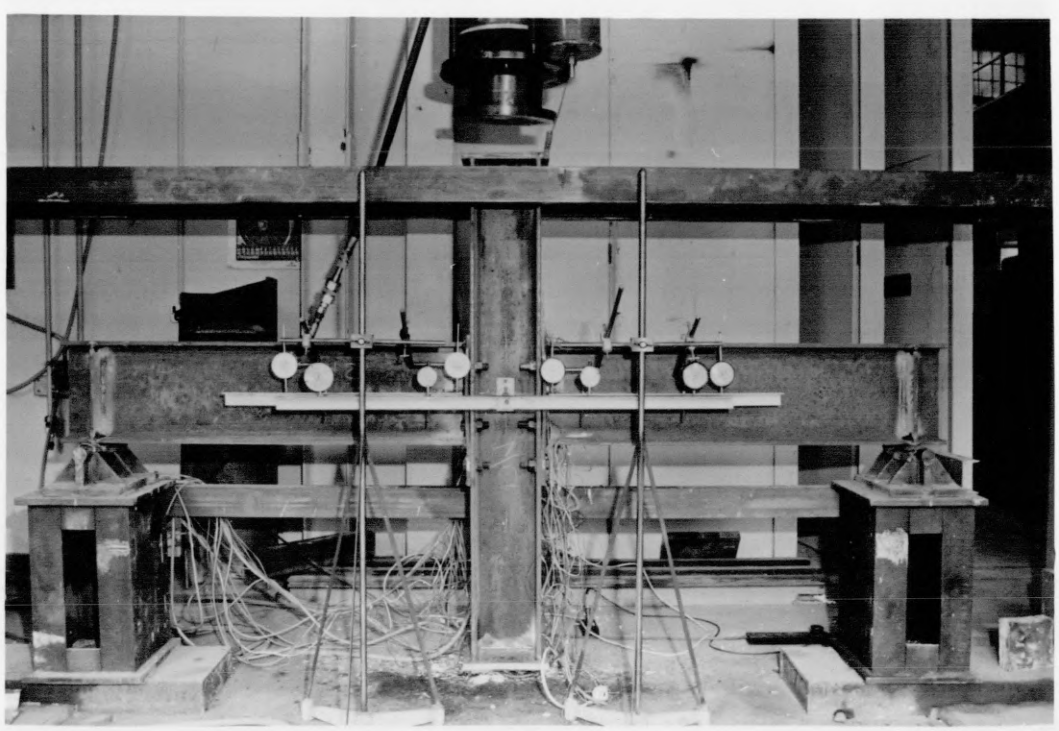

(b)

Fig. 6.1 (a) Arrangement for measuring rotation
(b) Test Rig

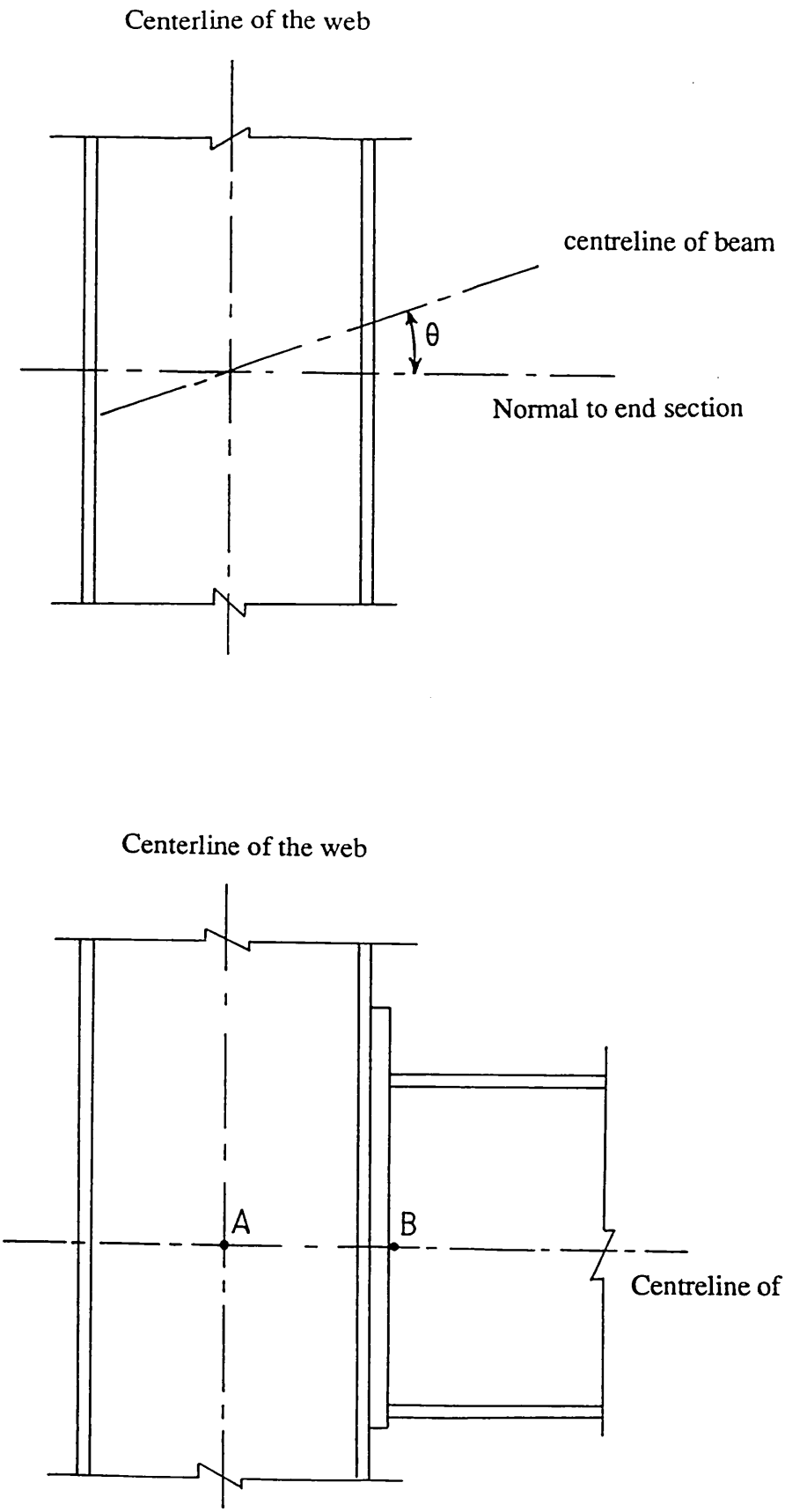

Fig. 6.2 The position at which the rotation is measured

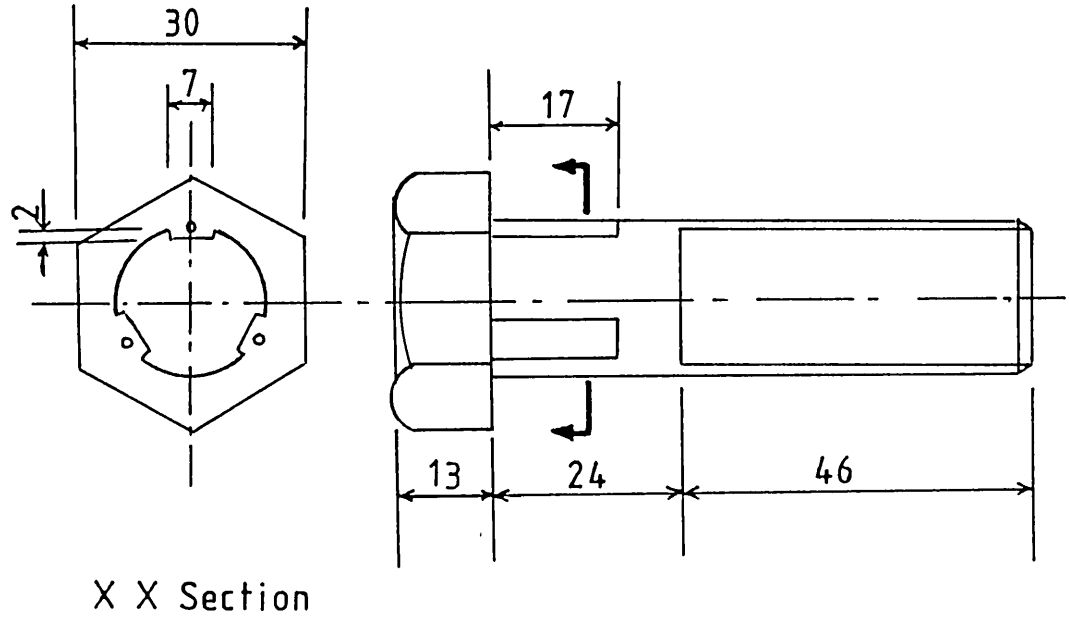

Fig. 6.3 Machined M20 bolt

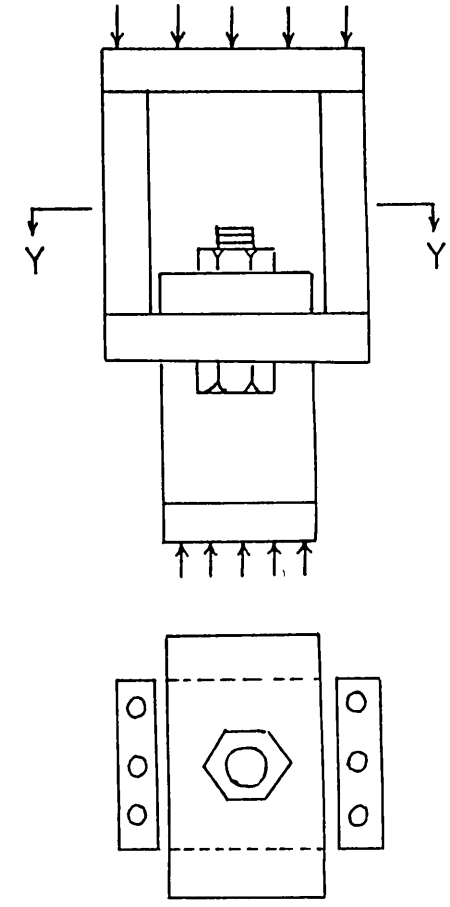

Fig. 6.4 Bolt tensile testing rig

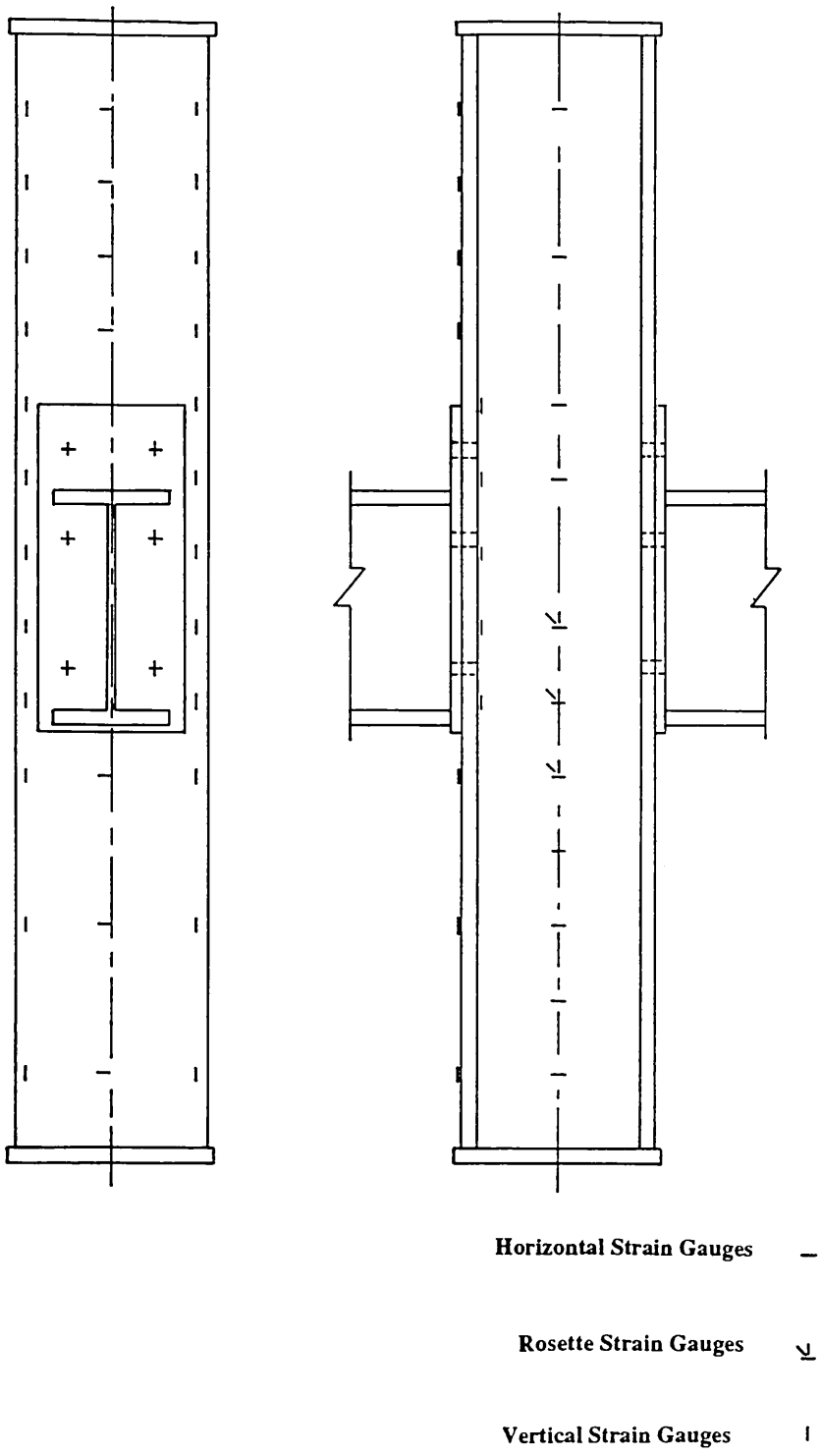

Fig. 6.5 Gauging pattern for the first set of tests

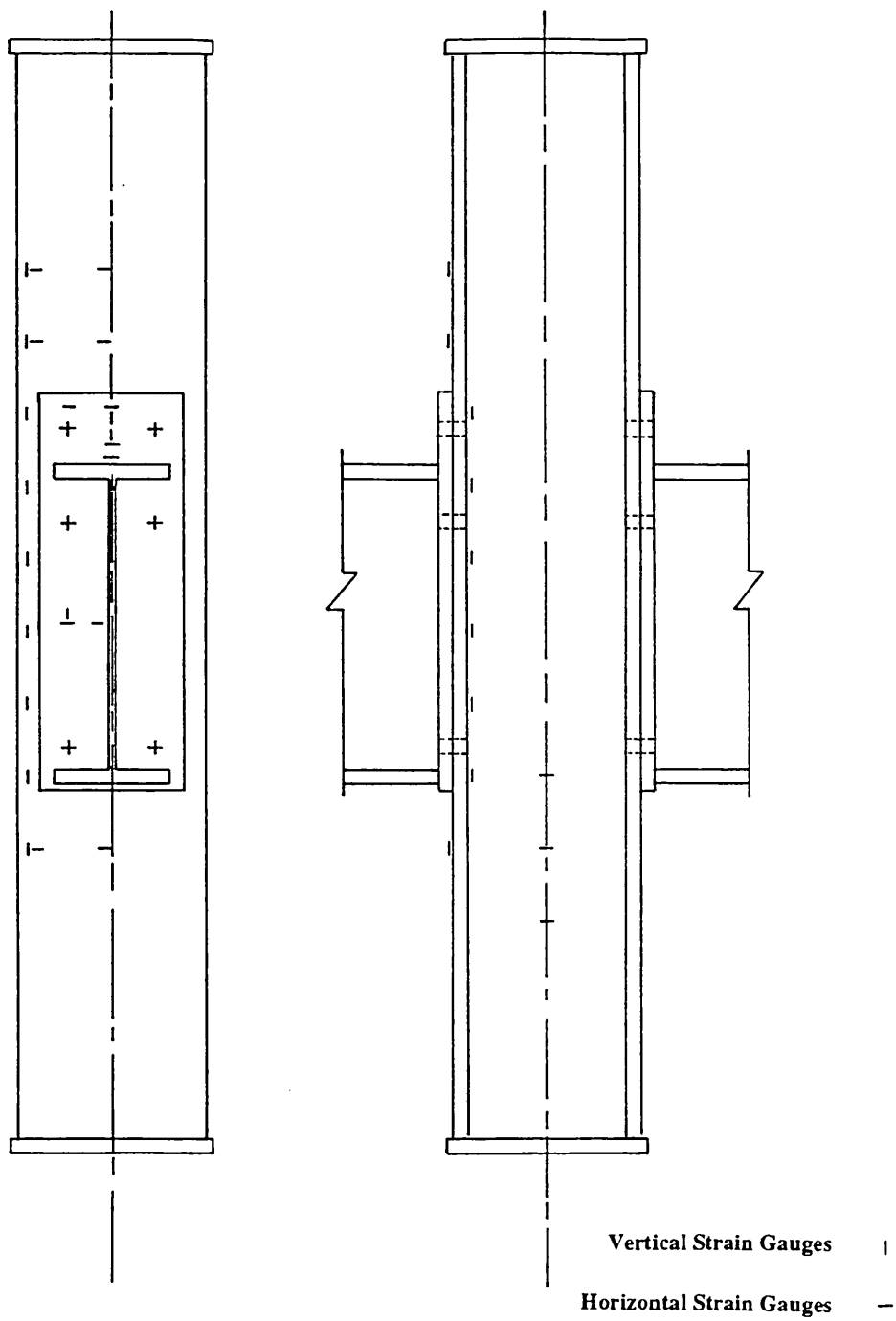

Fig. 6.6 Gauging pattern for the second set of tests

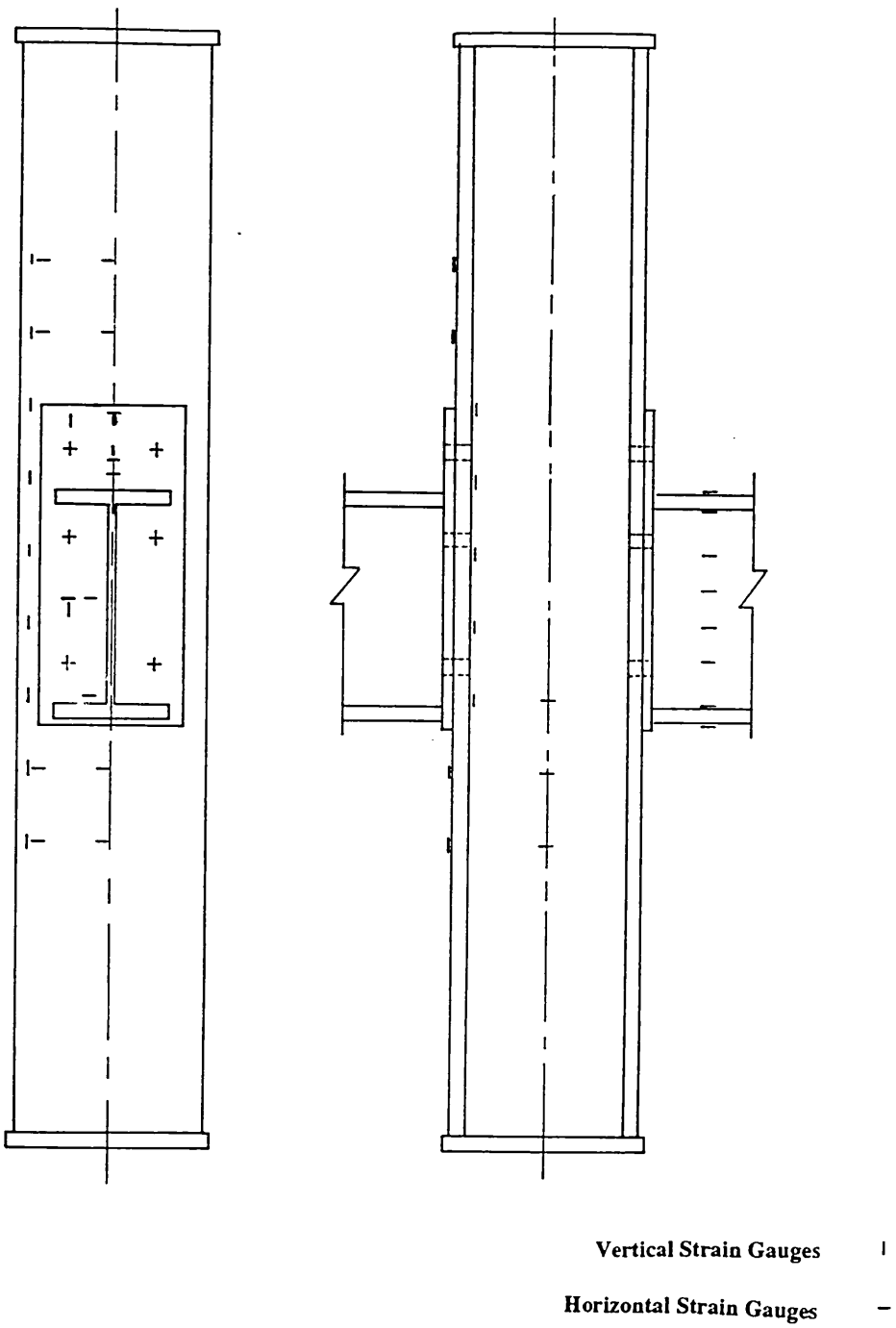

Fig. 6.7 Gauging pattern for the third set of tests

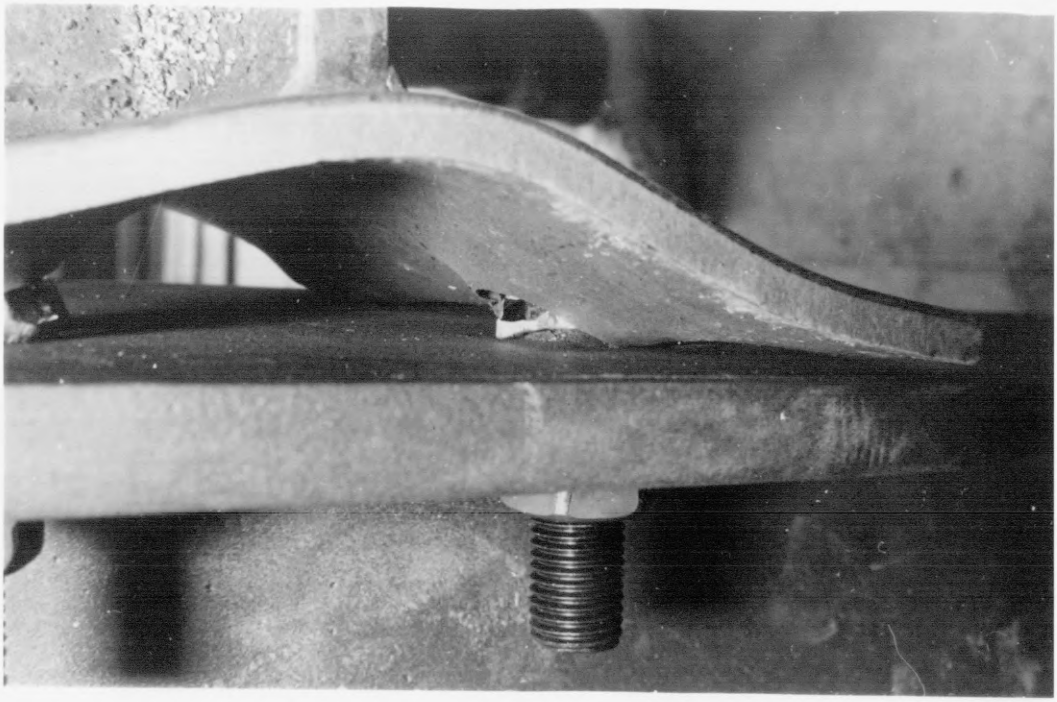

Fig. 6.8 Bolt punching through end plate around the inner tension bolts

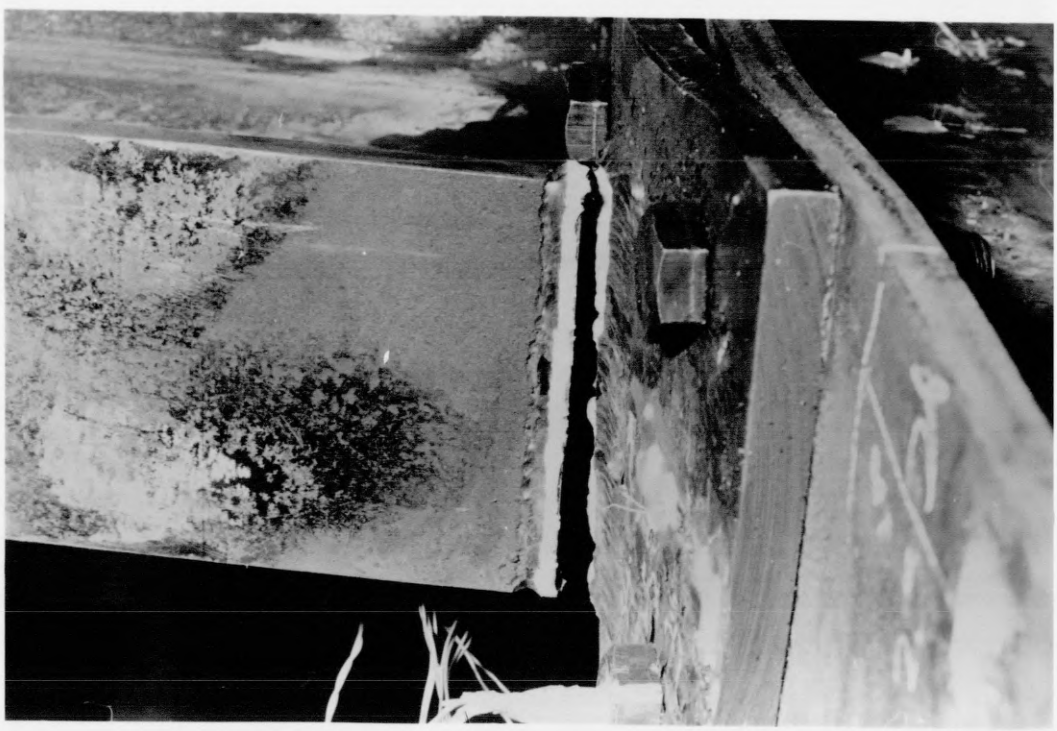

Fig. 6.9 Weld cracking at outer edge of beam tension flange

Fig. 6.10 Fractured M20 HSFG bolts

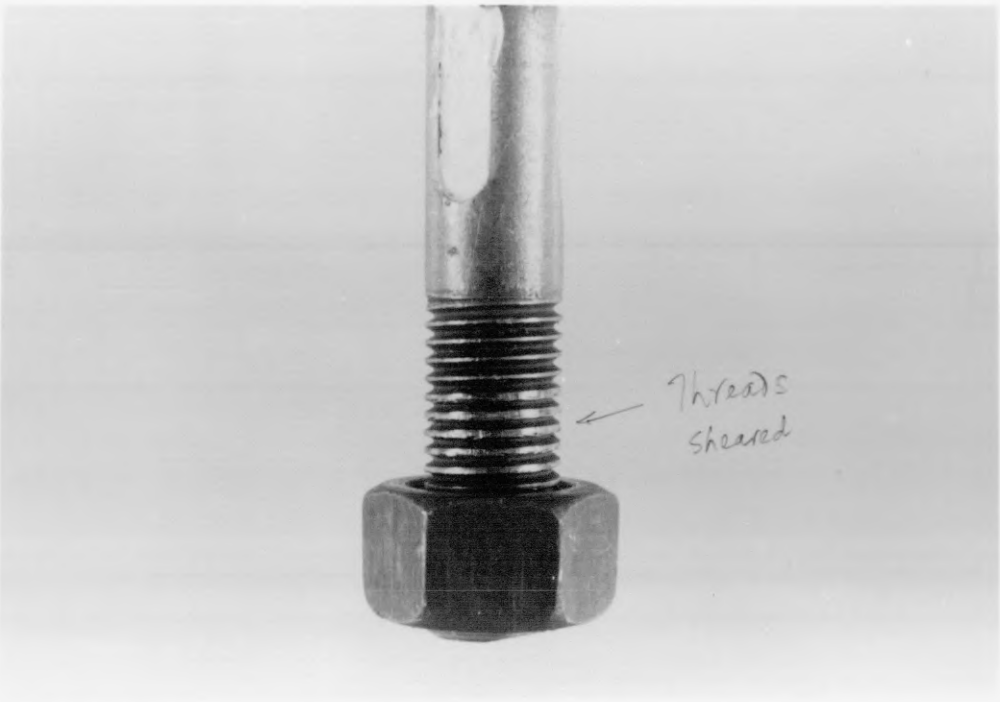

Fig. 6.11 Sheared threads of M20 grade 8.8 bolts

Fig. 6.12 Buckled web of light column section

Fig. 6.13 Moment - Rotation curves for the first set
254x254x132U.C., 305x165x54U.B.
10, 15, 22, 25mm end plates, M20 H.S.F.G. bolts

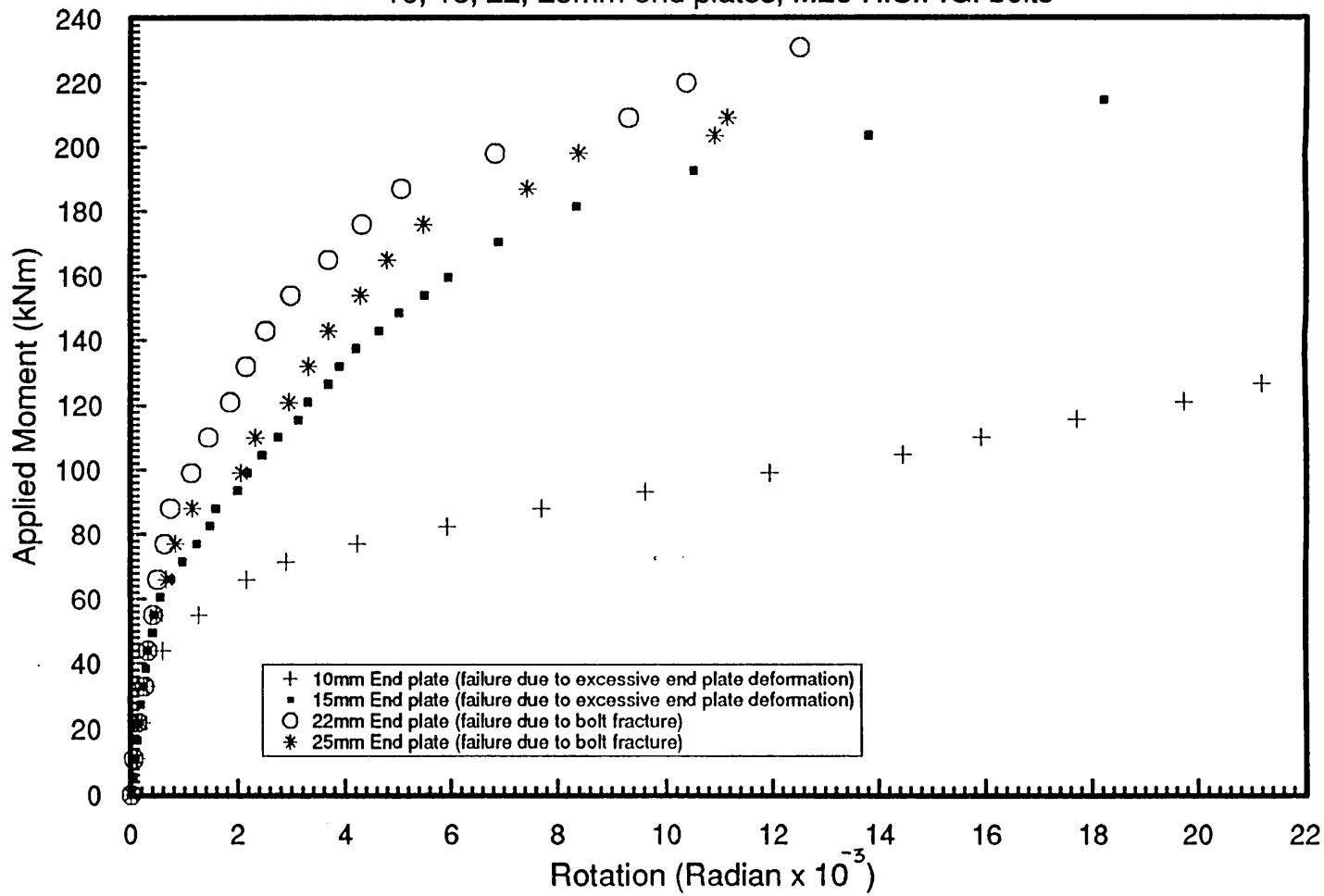

Fig. 6.14 Moment - Rotation curves for the second set
254x254x89 UC, 406x178x74 UB
10,15,20,25mm end plates, M20 grade 8.8 bolts

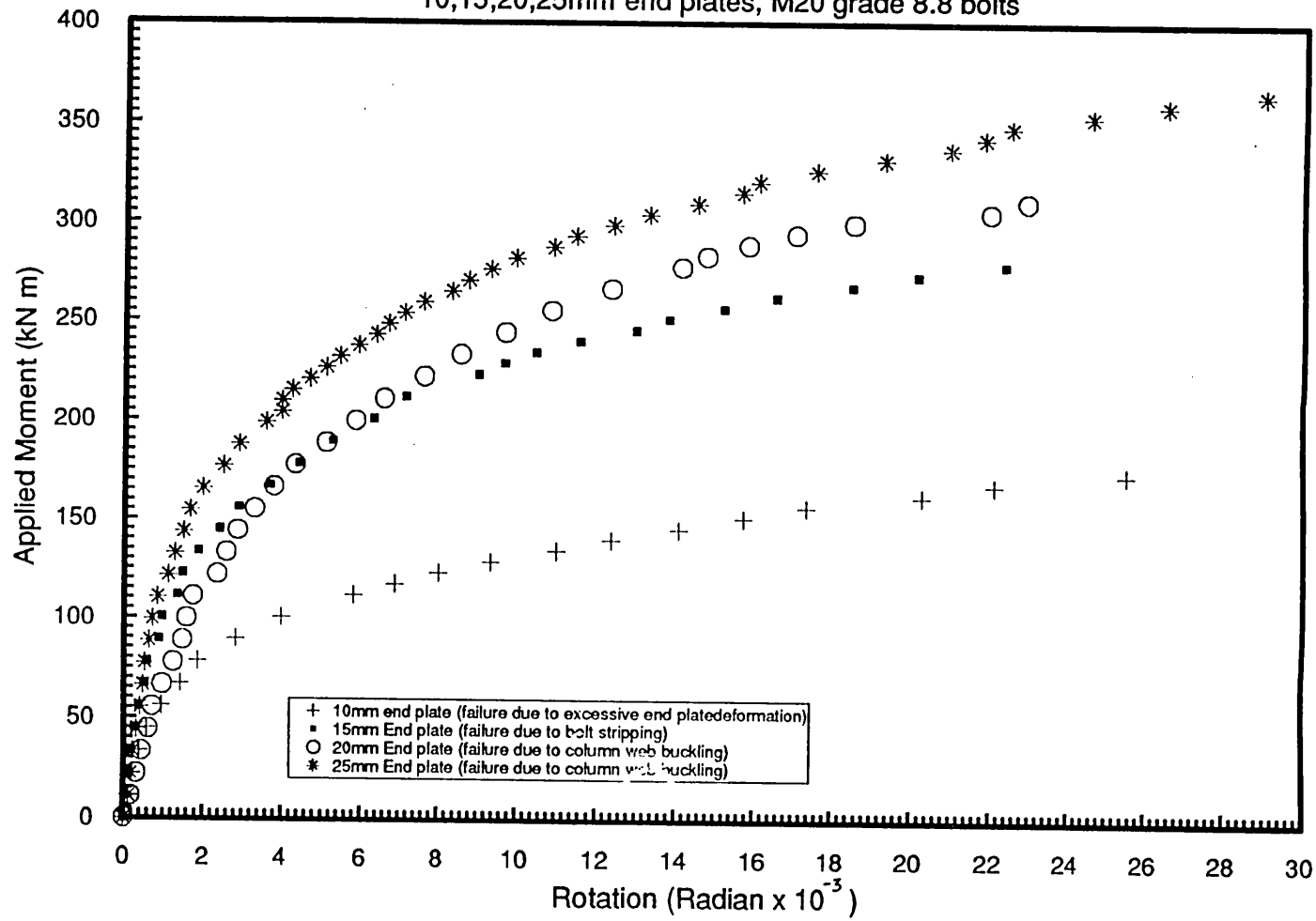

Fig. 6.15 Moment - Rotation curves for the third set
203x203x60 UC, 305x127x48 UB
10,12,15,20mm end plates, M20 grade 8.8 bolts

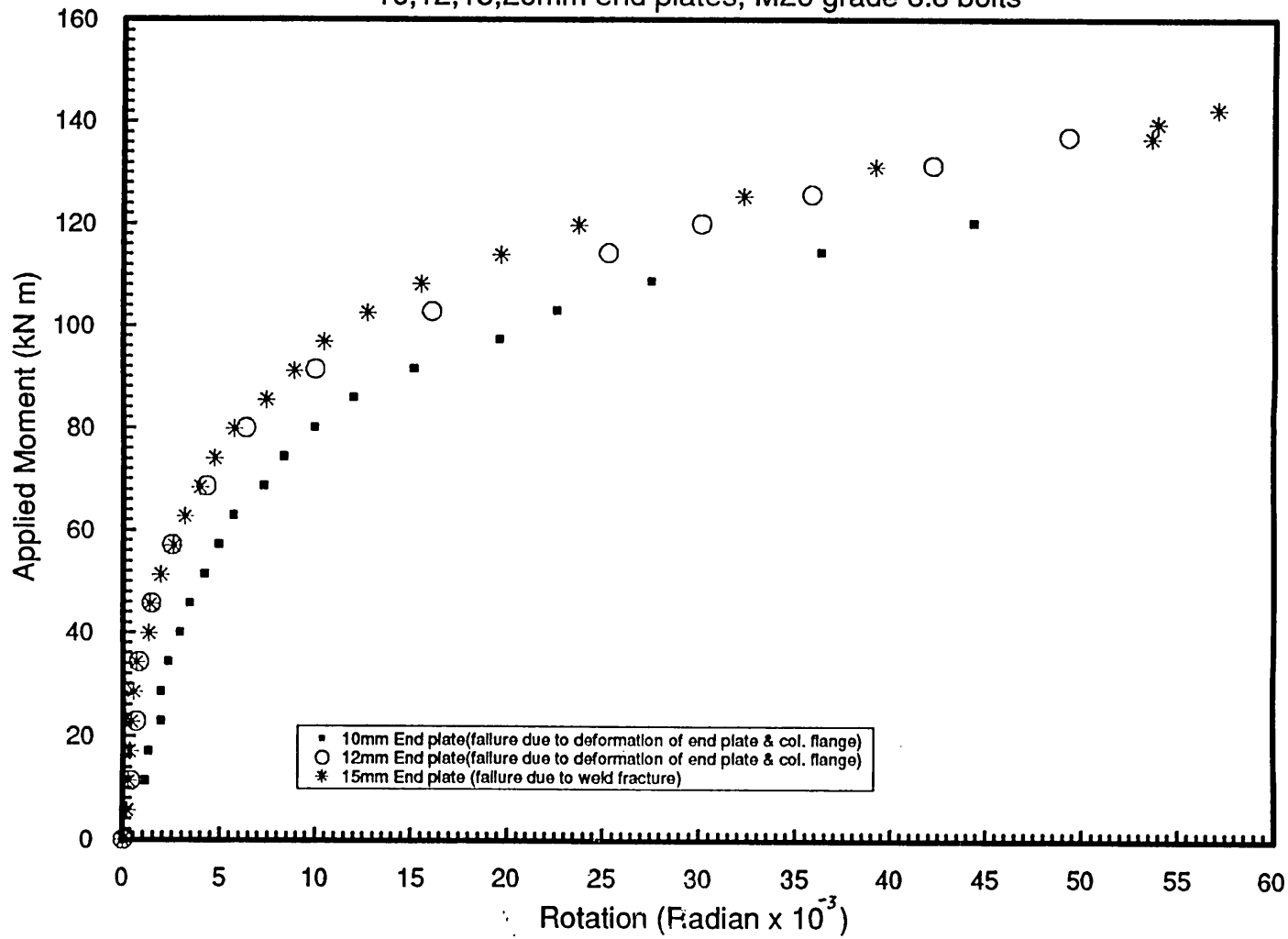

Fig. 6.16 Moment - Rotation curves for 10mm end plate connections;
Effect of variation in beam and column sections

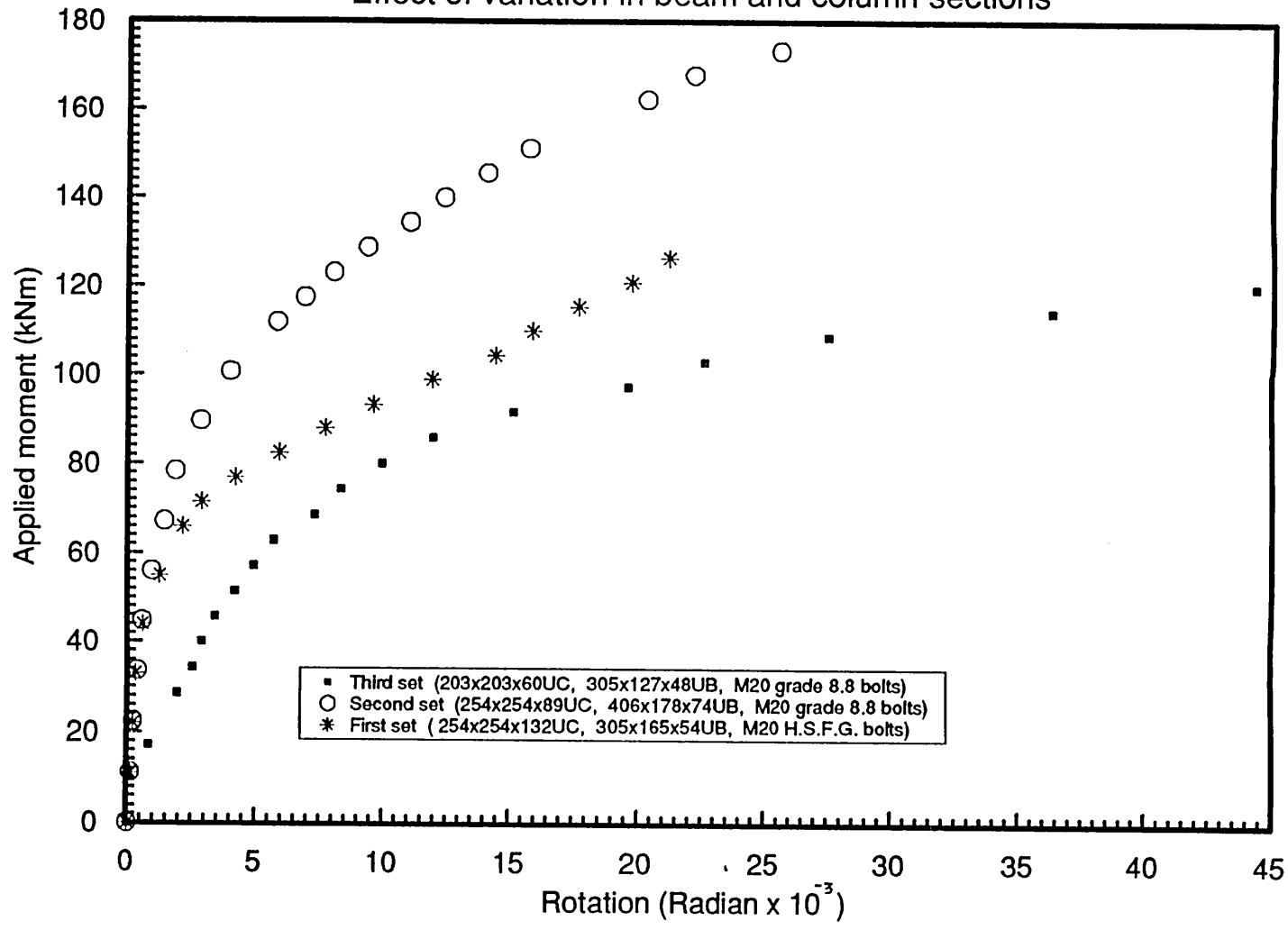

Fig. 6.17 Moment - Rotation curves for 15mm end plate connections;
Effect of variation in beam and column sections

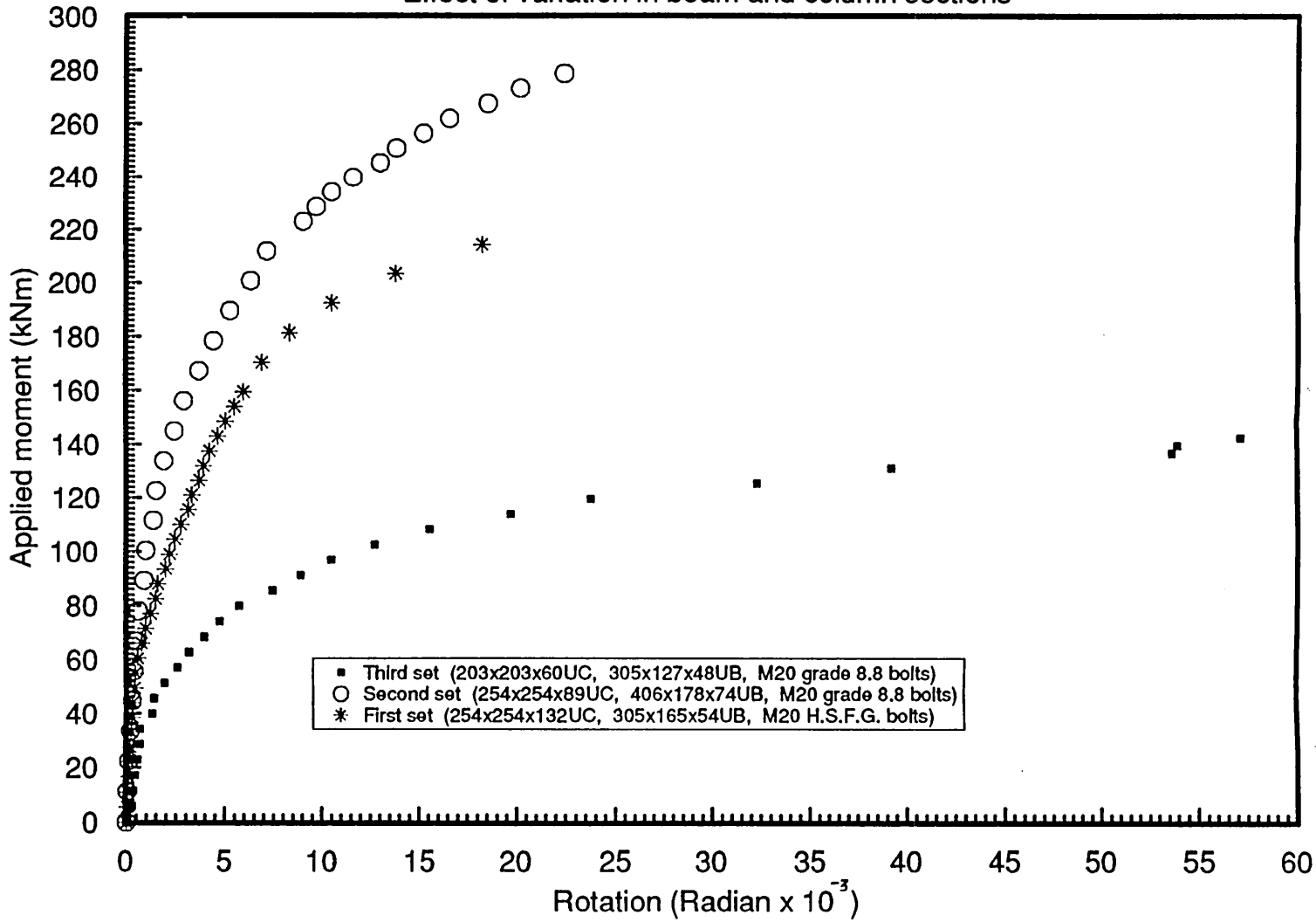

Fig. 6.18 Moment - Rotation curves for 25mm end plate connection;
Effect of variation in beam and column sections

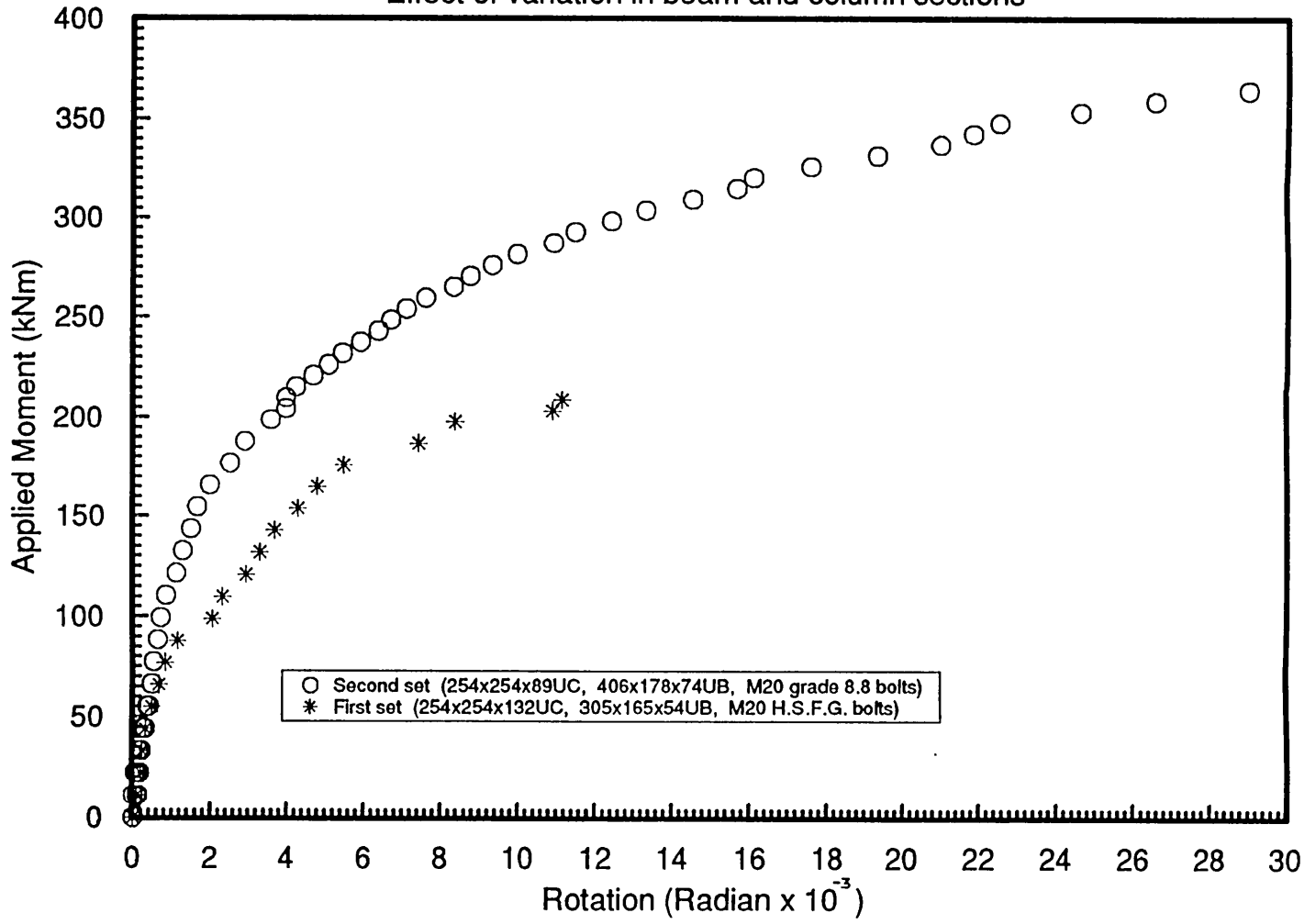

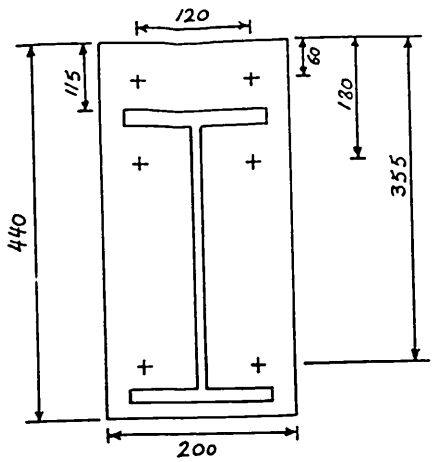

(a) First Set

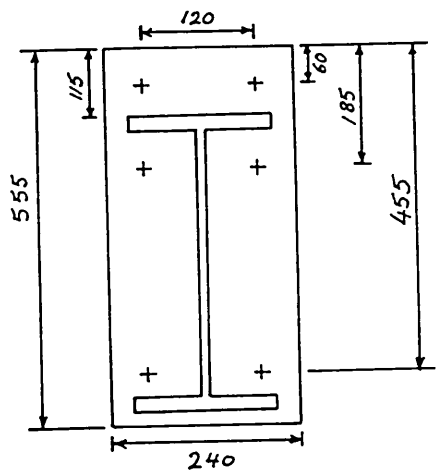

(b) Second Set

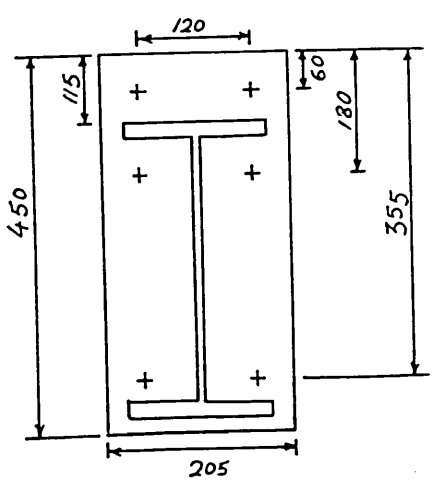

(All dimensions in mm)

(c) Third set

Fig. 6.19 End plate configuration

Fig. 6.20 Applied moment - Bolt force for 25mm end plate connection
in second set
(254x254x89U.C., 406x178x74U.B. with 20mm grade 8.8 bolts)

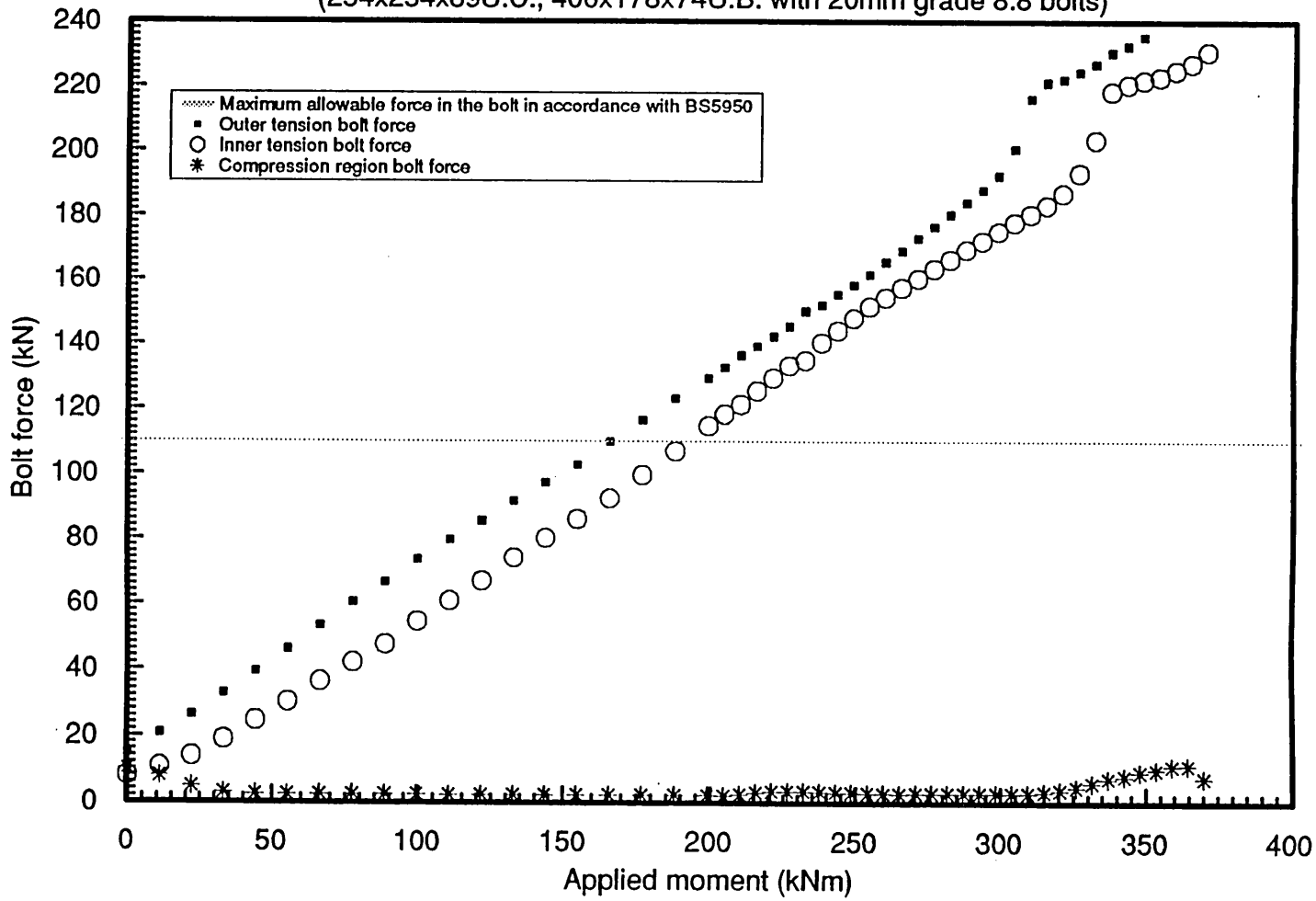

Fig. 6.21 Applied moment - Bolt force for 10mm end plate connection in first set
(254x254x132U.C., 305x165x54U.B. with 20mm H.S.F.G. bolts)

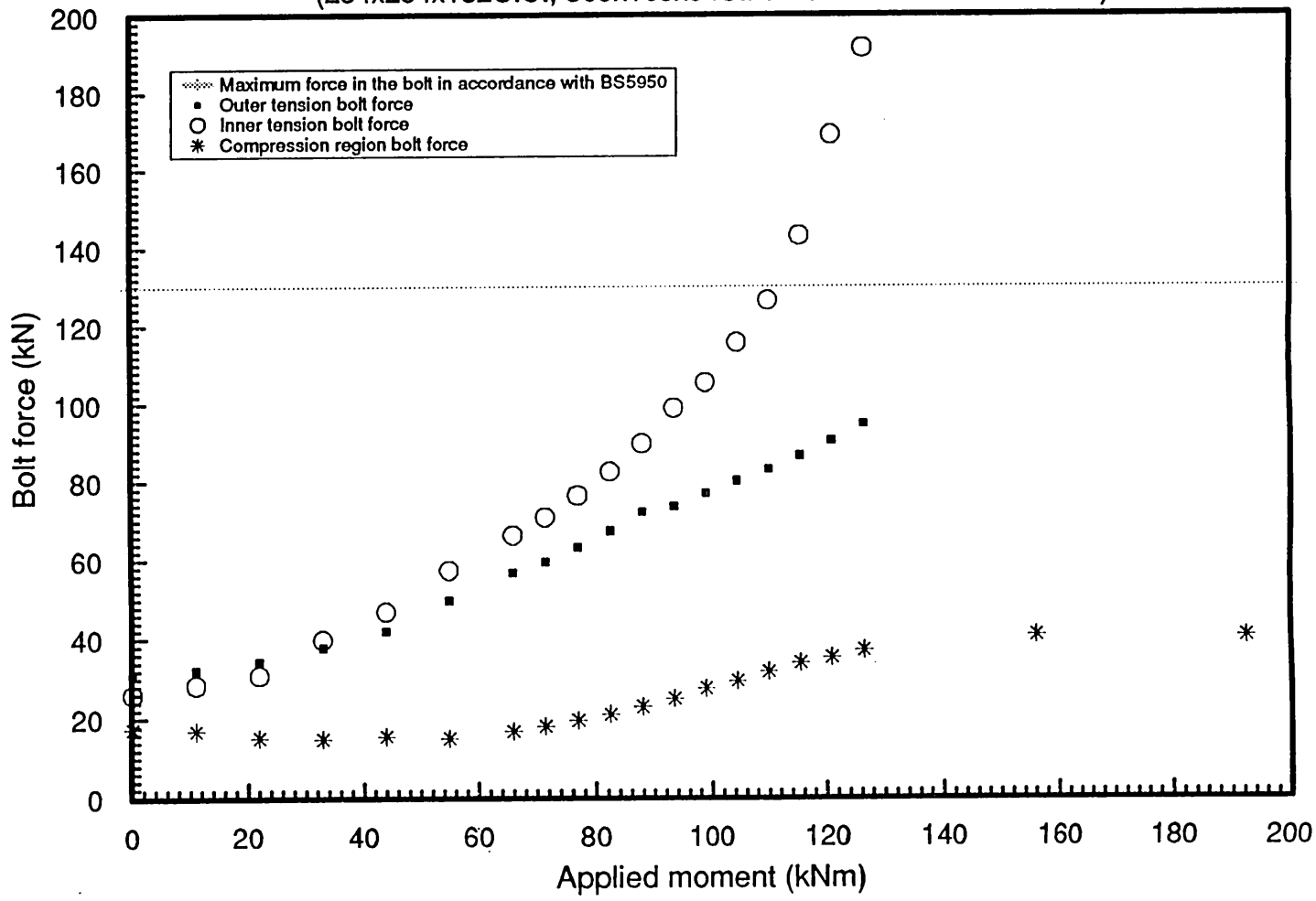

Fig. 6.22 Applied moment - Bolt force for 15mm end plate connection in first set
(254x254x132U.C., 305x165x54U.B. with 20mm H.S.F.G. bolts)

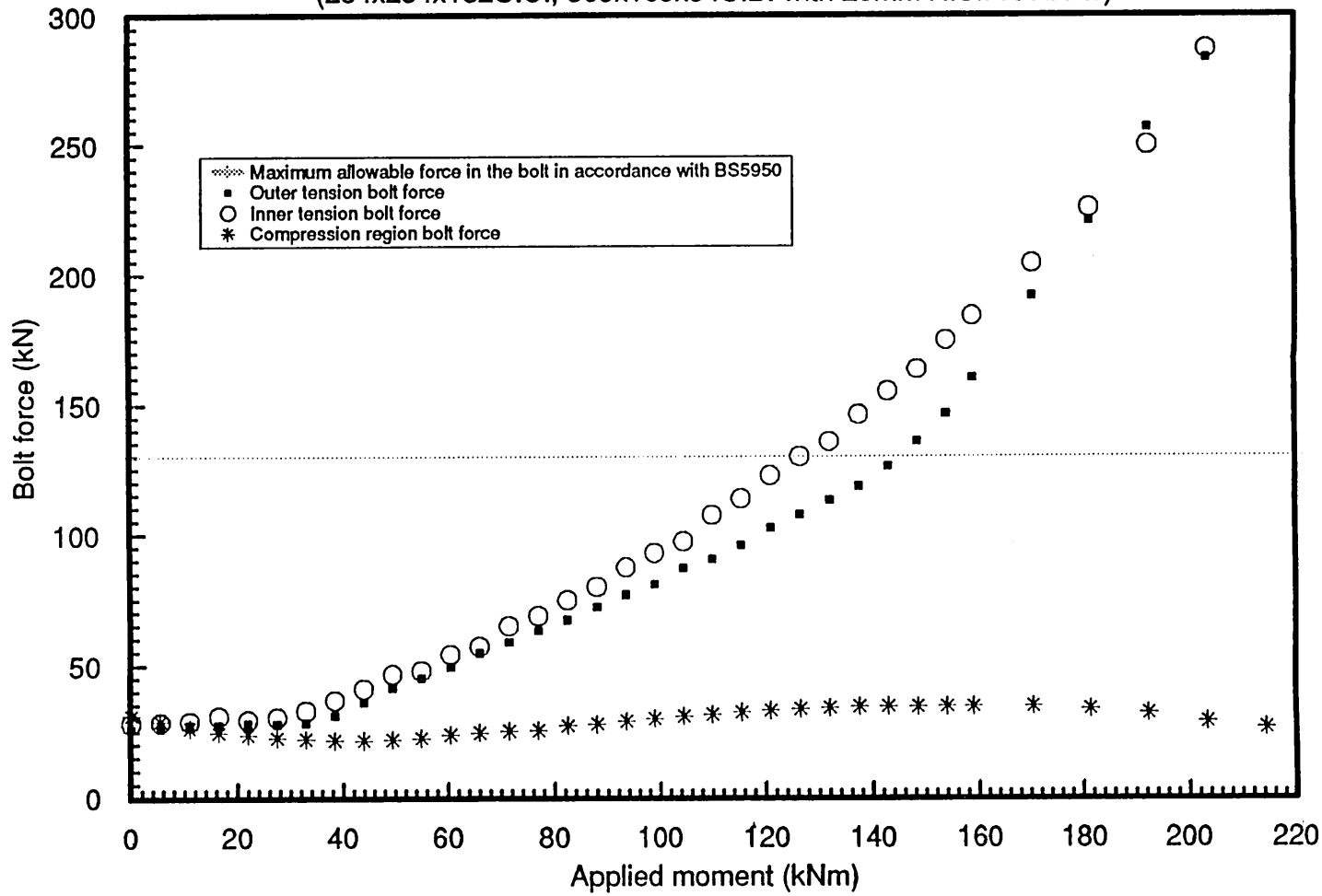

Fig. 6.23 Applied moment - Bolt force for 10mm end plate connection in second set
(254x254x89U.C., 406x178x74U.B. with 20mm grade 8.8 bolts)

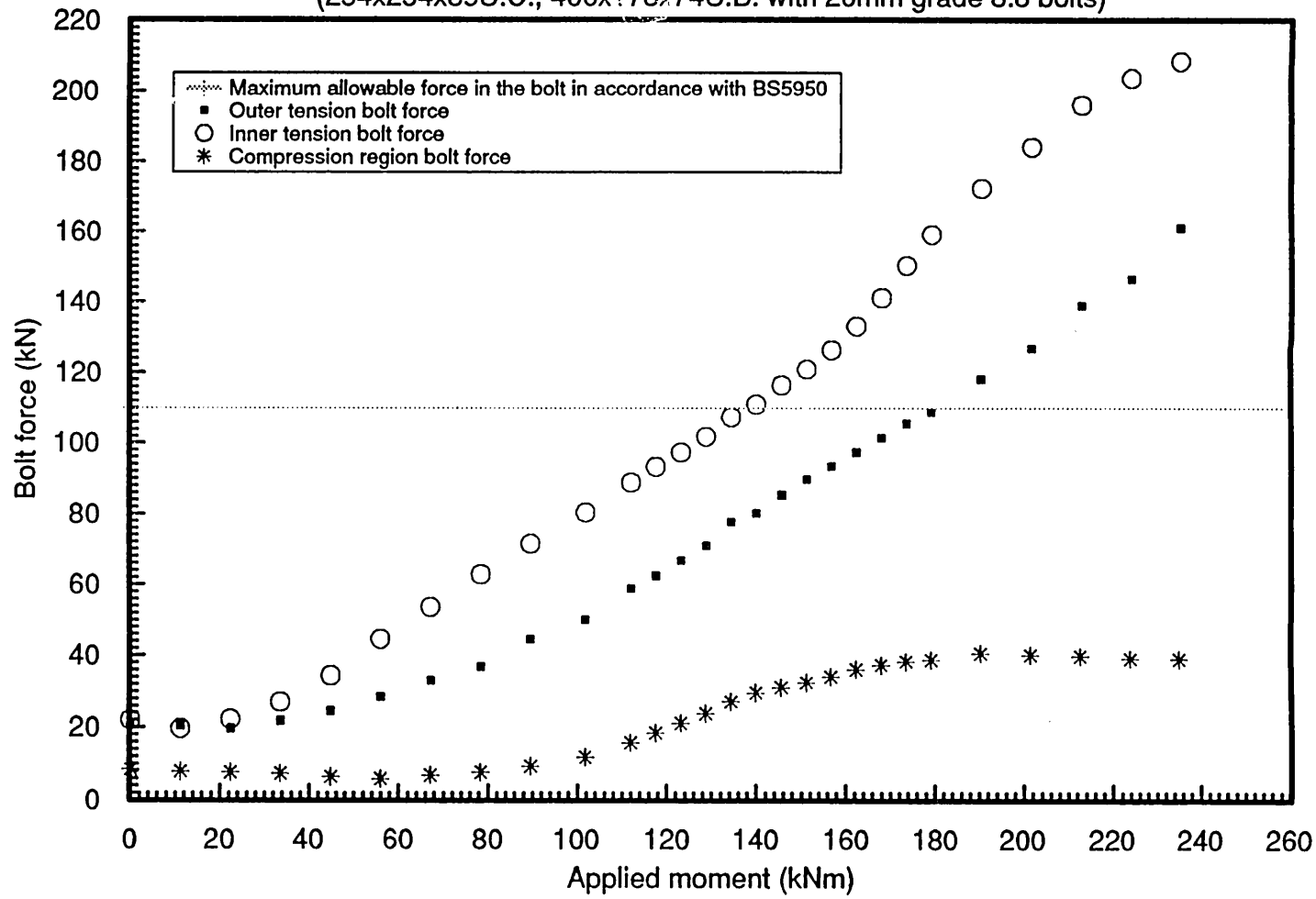

Fig. 6.24 Applied moment - Bolt force for 20mm end plate connection
in second set
(254x254x89U.C., 406x178x74U.B. with 20mm grade 8.8 bolts)

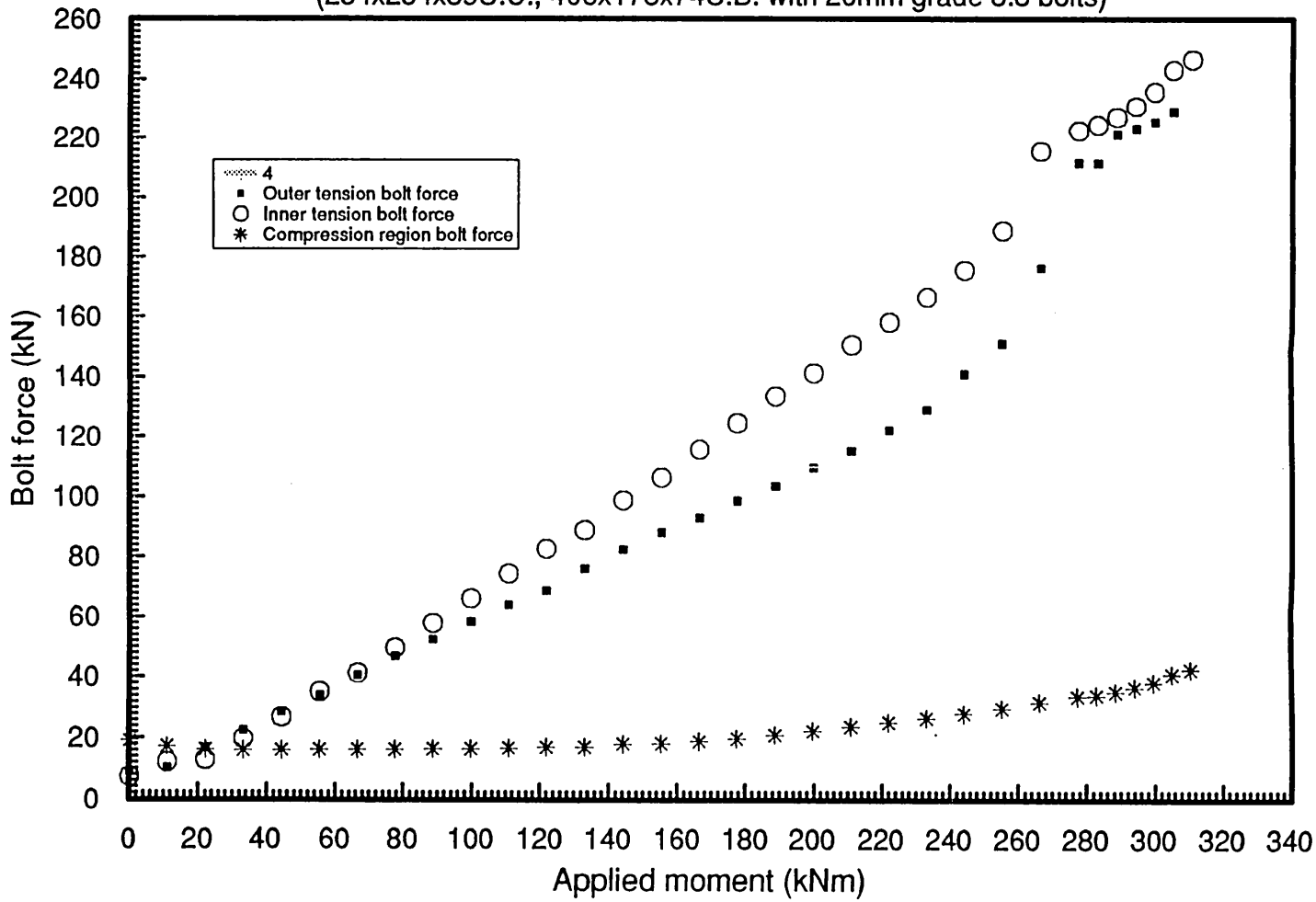

Fig. 6.25 Applied moment - Bolt force for 10mm end plate connection in third set
(203x203x60U.C., 305x127x48U.B. with 20mm grade 8.8 bolts)

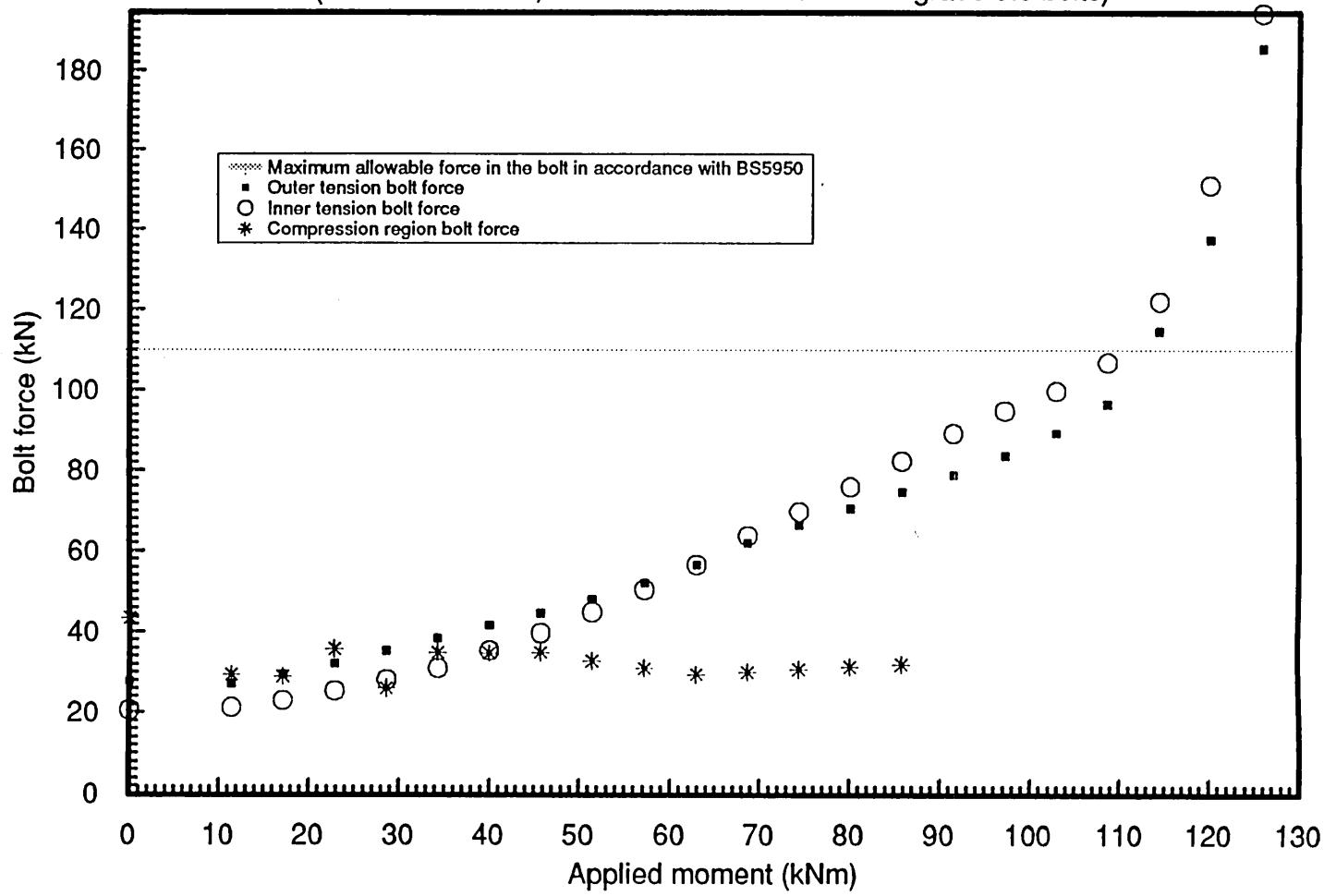

Fig. 6.26 Applied moment - Bolt force for 12mm end plate connection in third set
(203x203x60U.C., 305x127x48U.B. with 20mm grade 8.8 bolts)

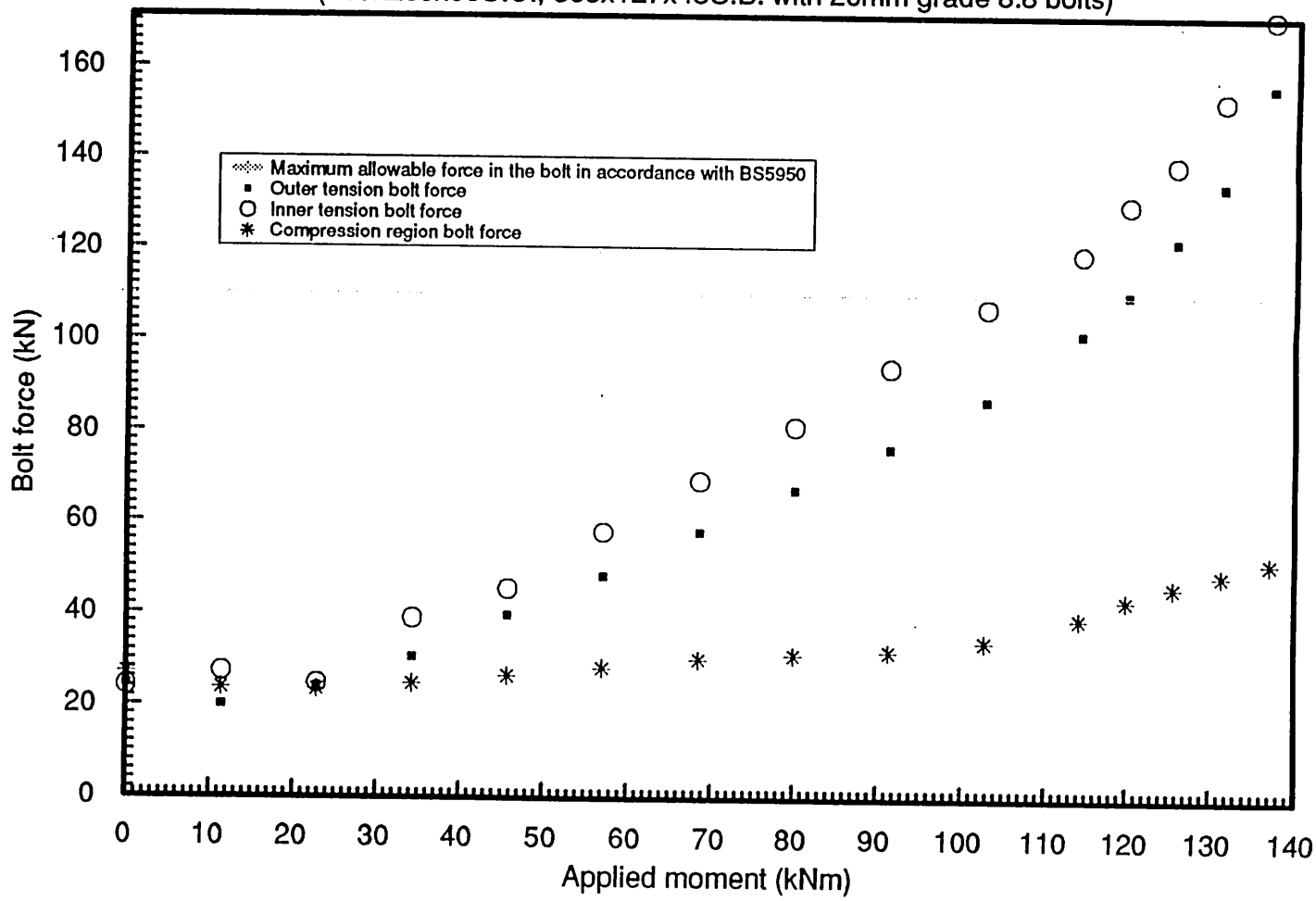

Fig. 6.27 Applied moment - Bolt force for 15mm end plate connection in third set
(203x203x60U.C., 305x127x48U.B. with 20mm grade 8.8 bolts)

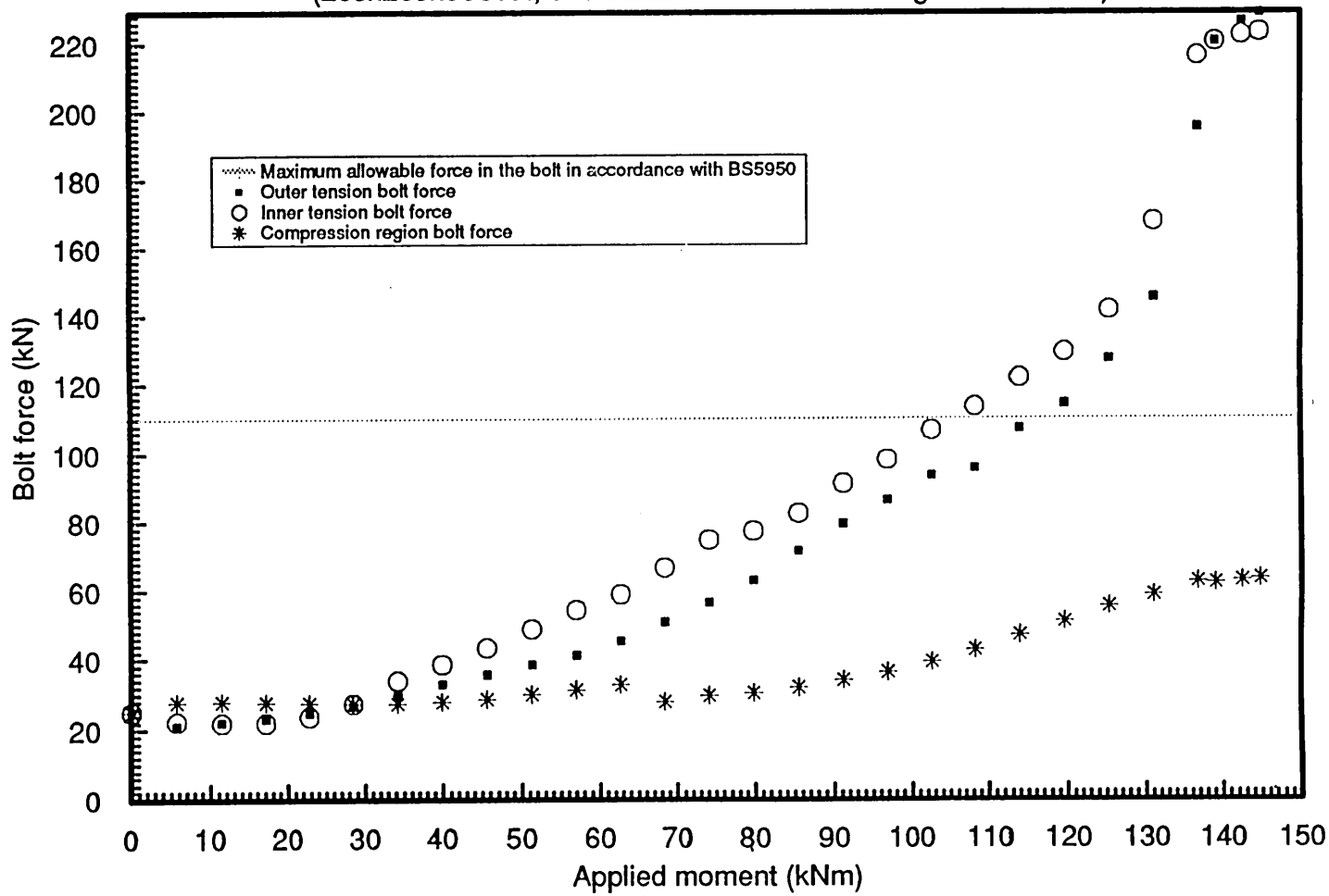

Fig. 6.28 Applied moment - Bolt force for 22mm end plate connection in first set
(254x254x132U.C., 305x165x54U.B. with 20mm H.S.F.G. bolts)

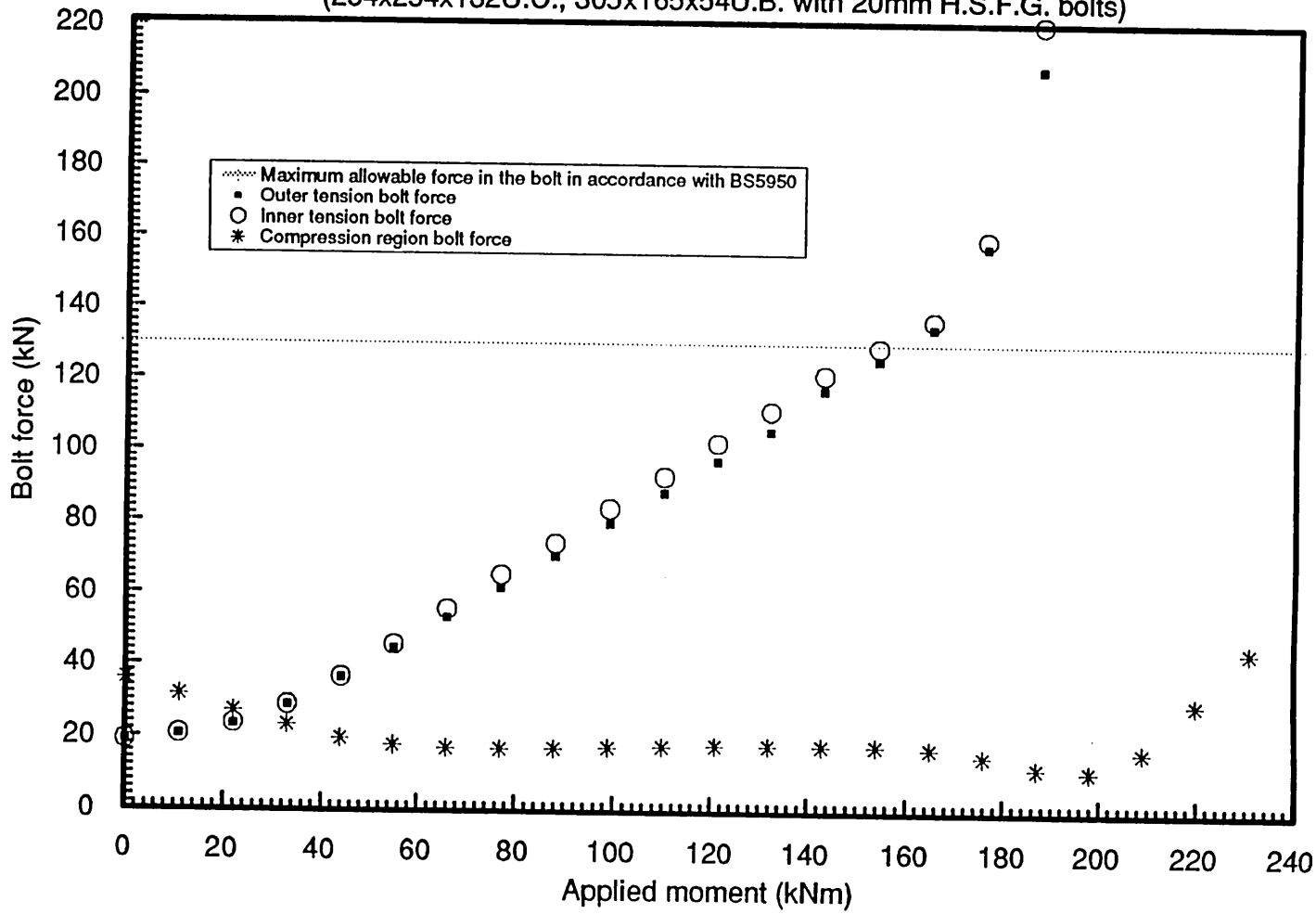

Fig.(6.29) Applied Moment - Bolt Force for 15mm end plate in second set (254X254X89U.C., 406X178X74U.B. with 20mm grade 8.8 bolts)

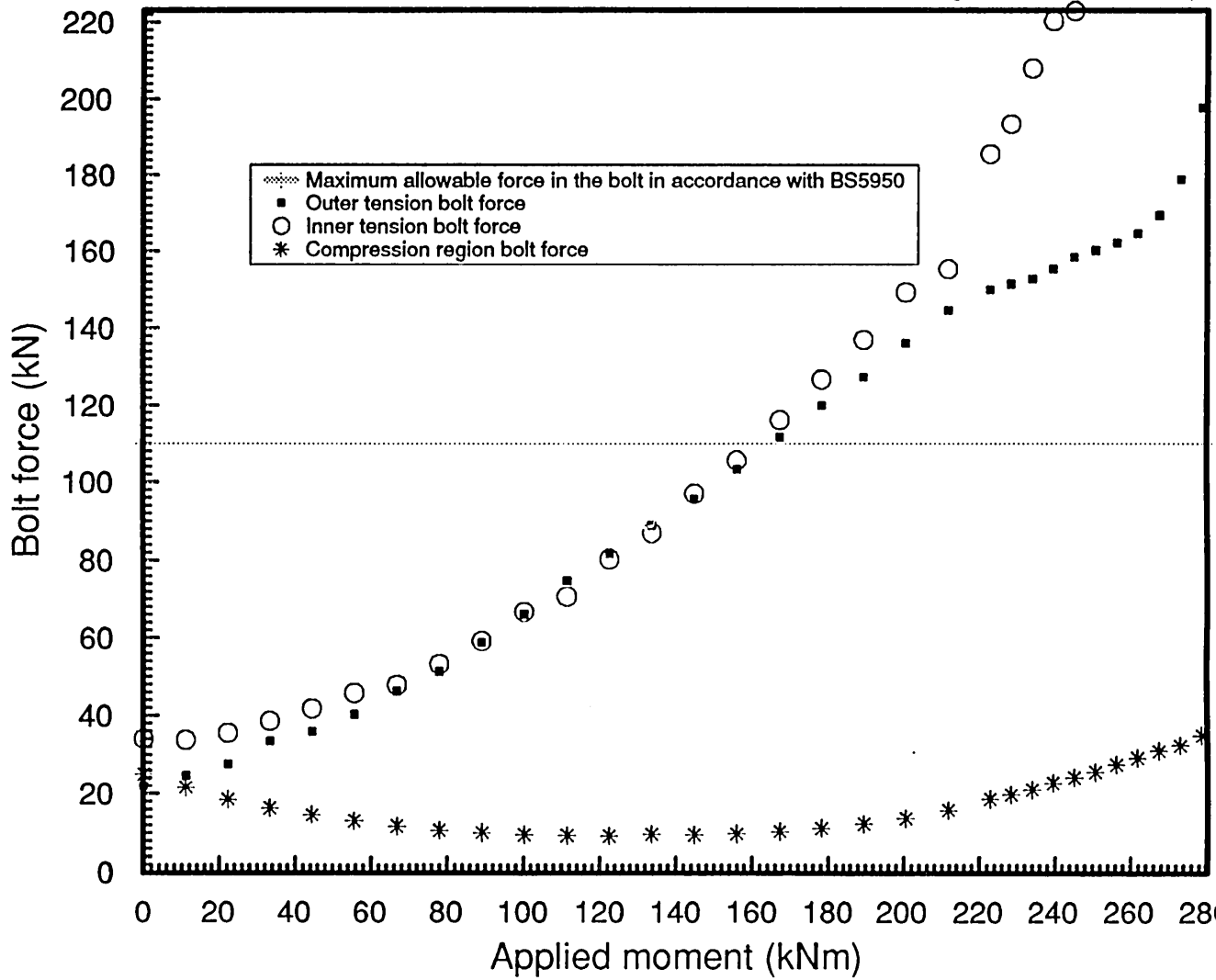

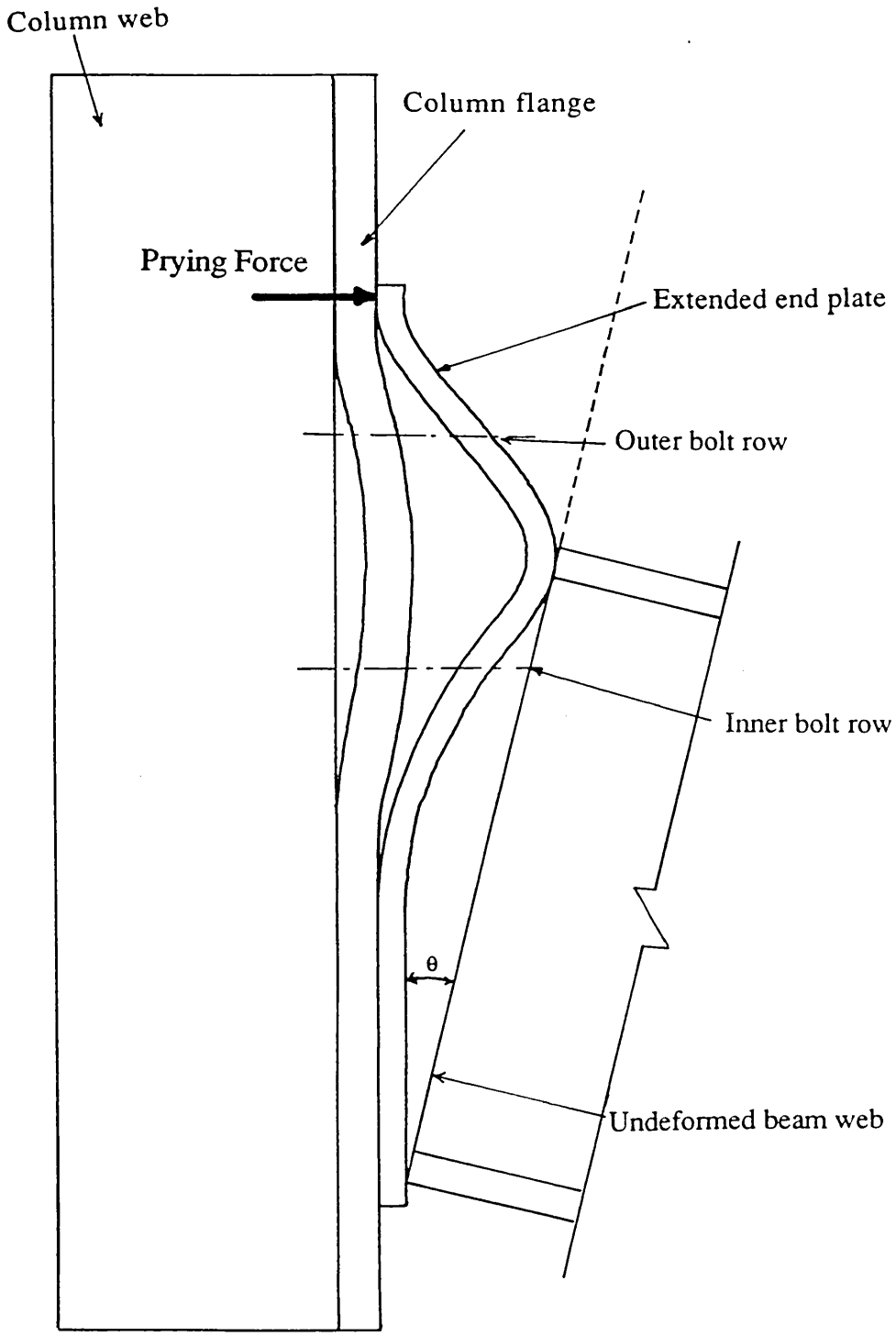

Fig. 6.30 Prying force diagram.

Fig. 6.31 Moment due to bolt forces - Applied moment for 22mm end plate connection (first set)
(254x254x132U.C., 305x165x54U.B. with 20mm H.S.F.G. bolts)

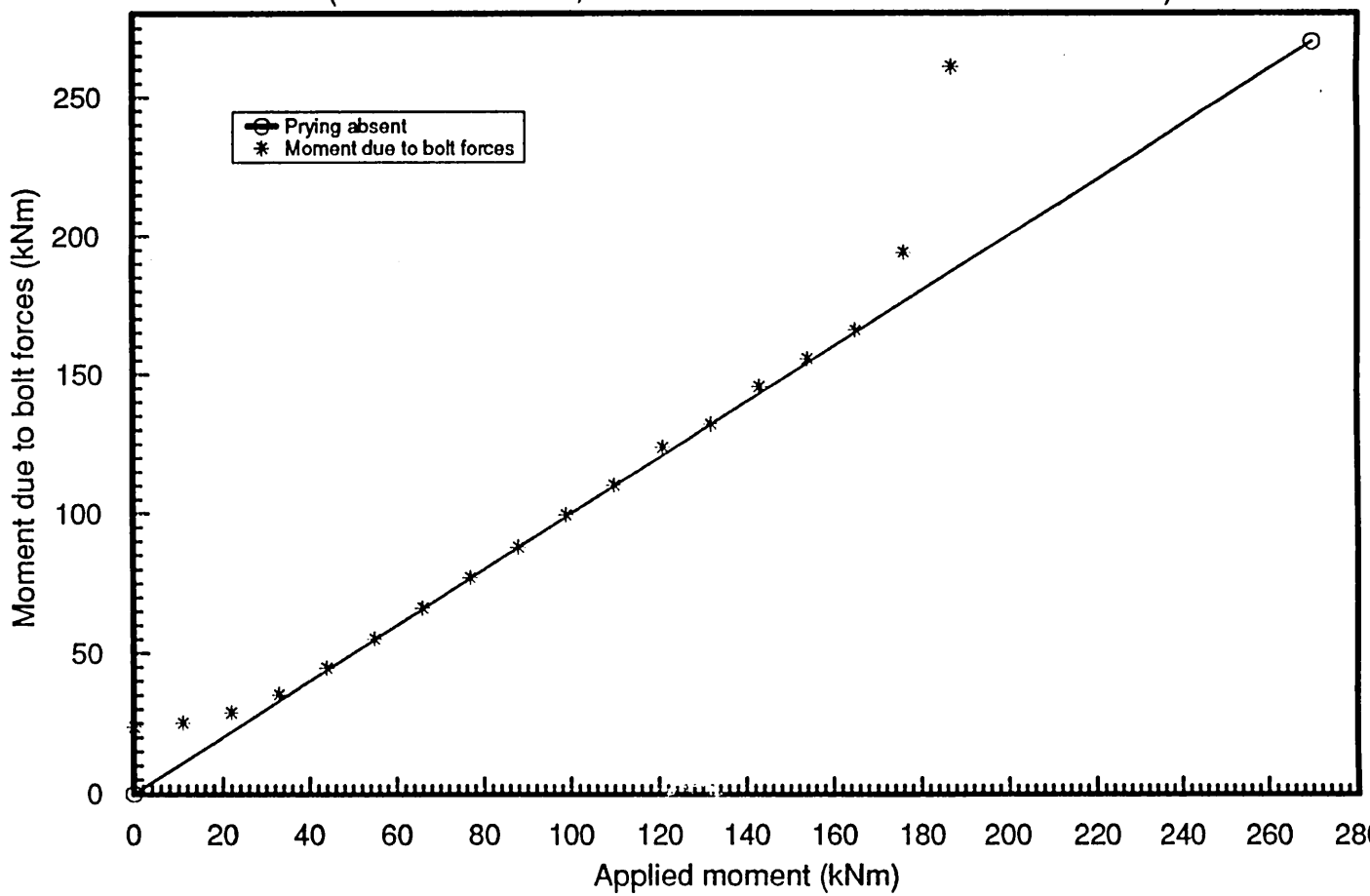

Fig. 6.32 Moment due to bolt forces - Applied moment for 20mm end plate connection (second set)
(254x254x89U.C., 406x178x74U.B. with 20mm grade 8.8 bolts)

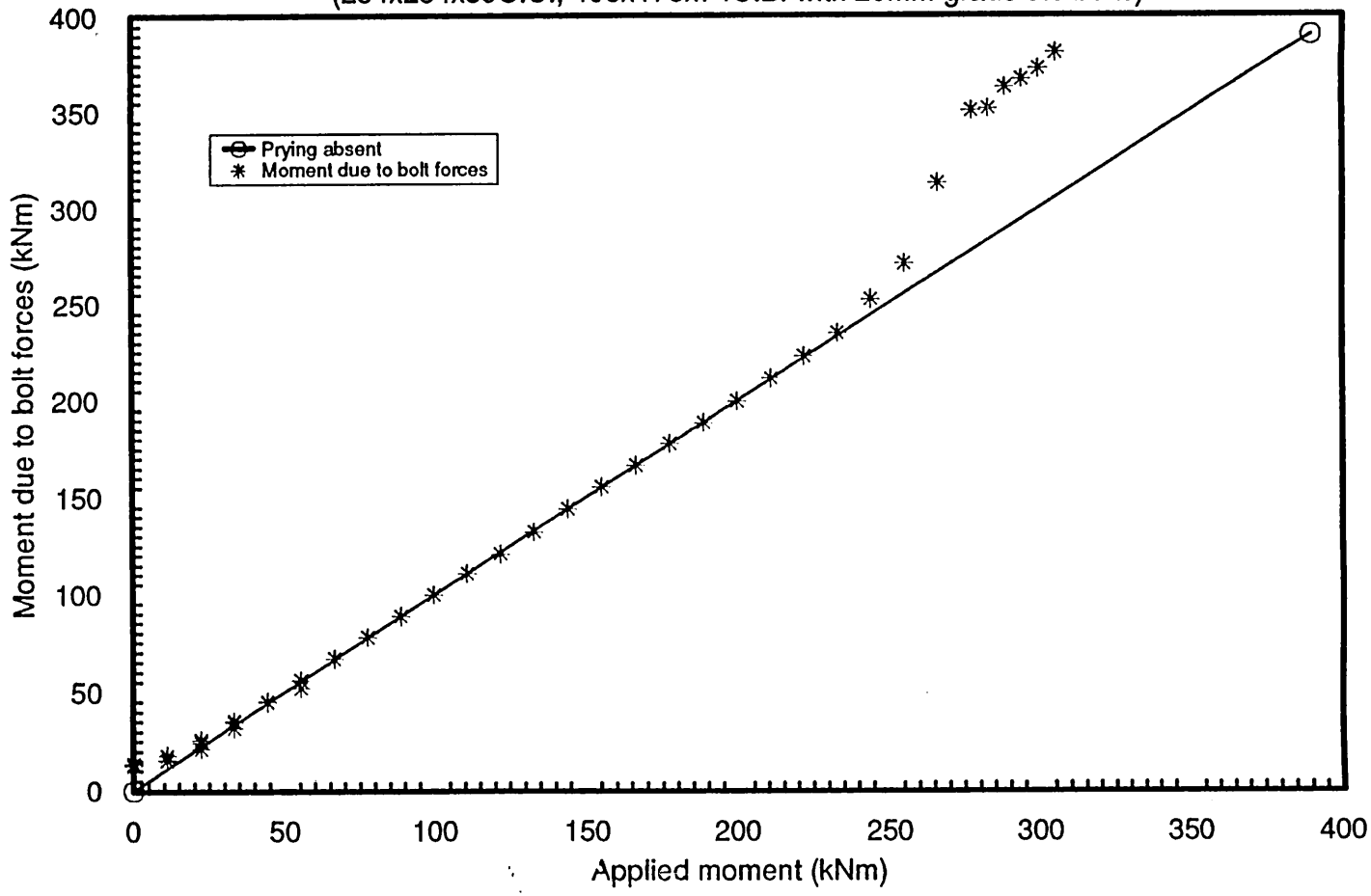

Fig. 6.33 Moment due to bolt forces - Applied moment for 25mm end plate connection (second set)
(254x254x89U.C., 406x178x74U.B. with 20mm grade 8.8 bolts)

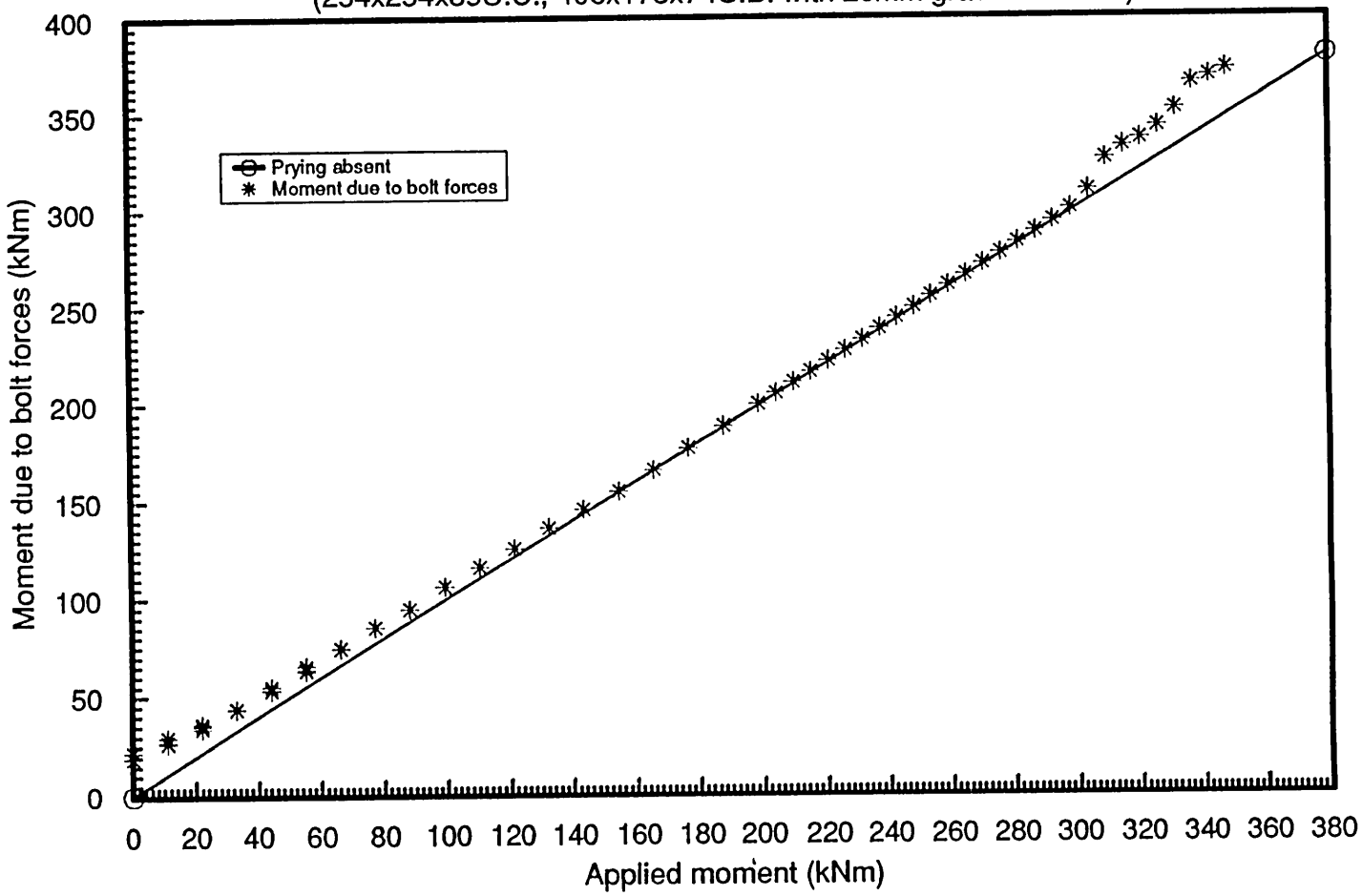

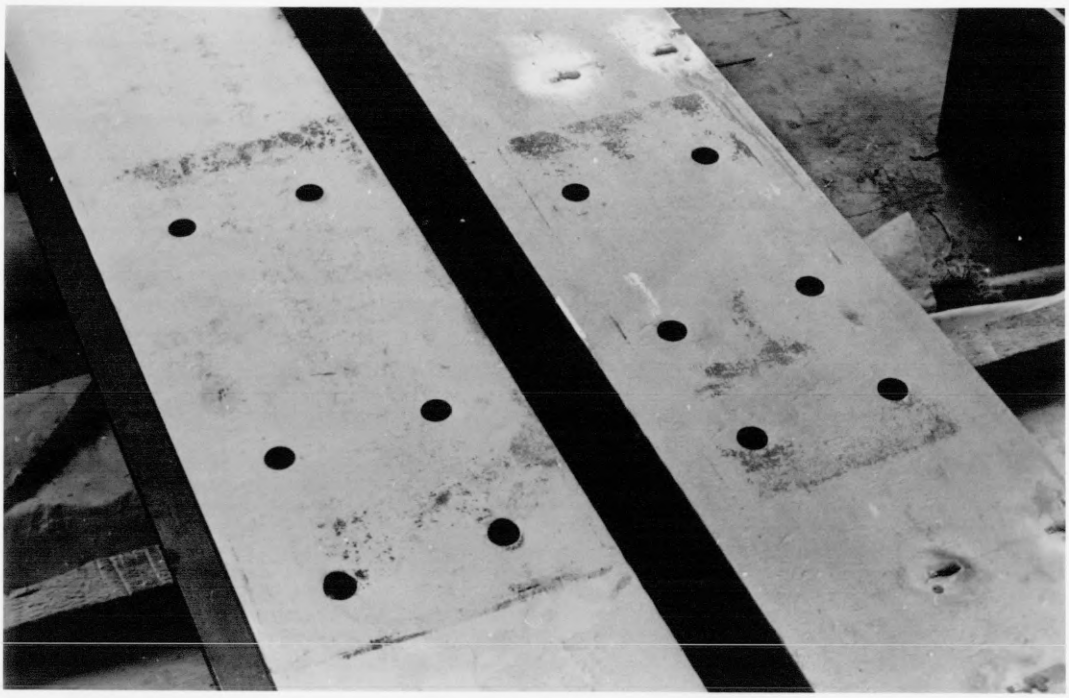

Fig. 6.34 Prying pattern for 20 and 15mm end plate connection (second and third set)

Fig. 6.35 Moment due to bolt forces - Applied moment for 10mm end plate connection (first set)
(254x254x132U.C., 305x165x54U.B. with 20mm H.S.F.G. bolts)

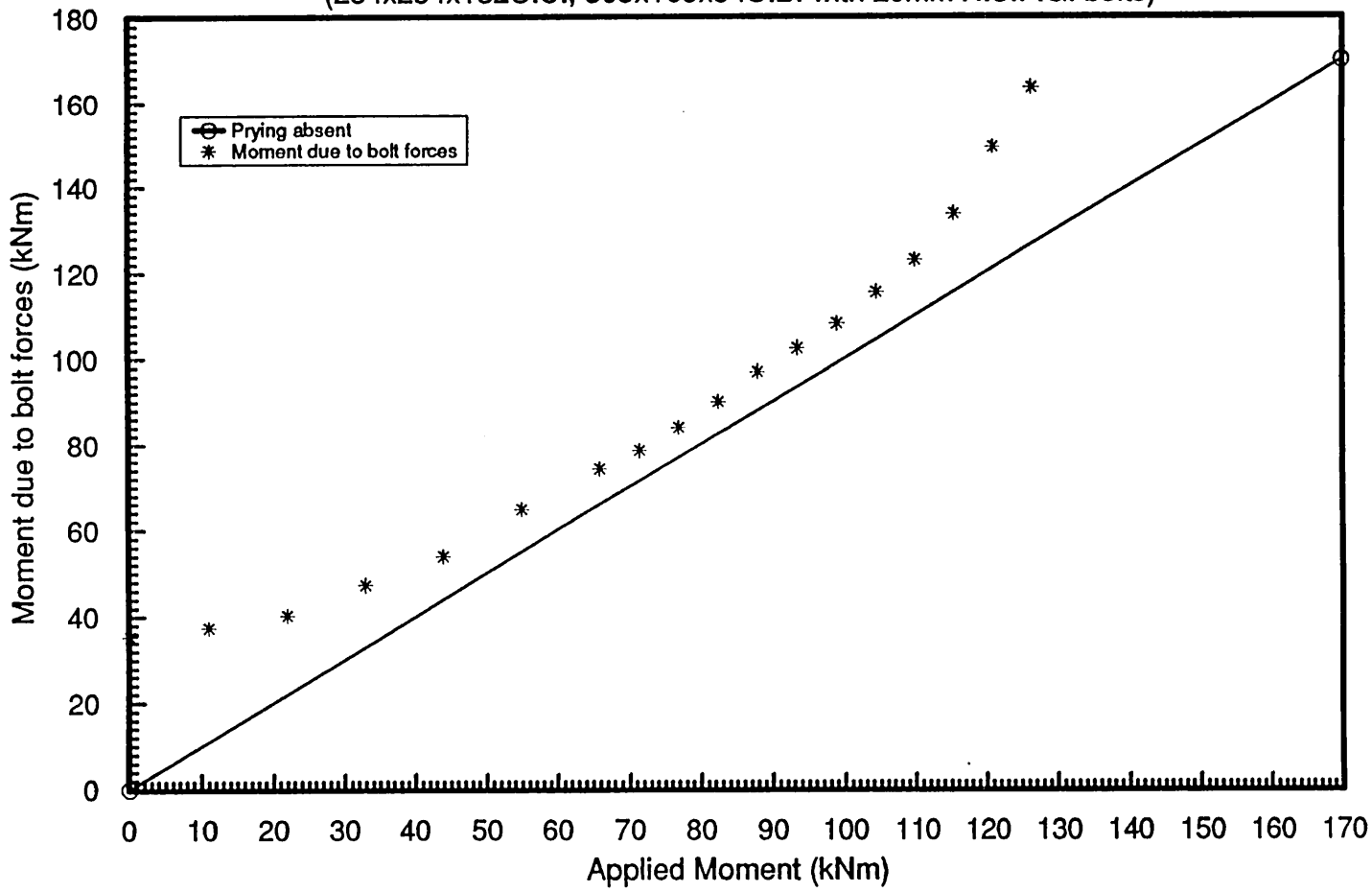

Fig. 6.36 Moment due to bolt forces - Applied moment for 12mm end plate connection (third set)
(203x203x60U.C., 305x127x48U.B. with 20mm grade 8.8 bolts)

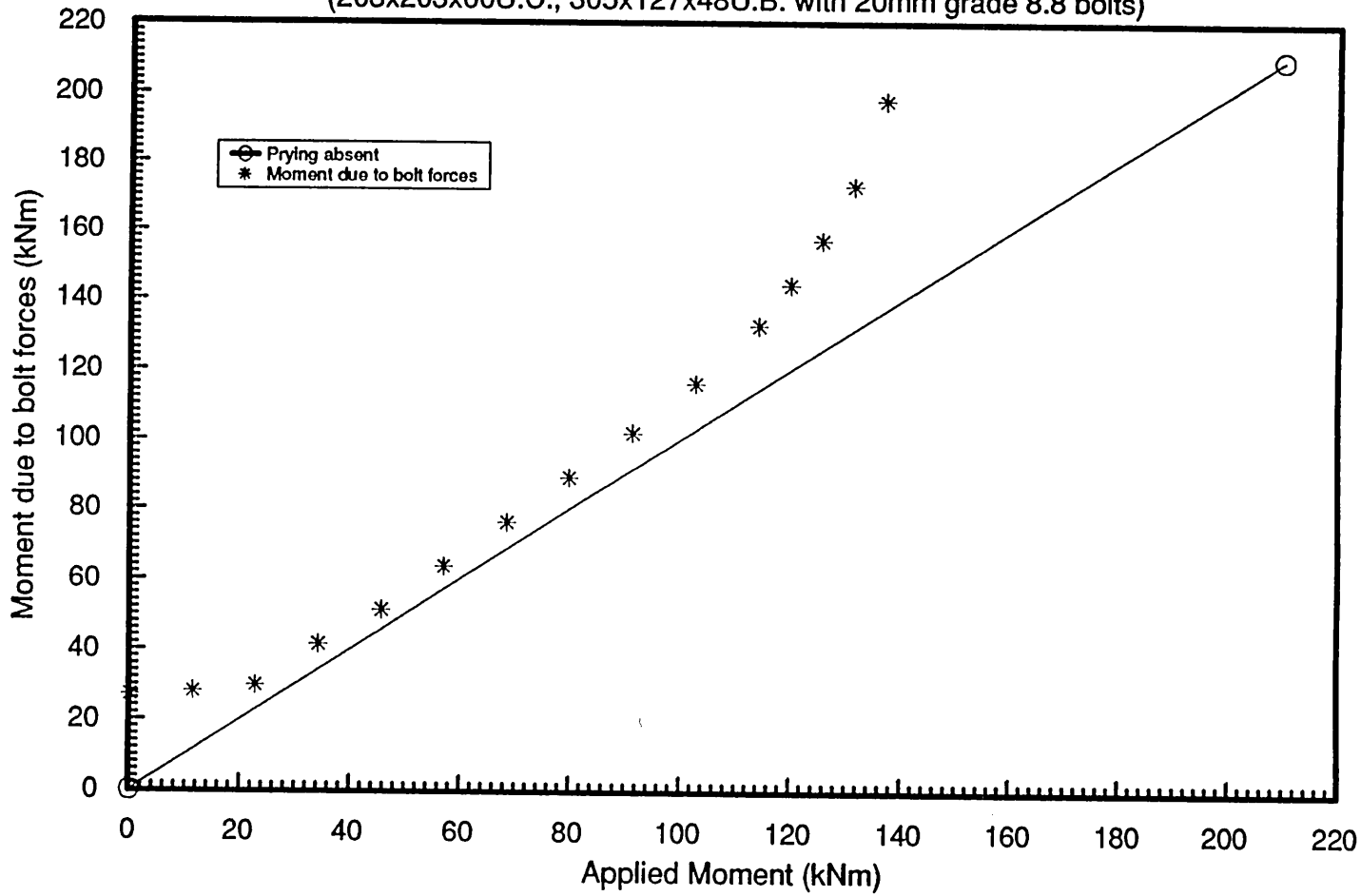

Fig. 6.37 Moment due to bolt forces - Applied moment for 10mm end plate connection (third set)
(203x203x60U.C., 305x127x48U.B. with 20mm grade 8.8 bolts)

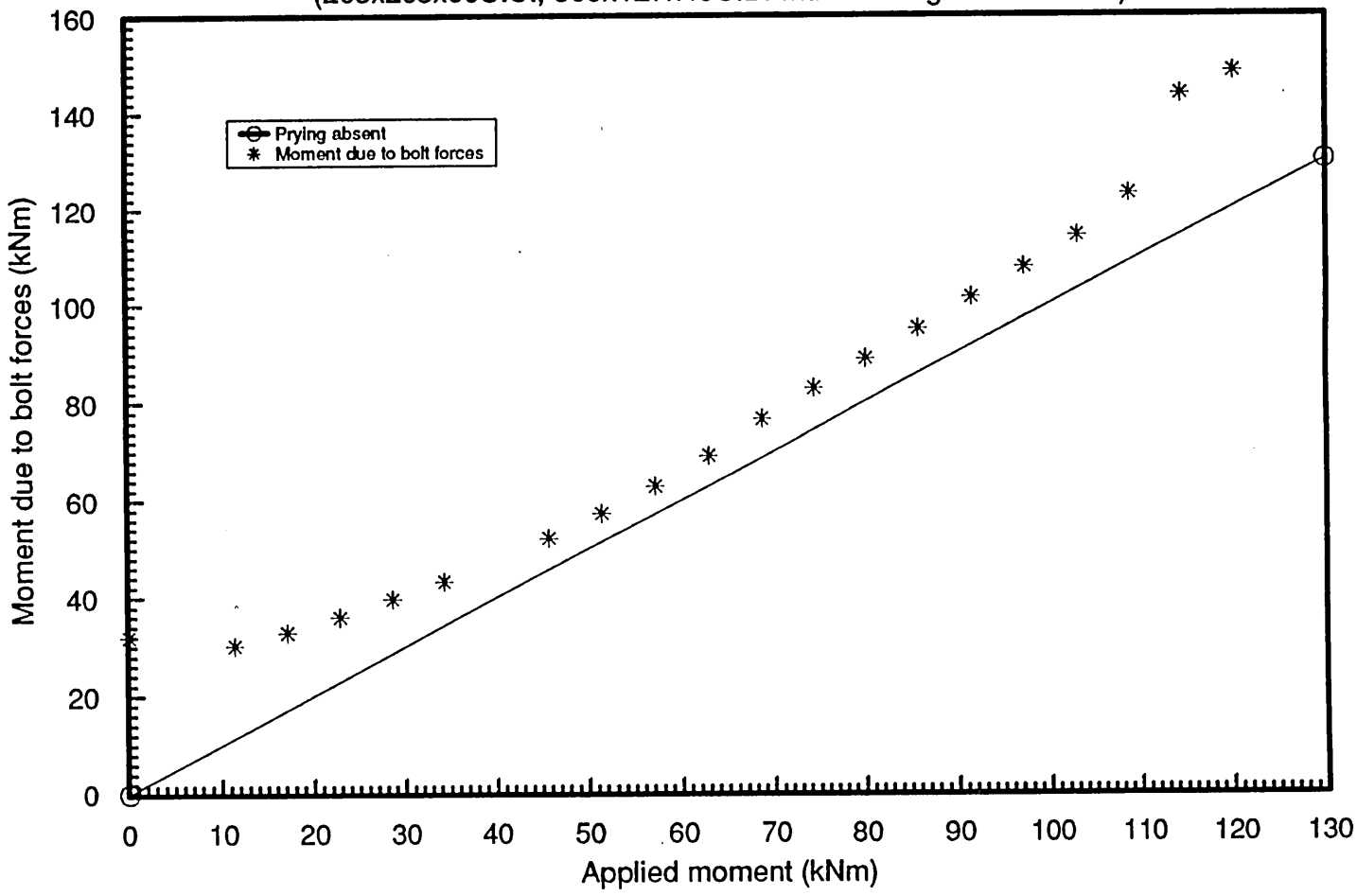

CHAPTER 7

Comparison between Experimental and Theoretical Results

7.1 Introduction

As stated previously, the most important properties of a connection which have significant effect on the overall performance of the structure are its strength, stiffness and rotational capacity. These properties can be obtained directly if the moment-rotation curve of the connection is available. Thus the knowledge of moment-rotation curve is a prerequisite for the design of any type of connection. It is therefore not surprising to find numerous studies in which the objective has been to provide a method of predicting the moment-rotation characteristics of semi-rigid joints. A meaningful study of the extended end plate joint behaviour would need to consider its three dimensional nature, which had rarely been appreciated. It was with this in mind that the current research was undertaken by the author. It was hoped that the investigation would culminate in the formulation of a limit state design for this type of connection.

The finite element analysis of the unstiffened extended end plate connection was divided into three stages. In the initial stage the main objectives were to examine the applicability of three dimensional finite element analysis method to extended end plate connection and to assess the validity of the few simplifying assumptions made in modelling the connection. These were realized by comparing the results of the linear elastic analysis with experimental results. Introduction of the finite element package LUSAS caused some uncertainty and offered challenge at this stage of project. Hence, familiarizing with LUSAS and assessing its potentialities became the first priority. Such task was more daunting and time consuming than it was originally realized due to a variety of reasons, e.g. vagueness of the LUSAS manual, frequent updating of the package and the lack of expert guidance.

This was to be the first comprehensive three dimensional analysis attempted of the unstiffened extended end plate connection and initially an elastic analysis of 15mm end plate connection from the first series of tests(254x254x132UC, 305x165x54UB and M20 H.S.F.G. bolts) was carried out. In order to test the validity of the proposed model it was necessary to check the balance of the forces and applied moments, observe the general pattern of deformation of the end plate and column flange and compare between the theoretical and experimental bolt forces and moment-rotation relationship. Also the interaction between the end plate and column flange was investigated. The comparison between the moment-rotation curves showed that for the same rotation the theoretical solution produced lower moment than the

experimental value. This was because an arbitrarily high modulus of elasticity of steel (210 kN/mm^2) was used in the analysis. Similarly the theoretical values of bolt forces were lower than the experimental values. Nevertheless the results of this analysis demonstrated that the three dimensional model of the 15mm end plate connection (first series) behaved in an appropriate manner and all the assumptions made were correct.

The objective in the second stage of the investigation was to ascertain the overall performance of unstiffened extended end plate connections over the entire range covering elastic and plastic states until failure occurred. A total of three models were investigated (15mm end plate connection in the first and second set and 10mm end plate connection in the third set) to evaluate the accuracy of the proposed modelling technique and the effect of the simplifying assumptions made. In the investigation the actual material properties obtained from the tensile tests of grade 43A steel and bolts (grade 8.8 or H.S.F.G.) were used. The output from the finite element analysis covering the entire elastic-plastic range consisted of the following:

(a) stresses and strains in the solid elements;

(b) forces and strains in the bar elements;

(c) forces and strains in the joint elements; and

(d) displacements at nodes.

The accuracy of the nonlinear finite element analysis was established by comparing the following connection properties derived from the theoretical results with the results obtained from the experimental investigation:

(a) moment- rotation curves;

(b) bolt forces;

(c) prying forces; and

(d) strains at preselected points on end plate and column flange.

In the final stage of investigation a parametric study of the above models was carried out with the aim of separating the input from various joint components towards the rotational stiffness of the connection. The ability to determine the contribution of each component is essential for the development of a suitable design method. In pursuit of such an objective each model was analysed twice. In the first analysis all the nodes on the column (flange and web) and at bolt positions on end plate were restrained in order to eliminate the contribution of the bolts and column towards the rotational behaviour of the joint, which could then be attributed to the end plate only. Second analysis was carried out with fictitiously very high modulus of elasticity and yield stress for bolts and end plate materials to reduce the deformation in these members to an insignificant level; hence the rotation of the connection was entirely due to column flange deformation.

7.2 Moment-Rotation Characteristics

The moment-rotation relationship of a connection demonstrates the rotation sustained by the joint under the influence of applied moment. This characteristic is fundamental in the behavioural analogy of all joints in structural analysis. Therefore, the accuracy of the finite element model of the connection can be assessed by comparing the theoretical with the experimental moment-rotation relationship.

As stated previously, the moment acting at the beam end is replaced by a couple whose forces act at the level of beam flanges. In these models the load is distributed uniformly on the beam tension and compression flanges. Hence the theoretical moment can be obtained by multiplying either tension or compression flange force with the depth of the beam. The calculation of joint rotation is complicated since centre of the rotation of the connection is not readily definable. The position of the rotational axis of the beam depends on the thickness of the end plate and column flange. From the theoretical and experimental results it can be seen that, at low moment, the centre of rotation is located above the compression flange of the beam which moves towards the bottom edge of the end plate with increasing moment. However, in the subsequent calculation of the theoretical rotation, it is assumed that the beam rotates about an axis at the mid-depth of its compression flange. Therefore, the joint rotation can be determined by dividing the difference between the displacements at the tension and compression flanges by the depth of the beam.

The comparison between the experimental and theoretical moment-rotation curves obtained for three connections (15mm end plate connection from the first and second set and 10mm end plate connection from the third set) are presented in Figs. 7.1, 7.2 and 7.3. There is a good agreement between the experimental and theoretical results for each of the connections. However, in the elastic range the theoretical moment-rotation curves are linear whereas the experimental ones are not. This non-linearity in the experimental curve can be attributed to the combination of pretensioning effect, imperfection in the set up and lack of fit. As none of these effects could be included in the analytical model, the results could only be linear. The theoretical moment-rotation curves for 15mm end plate connections (first and second set) indicate lower moment than the experimental value for similar rotation, particularly in the elastic range. This discrepancy may be caused by the lack of consideration of weld, heat affected zone and bolt head in the modelling of the connection. Although it can be argued that omitting bolt holes will compensate some of the losses in joint rigidity due to the above simplification, it does not fully restore the loss of stiffness caused by them. Also, in the theoretical analysis an element is assumed to yield if the stress in the element reaches the specified yield stress, while in practice plastification begins and spreads in the plane of the plate as well as through its thickness. Therefore, the theoretical strength of the element is less than the actual value. The theoretical results in the plastic range can be improved if a finer element mesh is adopted in the modelling of the connection.

The finite element analysis of 10mm end plate connection (third set) was terminated prematurely. This was caused by failure in the power supply of the computer system. However, from the graph (Fig. 7.3) it can be seen that in the plastic range the theoretical analysis overestimates the rigidity of the connection. This problem was more acute in joints where the failure was due to web buckling. In the analysis only a quarter of the column section was considered taking advantage of the symmetry of the connection configuration and all the nodes at the outer plane of the web were restrained from any out-of-plane displacement and rotation. Similarly, at the column mid-depth all the nodes in the plane of symmetry were restrained in all directions. These boundary conditions prevent any out-of-plane deformation of the web. Therefore, the web contribution as a result of bowing towards the overall joint rotation has not been included in the analysis. Also, the theoretical analysis only considers the material non-linearity in which both strains and displacements in the structure are assumed to be relatively small. Such assumptions mean that the geometry of the element remains basically unchanged during the loading process. In practice such assumptions are not always correct, especially when the structure has yielded. Experimental results confirm that in steel structures actual displacements at failure are larger than the theoretical values derived in which geometrical non-linearity has been ignored. These result in overestimating the element strength in a thin end plate and column flange.

The rotational stiffness of a connection is composed of the contributions from individual components and for the formulation of a design method it is essential to determine the separate contribution of each component. The results of such study are presented in Figs. 7.4, 7.5 and 7.6. They clearly demonstrate that the rotations in all finite element models are attributable to the combination of deformation due to end plate flexure and to a lesser extent of column deformation with very little contribution from the bolts. Since the bolts and in particular H.S.F.G. bolts are made of high-tensile steel, they exhibit very low extension properties. From these graphs the rotational stiffness of each component can be determined which can lead to a design method for unstiffened extended end plate connection.

7.3 Bolt Forces

In bolted end plate connections the applied load is normally transferred to the bolts through the end plate. In order to understand the overall behaviour of the connection, it is essential to know the response of the bolts to gradually increasing moment. Although the behaviour of individual bolts has been extensively investigated, their exclusive response within the connection has received scant attention. Such lack of information has forced the design engineers to provide a large load factor in order to ensure the strength of the steel structure. In order to bridge the existing gap it was decided to include the bolts in the theoretical model of bolted end plate connection.

As stated previously, in all specimens the applied moment was resisted by six bolts, four of which were located near the beam tension flange and the remaining two were placed near the beam compression flange. From the experimental results it was confirmed that the tensile force induced by the beam tension flange is carried primarily by tension group of bolts while the compressive force in the beam compression flange is resisted by bearing acting over an area near the bottom of the connection. Although some tensile force was measured in the compression bolts it was not included in the finite element model since its contribution towards the moment capacity of the connection was considered to be insignificant. In order to establish the accuracy of the proposed model a comparative study of forces in the inner and outer tension bolts was carried out for three extended end plate connections and the results are presented in Figs. 7.7, 7.8 and 7.9. They indicate good agreement between theoretical and experimental bolt forces over a wide range of loading. However, in the early stage of loading the experimental bolt forces are higher than their corresponding theoretical value. These differences are considered to be due to the effect of pretensioning. Although throughout the experimental programme the pretensioning of bolts was kept to a minimum, a degree of tightening was necessary to provide a reasonable contact between the end plate and column flange. This initial force had not been considered in the theoretical analysis. Once the pretensioning is overcome, both experimental and theoretical curves follow a similar path. The discrepancy between the two results at high load can be attributed to severe bending deformation of the bolts induced by large deformation of the plates which causes

flexural stress in the bolts. The bar elements representing the bolts in the finite element model could not take account of any bending deformation in the bolts.

The theoretical bolt force results also indicate that the forces are not distributed equally between the two rows of bolts in the tension region. The distribution of the bolt forces is influenced by the relative thickness of the end plate and column flange and the depth of the beam. From Fig. 7.7 it can be seen that, for 15mm extended end plate connection (first set), the inner bolt row attracts higher percentage of the applied load. Such pattern of force distribution within a bolt group is typical of the joints with relatively thin end plates as discussed in chapter 6. However, the experimental results suggest that the onset of yield in any of the components will reverse the rate of increase of the force in the inner and outer bolt rows (ie. the force in the inner bolt row increases at a slower rate than the force in the outer bolt row) until the forces are equal in both rows. Such behaviour is not evident from the theoretical bolt force results which could again be attributed to the effects of bending deformation of bolts.

Investigation of extended end plate connection will be incomplete without the determination of the magnitude and location of prying forces. The bolt force distribution for an applied moment cannot be ascertained by consideration of statics alone. Equilibrium and compatibility must be taken into account and the existence of prying forces must be acknowledged. Prying forces can develop and change position during loading. From previous research[21] it has been established that for an extended

end plate connection, there is a concentration of heavy pressure at the compression edge of end plate due to load transfer from the beam compression flange. Also at the upper and side edges further concentration of pressure occurs due to bending curvature of the end plate. The effect of these contact forces is to increase the actual bolt forces which can be important in extended end plate connections. This has been demonstrated in Figs. 7.10, 7.11 and 7.12 in which the moment obtained by multiplying bolt forces with the distance between the bolts and the beam compression flange is plotted against the applied moment. It can be observed that the moment due to bolt forces is consistently higher than the applied moment for thin end plate connection (10mm end plate). The comparative study of the theoretical and experimental prying results indicate that their degree of compatibility is similar to the bolt force results and the discrepancies which exist between them is the result of bolt pretensioning, lack of fit and bending effects as explained before. For 10mm extended end plate connection (third set) the theoretical interactive forces are higher than the experimental values. This could be due to welding distortion as well as the assumption made with regard to the position of the rotational axis of the connection which produces error in calculating the moment due to bolt forces. This is more noticeable for 15mm end plate connection (second set) where the moment due to bolt forces is less than the actual applied moment at ultimate load stage. From the theoretical results it is found that for 10mm end plate connection the increase in bolt forces due to prying ranges between 33 per-cent at low moment to 11 per-cent at high moment. The position of interactive forces and the extent by which they can affect the

bolt forces are dependent upon the rigidity of end plate and column flange as well as the extensibility of the bolts. It is very difficult to determine their magnitude and position by experimental means. Although Surtees and Mann[21] found that prying forces generally act at the horizontal edge of the extension plate and some parts of the end plate's vertical boundary, their precise location and progression with increasing load is not known (Fig. 7.13). In order to model the interaction of the end plate and column flange, a number of joint elements with infinite stiffness in compression and zero stiffness in tension were inserted between the coincidental nodes on both end plate and column flange as stated previously. Prying pattern can be ascertained from determination of forces in these elements, since a zero force in the joint element represents the separation between the end plate and column flange while a compressive force indicates contact between them. A series of prying patterns for the three finite element models are presented in Figs. 7.14, 7.15 and 7.16. From these figures three distinct regions of contact between the end plate and column flange can be observed at low moment. These contact points are located in the compression region, along the vertical edge of the end plate just below the inner tension bolt position, upper corner and horizontal edge of the extension plate. For thin end plate (10mm end plate connection third set) the prying spreads from the edge towards the outer and inner tension bolts. It indicates a very good agreement with the interaction pattern presented by the above authors[21]. However, with increasing moment and the resulting separation between the end plate and column flange, prying decreases and

ultimately the only contact between them occurs at the compression region and horizontal edge of the extension plate.

As stated previously, the development and location of prying forces are dependent on the relative stiffnesses of the end plate and column flange and in order to understand the influence of plate thickness on prying a parametric study of all finite element models was carried out. The result of this study show that for a connection with 10mm end plate and infinitely stiff column flange the prying occurs at points just above the outer tension bolt row which expands towards the top corner and continues along the horizontal edge extension plate (Fig. 7.17). The intensity of the interaction force varies over the contact area with the highest value recorded at a point located on the end plate top edge in line with the centre-line of the bolt holes. There is some prying along the vertical edge of the end plate just below the inner bolt row. The compression force is resisted by a rectangular region in line with the beam compression flange. However at high load stage the interaction of the end plate and column flange will only be at the top boundary of the end plate and compression region as shown in Fig. 7.17. The analysis of 15mm end plate connection (first and second set) with infinitely rigid column flange and bolts showed an almost similar prying pattern as shown in Figs. 7.18 and 7.19. The minor difference which exists between the prying pattern of the three models is due to the end plate thickness as well as the differences in the geometrical properties of the connection ie, beam depth, bolt pitch, etc.

A similar parametric study was carried out in order to determine the effect of column flange thickness on prying. The result of this analysis clearly indicates that for all the finite element models prying at low load is confined along the vertical boundary of the end plate from just below the inner tension bolt row to some point above the outer tension bolt. Also the bearing zone in the compression region is almost L-shaped with one leg along the bottom edge of the end plate and the other bears on the column web. The increasing column flange deformation causes the prying to move towards the inner tension bolt row until it disappears as shown in Figs. 7.20, 7.21 and 7.22. On the basis of the parametric study it can be concluded that the relative rigidities of end plate and column flange dictate the development of prying and its location; they also determine the shape and dimension of the compression bearing zone. Also the geometrical properties of the connection can influence the interaction of the plates.

7.4 Strain Comparison

As stated previously, the primary objectives of this research were to establish the validity of the finite element model and to determine the overall behaviour of the unstiffened extended end plate connection. In sections 7.2 and 7.3 the ability of the model to predict the moment-rotation characteristics, bolt forces and the interaction pattern between the end plate and column flange with high degree of accuracy has been demonstrated. However, in order further to investigate the reliability of the finite element technique, it was thought necessary to examine the deformational response of

each component of the connection. It was also intended to determine the yield propagation within the end plate as well as column flange and web.

The deformation of each member is governed by the system of forces it is resisting. Throughout this research it was assumed that the moment applied to the connection could be replaced by an equivalent couple whose force components act at the beam flanges and the contribution of the beam towards the joint rotation is negligible. A short length of beam with an artificially high modulus of elasticity was used in the modelling. This would ensure that all the nodes common to beam and end plate would remain in the same plane during the analysis. From the displacement results it was confirmed that the above requirement had been met (Fig. 7.23).

The end plate is subjected to tension and compression forces through the respective beam flanges as well as the resisting bolt forces on either side of the beam tension flange. This system of forces induce internal forces and stress resultants in the plate and cause deformation. The end plate bends about beam flanges and web which results in its prying into column flange creating another set of forces. The prying action increases forces in the bolts and at the same time it enhances the end plate rigidity by forcing it into double curvature. The stress distribution and displacement contours for 10mm end plate connection (third set) are presented in Fig. 7.24. They indicate good agreement with the general observations made during the test. Form the displacement contours it can be seen that major displacement occurs in the plate near

beam tension flange and at bolt position. The stress contours for the end plate demonstrate the highest concentration of stress at bolt location and at the outer junction of beam tension flange with end plate. This stress pattern is typical of the extended end plate responses from which it can be seen that the critical parameters in the design of end plate joint are the strength of the plate at bolt locations as well as the strength of the weld around the beam tension flange. This was confirmed by the results of test 5 (254x254x89UC, 406x178x74UB, 10mm end plate and grade 8.8 bolts) where the failure was due to bolt punching through the end plate and of test 11 (203x203x60UC, 305x127x48UB, 15mm end plate and grade 8.8 bolts) where the failure was caused by weld cracking at the outer edge of the beam tension flange. From the yield pattern (Figs. 7.25) it can be seen that plastification starts at bolt, tension and compression beam flange locations simultaneously. In compression zone the spread of plastification is limited to the flange region while in the tension region the plastic zone spreads rapidly towards the beam web and finally covers the entire tension region of the end plate. The corresponding moment-rotation curve indicates that the end plate starts to yield at 83 kNm which is the transitional point of the curve from elastic to plastic region.

A comparison between the theoretical and experimental strains in the column flange was carried out as shown in Figs. 7.26 to 7.30. From the graphs it can be seen that the experimental strain results obtained at various points on the column flange are close to their corresponding theoretical values. The small differences between the two sets

of values can be attributed to the approximate nature of the finite element method. These discrepancies could probably be minimized by adopting finer mesh in the modelling of the connection. From the displacement contour it can be seen that major displacement occurs in the tension region where the plate bends about the column web as well as at bolt locations as shown in Fig. 7.31. There is also some flange deformation in the compression region due to its bending about the web. These deformations which are highest at tension and compression beam flange location tend to dissipate quickly and will not travel far outwith the end plate boundaries. Stress and strain contours are presented in Fig. 7.32 from which it can be seen that the concentration of stress is also at bolt location and along the junction of flange and web in both tension and compression regions. However the degree of stress concentration is higher in the tension region than compression which is in agreement with the experimental observation. Also the yield pattern determined at different load increment indicates that the plastification starts at bolt locations and at some points on the intersection of the flange and web in line with beam compression flange. The degree of yield propagation in these regions is limited but increasing load caused the plastification to spread quickly along the line of intersection of flange with the web which extends between the inner and outer tension bolt rows (Figs. 7.33). A further investigation of the theoretical results highlighted two regions of high stress concentration in the web, one in the tension and other in the compression zone. The load in the tension region is transferred over an area in line with both tension group of bolts while in the compression region the load spreads out as it penetrates into the

web. However, the spread of load is not uniform over the whole area and a large proportion of the compressive force is transferred directly in line with the flange where an intense stress concentration is created at mid-depth of the web (Fig. 7.34). The yield propagation, presented in Fig. 7.35, also shows that the plastification of the web originates at a point directly below the beam compression flange and spreads out with increasing load.

Fig. 7.1 Comparison between theoretical and experimental moment-rotation.
254x254x132 UC, 305x165x54 UB
15mm end plate, M20 H.S.F.G. bolts (first set)

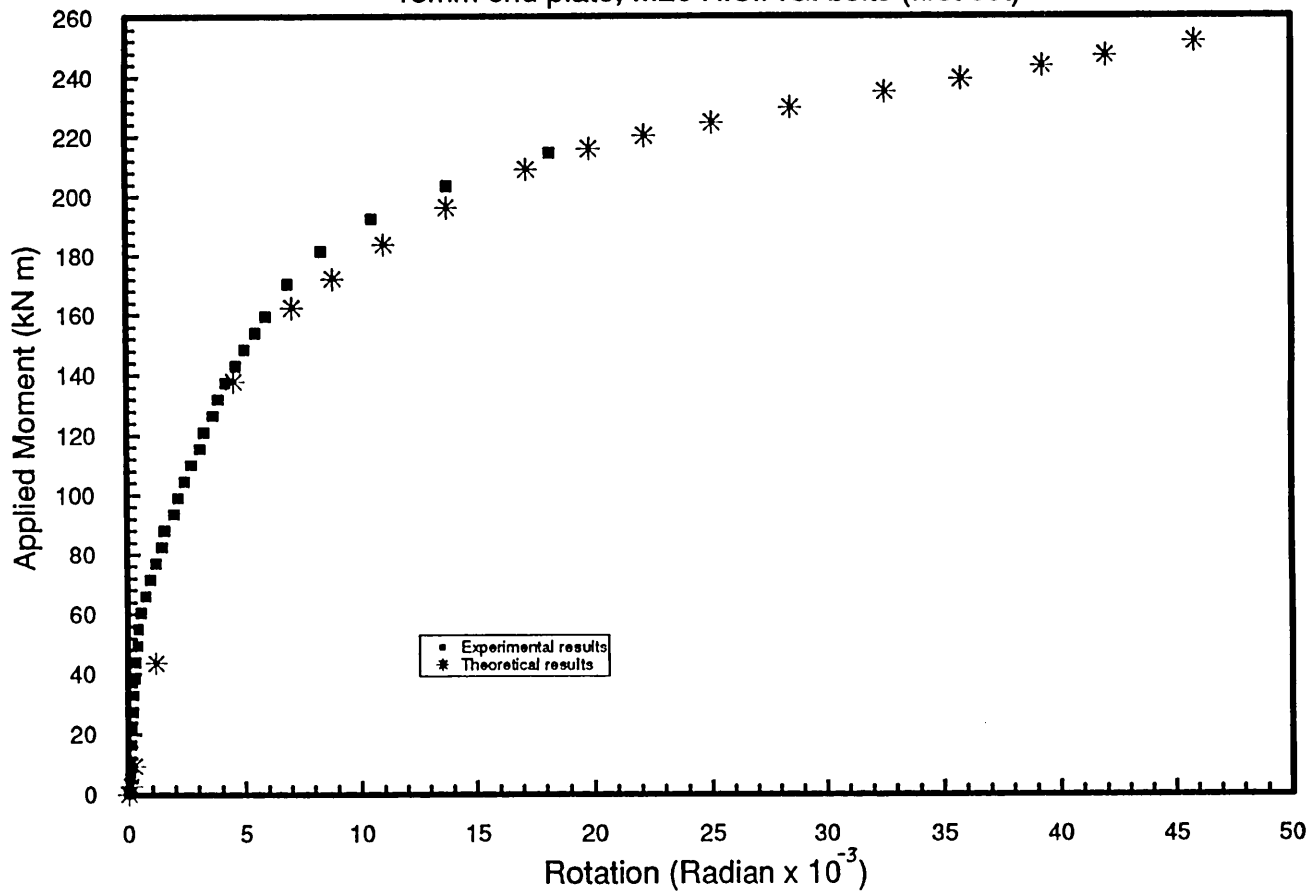

Fig. 7.2 Comparison between theoretical and experimental moment-rotation.
254x254x89 UC, 406x178x74 UB
15mm end plate, M20 grade 8.8 bolts (second set)

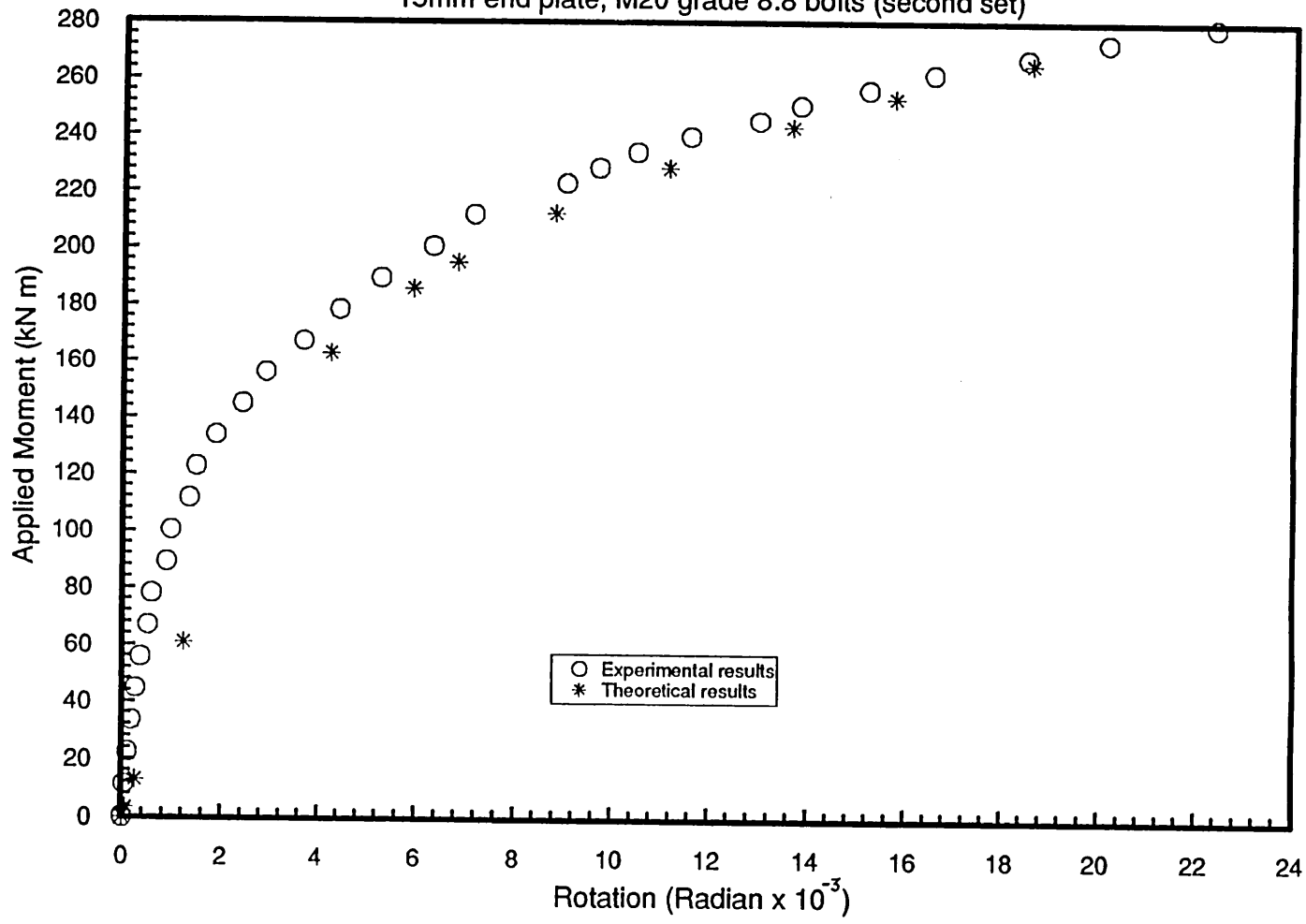

Fig. 7.3 Comparison between theoretical and experimental moment-rotation.
203x203x60 UC, 305x127x48 UB
10mm end plate, M20 grade 8.8 bolts (third set)

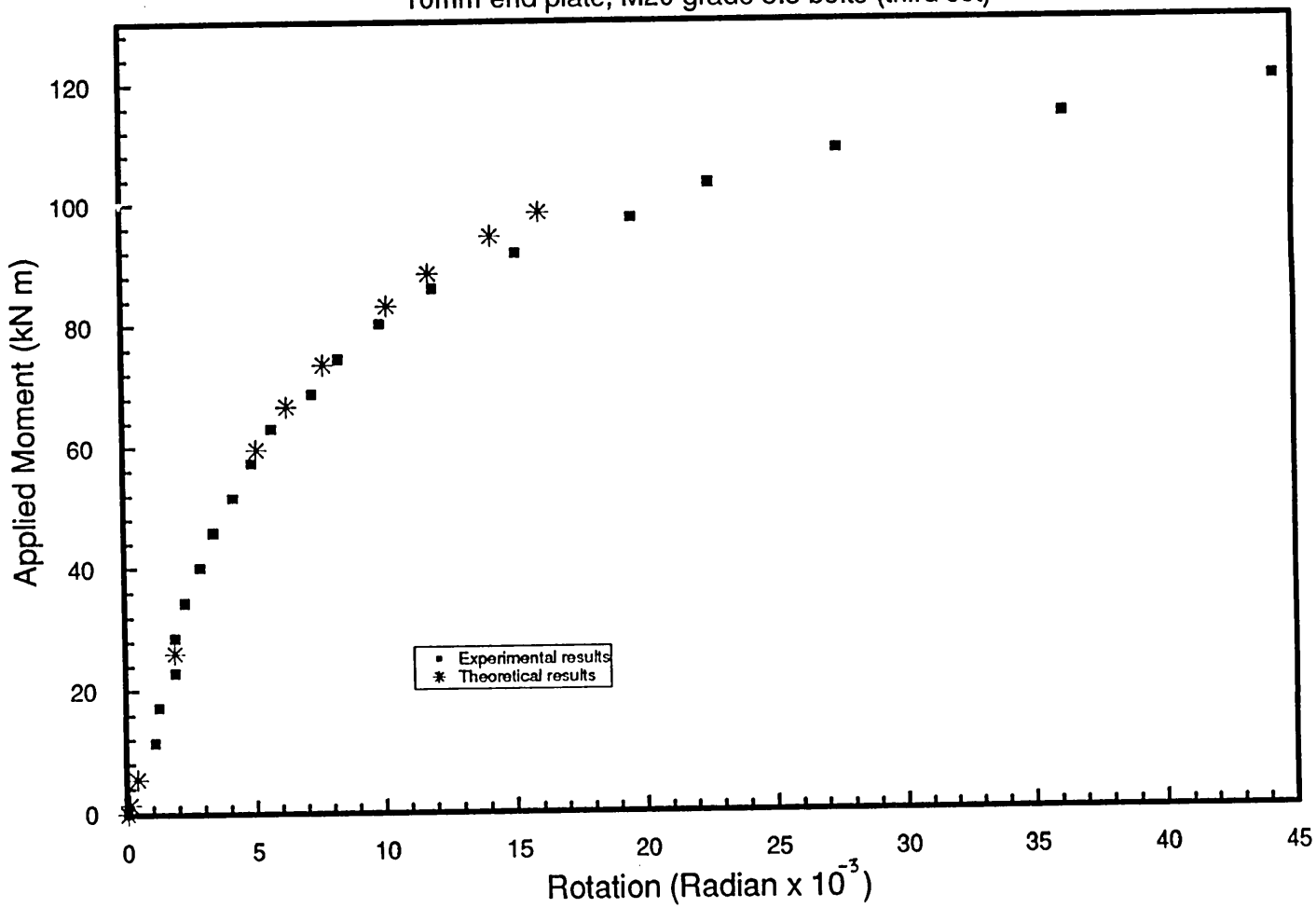

Fig. 7.4 Contribution of column flange and end plate
Towards joint rotation (15mm end plate connection, first set)

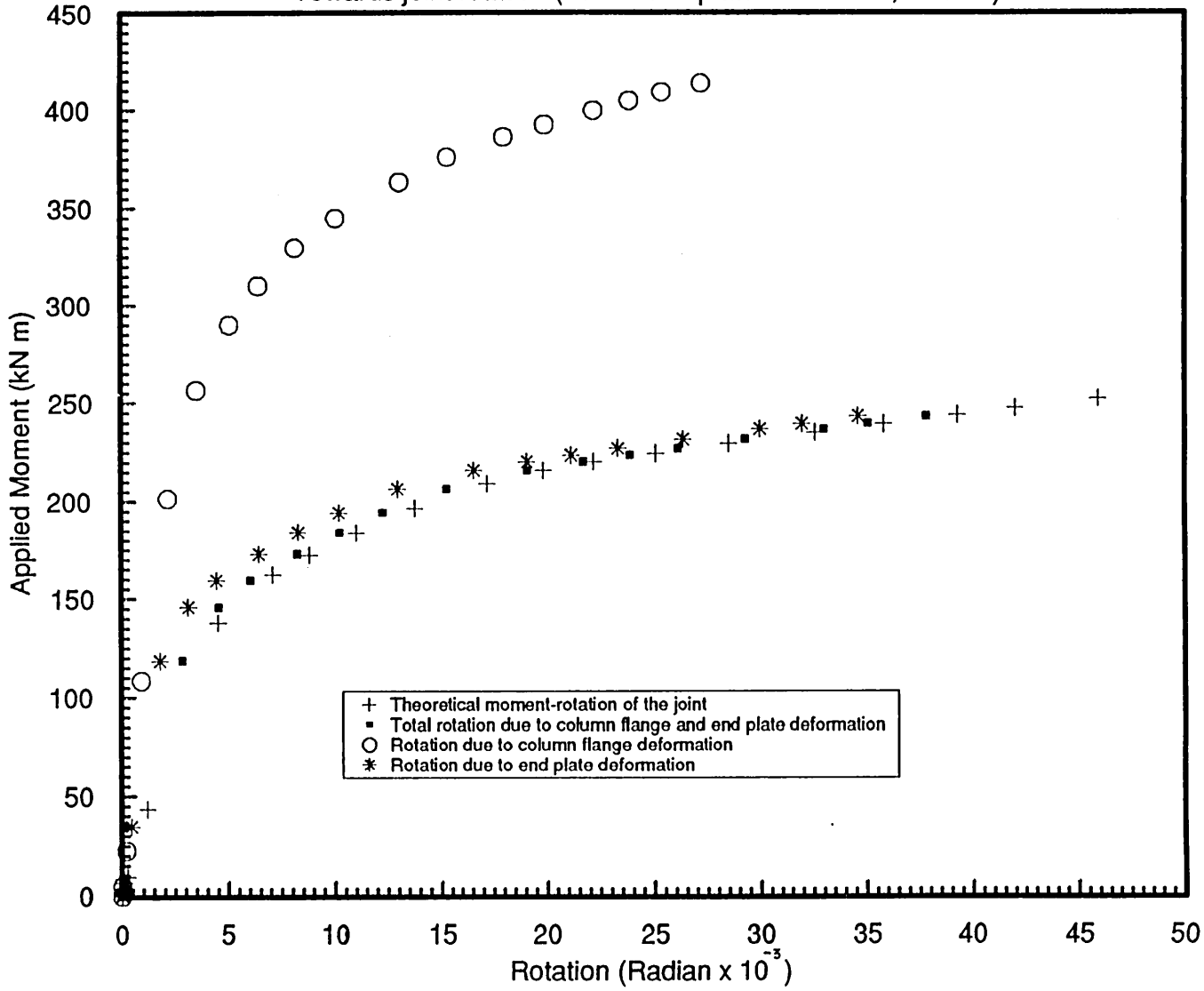

Fig. 7.5 Contribution of column flange and end plate towards joint rotation (15mm end plate connection, second set)

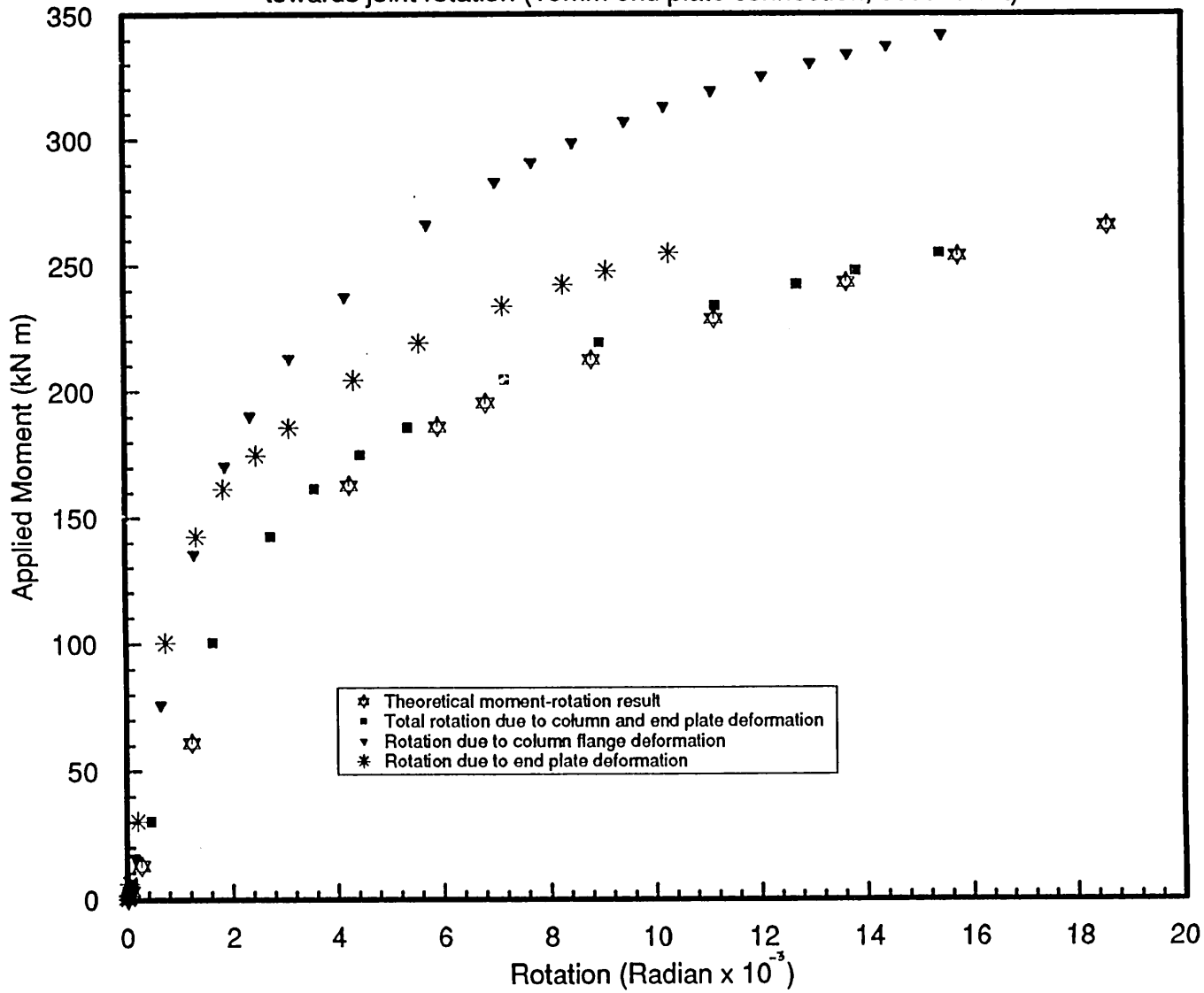

Fig. 7.6 Contribution of column flange and end plate towards joint rotation (10mm end plate connection, third set)

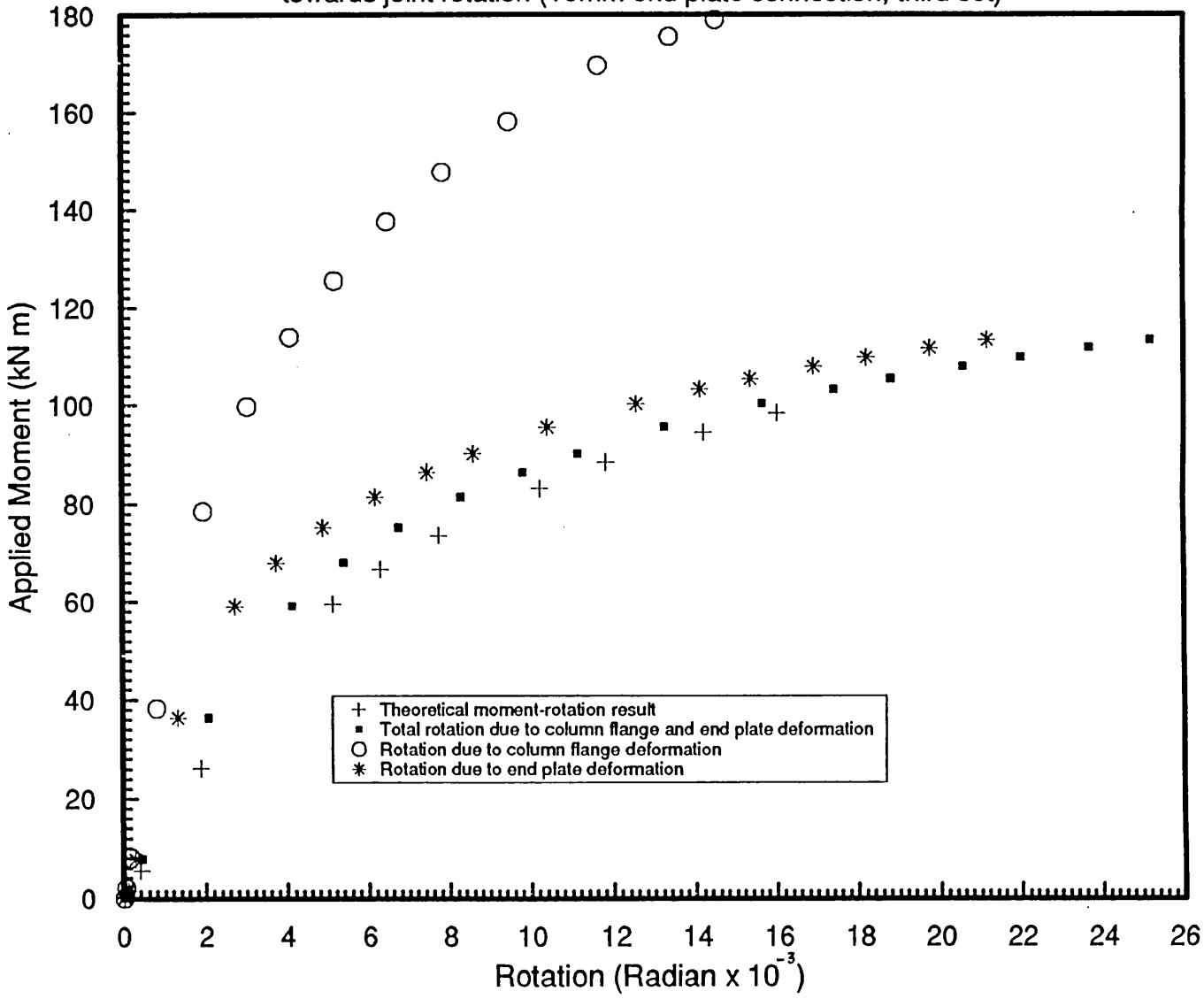

Fig. 7.7 Comparison between theoretical and experimental values of inner nad outer bolt forces (254x254x132U.C., 305x165x54U.B., 20mm H.S.F.G. bolts and 15mm end plate)

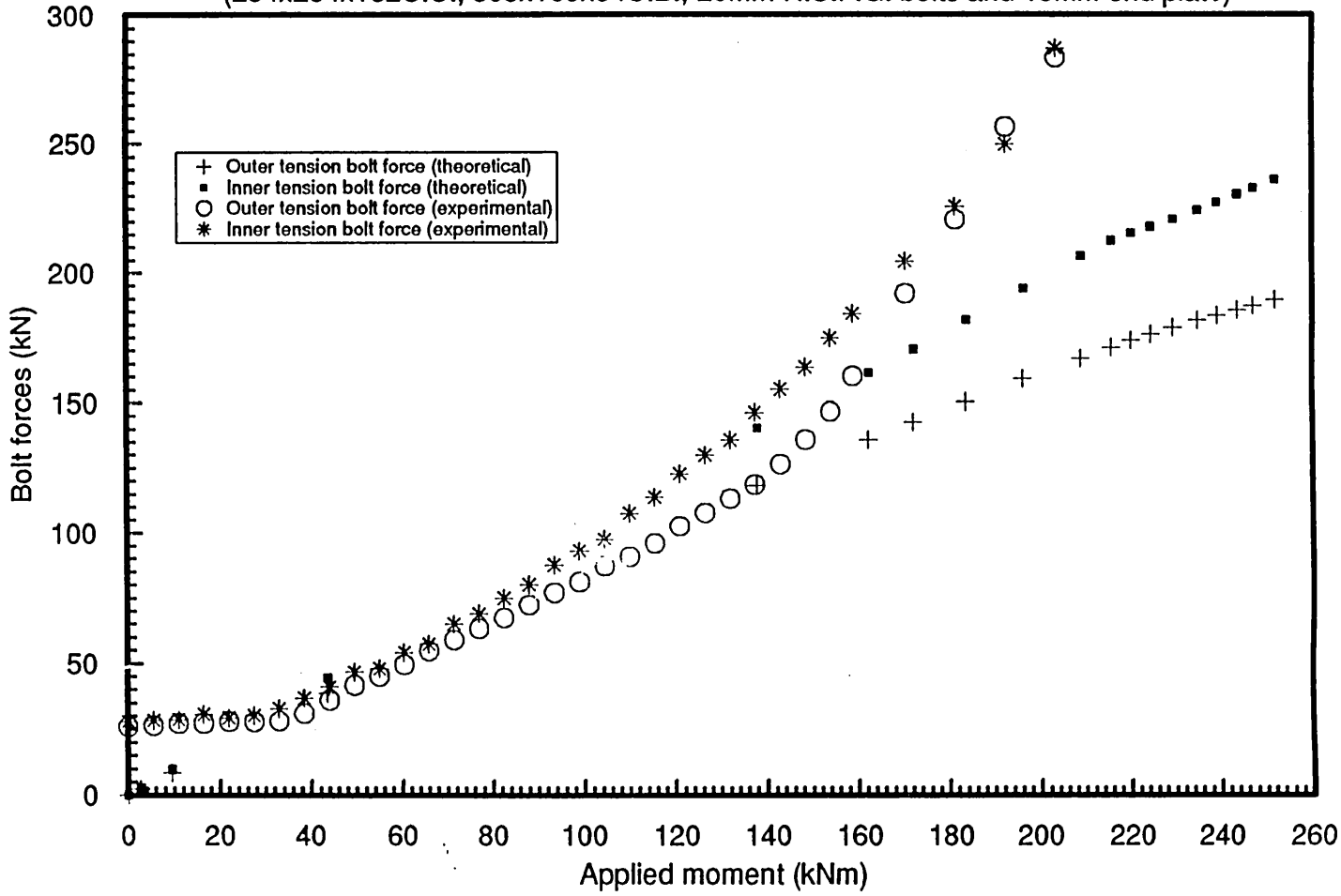

Fig. 7.8 Comparison between theoretical and experimental values of inner and outer bolt forces (254x254x89U.C., 406x178x74U.B., 20mm grade 8.8 bolts and 15mm end plate)

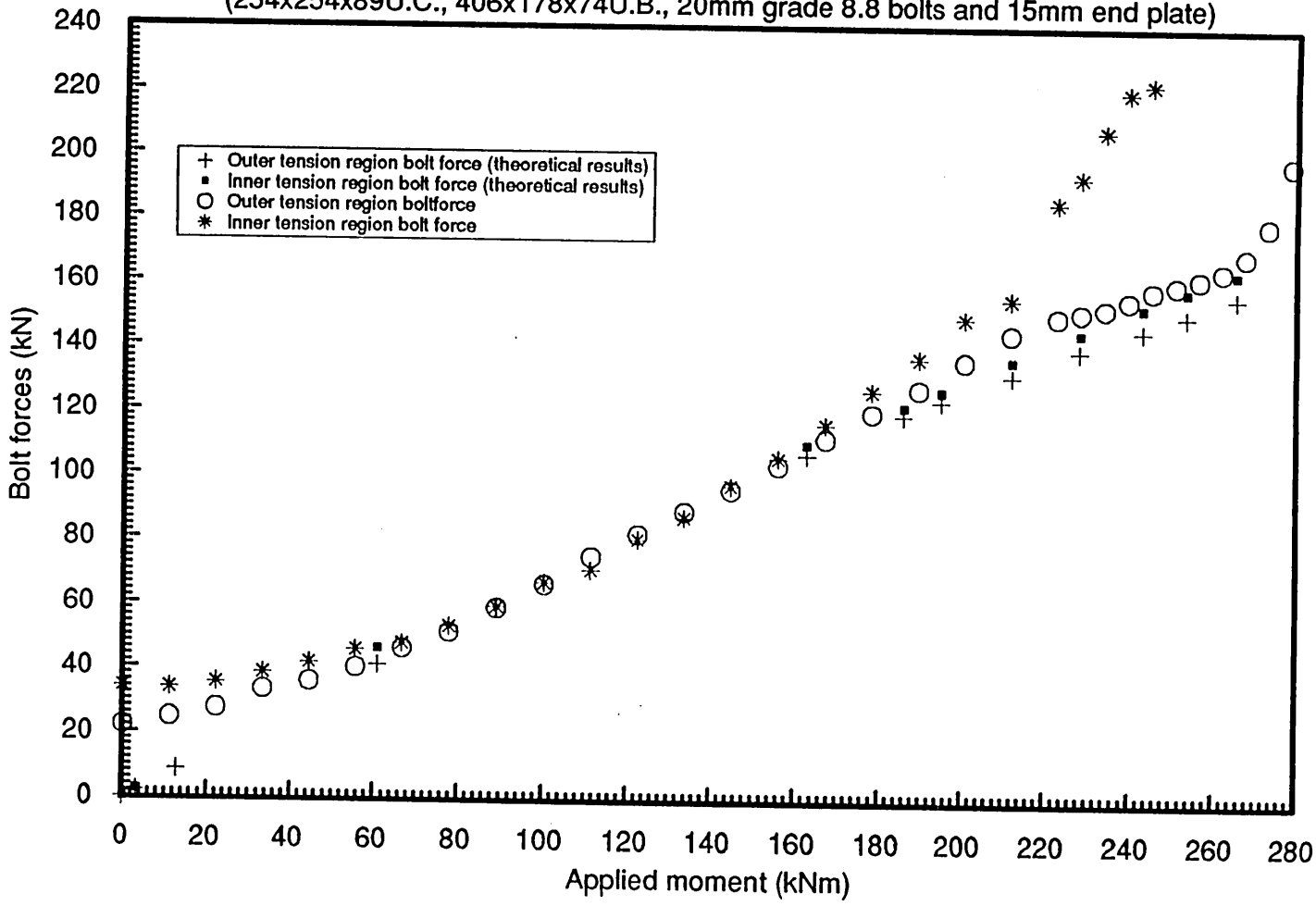

Fig. 7.9 Comparison between theoretical and experimental values of inner and outer bolt forces (203x203x60U.C., 305x127x48U.B., 20mm grade 8.8 bolts and 10mm end plate)

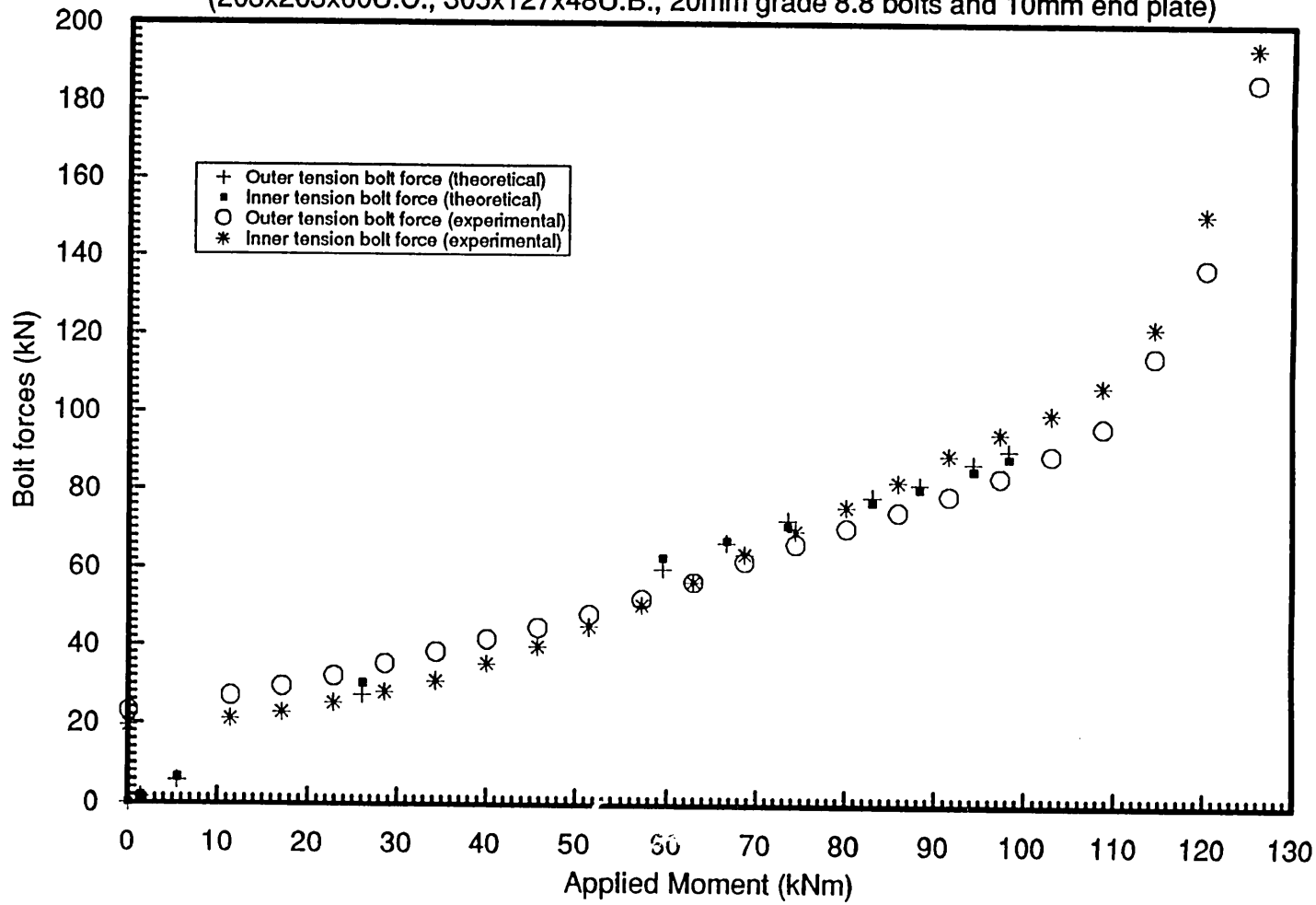

Fig. 7.10 Comparison of prying forces for 15mm end plate in first set
(254x254x132U.C., 305x165x54U.B., M20 H.S.F.G. bolts)

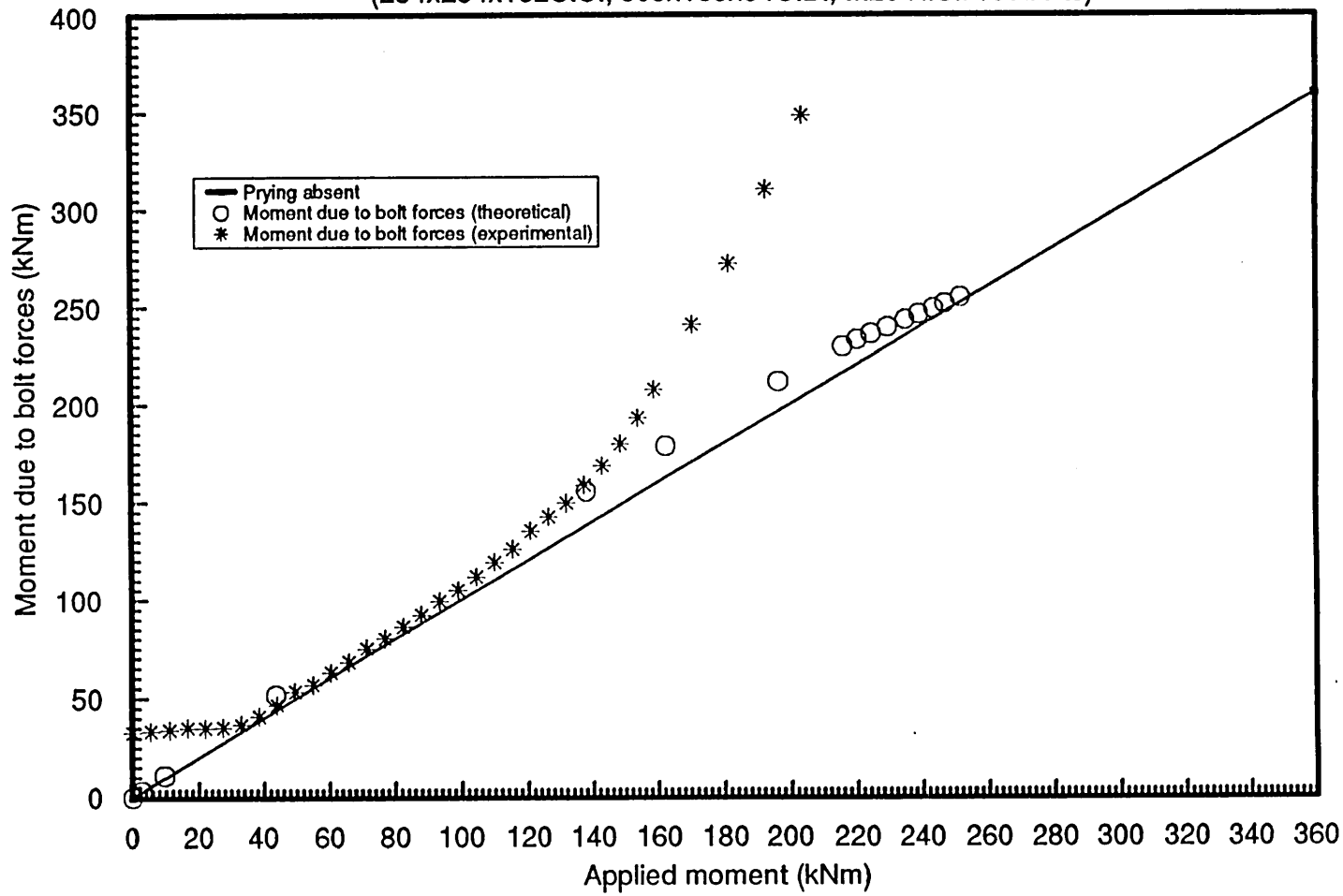

Fig. 7.11 Comparison of prying forces for 15mm end plate in second set
(254x254x89U.C., 406x178x74U.B., M20mm grade 8.8 bolts)

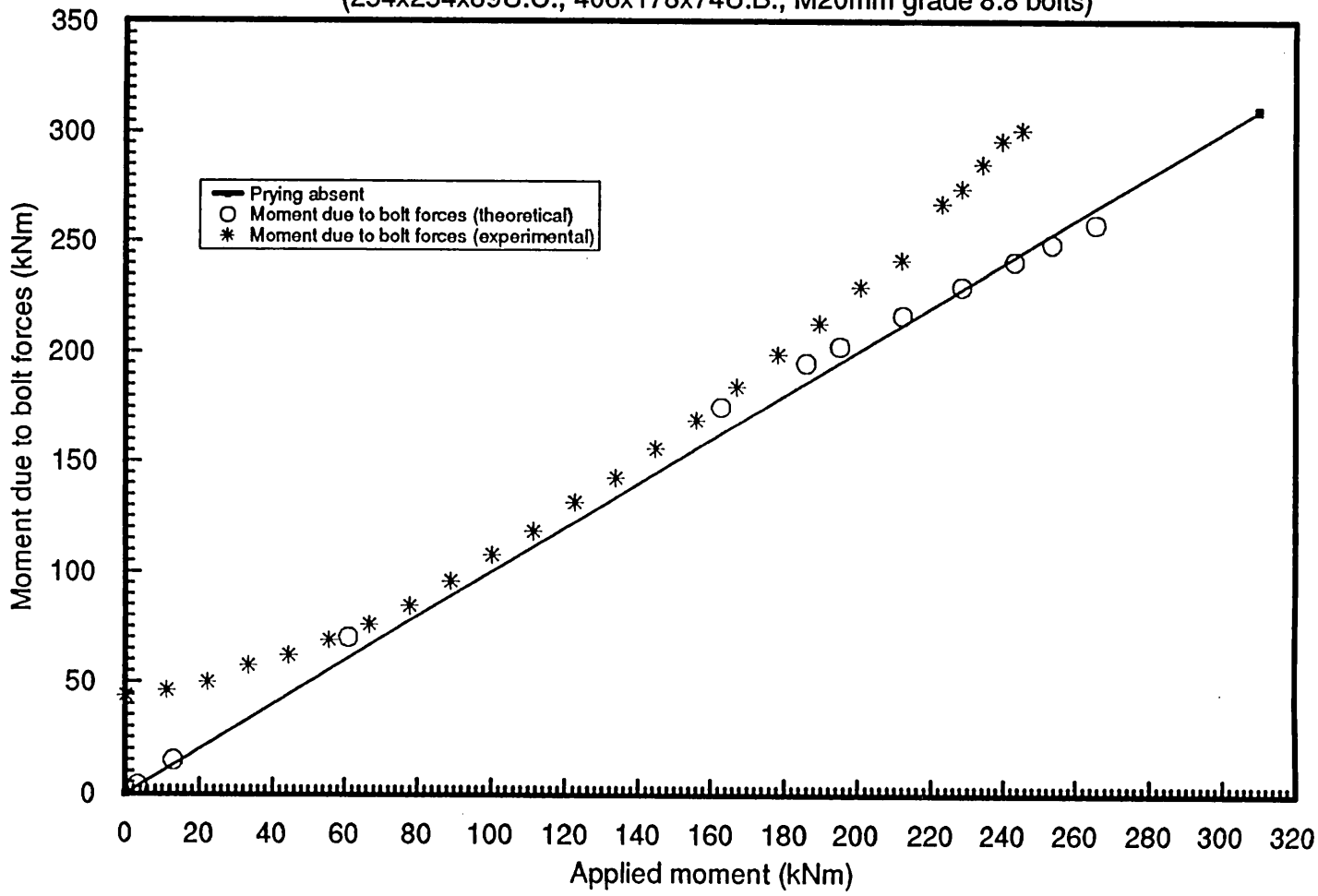

Fig. 7.12 Comparison of prying forces for 10mm end plate in third set
(203x203x60U.C., 305x127x48U.B., M20 grade 8.8 boltes)

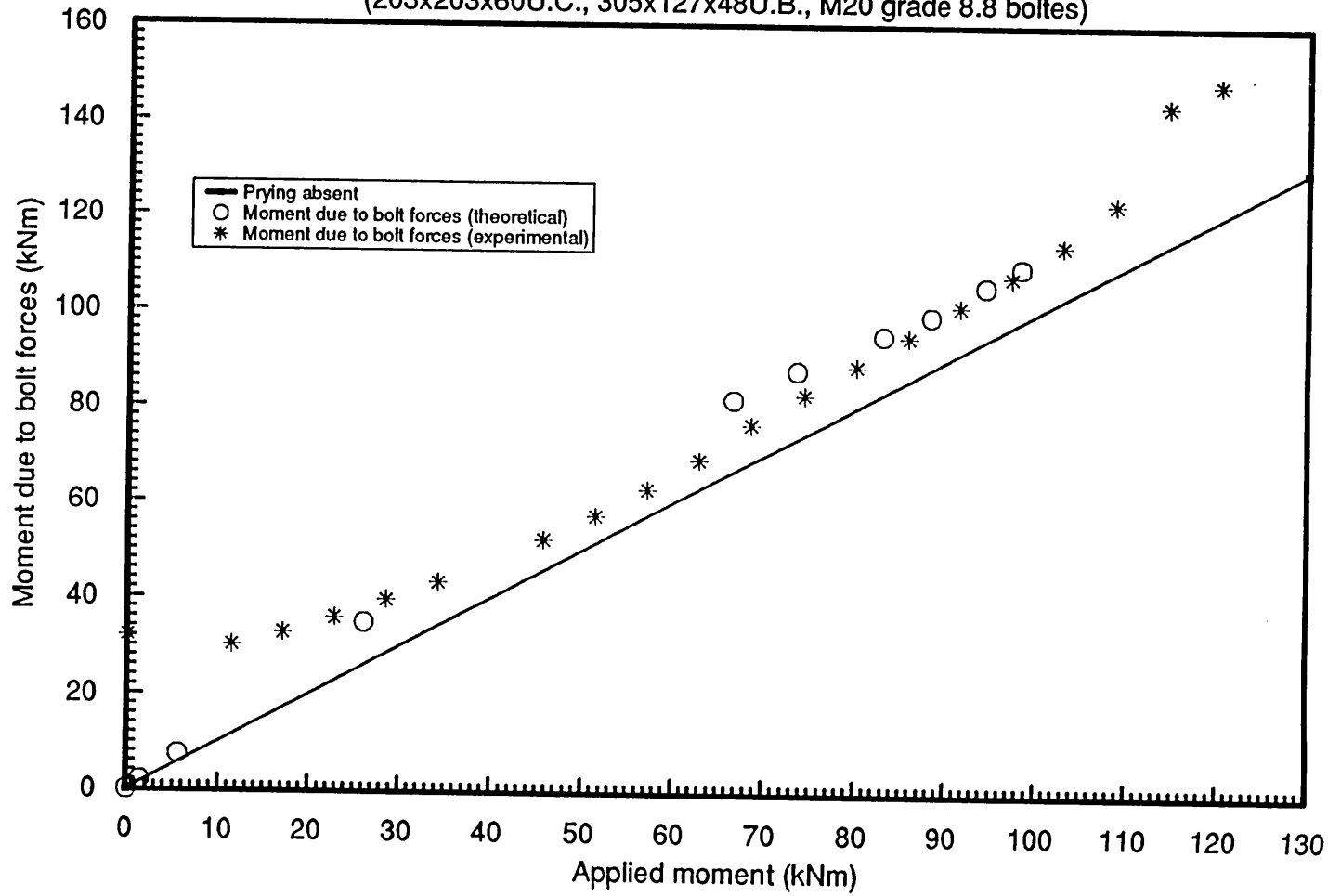

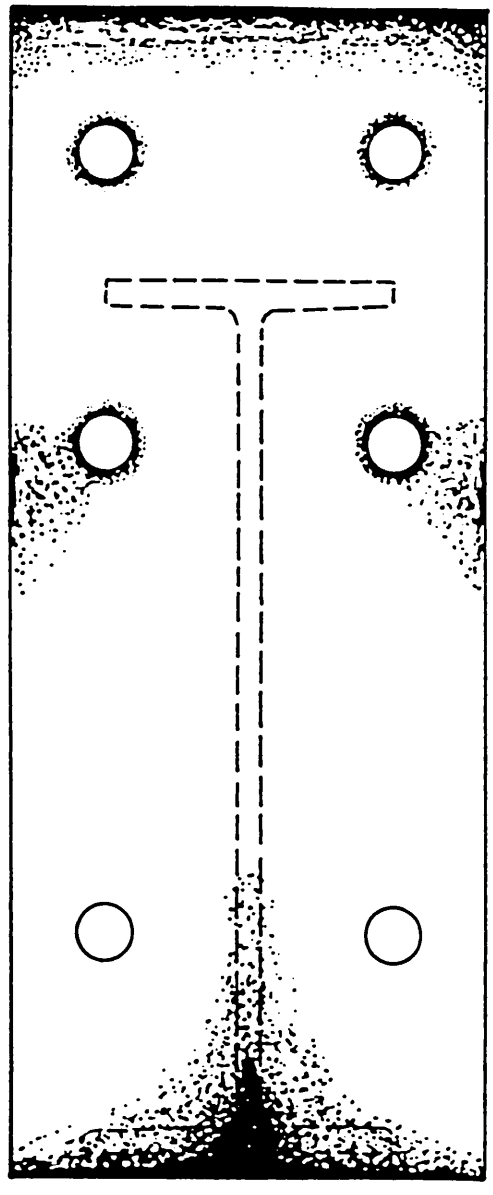

Fig. 7.13 Prying pattern determined by Surtees and Mann by experiment (Reproduced from Ref. 21)

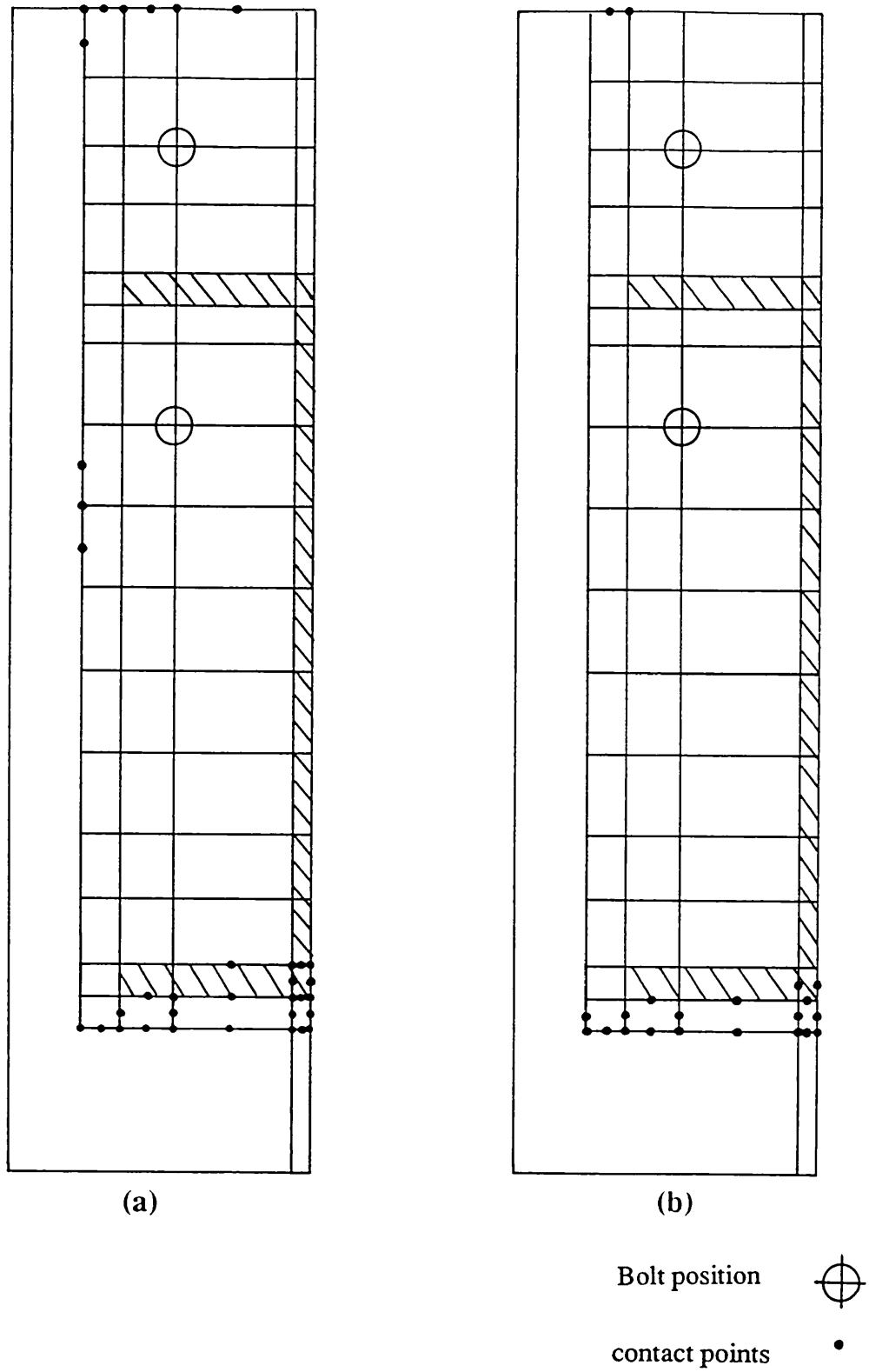

Fig. 7.14 Prying pattern for 15mm end plate connection (first set)
(a) at low moment, (b) at high moment

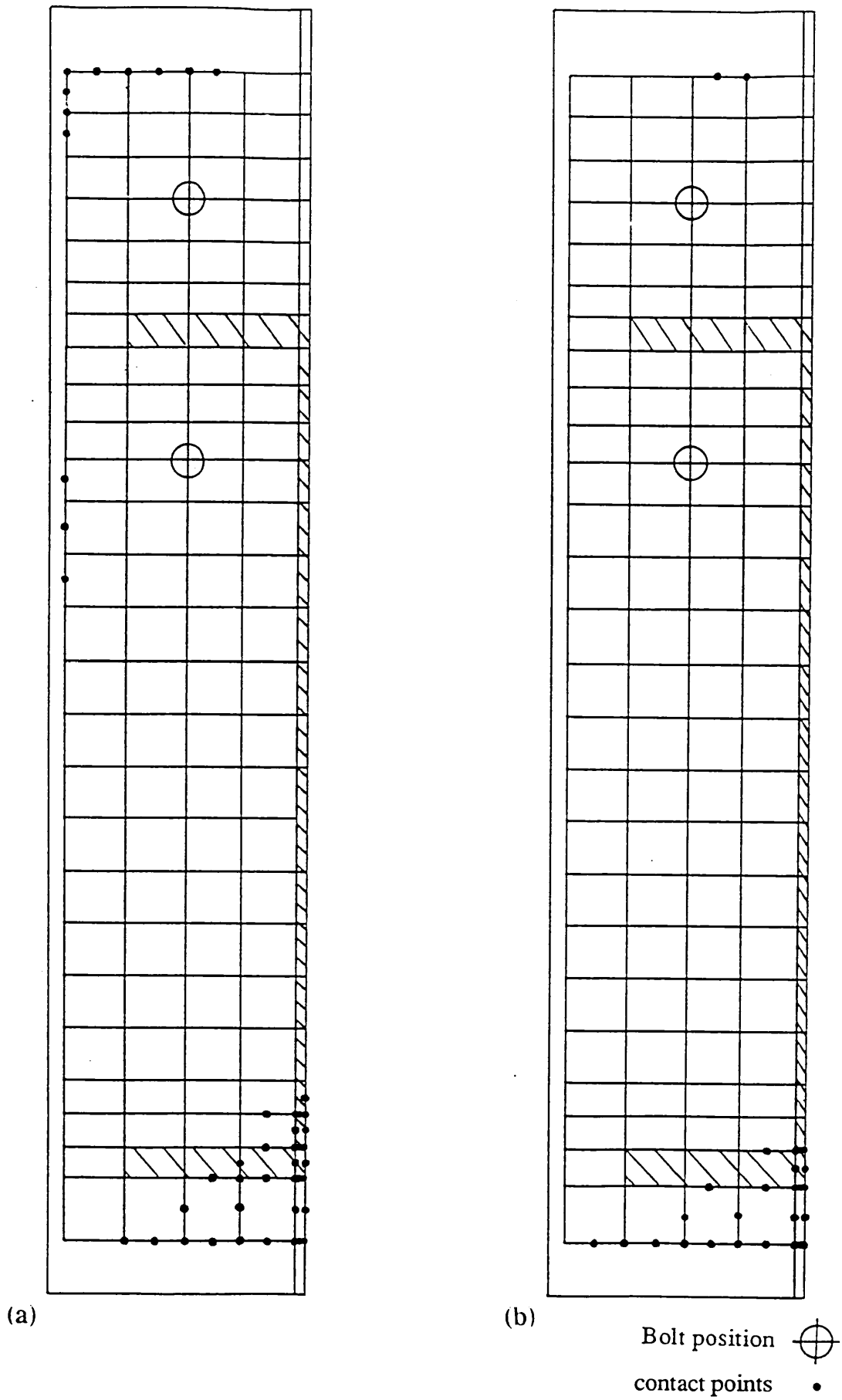

Fig. 7.15 Prying pattern for 15mm end plate connection (second set) (a) at low moment, (b) at high moment

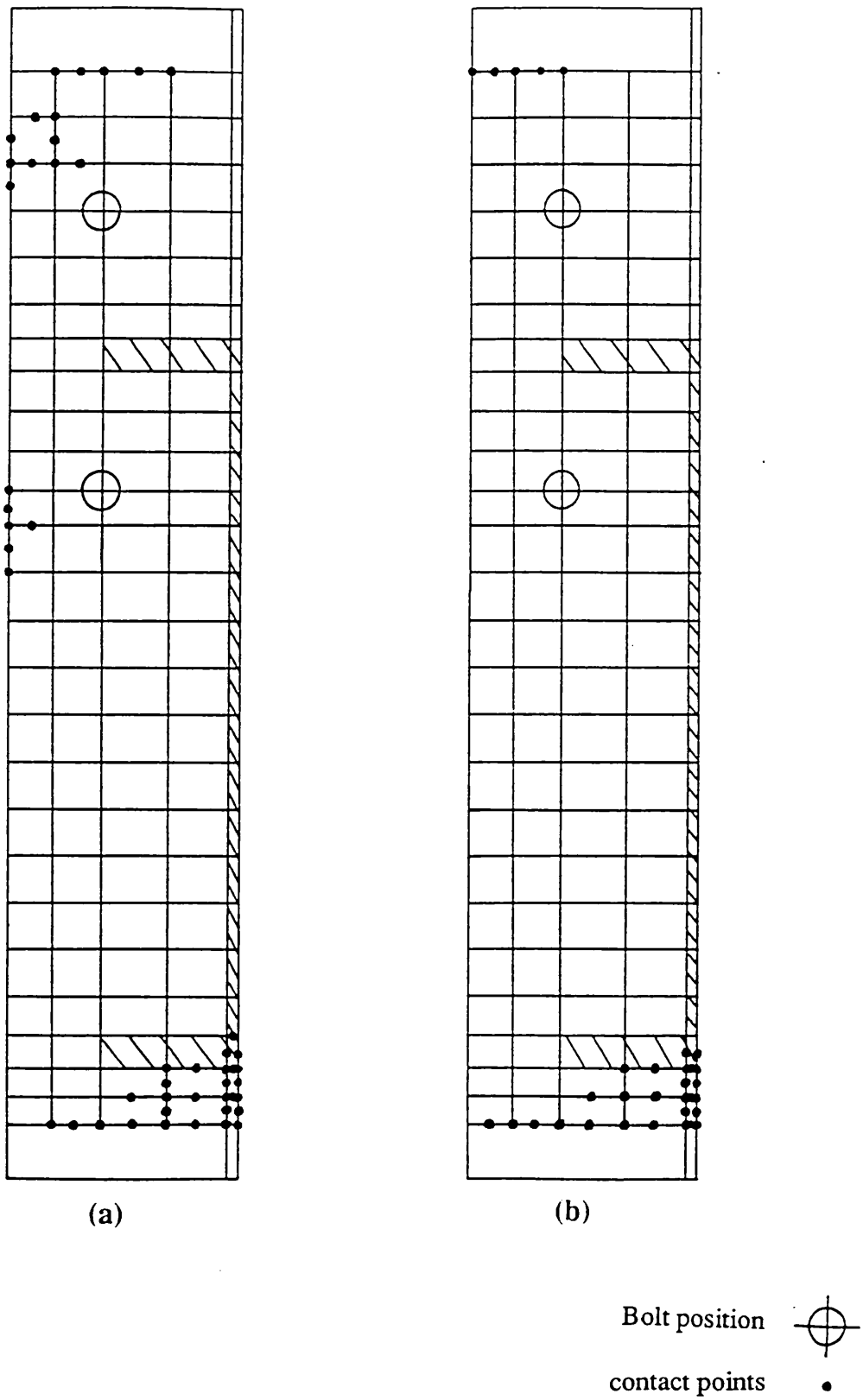

Fig. 7.16 Prying pattern for 10mm end plate connection (third set)
(a) at low moment, (b) at high moment

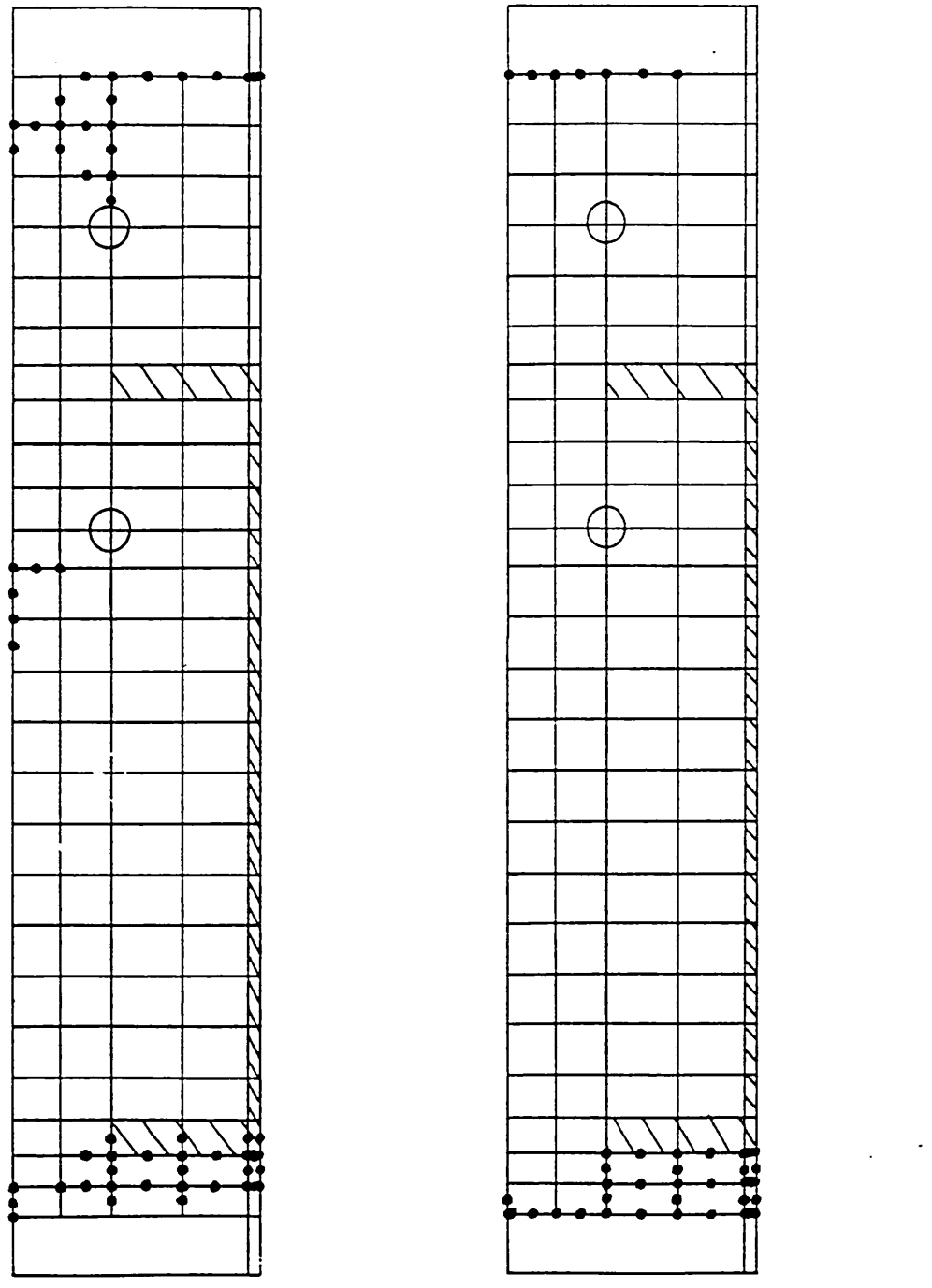

Fig. 7.17 Prying pattern for 10mm end plate connection when the column and bolts are infinitely rigid (third set)
(a) at low moment, (b) at high moment

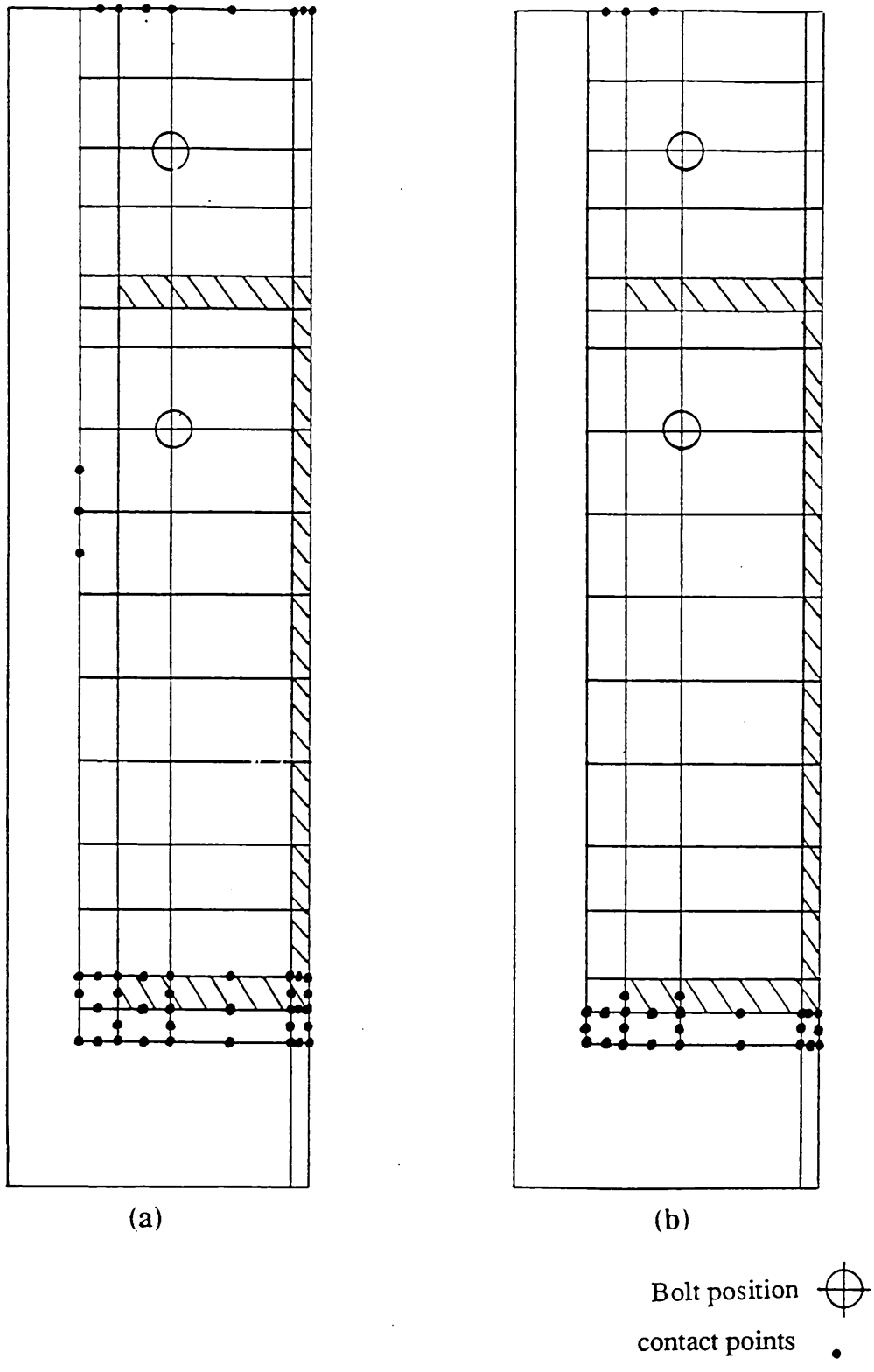

Fig. 7.18 Prying pattern for 15mm end plate connection when the column and bolts are infinitely rigid (first set)
(a) at low moment, (b) at high moment

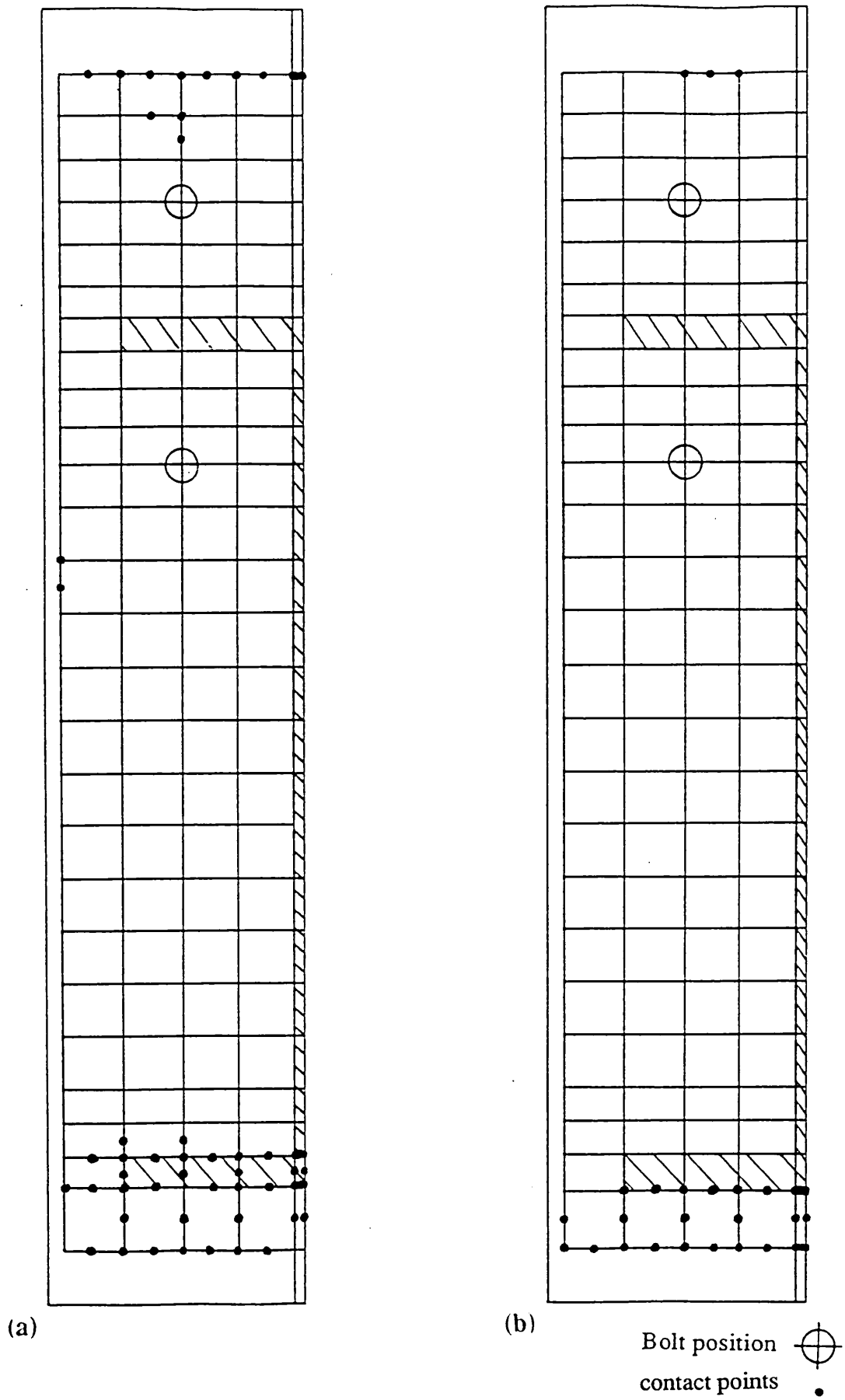

Fig. 7.19 Prying pattern for 15mm end plate connection when the column and bolts are infinitely rigid (second set)
(a) at low moment, (b) at high moment

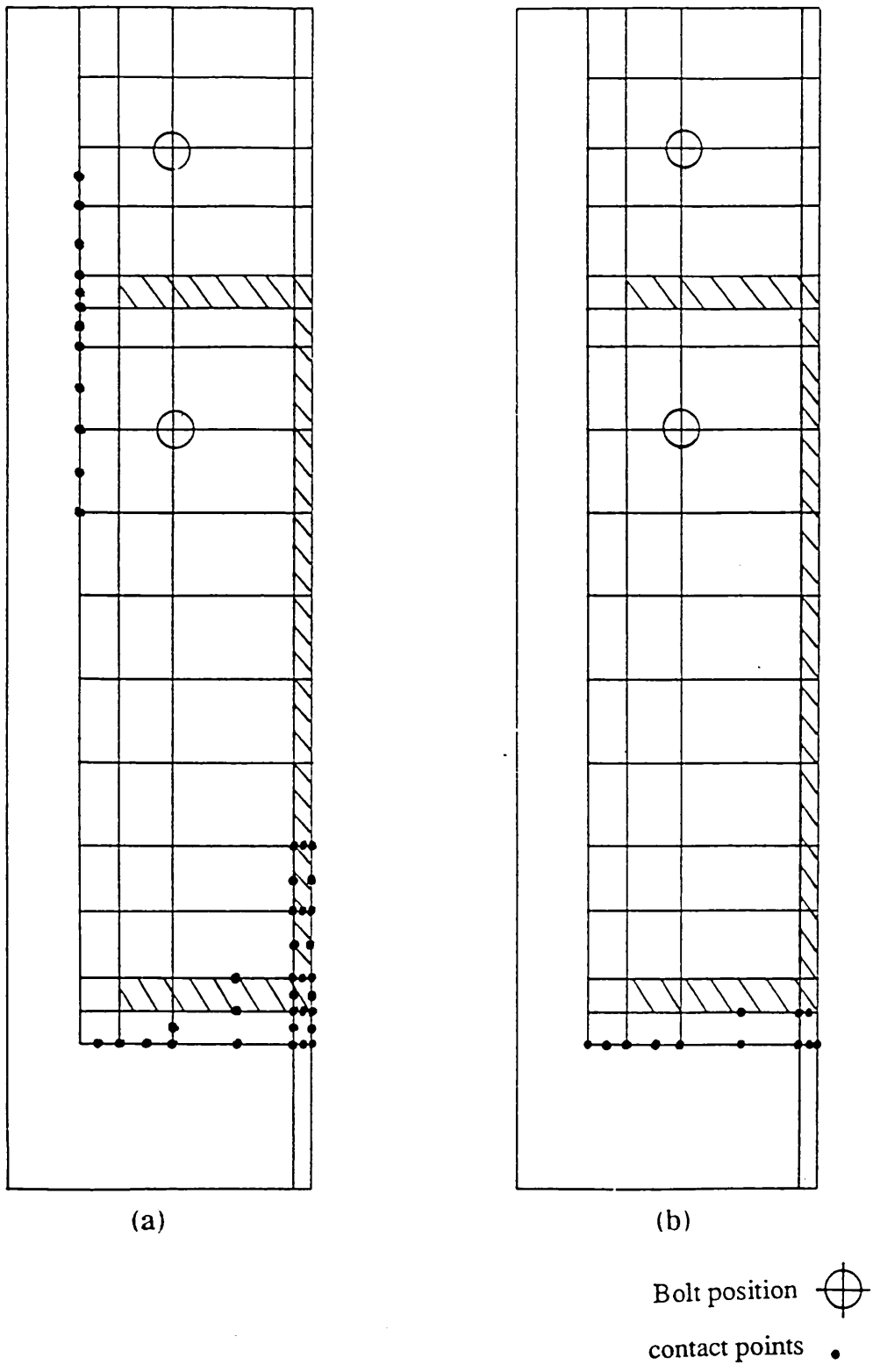

Fig. 7.20 Prying pattern for 15mm end plate connection when the end plate and bolts are infinitely rigid (first set) (a) at low moment, (b) at high moment

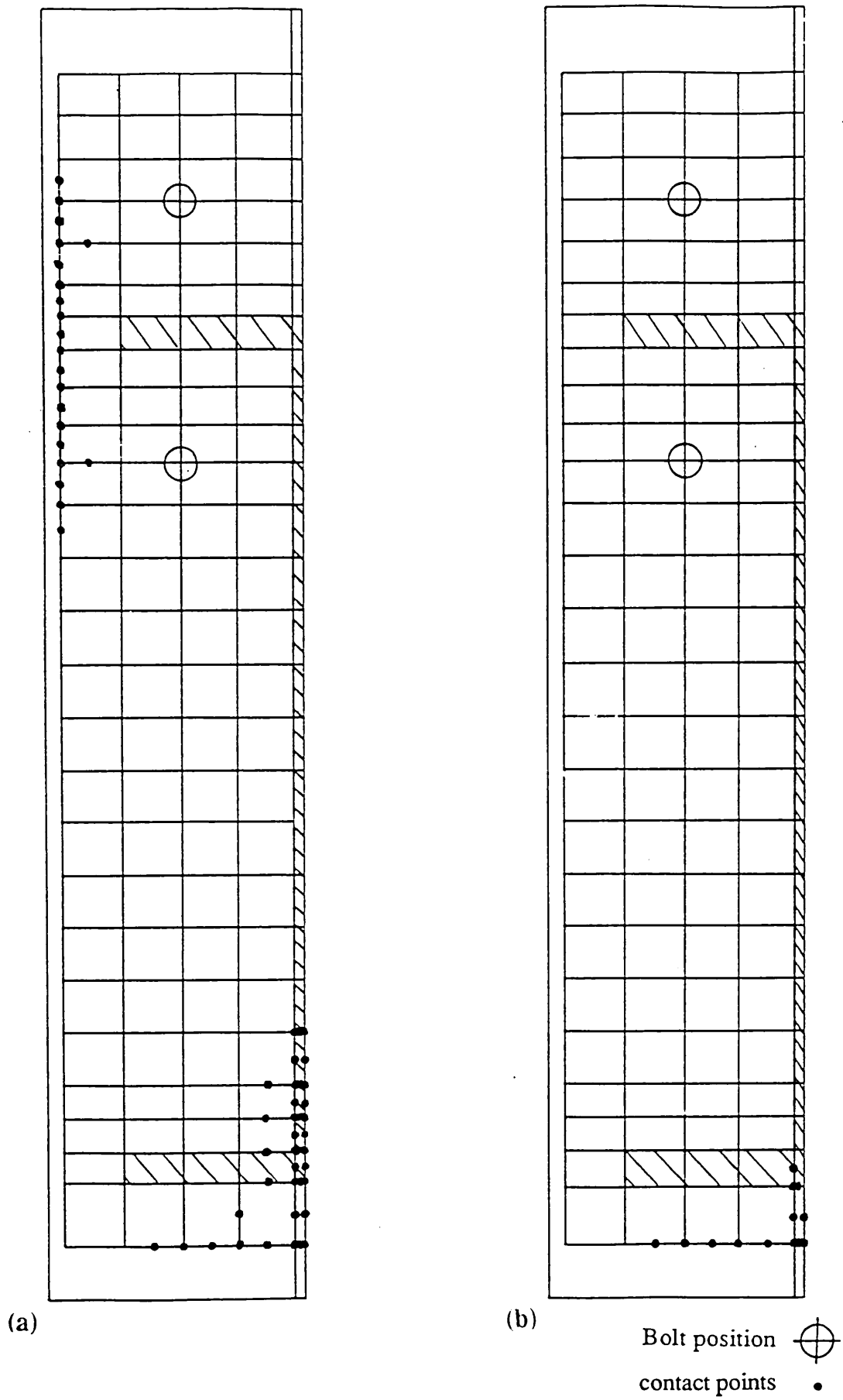

Fig. 7.21 Prying pattern for 15mm end plate connection when the end plate and bolts are infinitely rigid (second set) (a) at low moment, (b) at high moment

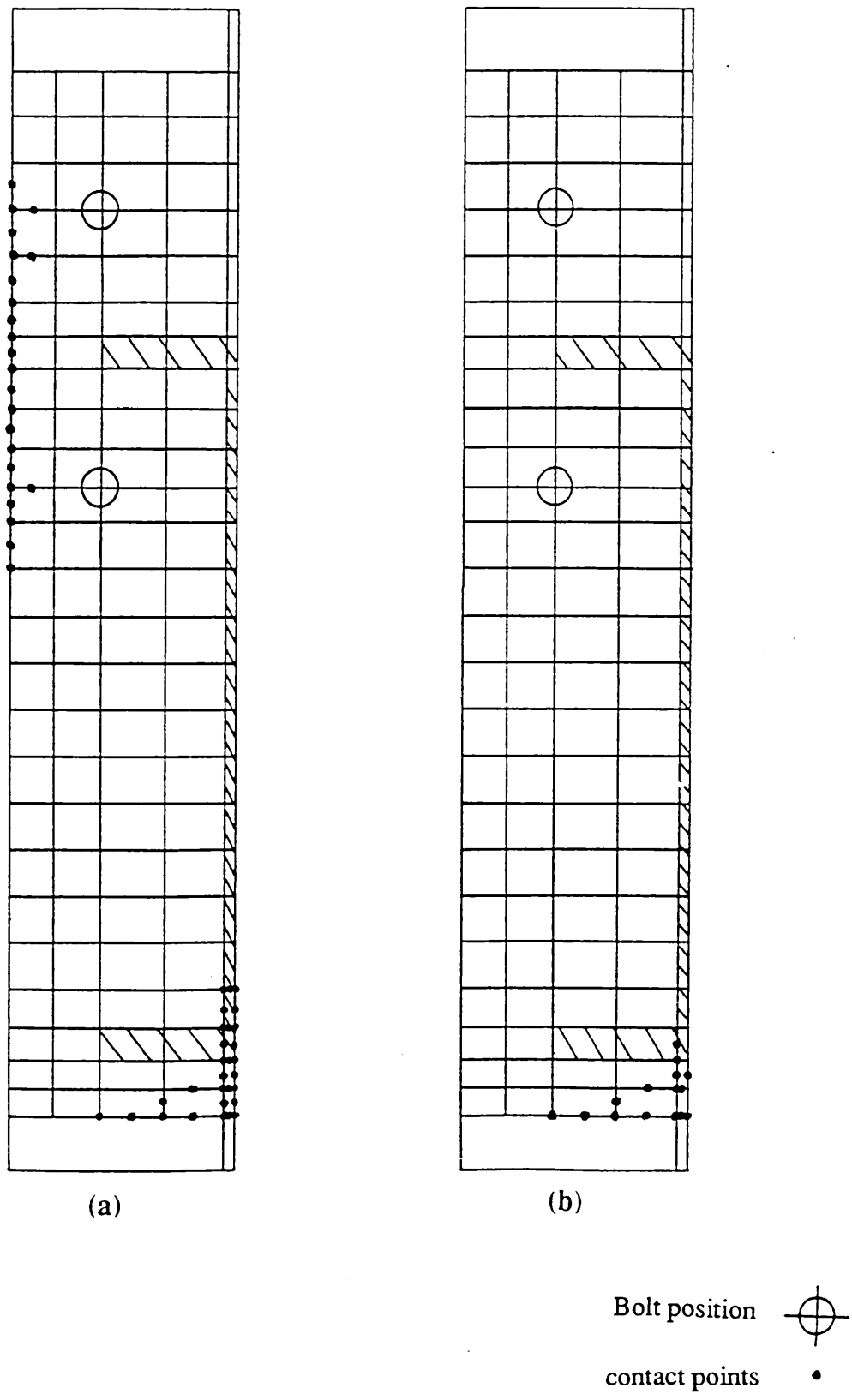

Fig. 7.22 Prying pattern for 10mm end plate connection when the end plate and bolts are infinitely rigid (third set) (a) at low moment, (b) at high moment

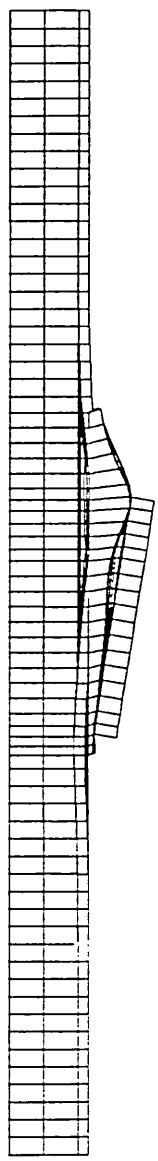

Fig. 7.23 Deformed shape of unstiffened extended end plate connection

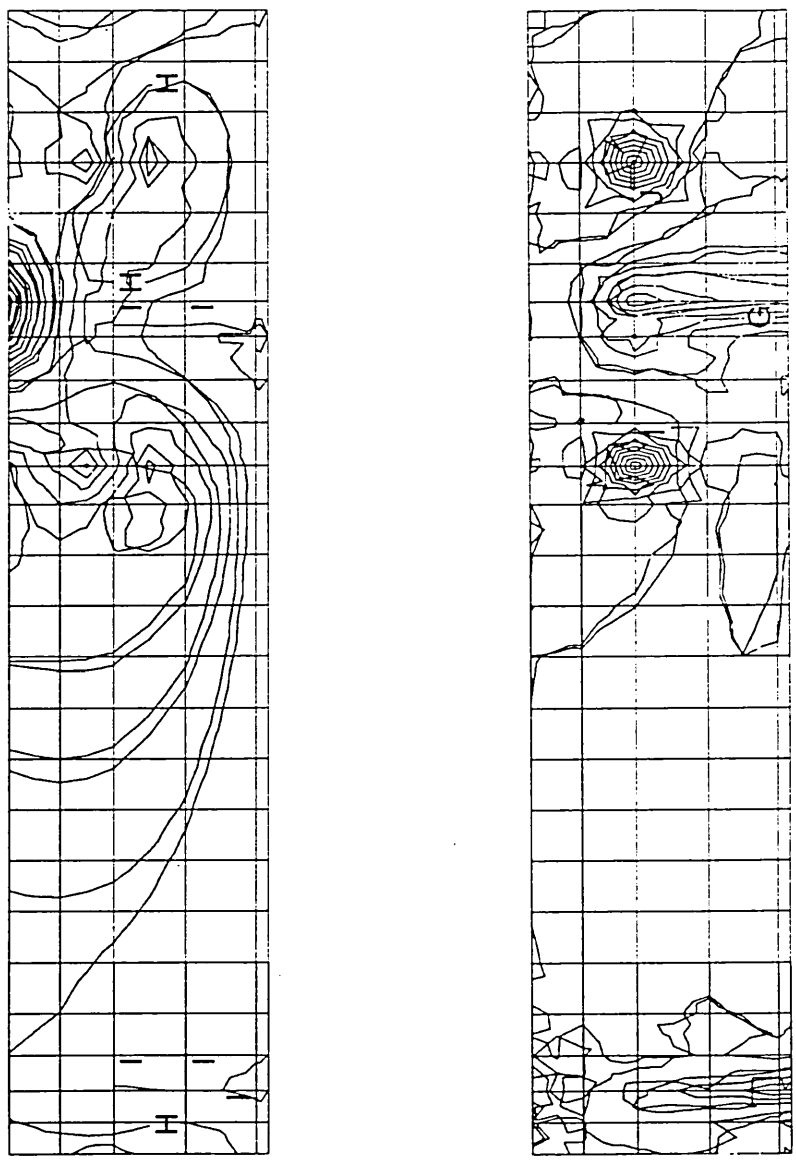

(a) (b)

Fig. 7.24 Displacement and stress contours for 10mm end plate (third set)

(a) Stress distribution contours (b) Displacement contours

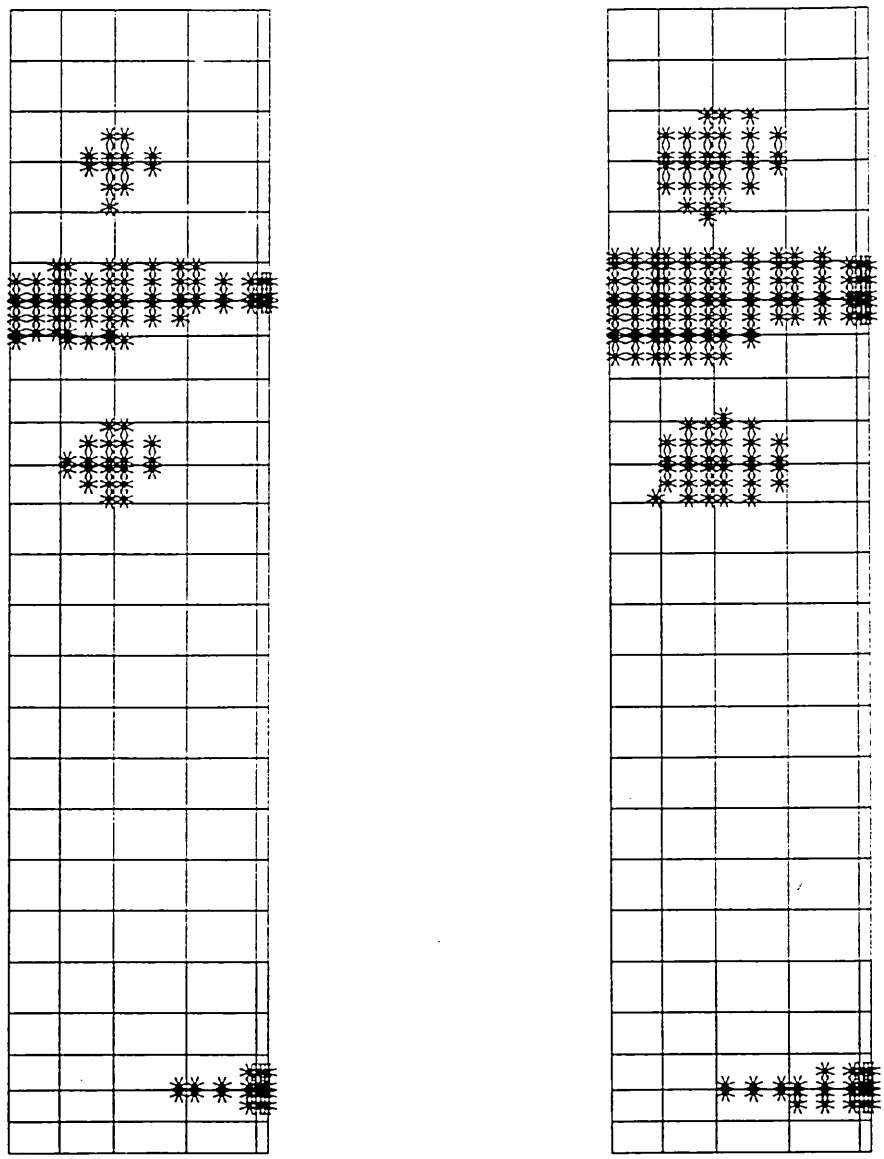

(a) (b)

Fig. 7.25 Yield propagation for 10mm end plate (third set)

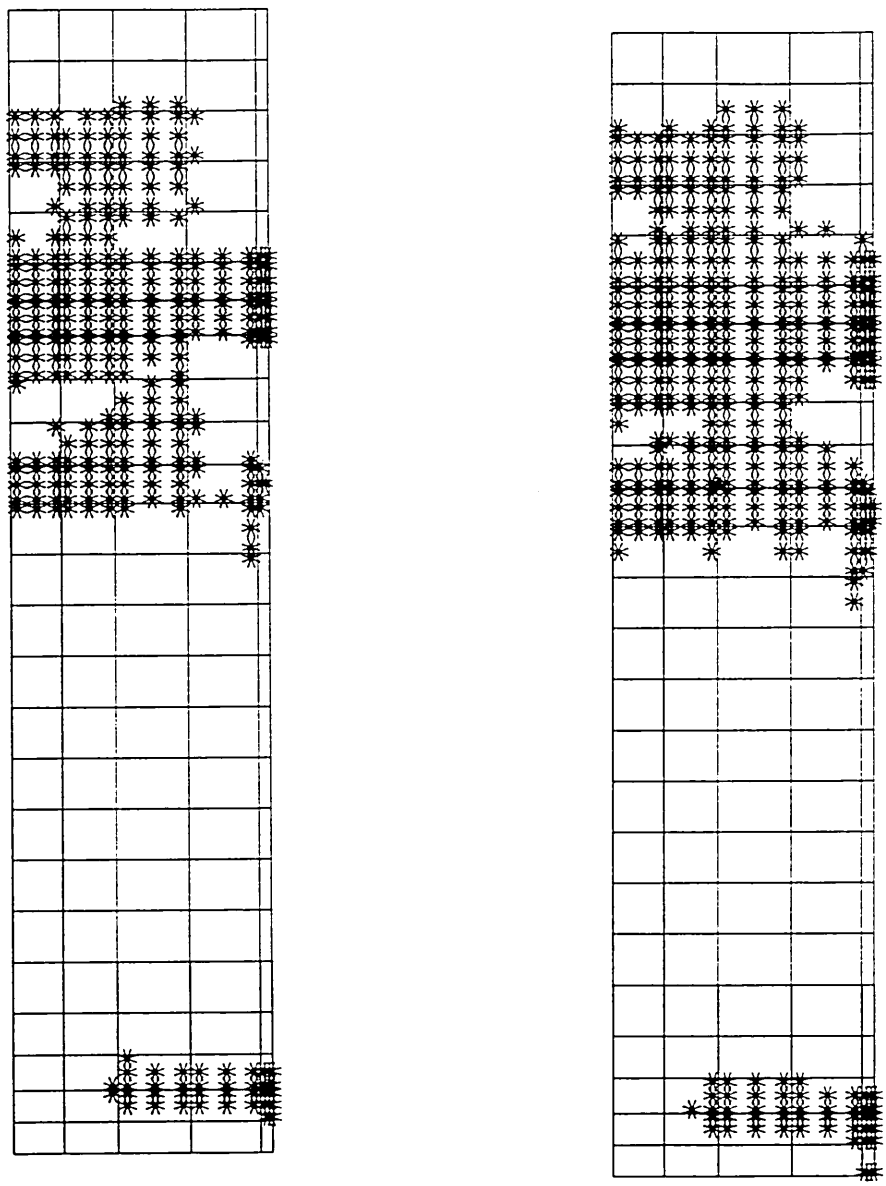

(c) (d)

Fig. 7.25 Yield propagation for 10mm end plate (third set)

Fig. 7.26 Comparison between theoretical and experimental column flange strain results for 15mm end plate connection (first set)

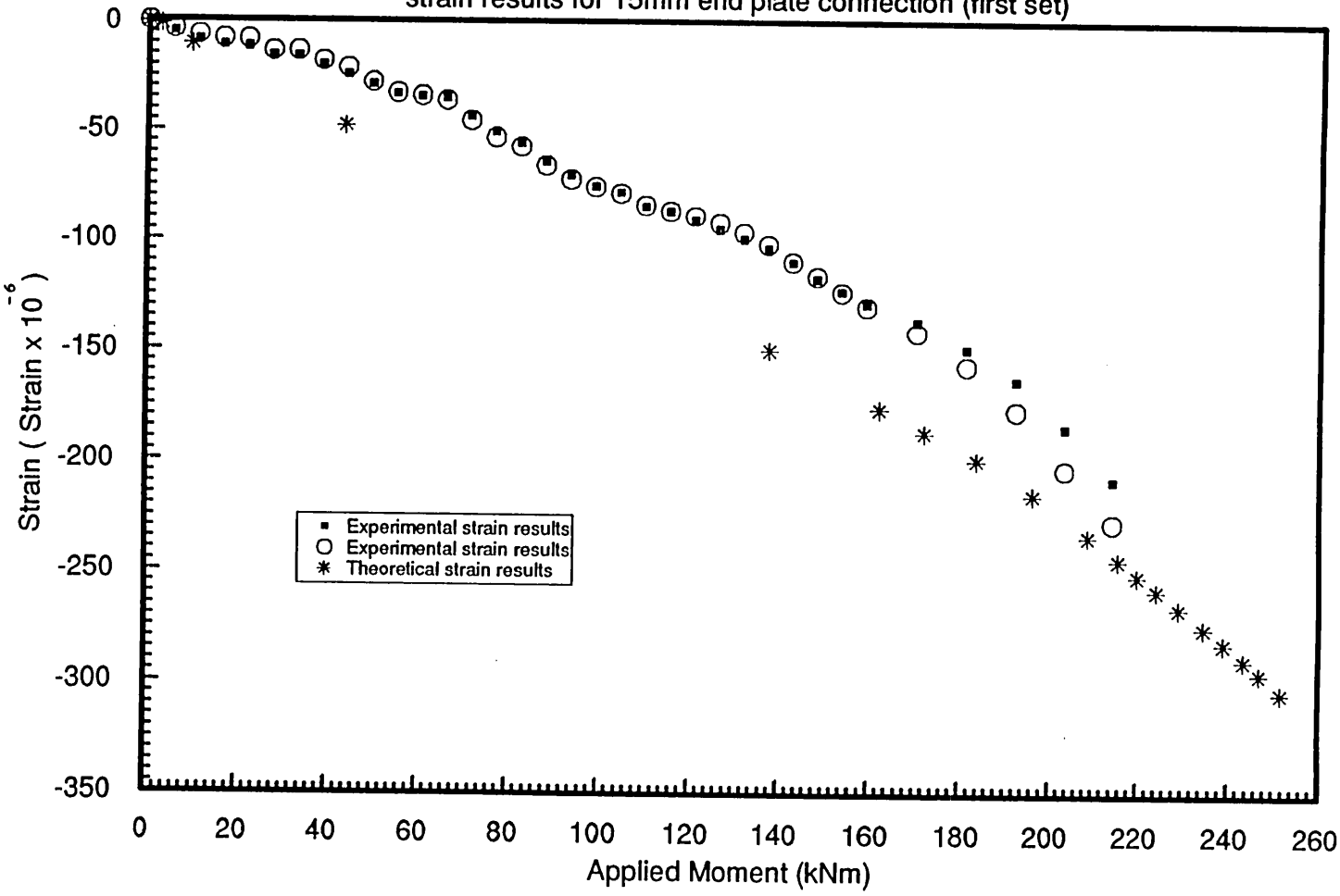

Fig. 7.27 Comparison between theoretical and experimental column flange strain results for 15mm end plate connection (first set)

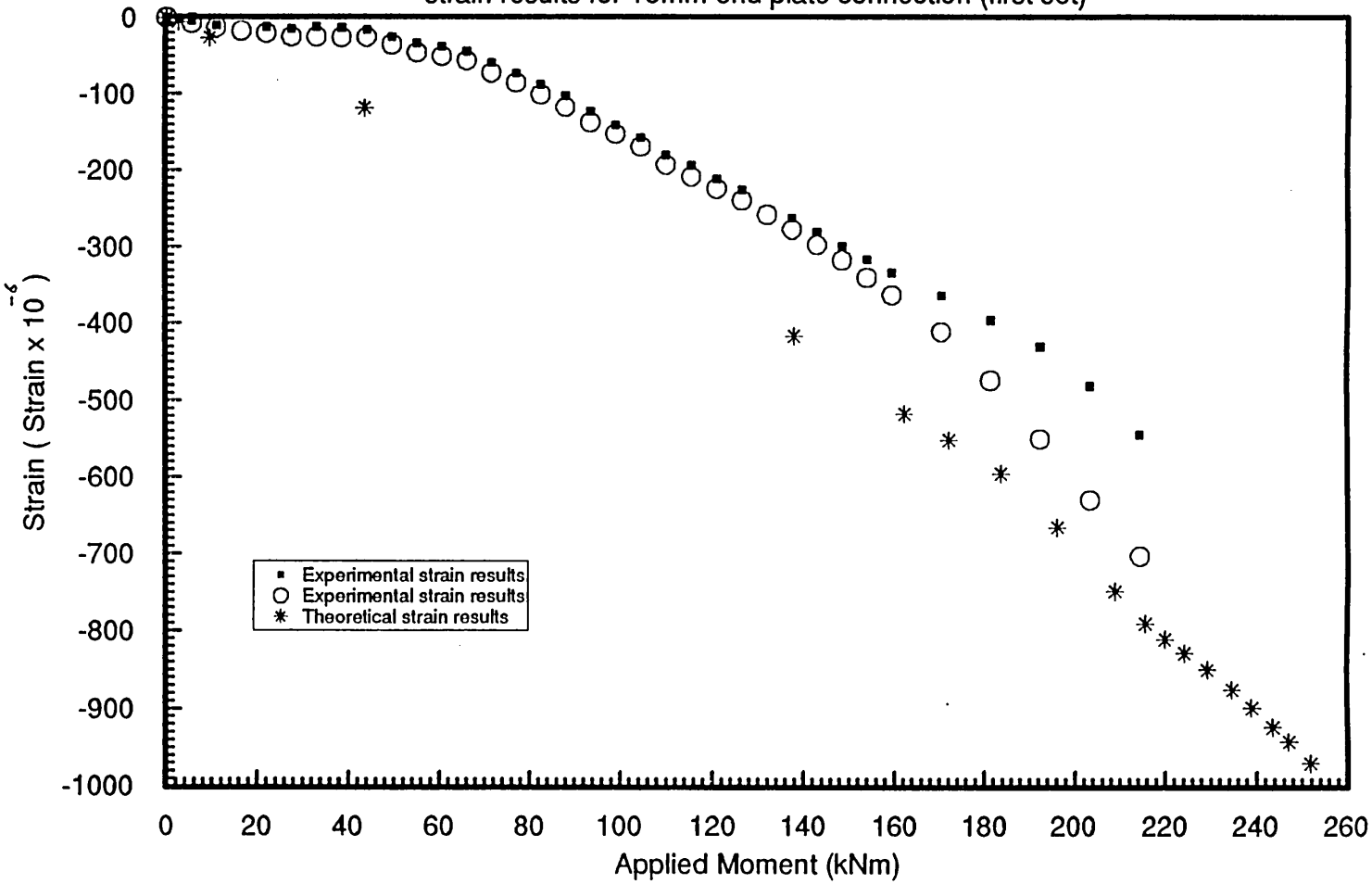

Fig. 7.28 Comparison between theoretical and experimental column flange strain results for 15mm end plate connection (first set)

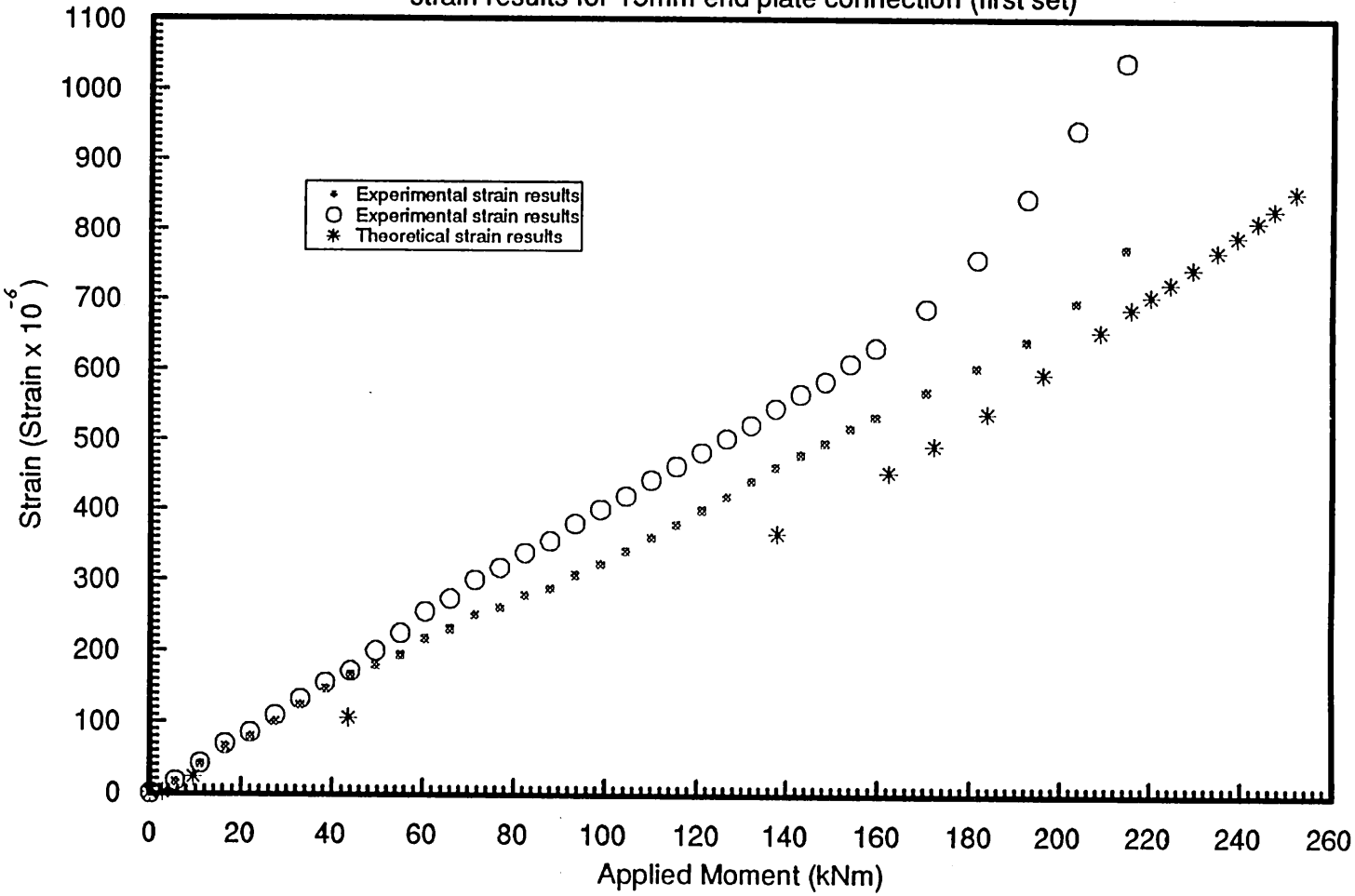

Fig. 7.29 Comparison between theoretical and experimental column flange strain results for 15mm end plate connection (second set)

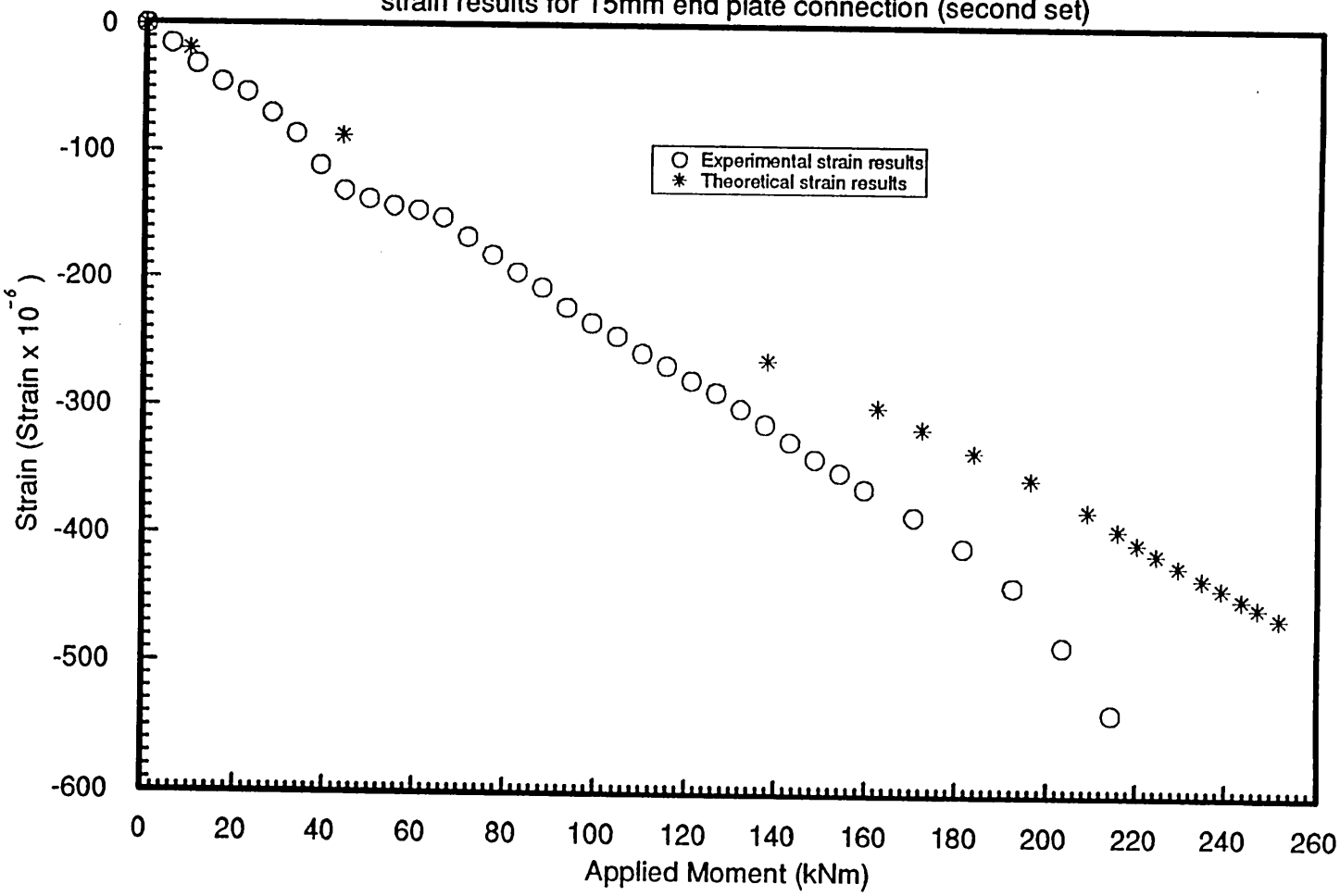

Fig 7.30 Comparison between theoretical and experimental column flange strain results for 15mm end plate connection (second set)

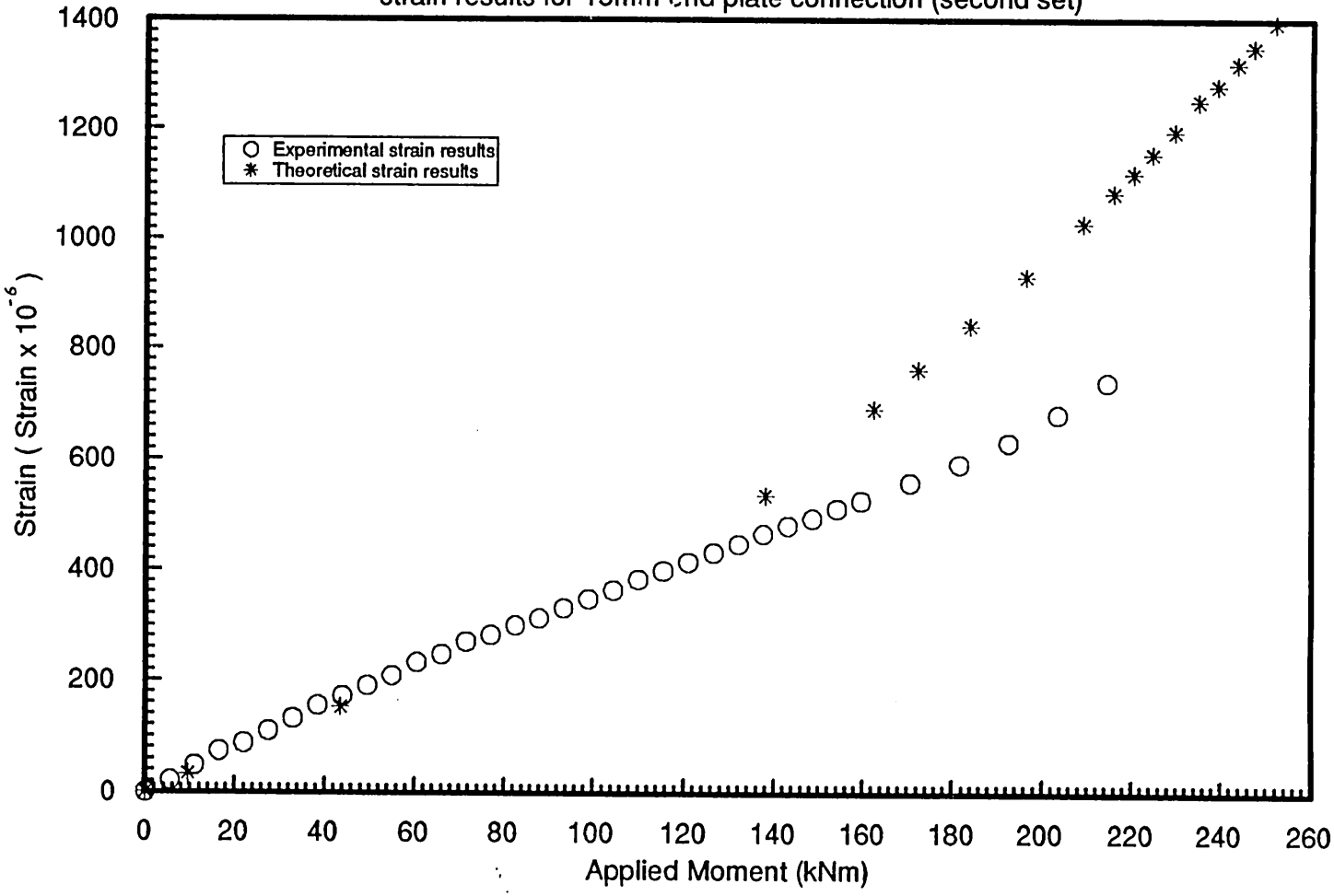

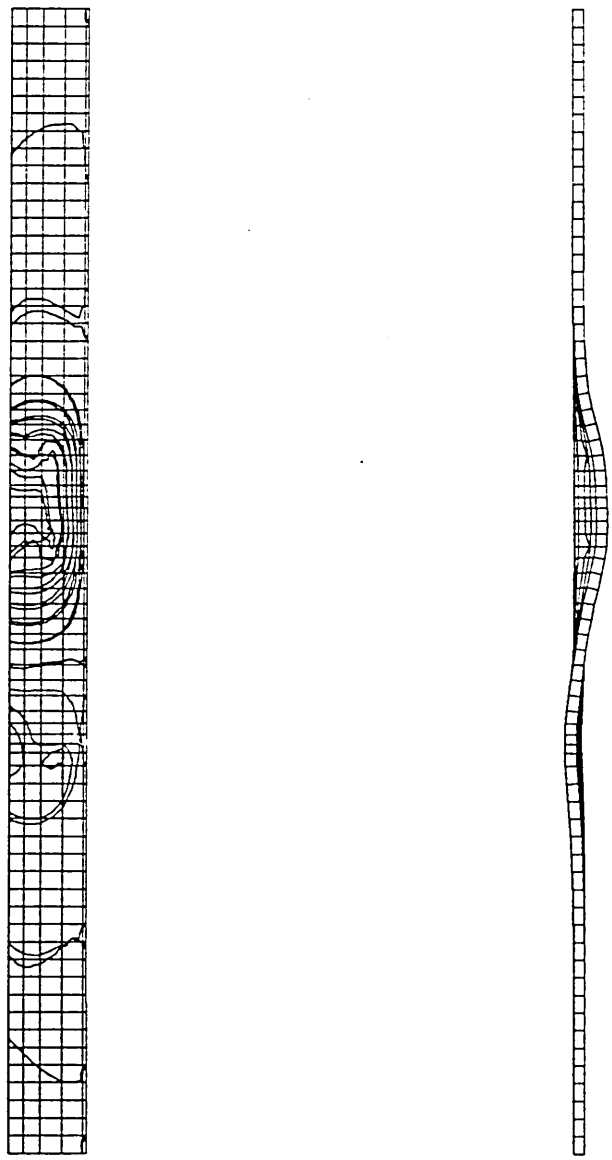

Fig. 7.31 Displacement contours for column flange (10mm end plate connection, third set)

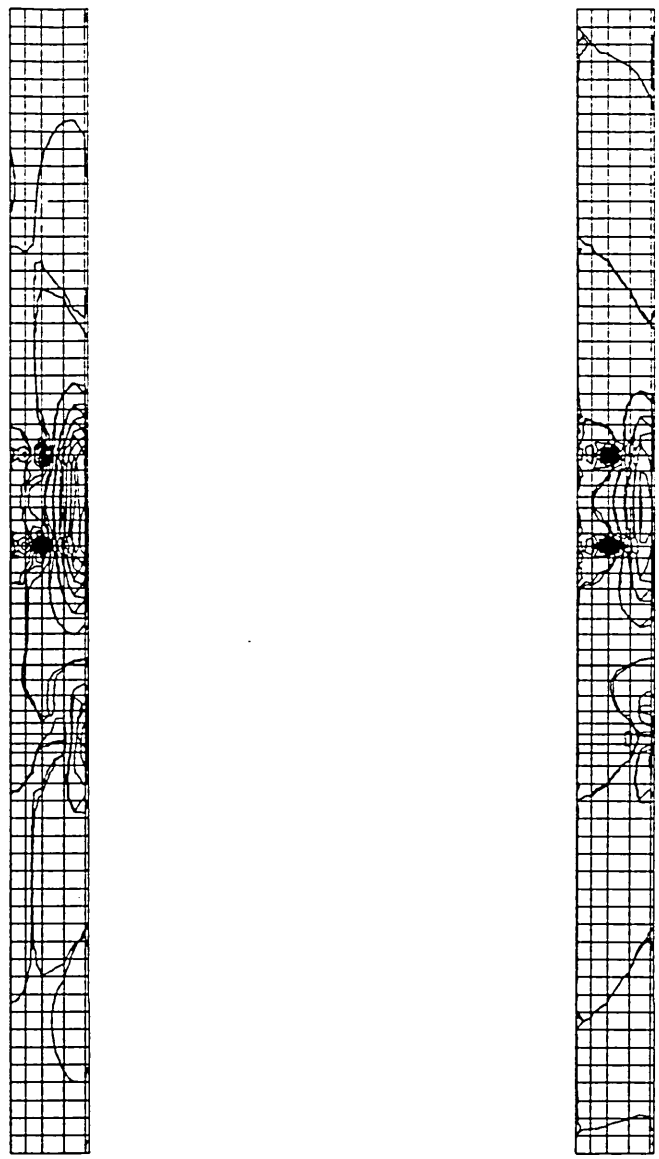

(a) (b)

Fig. 7.32 Strain and stress contours for column flange
(10mm end plate connection, third set)
(a) Stress distribution contours (b) Strain contours

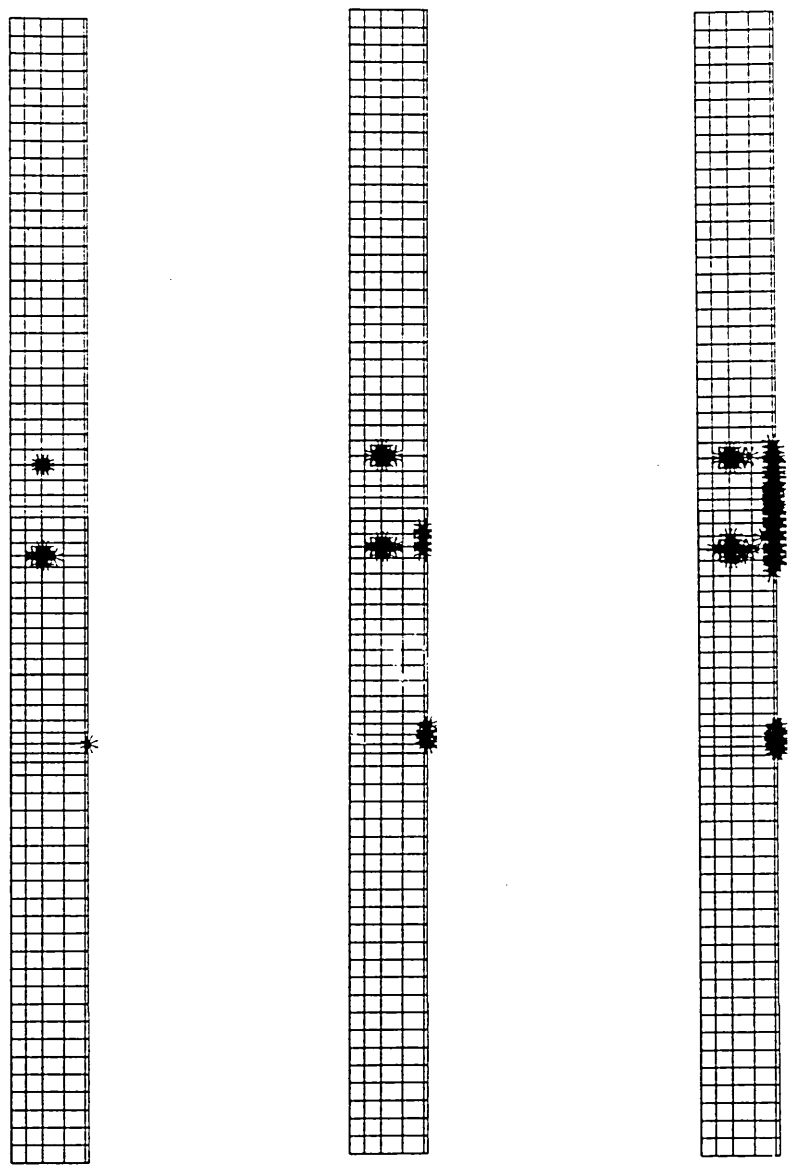

Fig. 7.33 Yield propagation for column flange (10mm end plate connection, third set)

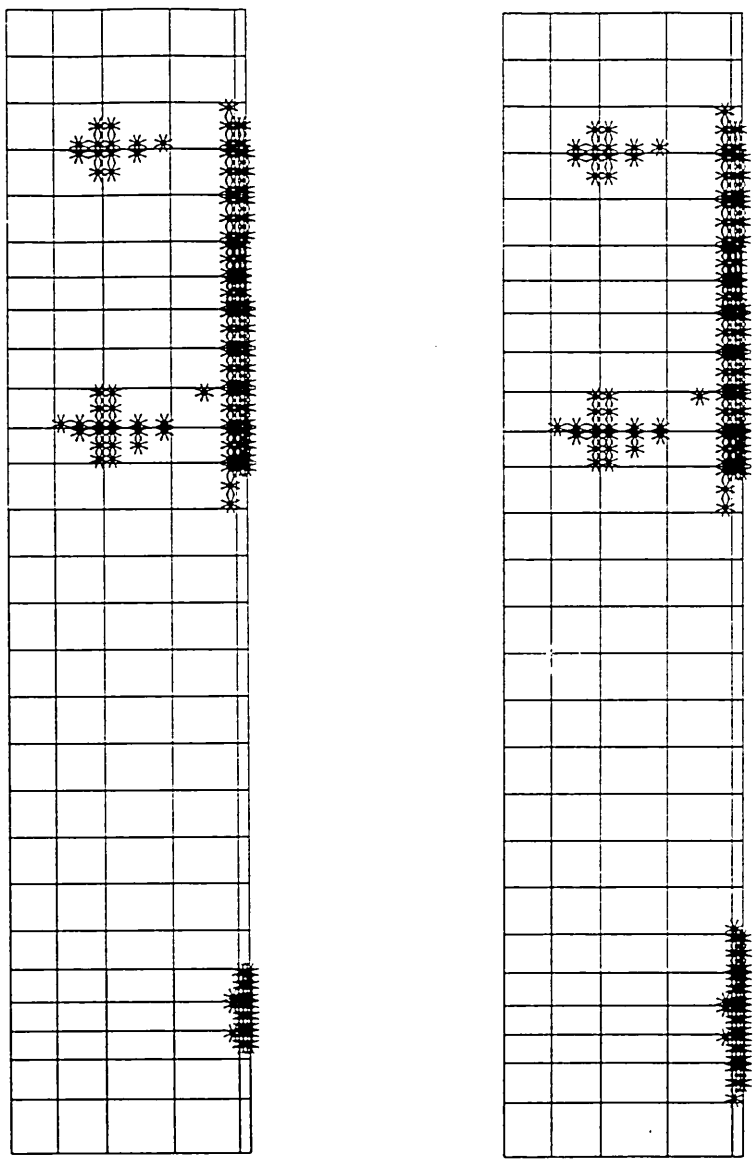

(d) (e)

Fig. 7.33 Yield propagation for column flange

Fig. 7.34 Stress contours for column web 10mm end plate connection, third set)

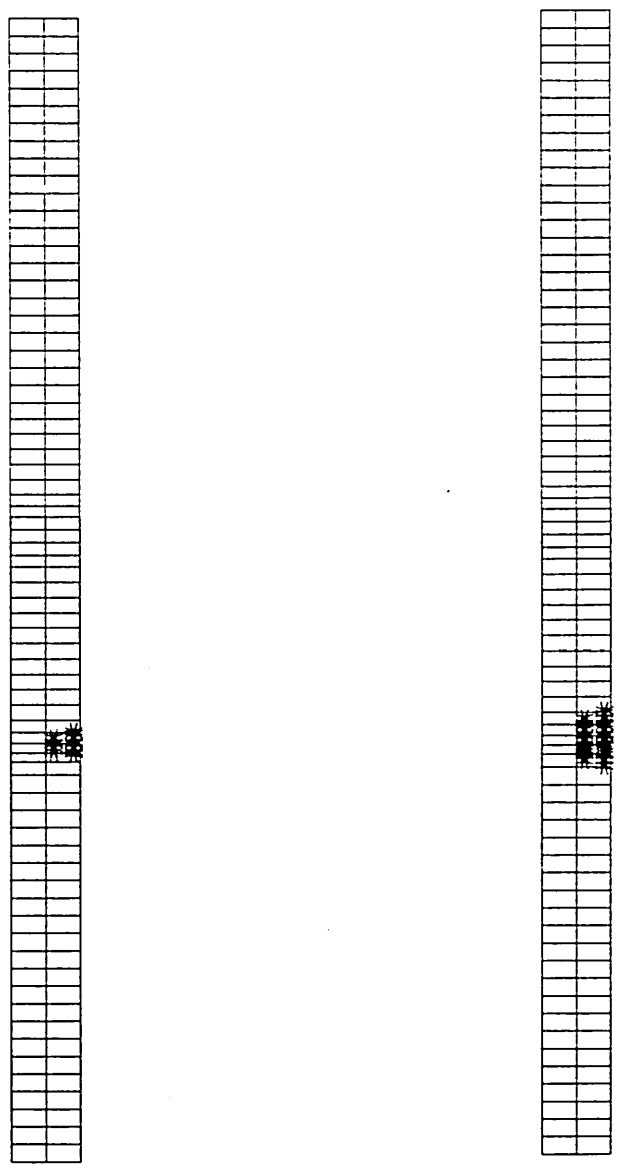

(a) (b)

Fig. 7.35 Yield propagation for column web (10mm end plate connection, third set)

CHAPTER 8

Design Method

8.1 Introduction

As stated previously, the primary objectives of the research project were to carry-out an in-depth investigation into the behaviour of the unstiffened extended end plate connection and to develop a limit state design method for this type of connection. However, an inordinately long time had to be spent to understand and then use the LUSAS finite element package to solve the complex three dimensional, nonlinear problem. It was demonstrated in chapter 7 that the performance of the connection could be predicted, with a high degree of accuracy, by the LUSAS finite element package. It would require the generation of large number of models and computer runs to collect adequate data for the purpose of producing design curves for the connection. Because of the time factor the author was unable to complete the task and he would strongly recommend that, in future, the routine work be carried out to complete the investigation. Professor Jenkins, one of the author's supervisors, had proposed a design method for flush end plate connection [32]. A similar method could be employed for the limit-state design of Extended End Plate Connection and a preliminary attempt to this end has been made by the author. A resume of Professor Jenkin's design method is given in the subsequent sections.

The flexural behaviour of a connection is best described by the relationship between the moment transmitted by the connection and the relative rotation of the two members fastened by the connection. Due to the variety of reasons mentioned before the moment-rotation curves are usually non-linear over the entire range of the curve. This non-linearity is the product of decreasing stiffness of the connection as the load increases. Therefore, the stiffness of a connection, which is represented by the slope of the moment-rotation response at any moment, would follow a non-linear pattern. Similar to rotational charateristics, the stiffness of a connection depends on the following factors:

(i) depth of the connected beam;

(ii) cross-centre distance between bolt holes;

(iii) type and size of bolts;

(iv) whether connection is to column web, column flange or grider web;

(v) end plate yield load;

(vi) column flange yield load;

(vii) column web yield load;

(viii) local beam and column flange buckling; and

(ix) end plate and column contact during deformation.

A reliable estimate of the connection stiffness is a prerequisite for the formulation of a design method for semi-rigid connections.

8.2 Connection Strength

The most appropriate parameter in the assessment of connection strength is the ultimate moment, which is the maximum moment which can be transmitted by the connection. The ultimate moment of a connection is the smallest of the values of M_{UB}, M_{UP} and M_{UC}, the ultimate moment based on bolt tension, end plate bending and column flange bending respectively. High-tensile bolts are brittle and the failure of these bolts are abrupt. Hence it is not a good practice to allow the ultimate moment of a connection to be based on the ultimate bolt tension. In the design method the bolt strengths recommended by BS5950 was adopted, which include provisions for such effects as the increase in the actual bolt force due to prying action and are in general conservative. Such analysis of the connection strength assumes that the failure can only take place in one of the above three elements, namely bolt, end plate and column flange. However, the design procedure should consider welds, shear capacity of the connection and buckling in the column web.

In order to evaluate the ultimate moment of the connection a series of charts were produced from the two dimensional finite element analysis of the end plate, reinforced column flange and the bolt strength recommended by BS5950. These design charts are for stiffened flush end plate connection with four tension bolts. The ultimate moment of the grade 8.8 bolts were determined using a linear bolt force relationship. These values of M_B are plotted against the overall depth of the beam, D

for M16, M20 and M24 bolts (Fig. 8.1), from which the diameter of the bolts for a particular beam section can be determined.

The strength of the connection due to plate bending was determined from elastic-plastic finite element analysis. Such study resulted in a series of graphs where the M_{UP} and θ_{UP} were plotted agaist the end plate thickness, t, for various universal beam sections (Figs. (8.2) and (8.3)). These charts would allow the resistance exhibited by the end plate and the resulting rotation to be determined for various end plate thickness and beam sections. A similar parametric study was used to produce two sets of curves for M_{UC} and θ_{UC} agaist the depth of the beam, D, for four different column sections (Figs. (8.4) and (8.5)). In producing these curves it was assumed that column web was stiffened with conventional stiffeners in line with the flanges of the beam.

8.3 Principal Design Parameters

The principal parameters in the design of the bolted end plate connection are the moments M_L and M_U and the corresponding rotations θ_L and θ_U. The first pair (M_L, θ_L) indicates the limit of the elastic behaviour of the connection and the range within which the theoretical stiffness of the joint is constant and is given by:

$$K_T = \frac{M_L}{\theta_L} \qquad (8.1)$$

where K_T is theoretical (linear) elastic stiffness of the connection, and

M_L is the maximum moment for linear behaviour of the connection.

This value of connection stiffness is important when assessing the serviceability limit state design of the beam and also in assessing the strength of the beam in the elastic range of connection behaviour. Moreover, in the ultimate limit state design of connection the critical parameters are the ultimate moment capacity of the joint M_U and the corresponding value of rotation, θ_U; and for the plastic hinge to form in the beam at ultimate load, the connection must have sufficient rotational capacity.

Stiffness of a connection is defined as the moment necessary to produce unit rotation of the joint. The distribution of stress resultant throughout the steel frame structure will depend on the connection stiffness as well as the stiffness of the structural elements. The connection stiffness, which can be determined from the analysis of the moment-rotation curve, behaves non-linearly and reduces progressively as the bending moment increases. A degree of approximation is essential in the design approach to obtain a practical representation of the moment-stiffness relationship. A bi-linear relationship was proposed in the design method. The idealized moment-stiffness relationship assumes the stiffness of the connection to be constant from zero load upto a moment level M_L from where the stiffness decreases linearly to zero at ultimate moment of the connection, M_U, as shown in Fig. (8.6a). The rotations corresponding to the moments M_L and M_U are θ_L and θ_U respectively.

The implication of such assumption is that the moment-stiffness characteristics of a connection can be defined by just three parameters, K_T, M_L and M_U and once K_T and

M_L are determined the elastic behaviour of the connection is determined upto its maximum elastic limit. At higher values of moment, $M > M_L$, the stiffness of the connection is assumed to decrease linearly (Fig. (8.6a)).

The assessment of M_L and consequently K_T for the connection was based on the experimental investigation which exhibited a considerable variability in the actual stiffness by supposedly identical connections. If K_T is the theoretical value of stiffness, actual stiffness had been observed to lie within the range of $K_T/3$ to $2K_T$. It was proposed that upto a moment level M_L the beam design should be based on a connection stiffness of $K_T/3$. At end moment (M_E) level between M_L and $1/2(M_L + M_U)$ a connection stiffness of $K_T/6$ was proposed. Above $1/2(M_L + M_U)$ the connection was deemed to have no stiffness and the beam design should be based on the constant end moment M_U. The connection stiffness for different end moments are indicated in Fig. (8.6b).

8.4 Determination of Connection Stiffness

As stated previously, Prof. Jenkins proposed design method was based on two dimensional finite element analysis of stiffened flush end plate connection. Separate analyses of end plate and column flange were carried out. Moment-rotation graphs were constructed from which the values of M_L, θ_L, M_U and θ_U were obtained for both components. These values were denoted by the additional subscripts **P** and **C** for the end plate and column flange respectively. Therefore, the estimation of elastic

connection stiffness, K_T, can be carried out as follows. For a particular connection determine:

$$K_{LP} = \frac{M_{LP}}{\theta_{LP}}$$

$$K_{LC} = \frac{M_{LC}}{\theta_{LC}} \qquad (8.2)$$

$$K_{LB} = \frac{M_{LB}}{\theta_{LB}}$$

Since the bolt behaviour is elastic upto 85% of its ultimate moment and its fracture would be catastrophic, the design bolt strength was assumed to be within the linear elastic region. Therefore, $M_B = M_{LB} = M_{UB}$. This moment was calculated on the assumption that the bolt force distribution was linear and that the centre of rotation was located at the centre-line of the beam compression flange. The corresponding rotation, θ_B would be proportional to

$$\frac{g}{A\,E}$$

where, g is the grip length of the bolt which is the total thickness of end plate and column flange;

A is the effective area of the bolt; and

E is the modulus of elasticity of the bolt material.

The third of equations (8.2) may be rewritten as:

$$K_B = \frac{M_B}{\theta_B} \tag{8.3}$$

The stiffness of the connection could then be determined by combining the individual stiffnesses. At any level of connection moment $M_E \leq M_L$ the connection rotation will be

$$\theta = \theta_P + \theta_C + \theta_B$$

$$\theta = M_E \left[\frac{\theta_{LP}}{M_{LP}} + \frac{\theta_{LC}}{M_{LC}} + \frac{\theta_B}{M_B} \right] \tag{8.4}$$

and the connection stiffness will be

$$K_T = \frac{M_E}{\theta}$$

$$= \frac{1}{\left[\frac{\theta_{LP}}{M_{LP}} + \frac{\theta_{LC}}{M_{LC}} + \frac{\theta_B}{M_B} \right]} \tag{8.5}$$

8.5 Design Equations

A series of design equations were derived by Prof. Jenkins [32], assuming symmetrical end conditions and loading. The basic equation is dependent upon a parameter, α, which is given by

$$\alpha = \frac{2EI}{K_T L} \qquad (8.6)$$

This parameter is used to relate the fixed end moment of the beam M_F to the actual end moment M_E, which can be expressed as:

$$\frac{M_E}{M_F} = \frac{1}{(1+\alpha)} \qquad (8.7)$$

The value of α varies between zero and infinity in the extreme cases which correspond to the ideally rigid and ideally pinned connection respectively. The practical range of α for flush end plate connection has been estimated to lie between 0.1 and 0.7 with lower values being applicable to stiffer connections. The above equations, (8.6) and (8.7), can be used to assess the connection moment under actual or assumed linear elastic conditions. Moreover, the central deflection of the beam Y_C can be determined from:

$$Y_C = Y_{CO} - M_E \frac{L^2}{8EI} \qquad (8.8)$$

where, Y_{co} is the central deflection at applied service load on simply supported span and is given by:

$$Y_{co} = \frac{5wL^4}{384EI} \qquad (8.9)$$

In the ultimate load design there is a need to check that the connection has sufficient rotation capacity to allow the plastic hinge to develop in the span of the beam. Therefore the ultimate rotation of the connection has to be determined. Three cases have to be considered depending upon which component defines the ultimate moment.

(1) If $M_U = M_{UP}$, then

$$\theta_U \approx \theta_{UP} + \left[\theta_{LC} + (M_U - M_{LC}) \frac{(\theta_{UC} - \theta_{LC})}{(M_{UC} - M_{LC})} \right] \qquad (8.10)$$

(2) If $M_U = M_{UC}$, then

$$\theta_U \approx \theta_{UC} + \left[\theta_{LP} + (M_U - M_{LP}) \frac{(\theta_{UP} - \theta_{LP})}{(M_{UP} - M_{LP})} \right] \qquad (8.11)$$

(3) if $M_U = M_B$, then

$$\theta_U \approx \left[\theta_{LC} + (M_U - M_{LC}) \frac{(\theta_{UC} - \theta_{LC})}{(M_{UC} - M_{LC})} \right] + \left[\theta_{LP} + (M_U - M_{LP}) \frac{(\theta_{UP} - \theta_{LP})}{(M_{UP} - M_{LP})} \right] \qquad (8.12)$$

The above equations are developed on the simplfying assumption that the moment-rotation relationships are bi-linear between the origin, (M_L, θ_L) and (M_U, θ_U). If the terms in the parenthesis become negative, they should be considered to be zero and the equations (8.10), (8.11) and (8.12) should be replaced by:

$$\theta_U \approx \theta_{UP} + \left[\theta_{LC} \frac{M_{UP}}{M_{LC}} \right] \tag{8.13}$$

$$\theta_U \approx \theta_{UC} + \left[\theta_{LP} \frac{M_{UC}}{M_{LP}} \right] \tag{8.14}$$

$$\theta_U \approx \left[\theta_{LC} \frac{M_{UP}}{M_{LC}} \right] + \left[\theta_{LP} \frac{M_{UC}}{M_{LP}} \right] \tag{8.15}$$

8.6 Design Procedure

The first step in the design of the flush end plate connection is to calculate the maximum free bending moment on the beam, M_O. By choosing a trial ratio of M_U/M_P between 0.3 and 0.5 (the lower value being appropriate for long spans and the higher value for short spans) the ultimate moment of the beam, M_U and ultimate moment of end plate, M_P can be determined from the following relationship:

$$M_U + M_P \geq M_O$$

This would allow a tentative choice of beam size. Once the beam depth, D, is known the bolt diameter can be determined from the graph of M_B against the beam depth

Fig.(8.1). It is necessary to ensure that the moment due to bolt forces, M_B, is not less than the ultimate moment of the connection. A choice of end plate thickness is then made using Fig. (8.2), such that M_{UP} is not less than the M_U required. Assuming that a trial section has been chosen for the column, M_{UC} can be determined from Fig. 8.4. The ultimate moment of the connection, M_U is now the smallest of the three values of M_B, M_{UP} and M_{UC}. The corresponding rotations θ_B, θ_{UP} and θ_{UC} can be obtained from Figs. (8.1), (8.3) and (8.5) . At this stage M_{LP}, M_{LC}, θ_{LP} and θ_{LC} are known. Therefore, using equation (8.5) the theoretical stiffness of the connection can be calculated. The beam design should be checked for the moment consistent with the elastic behaviour of the connection at $K = K_T/3$. This stiffness is valid upto a moment level M_L where M_L is the smallest of the M_B, M_{LP} and M_{LC}. Using equations (8.6) and (8.7) the end moment is determined which should be less than M_L. Above this level of moment the connection stiffness reduces and at moment levels between M_L and $1/2(M_U + M_L)$ it was proposed that a reduced connection stiffness of $K_T/6$ be considered. Once adequacy of the connection is proven by recalculating the end moment, the serviceability displacement requirement of the beam due to unfactored imposed load is checked by equation (8.8). A value of stiffness is chosen in accordance with the moment due to unfactored imposed load. If the ratio of the deflection, Y_C to the span of the beam is below the 1/360 limit it is deemed to be satisfactory.

In order to ensure that the plastic hinge is formed in the beam it is necessary to check the rotational capacity of the connection. The ultimate rotation of the connection can

be determined using the appropriate equation from (8.10), (8.11) and (8.12). If the calculated rotation is more than the value obtained from the chart, Fig.(8.7), the design of the connection is complete. Any reader who wants to pursue the design procedure in greater detail should consult Reference 32.

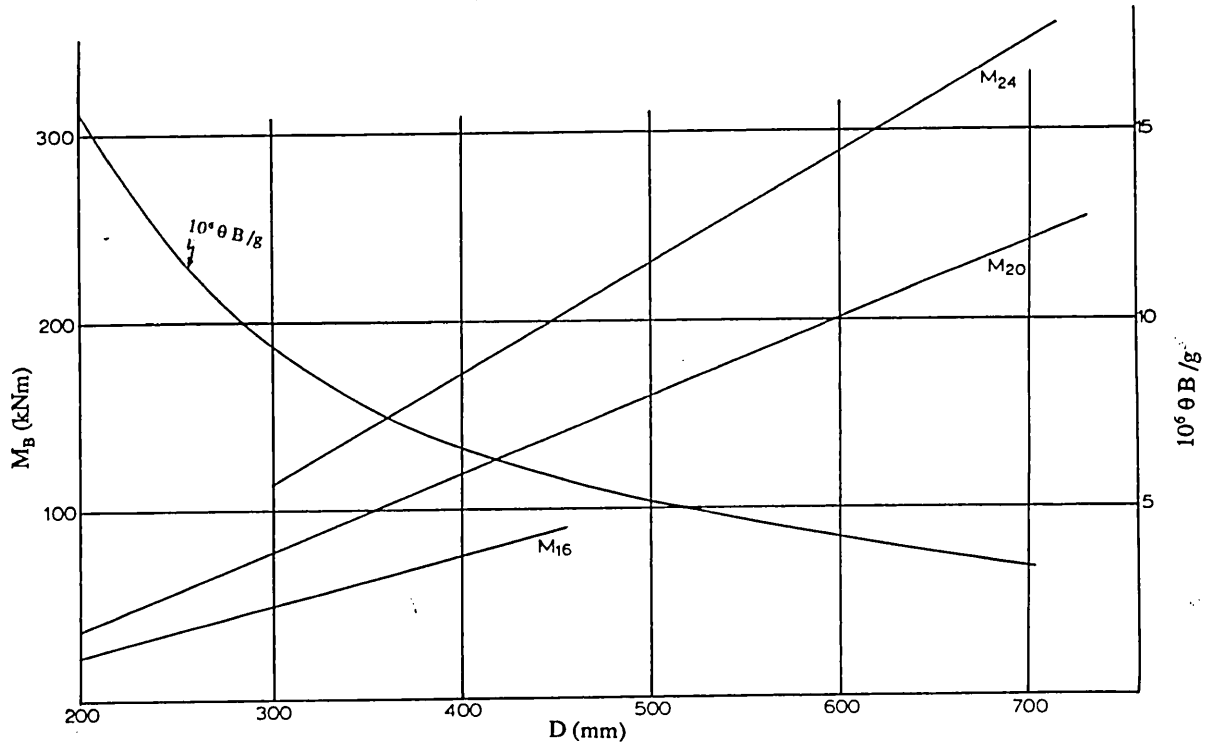

Fig. 8.1 Flush end plate with grade 8.8 bolts;
Moment capacity (M_B) and corresponding rotation (θ);
D, beam depth (mm), g, grip length (mm) (Reproduced from Ref. 32).

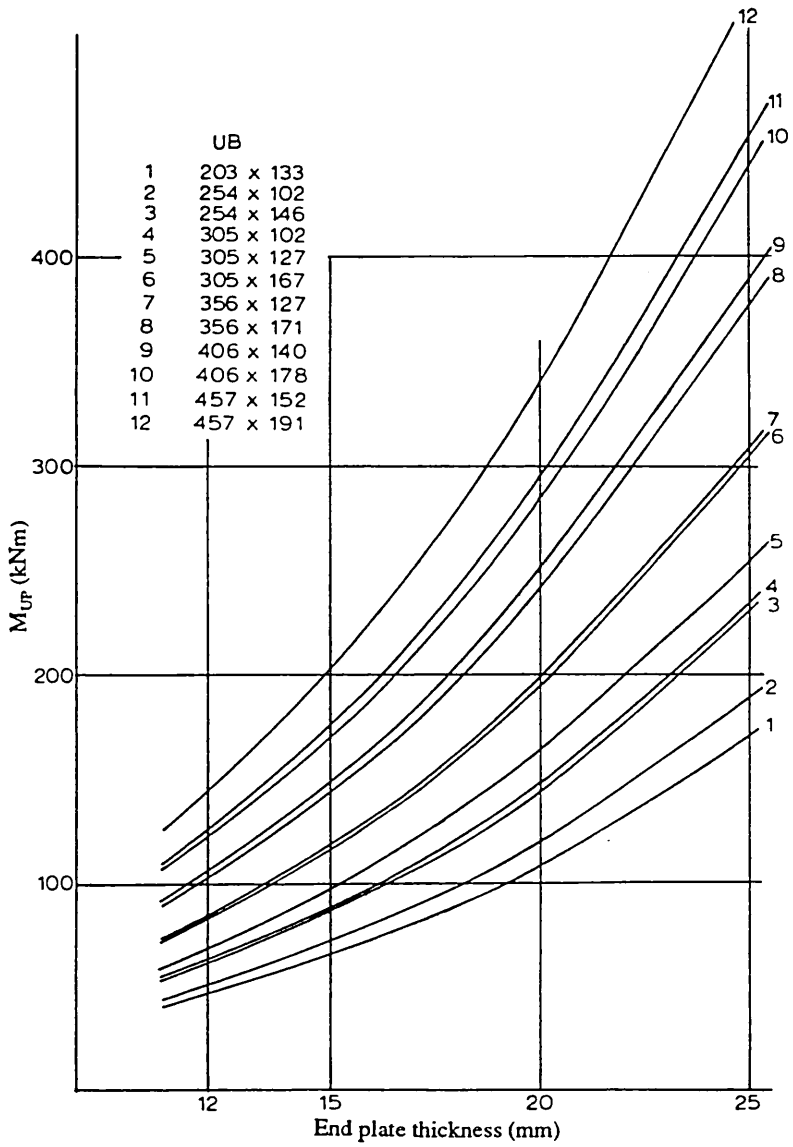

Fig. 8.2 M_{UP} for flush end plates with four tension bolts; $M_{LP} = 0.6\ M_{UP}$ (Reproduced from Ref. 32).

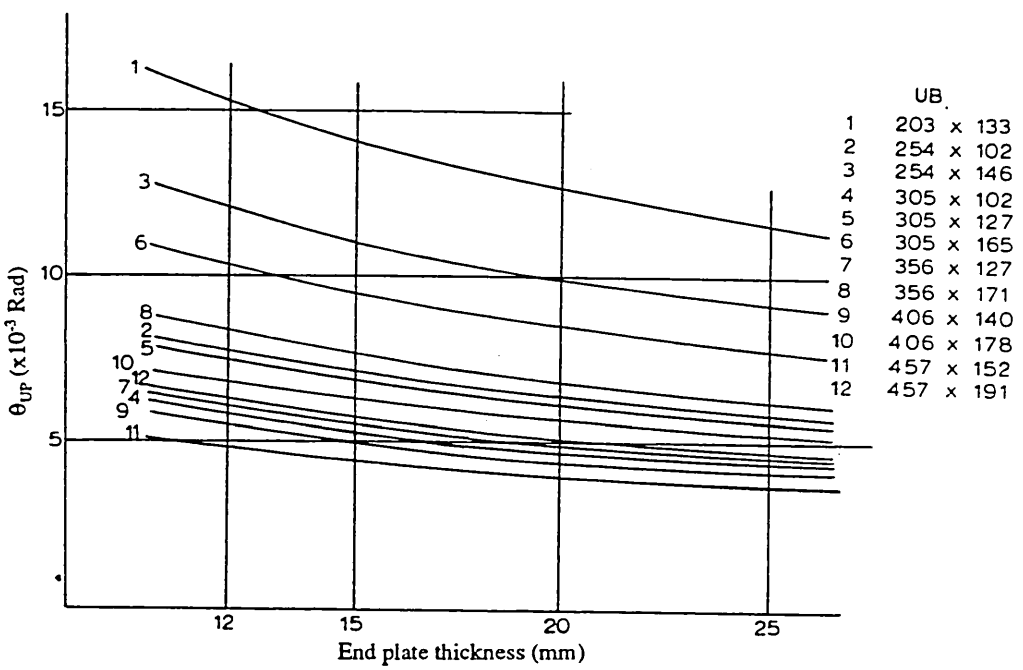

Fig. 8.3 Rotational capacity of end plate, θ_{UP} in flush end plate connection; $\theta = 0.2\ \theta_{UP}$ (Reproduced from Ref. 32).

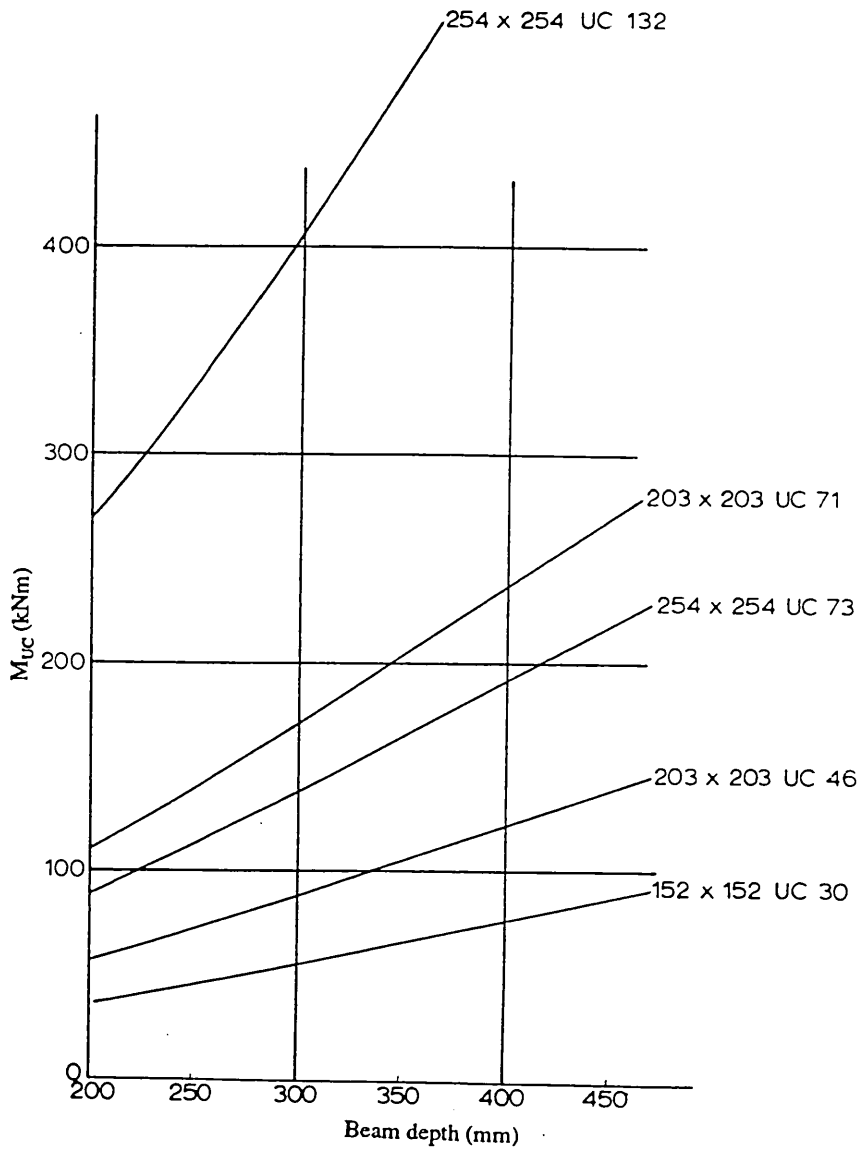

Fig. 8.4 M_{UC} for stiffened column; $M_{LC} = 0.6\ M_{UC}$ (Reproduced from Ref. 32).

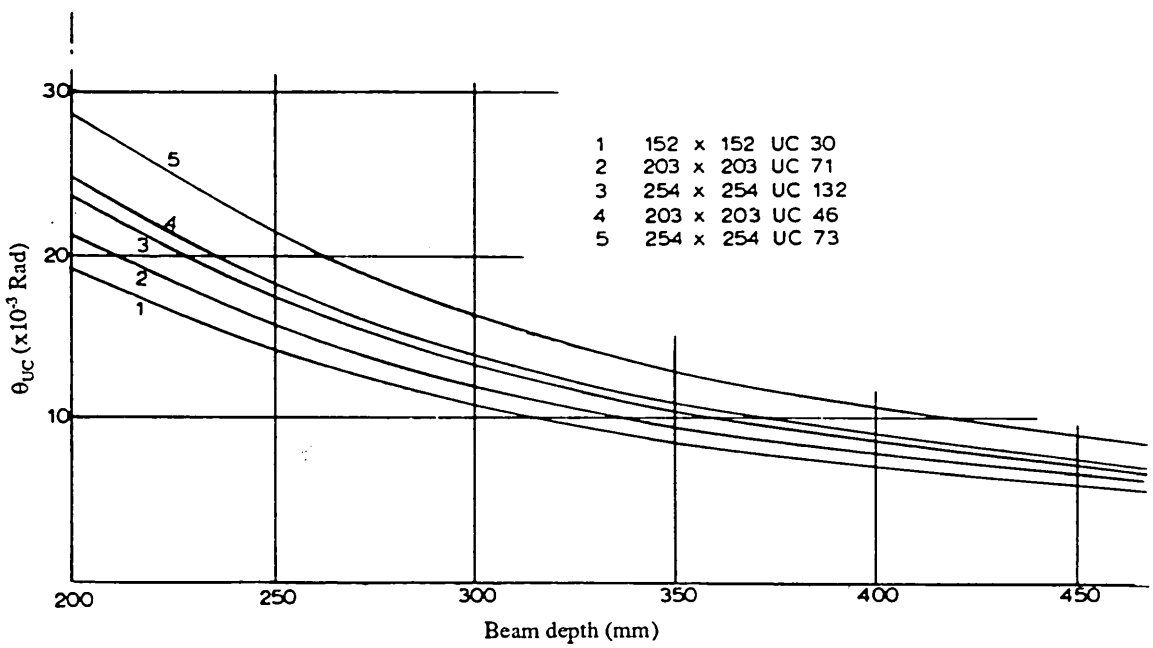

Fig. 8.5 Rotational capacity of end plate, θ_{UP}, in flush end plate connection, $\theta_{LP} = 0.2\ \theta_{UP}$ (Reproduced from Ref. 32).

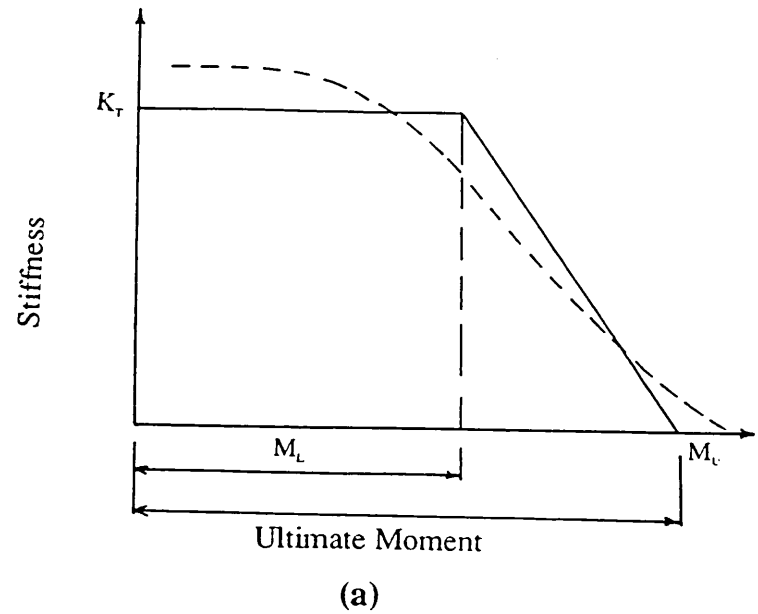

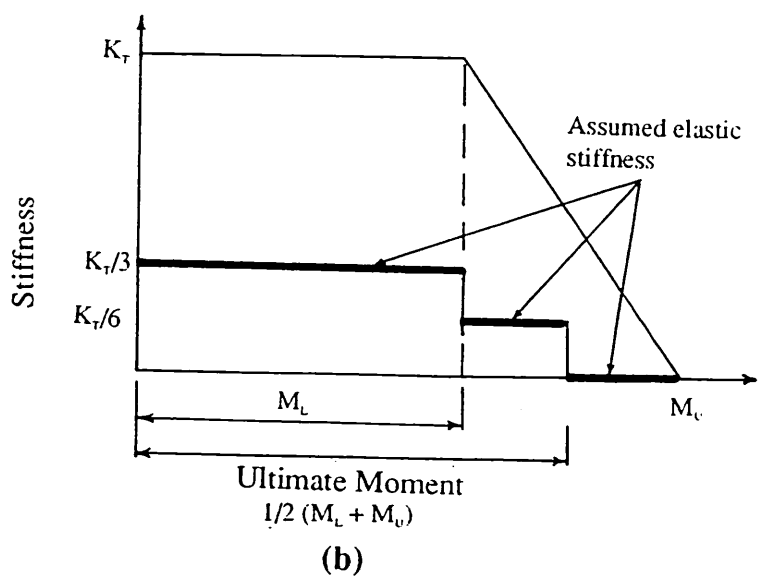

Fig. 8.6 Connection stiffness criterion for beam design (Flush end plate) (Reproduced from Ref. 32).

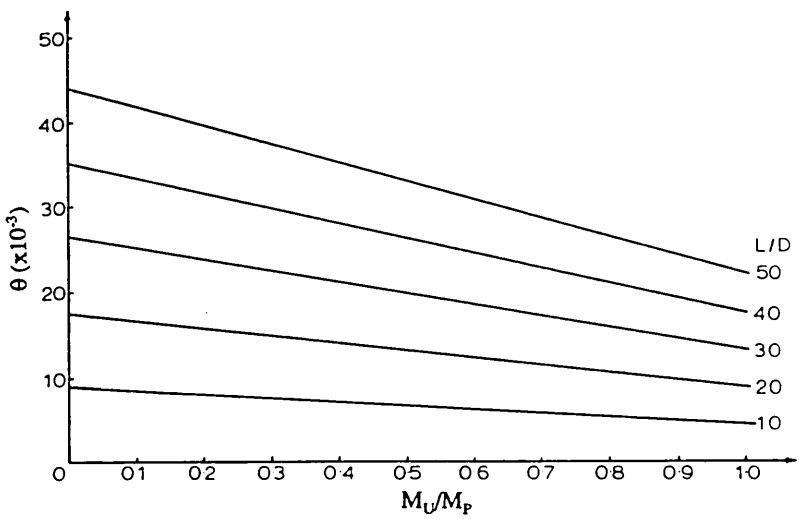

Fig. 8.7 Connection moment needed to allow development of plastic hinge at mid span of beam (Reproduced from Ref. 32).

CHAPTER 9

Conclusions and Recommendations

9.1 Conclusions

End plate connections are extensively used as moment resistant connections between members in steel frames. The popularity of these connections can be attributed to the simplicity and economy associated with their fabrication and erection. Both flush and extended end plate types are widely used in steel frame construction. Extended end plate is more rigid and has a higher moment capacity than flush end plate and is frequently used in steel framed structures to achieve rigid construction. Column stiffeners may be provided at the level of beam flanges to prevent overstressing of the column web in the compression region and column flange in the tension region. However, column stiffening involves costly fabrication and may interfere with the connection of cross beams to the web of the column; therefore it may be preferable to use a heavier column section to avoid column stiffening.

The extended end plate connection presents an extremely complex and highly indeterminate problem with a large number of parameters affecting its structural behaviour. Early attempts to solve the problem by classical structural principles involved many simplifying assumptions and resulted in simple but conservative

design formulae. In recent years efforts have been made to carry out a thorough investigation of the connection with the aim of predicting its behaviour more accurately and formulating a rational and economic design procedure. Two advanced techniques which have been frequently employed in the investigation are the yield line method and the finite element method. Early attempts to analyse the end plate connections using finite element technique were based on two dimensional analysis, treating the connection as a plane stress problem in the plane of the beam web. The column flange was treated either as a rigid base, which did not make any contribution towards the rotational characteristics of the connection, or the column flange was stiffened and had limited deformability. Although attempts were made to model the interaction between the end plate and column flange and determine the position of prying forces, they were mainly unsuccessful. Hence the prying effects were either ignored or a percentage increase in the tension bolt forces was recommended to account for the prying action.

It should be recognised that an extended end plate connection is essentially a three dimensional problem. Although a three dimensional finite element analysis of the connection is much more complicated than a two dimensional one and is a lot more demanding in respect of computer time and facilities, it is nevertheless preferable as it enables a realistic and meaningful solution to the extremely complex problem. The author undertook to build a suitable model of the unstiffened extended end plate connection and to use finite element technique to carry out a three dimensional, non-

linear analysis of the connection. It was further hoped that a limit state design method would be developed in the final stage of the investigation. This task could not be accomplished due to the unforseen problems encountered during the investigation.

A finite element model of the unstiffened extended end plate connection was presented in chapter 4. In the model solid elements were used for the plates, bar elements for the tension bolts and joint elements for the interactive forces generated between the end plate and column flange. The joint elements employed had non-linear properties with infinite stiffness in compression and zero stiffness in tension. This ensured displacement compatibility at nodes where end plate and column flange were in contact but allowed separation at all other nodes except at bolt locations.

In view of the complexity of the problem and in order to provide economy in computer time and space a few simplifying assumptions were made in modelling the connection. Bolt holes were disregarded in the model. Welds and the effect of welding on the yield stress of steel in the heat affected zone were ignored. Also no consideration was given to account for the fillets in the column. The bolts in the compression region were not included in the model, since their contribution towards the moment capacity of the connection was considered to be insignificant.

Twelve full scale tests were conducted and the data obtained from the tests were analysed. These were compared with the results obtained from the finite element

analysis in order to assess the validity of the assumptions made and the accuracy of the three dimensional finite element model.The accuracy of the non-linear analysis was established by comparing the theoretical moment-rotation curves, bolt forces and strains at preselected points with their corresponding experimental values. Experimental investigation and comparison between theoretical and experimental results were reported in chapters 6 and 7 respectively.

The comparison between the experimental and theoretical moment-rotation curves obtained for three connections indicated good agreement between them. In the elastic range the theoretical results were linear whereas the experimental responses were not. This non-linearity was due to a combination of the pretensioning effect, imperfection in fabrication and lack of fit. As none of these effects were included in the analytical model, the results could only be linear in the elastic range. The weld, heat affected zone and bolt head were ignored in the model of the connection which resulted in slight loss of rigidity. It was assumed that omitting bolt holes would compensate for the above loss in the joint rigidity.The theoretical results in the plastic range can be improved if a finer mesh is adopted in the modelling of the connection. The proposed model overlooked the possibility of failure due to web buckling. This can be remedied if a combined material and geometrical non-linear analysis of the web is carried out and the whole of the column web is accommodated in the model instead of the quarter used in the author's model.

Comparative study of inner and outer tension bolt forces also indicated good agreement between the theoretical and experimental results over a wide range of loading. The small discrepancies which existed between them were due to effects of pretensioning and severe bending deformation of the bolts near failure. Throughout the experimental programme the pretensioning of the bolts was kept to a minimum; however a degree of tightening was necessary to ensure reasonable contact between the end plate and column flange. This initial force had not been considered in the theoretical analysis which caused the discrepancies at low load. Also the bar elements representing the bolts in the finite element model could not take account of bending induced on the bolts due to large deformation of the end plate at high moment.

The theoretical investigation of prying forces in the extended end plate connection indicated that, at low moment, the pressures were concentrated at the lower edge of the end plate due to load transfer from the compression flange, as well as along the vertical edge of end plate just below the inner tension bolt position, upper corner and horizontal edge of the extension plate. For thin end plates the prying spread from the edge towards the outer and inner tension bolts. It indicated a very good agreement with the interaction pattern presented by previous researchers. With increasing moment and resulting separation between the end plate and column flange prying decreased and ultimately the only contact between them occurred at the compression region and along horizontal edge of the extension plate. The comparison between theoretical and experimental prying results indicated a similar trend to the bolt force

results. This was expected because the theoretical prying results were derived from bolt forces. From the theoretical results it was found that for a relatively thin end plate connection the increase in the bolt forces due to prying varied from 33 per-cent at low moment to 11 per-cent at high moment.

The theoretical displacement, stress and strain distribution contours determined for end plate and column (flange and web) were typical of the extended end plate responses; the displacement results complied with the displacement pattern observed during the experimental programme. Comparison between the theoretical and experimental strains in the column flange indicated that they were close and the small difference between the two sets of values could be attributed to the approximate nature of the finite element method. These discrepancies can be minimized by adopting a finer mesh in the modelling of the connection. In the LUSAS manual it is recommended that the aspect ratio should not exceed 5:1. Although this was not exceeded in the author's model of the connection, the values for some of the elements were not far from the limiting value.

It was found that the finite element model could chart the development of plasticity throughout the connection.

9.2 Recommendation

It is evident from the investigation that the extended end plate represents a semi-rigid connection between members of a steel frame and exhibits a non-linear moment-rotation relationship over the entire loading history. The degree of rigidity and failure moment of this type of connection depend on a large number of parameters including the thickness of column flange and web, depth of beam, thickness of end plate, diameter and type of bolts, bolt pitch distances and size of the welds. It was found that the proposed three dimensional finite element model was capable of predicting the complex behaviour of this type of connection with a high degree of accuracy. A few simplifying assumptions were made in modelling of the connection. It would be appropriate to investigate the effect of these assumptions on the performance of the model. The unfulfilled task of formulating a limit state design method also needs to be completed. The author recommends that the following investigations be carried out in the future.

(1) The effects of bolt holes, bolt head and nut on the rotational behaviour of the end plate connection should be investigated. This would mean much more complex mesh generation and would require a lot more computer space and time for the analysis.

(2) Welds and the effect of welding on the yield stress of steel in the heat affected zone were ignored in author's model. Investigation should be carried out to determine their effects on the performance of the connection.

(3) It is not precisely known if the high value of aspect ratio used for a few elements of the model had any adverse effect on the analysis of the connection. A model of connection with finer mesh should be built and analysed.

(4) The possibility of column web buckling was ignored in the model. A model should be built which would include the whole of the column web and the analysis be carried out considering both material and geometrical non-linearity.

(5) Parametric study of the connection must be carried out in order to separate the contribution of various components towards the moment-rotation characteristics. This would enable the design curves to be drawn for carrying out a limit state design of the connection.

(6) A related type of connection which is widely used in industry and about which meagre research information is available is the flush end plate connection. Using a method similar to the one proposed by the author for the extended end plate connection, the performance of the flush end plate type should be studied.

REFERENCES

1 **Young G.R., and Jackson K.B.**
'The relative rigidity of welded and riveted connections'.
Canadian Journal of Research, Vol. 11, No. 1 and 2, pp 62-99, 1934.

2 **Ruthbun J.C.**
'Elastic properties of riveted connections'.
Transactions ASCE, Vol. 101, pp 524-563, 1934.

3 **Batho C.**
'Steel Structures Research Committee 1st, 2nd and 3rd reports'.
Department of Scientific and Industrial Research, HMSO, London, 1931, 1934 and 1936.

4 **PD3343**
'Recommendations for design'.
Suppliment No. 1 to BS449, British Standards Institution.

5 **Munse W.H., Bell W.G. and Chesson E.**
'Behaviour of riveted and bolted beam-to-column connections'.
Journal of Structural Division, ASCE, Vol. 85, ST3, pp 25-50, March 1959.

6 **Godly M.H.R. and Needham F.H.**
'Comparative tests on 8.8 and H.S.F.G. bolts in tension and shear'.
The Structural Engineer, Vol. 60A, N0. 3, pp 94-101, March 1982.

7 **Higgins T.R. and Rubles**
'Structural uses of High Strength bollts'.
Transactions ASCE, Vol. 120, 1955.

8 **Stewart W.C.**
'History of the use of High Strength bolts'.
Transactions ASCE, Vol. 120, 1955.

9 **Disque R.O.**
'End plate connections'
National Engineering Conference Proceedings, American Institute of Steel Construction pp 30-37, 1962.

10 **BS5950 Parts 1 and 2**
'Structural use of steelwork in building'
British Standards Institution, London, 1990.

11 **Bose B., Sarkar S. and Bahrami M.**
'Finite element analysis of unstiffened extended end plate connections'
Structural Engineering Review, No. 3, pp 211-224, 1991.

12 **Wilson W.M. and Moore H.F.**
'Tests to determine the rigidity of riveted joints in steel structures'
University of Illinois, Engineering Experiment Station, Bulletin No. 104, U.S.A, 1917.

13 **Hetchman R.A. and Johnson B.G.**
'Riveted semi-rigid beam-to-column building connections'
Progress Report No. 1, Committee of Steel Structures Research, AISC, November 1947.

14 **Schutz F.W.**
'Strength of moment connections using high tensile strength bolts'
Proc. Nat. Eng. Conference, AISC, 1959.

15 **Sherbourne A.N.**
'Bolted beam to column connexions'
The Structural Engineer, Vol. 39, No. 6, pp 203-210, June 1961.

16 **Douty R.T. and McGuire W.**
'High strength bolted moment connections'
Journal of Structural Division, ASCE, Vol. 91, ST2, pp 101-129, April 1965.

17 **Nair R.S., Birkemore P.C. and Munse W.H.**
'High strength bolts subjected to prying'
Journal of Structural Division, ASCE, Vol. 100, pp 1-3, 1974.

18 **Grundy P., Thomas I.R. and Bennetts I.D.**
'Beam-To-Column Moment Connections'
Journal of Structural Division, ASCE, Vol. 106, ST1, pp 313-330, January 1980.

19 **Surtees J.O. and Mann A.P.**
'End plate connections in plastically designed structures'
Conference in Joints in Structures, Vol. 1, Paper 5, University of Shefield, pp 1-20, 1970.

20 **Zoetermeijer P.**
'A design method for the tension side of statically loaded, bolted beam to column connections'
Heron 20, No. 1, Delft University, The Netherlands, 1974.

21 **Packer J.A. and Morris L.J.**
'A limit state design method for the tension region of bolted beam-to-column connections'
The Structural Engineer, Vol. 55, No. 10, pp 446-458, 1977

22 **Krishnamurthy N. and Graddy D.E.**
'Correlation between 2 and 3 dimensional finite element analysis of steel bolted end plate connections'
Computers and Structures, Vol. 6, No. 415, pp 381-389, August 1976.

23 **Krishnamurthy N.**
'Steel bolted end plate connections'
Proceedings of International Conference on Finite Element Methods in Engineering, Adelaide, Australia, pp 23.1-23.16, December 1976.

24 **Krishnamurthy N.**
'A fresh look at bolted end plate behaviour and design'
Engineering Journal of Structural Division, ASCE, Vol. 15, Part 2, pp 39-49, 1978

25 **Krishnamurthy N., Huang H., Jeffery P.K. and Avery L.K.**
'Analytical M-θ curves for the end plate connections'
Journal of Structural Division, ASCE, Vol. 105, ST1, pp 133-145, January 1979.

26 **Tarpy T.S. and Cardinal J.W.**
'Behaviour of semi-rigid beam-to-column end plate connections'
Proceedings of the International Conference on Joints in Structural Steelwork, Teesside Polytechnic, Middlesbrough, April 1981, Pentech Press, pp 2.3-2.25.

27 **Hewlett J.H., Jenkins W.H., Maxwell S.M. and Bose B.**
'The behaviour of semi-rigid connections in steel structures'
Intrim report, Teesside polytechnic, June 1980.

28 **Maxwell S.M., Howlett J.H., Jenkins W.M. and Bose B.**
'A realistic approach to the performance and application of semi-rigid joints in steel structures'
Proceedings of the International Conference on Joints in Structural Steelwork, Teesside Polytechnic, Middlesbrough, April 1981, Pentech Press, pp 2.71-2.98.

29 **Patel K.V. and Chen W.F.**
'Nonlinear anlysis of steel moment connections'
Journal of Structural Engineering, ASCE, Vol. 110, No. 8, pp 1861-75, 1984.

30 **Patel K.V. and Chen W.F.**
'Analysis of a fully bolted connection using NONSAP'
Computers and Structures, Vol. 21, No. 3, pp 505-11, 1985.

31 **Jenkins W.M., Tong C.S. and Prescott A.T.**
'Moment-transmitting end plate connections in steel construction and a proposed basis for flush end plate design'
The Structural Engineer, Vol. 64A, No. 5, pp 121-132, May 1985.

32 **Jenkins W.M.**
'Moment-transmitting bolted end plate end plate connections'
Structural Connections: Stability and Strength, ed. Narayanan, Elsevier Science Publishers, pp 219-251, 1989.

33 **Gendron G., Beaulieu D. and Dhatt G.**
'Finite element modelling of bolted connections'
Can. J. Civ. Eng., Vol. 16, pp 172-181, 1989.

34 **Tong C.S.**
'The elastic behaviour of semi-rigid connections in steel structures'
PhD Thesis, Hatfield Ploytechnic, Hatfield, 1985.

35 **Prescott A.T.**
'The performance of end plate connections in Steel structures and their influence on overall structural behaviour'
PhD Thesis, Hatfield Polytechnic, Hatfield, 1987.

36 **Pask J.W.**
'Manual on connections for beam and column construction'
BCSA Publication, No. 9/82, 1982.

37 **Zienkiewicz O.C.**
'Finite element method'
Fourth Edition, Vol. 1, McGrawhill, 1989.

38 **Owen D.R.J. and Hinton E.**
'Finite element in plasticity (Theory and Practice)'
Pineridge Press, 1980.

39 **Finite Element Analysis Ltd.**
'Advance procedure and training course manual'

40 **Honnor M.E.**
'Frictional gap model'
Finite Element Analysis Ltd. internal report, No. FEAL502, May 1985.

41 **Finite Element Analysis Ltd.**
'London University Structural Analysis System (LUSAS)'
Computer Package Developed by FEA Ltd., Forge House, 66 High St. Kingston Upon Thames, Surrey.

42 **Wilson W.M. and Hao C.C.**
'Residual stresses in welded structures'
The Welding Journal, Research Supplement, May 1974.

43 **Nethercot D.A. and Zandonini R.**
'Methods of prediction of joint behaviour: beam-to-column connections'
Structural Connections: Stability and Strength, ed. Narayanan, Elsevier Science Publishers, pp 23-62, 1989.

44 **BS4190**
'ISO Metric Black Precision Hexagon Bolts, Screws and Nuts'
British Standards Institution, London, 1967

45 **Shakir-Khalil H. and Hao C.M.**
'Black bolts under combined tension and shear'
The Structural Engineer, Vol. 57B, No. 4, pp 69-76, December 1979.

46 **BS449, Part 2:**
'The Use of Structural Steel in Building'
British Standards Institution, London, 1969.

47 **Anderson C.**
'Characteristics of H.S.F.G. bolts'
MPhil Thesis, Polytechnic of the South Bank, London, 1976.

48 **BS3692**
'ISO Metric Precision Hexagon Bolts, Screw and Nuts'
British Standards Istitution, London, 1967.

49 **Mann A.P. and Morris L.J.**
'Significance of lack of fit in flush beam-column connections'
International Conference on Joints in Structural Steelwork, Teesside Polytechnic, 1981, Pentech Press Ltd., pp 6.22-6.35.

50 **Mann A.P. and Morris L.J.**
'Lack of fit in steel structures'
CIRIA Report 87, 1982.

51 **Mann A.P. and Morris L.J.**
'Lack of fit in high strength bolted connections'
Journal of Structural Engineering, ASCE, Vol. 110, No. 6, June 1984.

52 Davidson J.B., Kirby P.A. and Nethercot D.A.
'Effect of Lack of fit on connection restraint'
J. Construct. Steel Research, Vol. 8, pp 55-69, 1987.

The published paper cited below has been removed from the e-thesis due to copyright issues:

Bose, B., Sarkar, S. and Bahrami, M. (1991). Finite element analysis of unstiffened extended end-plate connections. In *Structural Engineering Review*, 3, pp.211-224.